


For Reference

NOT TO BE TAKEN FROM THIS ROOM

Ex libris
UNIVERSITATIS
ALBERTAENSIS





Digitized by the Internet Archive
in 2022 with funding from
University of Alberta Libraries

<https://archive.org/details/Heinekey1982>

T H E U N I V E R S I T Y O F A L B E R T A

RELEASE FORM

Cycloheptatrienyl Complexes of Transition Metals

NAME OF AUTHOR Dennis Michael Heinekey

TITLE OF THESIS .. Cycloheptatrienyl Complexes of Transition ..
Metals
.....

DEGREE FOR WHICH THESIS WAS PRESENTED Ph.D.

YEAR THIS DEGREE GRANTED 1981

Permission is hereby granted to THE UNIVERSITY OF ALBERTA LIBRARY to reproduce single copies of this thesis and to lend or sell such copies for private, scholarly or scientific research purposes only.

The author reserves other publication rights, and neither the thesis nor extensive extracts from it may be printed or otherwise reproduced without the author's written permission.

RESEARCH REPORT

NAME OF STUDENT:
TITLE OF STUDY:
DATE:
BY:
IN:
OF:
AT:
ON:
FOR:
BY:
IN:
OF:
AT:
ON:
FOR:

The purpose of this study is to determine the effect of the treatment on the growth of the plants. The results of the study are as follows: The plants treated with the treatment showed a significant increase in growth compared to the control group. The results of the study are as follows: The plants treated with the treatment showed a significant increase in growth compared to the control group.



THE UNIVERSITY OF ALBERTA

FACULTY OF GRADUATE STUDIES AND RESEARCH

Cycloheptatrienyl Complexes of Transition Metals

by



Dennis Michael Heinekey

A THESIS

SUBMITTED TO THE FACULTY OF GRADUATE STUDIES AND RESEARCH
IN PARTIAL FULFILMENT OF THE REQUIREMENTS FOR THE DEGREE
OF DOCTOR OF PHILOSOPHY

DEPARTMENT OF CHEMISTRY

EDMONTON, ALBERTA

SPRING, 1982

THE UNIVERSITY OF ALBERTA
FACULTY OF GRADUATE STUDIES AND RESEARCH

The undersigned certify that they have read, and recommend to the Faculty of Graduate Studies and Research, for acceptance, a thesis entitled CYCLOHEPTATRIENYL COMPLEXES OF TRANSITION METALS submitted by DENNIS MICHAEL HEINEKEY in partial fulfilment of the requirements for the degree of Doctor of Philosophy in Chemistry.

TO MY PARENTS

Abstract

The synthesis, reactions and fluxional behaviour of a number of cycloheptatrienyl complexes of transition metals have been investigated. Monohapto, trihapto and pentahapto coordination of the cycloheptatrienyl group to transition metals has been explored. Fluxional behaviour in these complexes has been studied using variable temperature NMR spectroscopy.

Reaction of $\text{NaRe}(\text{CO})_5$ with $\text{C}_7\text{H}_7\text{BF}_4$ afforded $(7-\eta^1\text{-C}_7\text{H}_7)\text{Re}(\text{CO})_5$ (5), the first monohaptocycloheptatrienyl derivative of a transition metal. Study of the fluxional behaviour of 5 by spin saturation transfer techniques demonstrated that the metal migration process in this compound is a [1,7] sigmatropic migration. A concurrent carbonyl scrambling process was also detected. These results are interpreted in terms of conservation of orbital symmetry.

Successive decarbonylation of 5 afforded $(\eta^3\text{-C}_7\text{H}_7)\text{Re}(\text{CO})_4$, (8), $(\eta^5\text{-C}_7\text{H}_7)\text{Re}(\text{CO})_3$, (9) and $[(\eta^7\text{-C}_7\text{H}_7)\text{Re}(\text{CO})_2]_2$. Reaction of 8 and 9 with various phosphine ligands afforded monohapto and trihapto derivatives, some of which exhibit fluxional behaviour.

Reaction of $\text{NaCpRu}(\text{CO})_2$ with $\text{C}_7\text{H}_7\text{BF}_4$ formed $\text{CpRu}(\text{CO})_2(7-\eta^1\text{-C}_7\text{H}_7)$, (23), nearly quantitatively. This compound exhibits two metal migration pathways. The expected [1,5] sigmatropic migration of the metal moiety

was observed, as well as a [1,7] metal migration.

The stereochemistry of the metal migration process has been studied using a derivative of 23, $\text{CpRu}(\text{CO})(\text{PMe}_2\text{Ph})(7\text{-}\eta^1\text{-C}_7\text{H}_7)$, having a chiral metal center. The [1,7] metal migration in this compound proceeds with retention of configuration at the metal.

Acknowledgments

The author expresses sincere appreciation and gratitude to:

Dr. W. A. G. Graham for his enthusiastic guidance and encouragement throughout the course of this work.

The members of the research group, in particular Dr. James R. Sweet and Dr. James K. Hoyano for their friendship and many stimulating discussions.

Dr. R. E. D. McClung for helpful discussions and his contribution of the appendix to this thesis.

Dr. Josef Takats for his enthusiastic teaching and helpful discussions.

Jacki Jorgensen and Annabelle Wiseman for their assistance in the preparation of this manuscript.

Glen Bigam, Tom Brisbane and Dr. Tom Nakashima for their invaluable assistance and advice on NMR problems.

John Olekszyk for obtaining the mass spectra.

TABLE OF CONTENTS

CHAPTER		PAGE
I	INTRODUCTION	1
II	CYCLOHEPTATRIENYL COMPLEXES OF MANGANESE AND RHENIUM	
	Section I Introduction	11
	Section II Cycloheptatrienyl Compounds of Manganese	13
	Section III Preparation and Properties of $(7-\eta^1-C_7H_7)Re(CO)_5$	18
	Section IV Decarbonylation Reactions of $(7-\eta^1-C_7H_7)Re(CO)_5$	31
	Section V Experimental	43
III	PHOSPHINE ADDITION REACTIONS	
	Section I Introduction	59
	Section II Rhenium Compounds	61
	Section III Manganese Compounds	72
	Section IV Experimental	76
IV	COMPOUNDS OF CHROMIUM, MOLYBDENUM AND TUNGSTEN	
	Section I Introduction	83
	Section II Anion Reactions	86
	Section III Indirect Synthetic Methods	88
	Section IV Experimental	96

V	CYCLOHEPTATRIENYL COMPOUNDS OF IRON AND RUTHENIUM	
	Section I Introduction	102
	Section II Iron Compounds	105
	Section III Ruthenium Compounds	110
	Section IV Mechanistic Considerations	118
	Section V Preparation of Monohaptocycloheptatrienyl Alkyls With Asymmetric Metal Centers	123
	Section VI Experimental	135
VI	DINUCLEAR RUTHENIUM COMPOUNDS	
	Section I Introduction	148
	Section II Preparation of $[\text{CpRu}(\text{CO})(\text{PMe}_3)_2]_2$	150
	Section III Preparation of $[\text{CpRu}(\text{CO})(\text{PMe}_2\text{Ph})]_2$	159
	Section IV Experimental	161
VII	FLUXIONAL BEHAVIOUR OF MONOHAPTOCYCLOHEPTATRIENYL COMPOUNDS	
	Section I Introduction	
	A. Application of Orbital Symmetry Criteria to Sigmatropic Shifts	168
	B. σ -Cyclopolyenyl Metal Complexes: Previous Results	173
	C. Scope of the Present Studies	178

Section II Fluxional Processes in	
$(7-\eta^1-C_7H_7)Re(CO)_5$	
A. The Pathway of Metal Migration	180
B. Carbonyl Exchange and the Mechanism	
of Metal Migration	200
Section III Spin Saturation Transfer	
Experiments on Phosphine Sub-	
stituted Derivatives of	
$(7-\eta^1-C_7H_7)Re(CO)_5$	205
Section IV Metal Migration in	
$CpRu(CO)_2(7-\eta^1-C_7H_7)$	207
Section V Stereochemistry of Metal Migration	
in $CpRu(CO)(PMe_2Ph)(7-\eta^1-C_7H_7)$	217
Section VI Conclusions	226
Section VII Experimental	
A. General	227
B. Instrumentation and Methodology	227
C. Temperature Control and Calibration	229
D. Field Homogeneity and Probe Tuning	232
E. Integrals	232
VIII FLUXIONAL BEHAVIOUR OF TRIHAPTO AND PENTA-	
HAPTO CYCLOHEPTATRIENYL COMPOUNDS	
Section I Introduction	234
Section II Fluxionality in $(\eta^3-C_7H_7)M(CO)_4$	
(M = Mn, Re) and Phosphine Substituted	
Derivatives	236

A. $(\eta^3\text{-C}_7\text{H}_7)\text{Re}(\text{CO})_4$ and $(\eta^3\text{-C}_7\text{H}_7)\text{Mn}(\text{CO})_4$	236
B. Phosphine Substituted Derivatives	240
Section III Fluxionality of $\text{CpRu}(\text{CO})(\eta^3\text{-C}_7\text{H}_7)$	245
Section IV Fluxional Processes in	
$(\eta^5\text{-C}_7\text{H}_7)\text{Re}(\text{CO})_3$	247
Section V Experimental	252

LIST OF TABLES

TABLE		PAGE
<u>CHAPTER II</u>		
I	^1H NMR data for some $(\eta^7\text{-C}_7\text{H}_7)$ compounds	41
II	Crystal Data for $(7\text{-}\eta^1\text{-C}_7\text{H}_7)\text{Re}(\text{CO})_5$	52
III	$(7\text{-}\eta^1\text{-C}_7\text{H}_7)\text{Re}(\text{CO})_5$ -Bond lengths	53
IV	$(7\text{-}\eta^1\text{-C}_7\text{H}_7)\text{Re}(\text{CO})_5$ -Bond angles	54
V	$(7\text{-}\eta^1\text{-C}_7\text{H}_7)\text{Re}(\text{CO})_5$ -Positional and thermal parameters	55
<u>CHAPTER VI</u>		
VI	Crystal Data for $[\text{CpRu}(\text{CO})(\text{PMe}_3)]_2$	164
VII	$[\text{CpRu}(\text{CO})(\text{PMe}_3)]_2$ -Bond lengths	165
VIII	$[\text{CpRu}(\text{CO})(\text{PMe}_3)]_2$ -Bond angles	166
IX	$[\text{CpRu}(\text{CO})(\text{PMe}_3)]_2$ -Positional and thermal parameters	167
<u>CHAPTER VII</u>		
X	^1H SST data for $(7\text{-}\eta^1\text{-C}_7\text{H}_7)\text{Re}(\text{CO})_5$	188
XI	^{13}C SST data for $(7\text{-}\eta^1\text{-C}_7\text{H}_7)\text{Re}(\text{CO})_5$	198
XII	^{13}C SST data for $\text{CpRu}(\text{CO})_2(7\text{-}\eta^1\text{-C}_7\text{H}_7)$	211
<u>CHAPTER VIII</u>		
XIII	Rate constants for the (1,2) Re migration in $(\eta^3\text{-C}_7\text{H}_7)\text{Re}(\text{CO})_4$	238
XIV	Rate constants for the (1,2) Re migration in $(\eta^5\text{-C}_7\text{H}_7)\text{Re}(\text{CO})_3$	249
XV	Rates of CO scrambling in $(\eta^5\text{-C}_7\text{H}_7)\text{Re}(\text{CO})_3$	250

LIST OF FIGURES

FIGURE		PAGE
<u>CHAPTER II</u>		
I	Infrared spectrum of $C_7H_7-\overset{O}{\overs{ }}C-Mn(CO)_5$	14
II	Infrared spectrum of $(\eta^3-C_7H_7)Mn(CO)_4$	16
III	1H NMR spectrum of $(7-\eta^1-C_7H_7)Re(CO)_5$	22
IV	^{13}C NMR spectrum of $(7-\eta^1-C_7H_7)Re(CO)_5$	24
V	Molecular structure of $(7-\eta^1-C_7H_7)Re(CO)_5$	28
VI	Mass spectrum of $[(\eta^7-C_7H_7)Re(CO)_2]_2$	37
VII	Infrared spectrum of $[(\eta^7-C_7H_7)Re(CO)_2]_2$	39
<u>CHAPTER III</u>		
VIII	Infrared spectrum of $(\eta^3-C_7H_7)Re(CO)_3(PMe_3)$	65
IX	Infrared spectrum of $(\eta^1-C_7H_7)Re(CO)_3(PMe_3)_2$	69
<u>CHAPTER IV</u>		
X	Infrared spectrum of $CpW(CO)_3-\overset{O}{\overs{ }}C-C_7H_7$	90
<u>CHAPTER V</u>		
XI	Infrared spectra of $KCpRu(CO)_2$ and $CpRu(CO)_2(7-\eta^1-C_7H_7)$	111
XII	1H NMR spectrum of $CpRu(CO)_2(7-\eta^1-C_7H_7)$	113
XIII	Infrared spectrum of $CpRu(CO)_2(7-\eta^1-C_7H_7)$	114
XIV	1H NMR spectrum of $CpRu(CO)(PMe_3)(1,2-\eta^2-C_7H_8)-$ PF_6	128
XV	1H NMR spectrum of $CpRu(CO)(PMe_2Ph)(7-\eta^1-C_7H_7)$	131
XVI	^{13}C NMR spectrum of $CpRu(CO)(PMe_3)(7-\eta^1-C_7H_7)$	133

CHAPTER VI

XVII	^1H NMR spectrum (hydride region) of $[\text{CpRu}(\text{CO})(\text{PMe}_3)]_2(\mu_2\text{-H})\text{PF}_6$	151
XVIII	Infrared spectrum of $[\text{CpRu}(\text{CO})(\text{PMe}_3)]_2\text{-}$ $(\mu_2\text{-H})\text{PF}_6$	153
XIX	Molecular structure of $[\text{CpRu}(\text{CO})(\text{PMe}_3)]_2$	158

CHAPTER VII

XX	^1H SST difference spectrum of $(7\text{-}\eta^1\text{-C}_7\text{H}_7)\text{Re}(\text{CO})_5$	183
XXI	^1H SST difference spectra of $(7\text{-}\eta^1\text{-C}_7\text{H}_7)\text{Re}(\text{CO})_5$ at various temperatures	186
XXII	Eyring plot of ^1H rate constant data for $(7\text{-}\eta^1\text{-C}_7\text{H}_7)\text{Re}(\text{CO})_5$	191
XXIII	Plot of ^{13}C T_1 's of $(7\text{-}\eta^1\text{-C}_7\text{H}_7)\text{Re}(\text{CO})_5$ as a function of temperature	193
XXIV	^{13}C SST difference spectrum of $(7\text{-}\eta^1\text{-C}_7\text{H}_7)\text{-}$ $\text{Re}(\text{CO})_5$	195
XXV	^{13}C SST difference spectra for $(7\text{-}\eta^1\text{-C}_7\text{H}_7)\text{-}$ $\text{Re}(\text{CO})_5$ at various temperatures	196
XXVI	Eyring plot of ^{13}C rate constant data for $(7\text{-}\eta^1\text{-C}_7\text{H}_7)\text{Re}(\text{CO})_5$	199
XXVII	Proposed transition state geometry for the metal migration process in $(7\text{-}\eta^1\text{-C}_7\text{H}_7)\text{Re}(\text{CO})_5$	203
XXVIII	^{13}C SST difference spectrum of $\text{CpRu}(\text{CO})_2\text{-}$ $(7\text{-}\eta^1\text{-C}_7\text{H}_7)$	209

XXIX	^{13}C SST difference spectra for $\text{CpRu}(\text{CO})_2^-$ ($7-\eta^1\text{-C}_7\text{H}_7$)	210
XXX	Eyring plot of ^{13}C rate constant data for $\text{CpRu}(\text{CO})_2$ ($7-\eta^1\text{-C}_7\text{H}_7$)	213
XXXI	^{13}C SST difference spectrum of $\text{CpRu}(\text{CO})(\text{PMe}_2\text{Ph})(7-\eta^1\text{-C}_7\text{H}_7)$	220
XXXII	Observed and calculated $^1\text{H}\{^{31}\text{P}\}$ NMR spectra of the H_7 resonance of $\text{CpRu}(\text{CO})(\text{PMe}_2\text{Ph})-$ ($7-\eta^1\text{-C}_7\text{H}_7$)	222
XXXIII	Observed and calculated $^1\text{H}\{^{31}\text{P}\}$ NMR spectra of the methyl resonances of $\text{CpRu}(\text{CO})(\text{PMe}_2\text{Ph})-$ ($7-\eta^1\text{-C}_7\text{H}_7$)	224

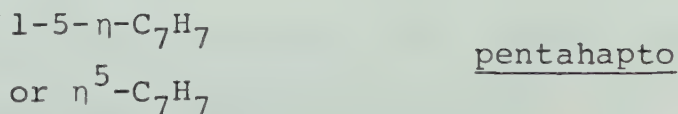
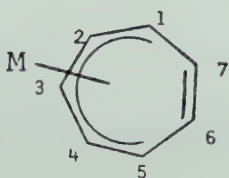
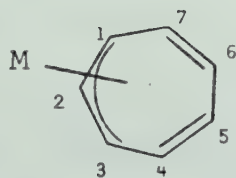
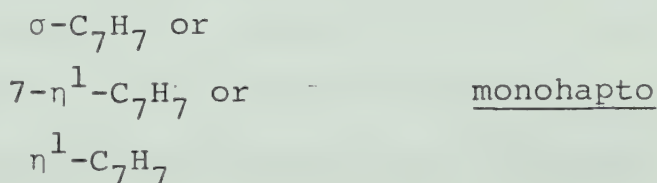
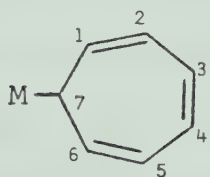
LIST OF ABBREVIATIONS

Me	methyl
Et	ethyl
dmpe	$\text{Me}_2\text{P}-\text{CH}_2\text{CH}_2-\text{PMe}_2$
Ph	phenyl
diglyme	bis(2-methoxy ethyl)ether
diphos	$\text{Ph}_2\text{P}-\text{CH}_2-\text{CH}_2-\text{PPh}_2$
THF	tetrahydrofuran
COD	1,5 cyclooctadiene
n-Bu	normal Butyl
Cp	η^5 -cyclopentadienyl, C_5H_5
Me_5Cp	η^5 -pentamethylcyclopentadienyl, C_5Me_5
COT	cyclooctatetraene
RF	radio frequency
FID	free induction decay
T_1	spin lattice relaxation time
NOE	nuclear Overhauser effect
M_z	equilibrium magnetization (z component)

CHAPTER ONE

INTRODUCTION

This thesis is concerned with the synthesis and properties of cycloheptatrienyl complexes of the transition metals. Cycloheptatriene is a very versatile ligand which can bond to transition metals in several different ways, employing between one and seven carbon atoms in bonding to the metal. It is convenient to have a shorthand notation to describe the number of carbon atoms attached to the metal. A system of notation suggested by Cotton will be employed.¹ The number of carbon atoms bonded to the metal is specified by a prefix such as monohapto, trihapto, tetrahapto, etc. Abbreviations for these prefixes are η^1 , η^3 , η^4 , etc. A standard numbering scheme² for the ring carbon atoms is outlined below.



In the monohapto bonding mode, only one metal-carbon σ bond is formed from the metal to C_7 . This general type of bonding between a transition metal and an organic group has a somewhat confusing history, which will be briefly outlined here.

Historically, the formation of metal-carbon σ bonds was first investigated in studies of compounds of the main group metals. One of the early discoveries of organometallic chemistry was the preparation by Frankland of diethylzinc in 1848.³ In 1853, Löwig prepared an ethyl compound of lead.⁴ By 1859, Buckton had identified this material as tetraethyllead,⁵ a material which was much later to have considerable industrial importance. The study of the alkyl compounds of the main group metals was firmly established by 1900, when the discovery of Grignard reagents opened up many new areas for study.⁶ More conveniently prepared and handled than the alkyls of zinc, the Grignard reagent allowed the convenient synthesis of many metal alkyls from the corresponding metal halides.

In contrast to the rapid development of main group alkyl chemistry, early attempts to apply synthetic methods of this type to the preparation of transition metal alkyls met with very limited success. For example, the reaction of phenylmagnesium bromide with $CrCl_3$

was reported by Bennett and Turner in 1914.⁷ This reaction gave a quantitative yield of biphenyl. (It should be noted that F. Hein obtained phenyl complexes of chromium from similar reactions in 1919,⁸ but the true nature of these complexes was not understood until much later). These and other results led to the impression that transition metal alkyls were less stable than those of main group metals. In a 1955 review of alkyls and aryls of the transition metals, F.A. Cotton summarized the available data with this statement: "It will be apparent from this overall picture of alkyls and aryls of the transition metals that the often heard generalization that they are much less stable and accessible than those of non-transition elements is quite true."⁹

Developments of the late 1950's led to some revision of these ideas. Compounds such as $\text{CH}_3\text{-Mn(CO)}_5$,¹⁰ $\text{CH}_3\text{-Pt(Cl)(PEt}_3)_2$ ¹¹ and $(\eta^5\text{-C}_5\text{H}_5)\text{W(CO)}_3\text{-CH}_3$ ¹² were prepared, along with many other complexes where in addition to one or more metal carbon σ bonds, the complex contained π bonding or π acid ligands such as CO or phosphines. This led to the theory that "stabilizing" ligands were needed in order to increase the strength of the metal-carbon bond.¹³

More recent developments have shown that this view is not correct. Stable transition metal alkyls without any other ligands have been prepared. Kinetic stability

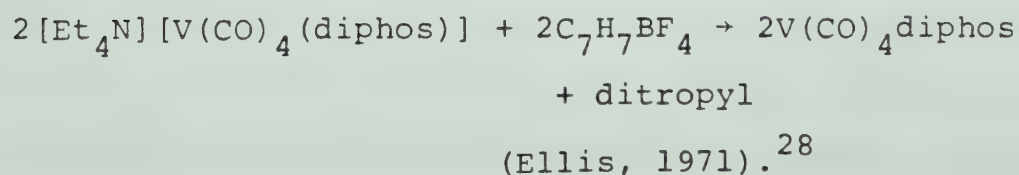
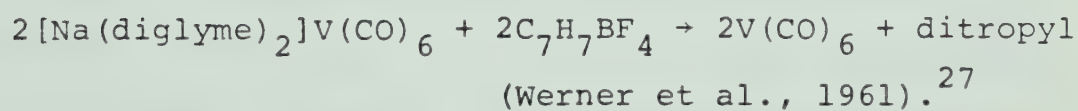
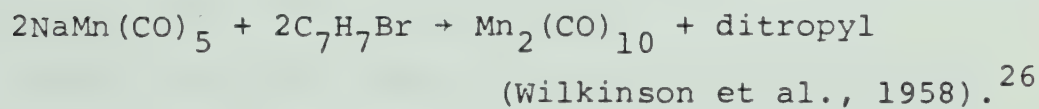
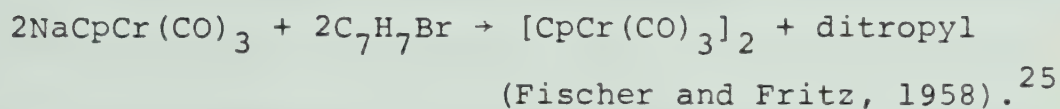
is assured by judicious choice of alkyl groups which prevent access to low energy decomposition pathways.^{14,15,16} Results in this area have been summarized in two recent reviews.^{17,18}

A monohaptocycloheptatrienyl alkyl is a special case of metal-carbon σ bonding. Due to the large resonance stabilization of the tropyli radical,¹⁹ metal-carbon σ bonds of this type are expected to be weakened, relative to bonds to ordinary alkyl groups such as methyl, ethyl, etc. At the outset of this research, the only organo-metallic examples of monohapto bonding of cycloheptatriene were found among the main group IV metals.²⁰ One of the objectives of this research was to develop synthetic methods which would allow the preparation of monohapto-cycloheptatrienyl alkyls of the transition metals, on the assumption that some of these compounds would be stable enough to isolate.

In contrast to cyclopentadiene, which is quite acidic due to the formation of the stable aromatic $C_5H_5^-$ anion, cycloheptatriene is a very weak acid. An estimated pK_a of 36 has been reported by Breslow and Chu.²¹ There is limited indirect evidence for the existence of the anion $C_7H_7^-$.^{22,23} The halides of cycloheptatriene are ionic, due to the great stability of the tropylium cation, $C_7H_7^+$,²⁴ which is isoelectronic with benzene. This

cation is a convenient starting point for synthesis.

The reaction of the tropylium cation with an nucleophilic transition metal center such as a metal carbonyl anion would be expected to yield a monohapto-cycloheptatrienyl alkyl. An examination of the literature reveals that this approach has been a complete failure in the past. Every reported reaction of a metal carbonyl anion with tropylium has resulted in oxidation of the anion and reduction of the cation to $(C_7H_7)_2$ (ditropyl). Some of these reactions are:



Tropylium cation has been used extensively by Ellis and coworkers as an oxidizing agent for metal carbonyl anions. In a recent paper, Ellis states that "tropylium ion is often used as a mild and convenient one-electron

oxidizing agent to convert carbonyl anions to analogous neutral species."²⁹

The failure of these reactions may be due to the occurrence of a one electron transfer from the anion to the cation, followed by coupling of the tropylium radicals to give ditropylium. An alternative explanation is that the metal carbon σ bond in the monohapto alkyls is too weak to allow isolation of these alkyl compounds, due to the stability of the tropylium radical.

In order to investigate this question, in this thesis a variety of indirect synthetic routes have been explored in attempts to prepare monohaptocycloheptatrienyl alkyls of various transition metals. The direct reaction of tropylium with carbonyl anions of the heavier transition metals has also been investigated.

Aside from the chemical interest and synthetic challenge of monohaptocycloheptatrienyl compounds, a major motive for investigation of these compounds was to study their fluxional behaviour. Fluxional molecules are defined³⁰ as systems which have more than one thermally accessible equivalent structure and undergo a degenerate rearrangement process which interconverts these structures. Organometallic compounds with cyclopolyenyl groups σ bonded to the metal form one class of fluxional molecules. The σ -cyclopentadienyl (or η^1 -C₅H₅) metal compounds have

been studied extensively.

An iron compound, $(\eta^5\text{-C}_5\text{H}_5)\text{Fe}(\text{CO})_2(\eta^1\text{-C}_5\text{H}_5)$, prepared by Piper and Wilkinson in 1956, was the first compound of this type recognized as a fluxional molecule. Based on the observation of a single resonance for the $(\eta^1\text{-C}_5\text{H}_5)$ group in the ^1H NMR spectrum, these authors correctly inferred that the metal moiety was rapidly migrating around the σ bonded cyclopentadienyl ring, breaking and reforming metal carbon σ bonds as it went.¹² A large number of σ -cyclopentadienyl compounds of the transition metals and the main group metals are now known. Most of them exhibit similar fluxional behaviour.

The question of how these rearrangements occur has been investigated extensively. In every case studied, it was found that the migration of the metal group is from one carbon atom to the adjacent carbon, a so-called (1,2) shift.³¹

In the 1960's a large amount of experimental data had accumulated on these and many other types of molecular rearrangements. At the same time, a theoretical basis for the mechanism of these reactions became available with advances in molecular orbital theory. The contributions of several workers led to what are now commonly referred to as orbital symmetry rules or the Woodward-Hoffmann rules.³² These rules apply the principle of conservation of orbital symmetry to predict the path of

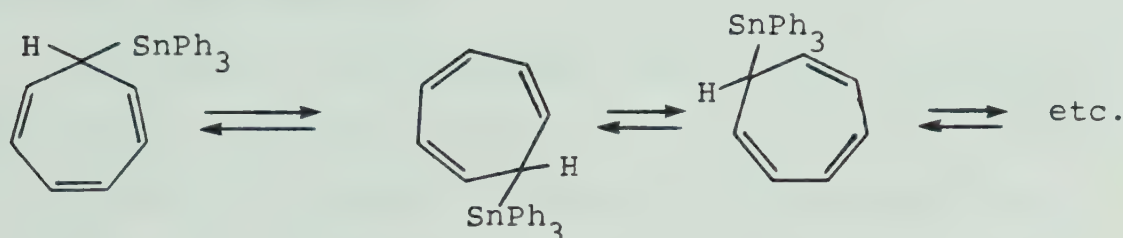
molecular rearrangements. One type of rearrangement governed by these rules is sigmatropic migration, defined by Woodward and Hoffmann³³ as an uncatalyzed, concerted intramolecular migration of a σ bond to a new position within a π electron system.

Application of orbital symmetry considerations to migrations in cyclic dienyl systems such as cyclopentadiene and cycloheptatriene is well established in organic chemistry and the extension to organometallic chemistry, particularly in main group IV derivatives, has generated a great deal of interest. In cyclopentadienyl systems, the observed (1,2) shifts are not distinguishable from the theoretically predicted [1,5] sigmatropic migration.* It is not clear whether orbital symmetry constraints or a preference for minimum motion of the migrating group ("least-motion" shifts) is the dominant factor. In σ -cycloheptatrienyl systems, the least motion (1,2) path can be readily distinguished from the theoretically allowed [1,5] pathway, in which the migrating group moves to the carbon atom furthest from the original point

*The convention of designating the pathway of sigmatropic migrations in square brackets will be followed. A complete explanation of this terminology and the basis of the theoretical predictions will be found in chapter VII.

of attachment.*

In a study of triphenyl-7-cycloheptatrienylnitin, Larrabee found that this molecule is fluxional via a [1,5] migration of the metal.²⁰ This result is very



important, since it establishes that orbital symmetry constraints can determine the pathway of a metal migration. The theoretical basis for the symmetry rules assumes that the migrating group presents an invariant orbital of σ symmetry as it migrates over the polyenyl framework. The results for this tin compound indicate that this assumption is probably valid for main group metals.

If the migrating group also has d orbitals which are at accessible energy levels and can participate in metal-carbon bond formation, the restrictions imposed by orbital symmetry conservation requirements based on s and p orbitals may be altered. As mentioned previously,

* Only the [1,5] shift is allowed if the stereochemistry of the migrating group remains unchanged. The consequences of inversion at the migrating group are discussed in Chapter VII.

the intensively studied monohaptocyclopentadienyl compounds of the transition metals, which all exhibit (1,2) metal migrations, do not allow this question to be addressed since the "least motion" and symmetry controlled pathways are degenerate.

The study of the fluxional behaviour of monohapto-cycloheptatrienyl compounds of the transition metals will allow the role of metal d orbitals in determining the pathway of metal migration to be investigated.

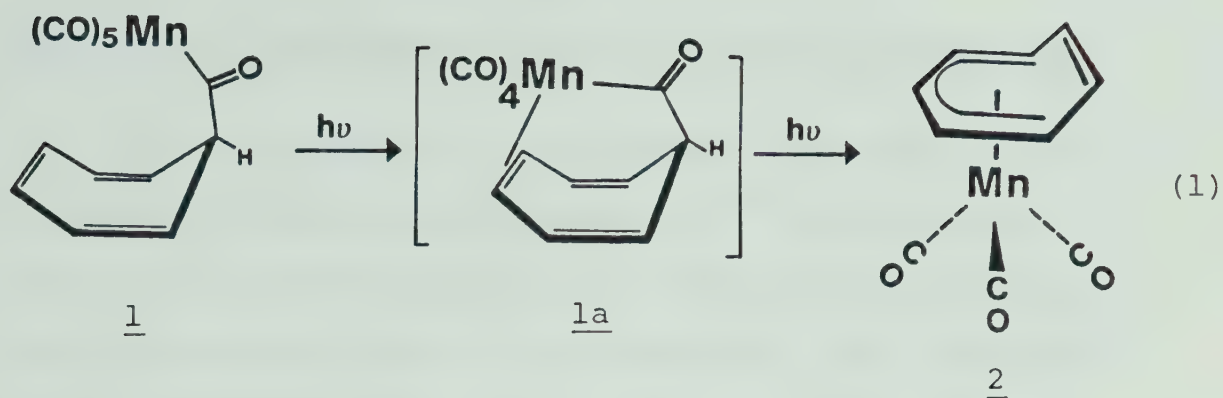
CHAPTER TWO

CYCLOHEPTATRIENYL COMPLEXES OF MANGANESE AND RHENIUM

Section I. Introduction

The reaction of the $\text{Mn}(\text{CO})_5^-$ anion with tropylium bromide was first reported in 1958 to yield only ditropyl and $\text{Mn}_2(\text{CO})_{10}$.²⁶ This result was later interpreted by King³⁴ as indicating that the manganese-carbon bond in the unknown σ -cycloheptatrienyl derivative $(7-\eta^1\text{-C}_7\text{H}_7)\text{Mn}(\text{CO})_5$ apparently is very weak. This reaction was reinvestigated recently by T.H. Whitesides and R. Budnik.³⁵ Reaction of $\text{NaMn}(\text{CO})_5$ with $\text{C}_7\text{H}_7\text{BF}_4$ in THF at -78°C gave only $\text{Mn}_2(\text{CO})_{10}$ and ditropyl. Irradiation of the reaction mixture at -78°C gave no additional products. It was concluded that any σ bonded alkyl intermediate was very unstable, even at -78°C .

In contrast to these results, a stable manganese acyl compound was isolated by these workers from the reaction of $\text{NaMn}(\text{CO})_5$ with 7-cycloheptatrienylacyl chloride. This acyl was photochemically decarbonylated at -65°C to give a low yield (11% after chromatography) of $(\eta^5\text{-C}_7\text{H}_7)\text{Mn}(\text{CO})_3$ (2) along with large amounts of ditropyl and $\text{Mn}_2(\text{CO})_{10}$ (eq. 1).



Whitesides postulated the chelated acyl intermediate 1a to explain the success of this indirect route. If this is correct, it seems unlikely that 2 is the sole product of further decarbonylation of 1a. We have reinvestigated this reaction in the hope of intercepting intermediates in the formation of 2.

The remainder of this chapter deals with the preparation and properties of the analogous rhenium compounds, with emphasis on decarbonylation reactions. Striking differences in thermal stability and ease of decarbonylation between manganese compounds and their rhenium analogs are explored.

Section II. Cycloheptatrienyl Compounds of Manganese

The acyl compound 1 was prepared according to the procedure of Whitesides and Budnik.³⁵ The reported physical and spectroscopic properties of this material are in agreement with our observations, with the exception of the infrared spectrum. The reported infrared spectrum (pentane solution) consists of four absorptions in the carbonyl stretching region: 2115, 2050, 2005 and 1652 cm^{-1} (acyl CO). Under higher resolution, a more complex spectrum is evident (see Figure I).

For a molecule LMn(CO)_5 of C_{4v} symmetry only three infrared active CO stretching vibrations are predicted from group theory ($2A_1$ and E).³⁶ In alkyl and acyl Mn(CO)_5 compounds with lower than C_3 symmetry in the alkyl or acyl groups, the normally infrared inactive B_1 stretching mode becomes infrared active and the doubly degenerate E mode splits into two components.³⁷ By comparison to other compounds of the R-Mn(CO)_5 and R-C(=O)-Mn(CO)_5 type,³⁸ the infrared spectrum of 1 can be assigned: (cyclohexane, $\nu_{\text{CO}}, \text{cm}^{-1}$) 2114 (w, A_1), 2050 (w, B_1), 2020 (s, E), 2009 (s, E), 2005 (s, A_1).

The acyl stretching frequency is also split into two bands at 1668 cm^{-1} and 1655 cm^{-1} . This is due to the existence of two different rotamers with respect to the carbon-carbon bond in the acyl group. Similar effects

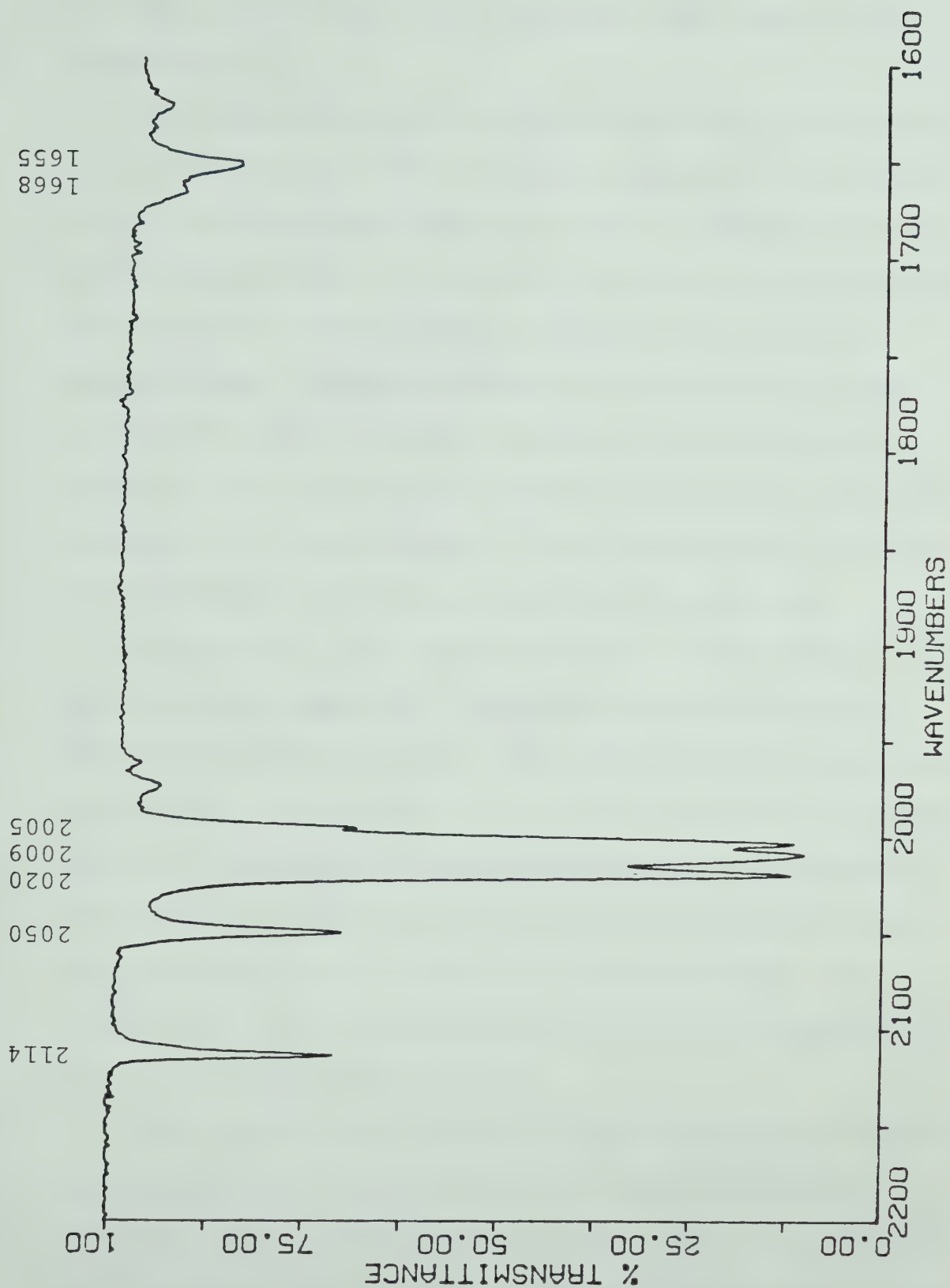


FIGURE I. Infrared spectrum of $(\text{C}_7\text{H}_7)\text{-C}(=\text{O})\text{-Mn}(\text{CO})_5$, cyclohexane.

in other $\text{R}-\overset{\text{O}}{\parallel}\text{C}-\text{Mn}(\text{CO})_5$ compounds have been reported by Calderazzo.³⁸

The photochemical decarbonylation of 1 was carried out in acetone at -50°C using an immersion well reactor with a refrigerated lamp jacket (450 W medium pressure Hg discharge lamp). A nitrogen purge was maintained and the progress of the reaction monitored by infrared spectroscopy. This procedure is very similar to that employed by Whitesides and Budnik. Chromatographic work-up (see experimental section for details) gave the expected $(\eta^5\text{-C}_7\text{H}_7)\text{Mn}(\text{CO})_3$ in 14% yield as well as a red compound identified by infrared spectroscopy as $(\eta^3\text{-C}_7\text{H}_7)\text{Mn}(\text{CO})_4$ (3) (see Figure II). NMR spectra of this material indicated contamination with ditropyl. Careful recrystallization from hexane affords 3 as large red needles and ditropyl in the form of large colourless plates. These were then physically separated and the red crystals were recrystallized once more from hexane to give pure 3 in 7% yield. All spectroscopic and analytical data are consistent with the formulation of 3 as a tetracarbonyl compound.

In view of the presence of this new compound among the products of the photochemical decarbonylation reaction, some of the physical properties of 2 reported by Whitesides which differ slightly from our observations

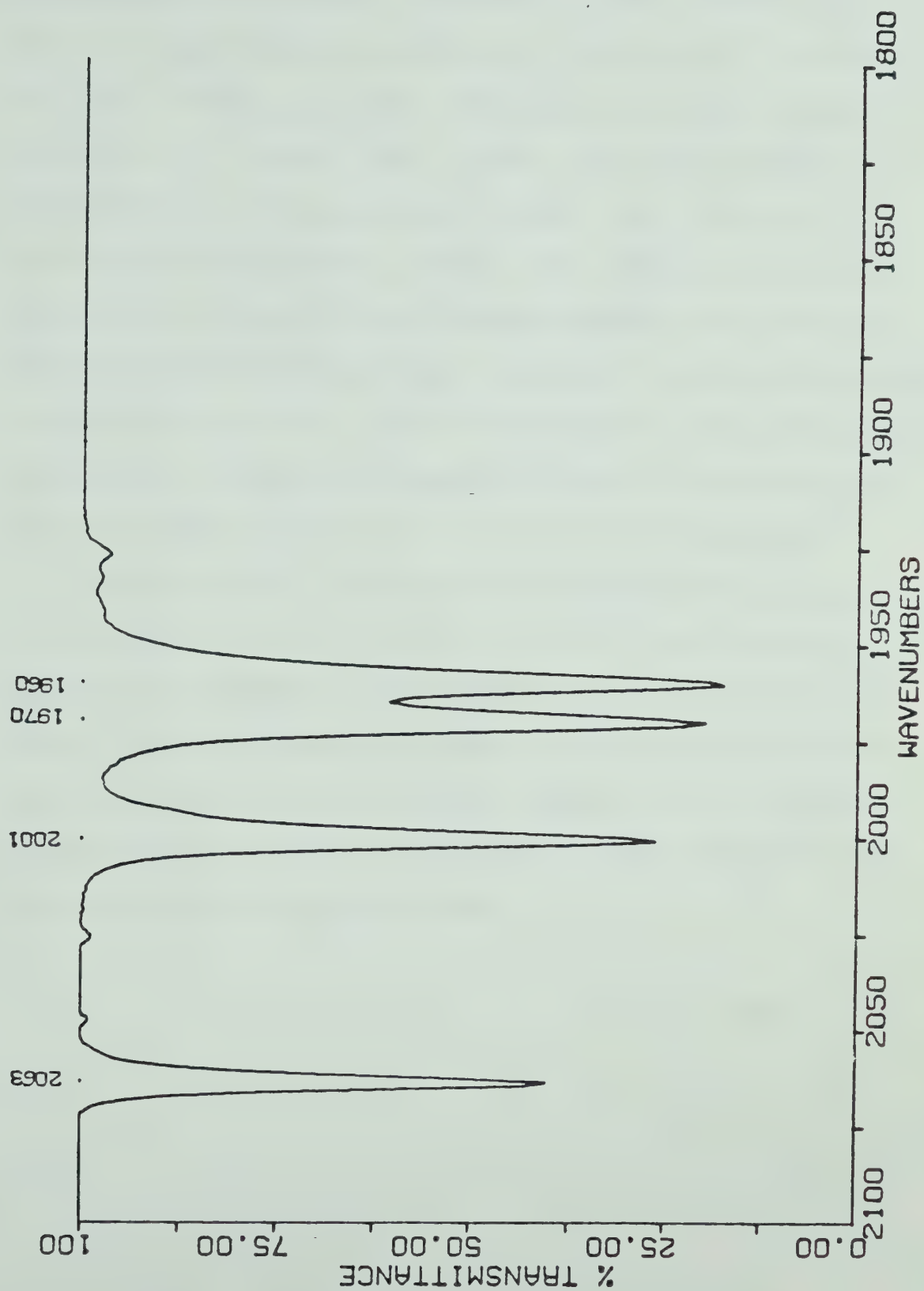


FIGURE II. Infrared spectrum of $(\eta^3\text{-C}_7\text{H}_7)\text{Mn}(\text{CO})_4$, cyclohexane.

are perhaps explicable. Compound 2 was reported as a bright orange solid, mp 64°C, λ_{max} (EtOH) 307 (ϵ 4500), 262 nm (ϵ 10400). In our hands, 2 is a yellow solid, mp 64°C, λ_{max} (EtOH) 374 (ϵ 3450), 311 nm (ϵ 10350). Contamination of 2 by a small amount of 3 (mp 66°C) would not substantially affect the elemental analysis. Detection of 3 by NMR spectroscopy under the conditions employed by Whitesides is not possible since 3 is fluxional and would give only a very broad signal at the temperatures indicated. (Refer to Chapter VIII for a discussion of the fluxional properties of 3 and related compounds.)

In principle, the intense red colour of 3 (λ_{max} (EtOH) 388 (ϵ 5150), 312 nm (ϵ 38700)) could lead to a detectable change in the UV/visible absorption spectrum of 2. The differences between our observed UV/visible spectrum of 2 and the spectrum reported by Whitesides are so large (ca. 50 nm) that some other source of this discrepancy must be considered.

Section III. Preparation and Properties of $(7-\eta^1-C_7H_7)Re(CO)_5$

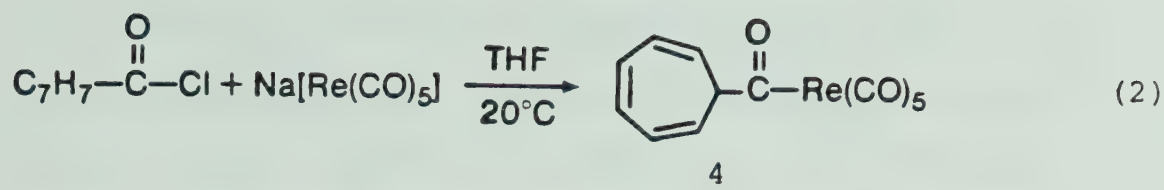
The failure of our attempts and those of other workers to prepare a monohaptocycloheptatrienyl compound of manganese could be attributed to two different factors. Whitesides³⁵ has suggested that $(7-\eta^1-C_7H_7)Mn(CO)_5$ would be very unstable due to weakness of the metal-carbon σ bond which arises from the stabilization of the tropyli radical. The other possible explanation is that under photolysis conditions, facile decarbonylation to the trihapto and pentahapto compounds prevents isolation of $(7-\eta^1-C_7H_7)Mn(CO)_5$.

A quantitative study of Mn-C versus Re-C bond strengths has been reported by Skinner et al.³⁹ The Mn-C bond dissociation energy $D[CH_3-Mn(CO)_5]$ is 27.9 ± 2.3 or 30.9 ± 2.3 kcal mol⁻¹ (the value depends on a choice between two different reported values^{40,41} for $D[Mn-Mn]$ in $Mn_2(CO)_{10}$). For rhenium $D[CH_3-Re(CO)_5]$ is 53.2 ± 2.5 kcal/mol. In a monohaptocycloheptatrienyl alkyl, the M-C σ -bond will be weakened by resonance stabilization of the tropyli radical. This stabilization relative to the methyl radical can be estimated by comparing the measured $D[C_7H_7-C_7H_7]$ for ditropyli of 35 kcal mol⁻¹¹⁹ with $D[CH_3-CH_3]$ for ethane, which is reported as 88 kcal mol⁻¹.⁴² On this basis, the stabilization of the $C_7H_7\cdot$ radical relative to $CH_3\cdot$ is approximately

26 kcal mol⁻¹. The apparent instability of (7- η^1 -C₇H₇)Mn(CO)₅ is to be expected, since D[C₇H₇-Mn(CO)₅] will be in the range of 2-5 kcal mol⁻¹. A similar estimate for the rhenium analog gives D[C₇H₇-Re(CO)₅] of about 27 kcal mol⁻¹, which should be sufficient bond strength to allow isolation of the compound.

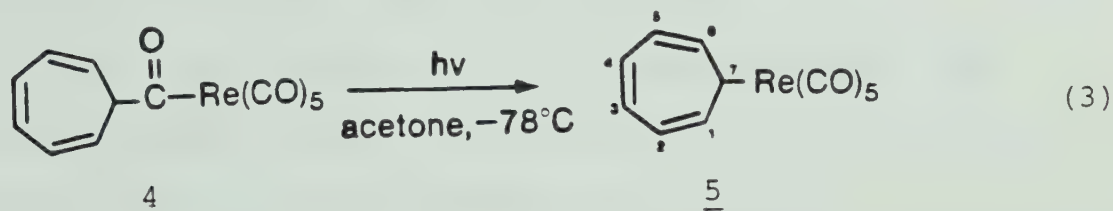
Another route by which a monohaptocycloheptatrienyl compound could decompose would be by decarbonylation to a trihapto compound, as noted in Section I in the synthesis of (η^3 -C₇H₇)Mn(CO)₄. Rhenium pentacarbonyl compounds are known to exhibit reduced CO lability compared to the manganese analogs.⁴³ For example, at the time that this research was undertaken a report of the synthesis of (η^1 -C₃H₅)Re(CO)₅ had appeared in which it was stated that "Limited attempts to decarbonylate this material were unpromising."⁴⁴ (the presumed product of decarbonylation, (η^3 -C₃H₅)Re(CO)₄, is a stable compound available by another route).⁴⁵ A subsequent reinvestigation of this work established that (η^1 -C₃H₅)Re(CO)₅ does undergo decarbonylation under UV irradiation to afford (η^3 -C₃H₅)Re(CO)₄ in 55% yield.⁴⁶

Based on the above considerations of greater Re-C σ bond strength and reduced lability toward decarbonylation of rhenium systems, the acyl C₇H₇- $\overset{\text{O}}{\parallel}$ C-Re(CO)₅ was prepared as an entry into the rhenium system (eq. 2).



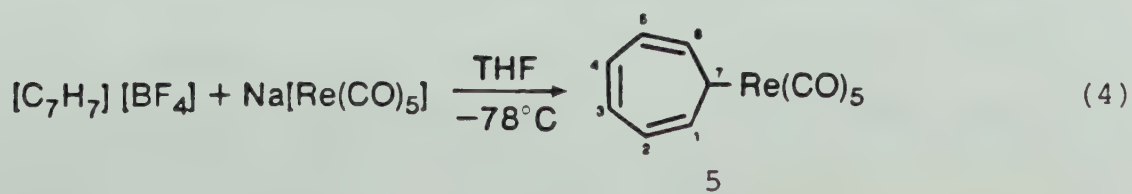
Compound 4 was fully characterized by infrared, NMR and mass spectroscopy as well as elemental analysis. The infrared spectrum is very similar to that of the manganese analog, again exhibiting splitting of the doubly degenerate E mode and a doubling of the acyl stretching frequencies due to rotational isomerism (see Section I for a discussion of these effects).

Photochemical decarbonylation of 4 in acetone at -78°C affords the monohaptocycloheptatrienyl compound in 60% yield (eq. 3). Compound 5 is an air stable, orange



crystalline solid which melts at 74°C . It has been fully characterized by elemental analysis and spectroscopic methods. The contrast between these results and those obtained in the manganese system is quite remarkable.

Since 5 is a stable compound, we investigated a more direct synthesis from $\text{C}_7\text{H}_7\text{BF}_4$ (eq. 4). Surprisingly,



this reaction is essentially quantitative, affording 5 in 90% isolated yield. As noted in the introduction, all previously reported reactions of metal carbonyl anions with tropylium led to oxidation of the anion and reduction of the tropylium cation to ditropyl.

The infrared spectrum of 5 in cyclohexane solution shows three ν_{CO} bands at 2120, 2015 and 1983 cm^{-1} . The positions and relative intensities of these bands are typical of an $\text{M}(\text{CO})_5$ derivative.^{47,48} Further confirmation of the formulation of 5 as a pentacarbonyl derivative was provided by the mass spectrum, which has a molecular ion corresponding to $(\text{C}_7\text{H}_7)\text{Re}(\text{CO})_5$ at m/e 418 with the correct isotope pattern. Ions corresponding to loss of up to five CO groups were also observed.

The ^1H NMR spectrum of 5 is shown in Figure III. The assignments shown on the spectrum are based on the following decoupling experiments:

- 1) the triplet of triplets at δ 3.16 integrates as one proton, therefore it is H_7 . Decoupling of this signal causes the signal at δ 5.44 to collapse to a broad doublet. This peak is assigned to $\text{H}_{1,6}$.
- 2) Decoupling of $\text{H}_{1,6}$ causes H_7 to collapse to a singlet while the complex resonances at δ 5.25 becomes much narrower (i.e., a large coupling is

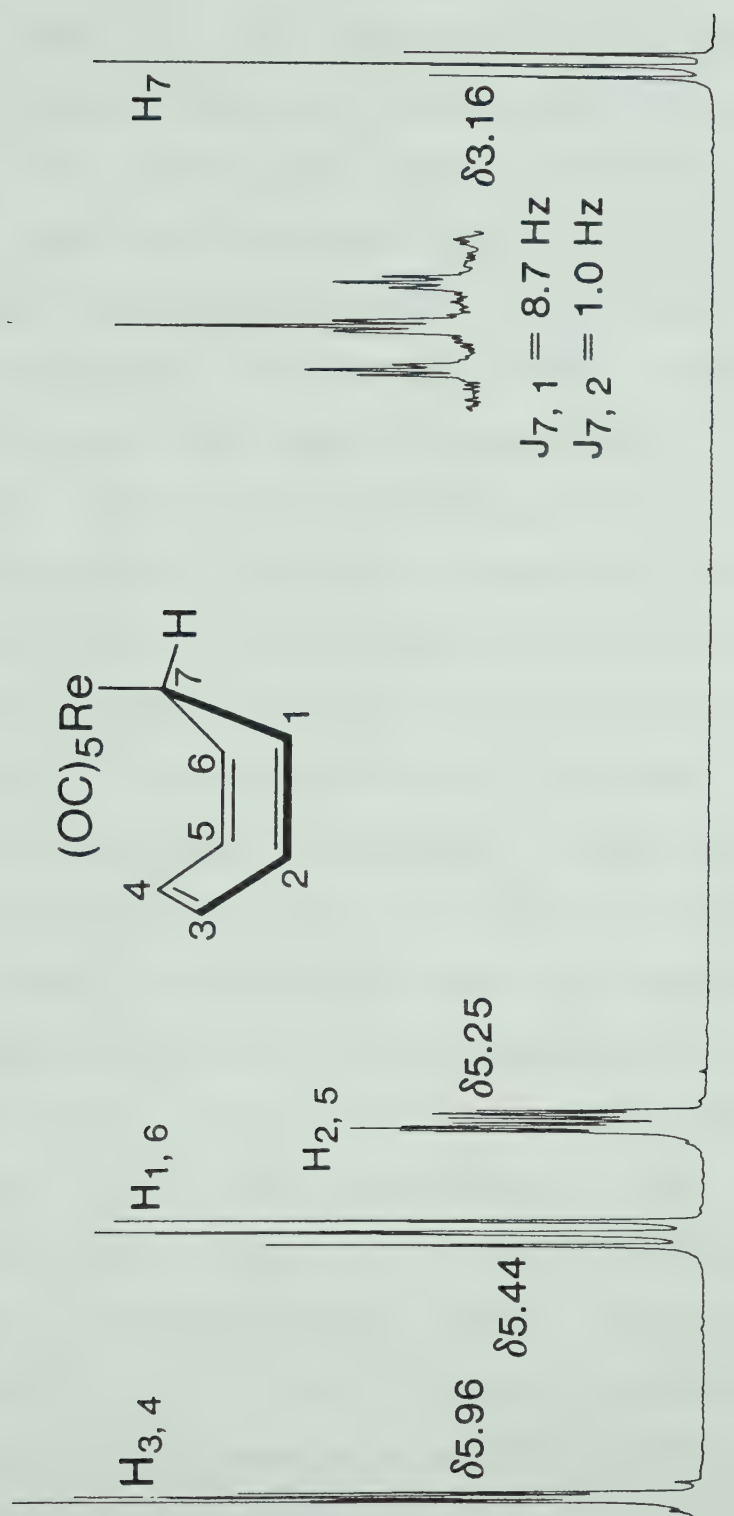


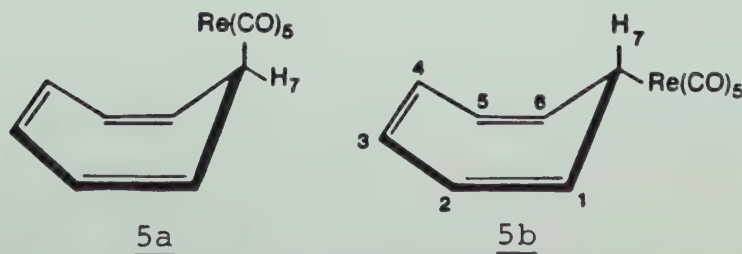
FIGURE III. ¹H NMR spectrum of (7-η¹-C₇H₇)Re(CO)₅, methylcyclohexane-d₁₄.

removed). This resonance is assigned to $H_{2,5}$.

- 3) Decoupling of $H_{2,5}$ causes the remaining resonance at δ 5.96 to collapse to a singlet, confirming that this resonance is due to $H_{3,4}$.

These assignments of the 1H spectrum can then be used as the basis for selective proton decoupling experiments to assign the olefinic resonances in the ^{13}C NMR spectrum. The 25.1 MHz ^{13}C NMR spectrum (broad band proton decoupled) is shown in Figure IV. The two carbonyl resonances can be assigned by inspection, based on their intensity ratio, to the axial and equatorial carbonyl positions. Confirmation of this assignment is provided by comparison with the reported ^{13}C NMR spectra of other $Re(CO)_5$ derivatives, where the equatorial CO resonances are at lower field than the axial CO resonance.⁴⁹

Inspection of the 1H NMR spectrum of 5 in methylcyclohexane- d_{14} reveals that the vicinal coupling constant $^3J_{1-7}$ in this compound is 8.7 Hz. This coupling is altered very slightly by a change in solvent to dioxane- d_8 or $CFHCl_2/CD_2Cl_2$ (4:1). In both of these solvents, $^3J_{1-7} = 8.5$ Hz. Compound 5 potentially has two different conformers in solution, which can be represented as 5a and 5b.



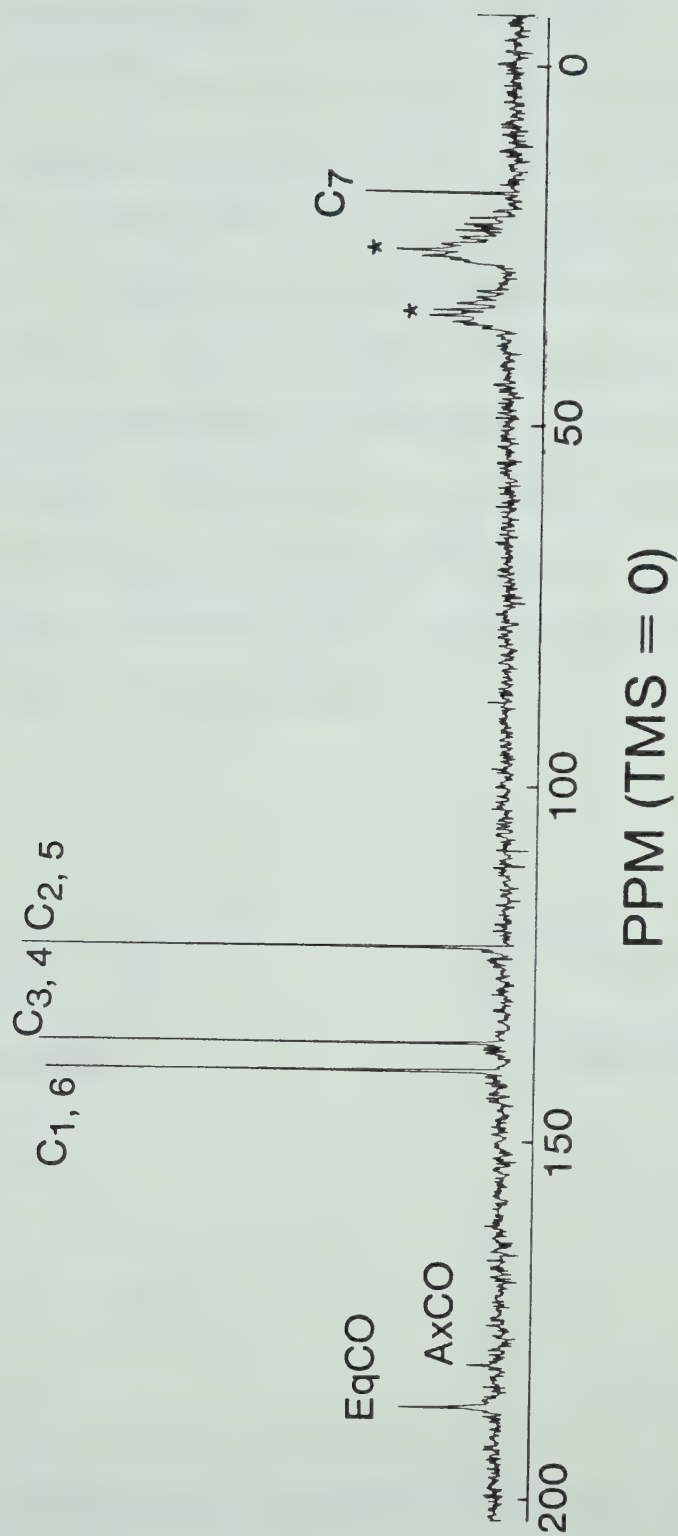
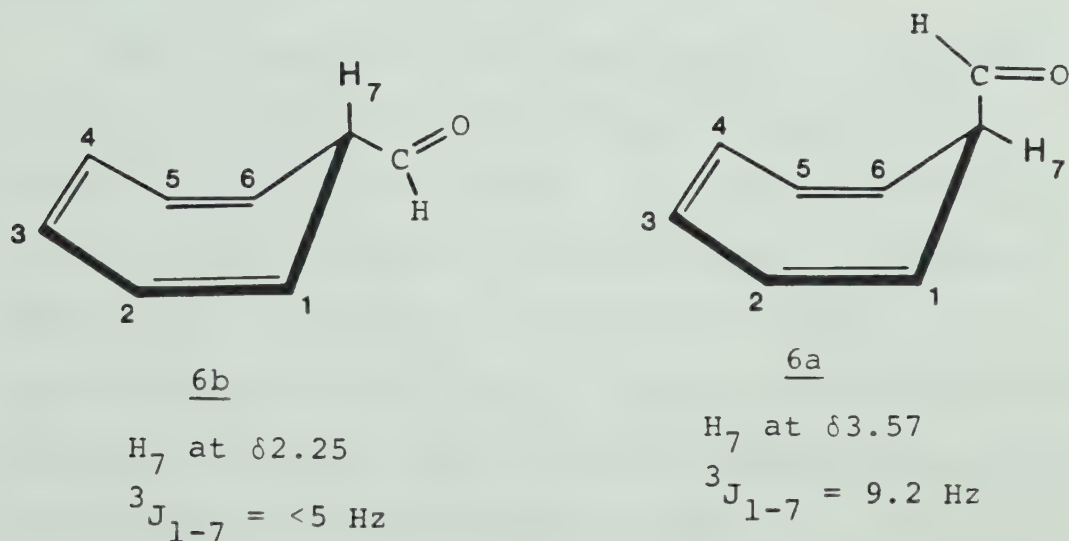


FIGURE IV. ^{13}C NMR spectrum of $(7-\eta^1\text{-C}_7\text{H}_7)\text{Re}(\text{CO})_5$, methylcyclohexane- d_{14} (* = solvent resonances).

In cycloheptatriene itself,^{50,51} and in 7-substituted derivatives,^{52,53} there is a rapid equilibrium between conformers analogous to 6a and 6b. This process can be slowed down (on the NMR time scale) at low temperatures (ca. -100°C). The H₇ resonances of the two conformers typically exhibit chemical shift differences of 1 ppm or more and also substantial differences in ³J₁₋₇. An example of these differences is provided by the recent study of Gunther et al. on C₇H₇-C(=O)H (6).⁵⁴ At -152°C in CD₂Cl₂/vinyl chloride (1:2), conformers 6a and 6b could be clearly distinguished.



These results for the vicinal coupling constants are in accord with predictions based on the Karplus curve.⁵⁵ The vicinal angle between H₇ and H₁₍₆₎ in 5b is ca. 120°,

so a vicinal coupling constant of about 4 Hz would be expected, while 5a should give a coupling constant of approximately 8 Hz.

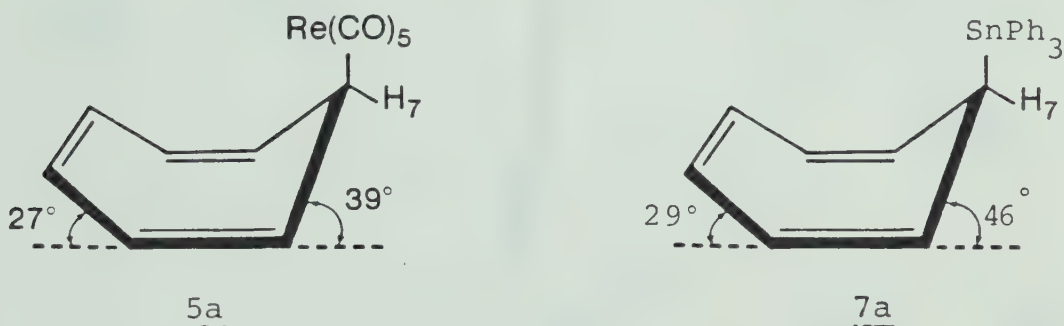
Since the vicinal coupling constant in 5 is 8.7 Hz, we tentatively conclude that 5a is the predominant form in solution. In order to investigate the 5a \rightleftharpoons 5b interconversion, a low temperature NMR study was carried out. A sample of 5 was dissolved in CFHCl₂/CD₂Cl₂ (4:1) and the 100 MHz ¹H NMR spectrum was examined at various temperatures down to -150°C. There is some line broadening and loss of resolution at this temperature, but the chemical shift and vicinal coupling constant are unchanged. No new signals are observed.

These results confirm that 5a is the predominant conformer in solution. The amount of 5b present is below ¹H NMR detection limits. These conclusions are based on the reasonable assumptions that the chemical shifts of H₇ in 5a and 5b would be different and that the activation energy for 5a \rightleftharpoons 5b interconversion is not substantially lower than that observed in other 7-substituted cycloheptatriene derivatives.

A similar vicinal coupling constant (³J₁₋₇ = 8.0 Hz) had been reported for Ph₃Sn(7-η¹-C₇H₇), (7),⁵⁶ implying a similar solution structure for the two compounds. It has also been established by crystallography that the

solid state structure of the tin compound is the conformer analogous to 5a.⁵⁷ In order to elucidate structural features of a transition metal monohapto compound, a determination of the structure of 5 was carried out by the crystallographic staff of Molecular Structure Corporation, College Station, Texas. Details of the data collection and refinement procedure as well as tables of structural parameters, bond lengths and bond angles will be found in the experimental section.

The crystal structure (see Figure V) establishes that the solid state structure of 5 is conformer 5a.



This is very similar to the reported structure for $\text{Ph}_3\text{Sn}(7\text{-}\eta^1\text{-C}_7\text{H}_7)$, 7a.⁵⁷ The length of the Re-C_7 bond is $2.348(11) \text{ \AA}$. This value is the same, within experimental error, as the Re-CH_3 bond in $(\eta^5\text{-C}_5\text{H}_5)\text{Re(CO)}_2\text{Br(CH}_3)$, $2.32(4) \text{ \AA}$,⁵⁸ and somewhat longer than the mean Re-CH_3 distance of 2.24 \AA in $(\eta^5\text{-C}_5\text{H}_5)(\eta^4\text{-C}_5\text{H}_5\text{CH}_3)\text{Re(CH}_3)_2$.⁵⁹ A Re-CH_3 distance of $2.308 \pm .017 \text{ \AA}$ in $\text{CH}_3\text{-Re(CO)}_5$ has been determined by

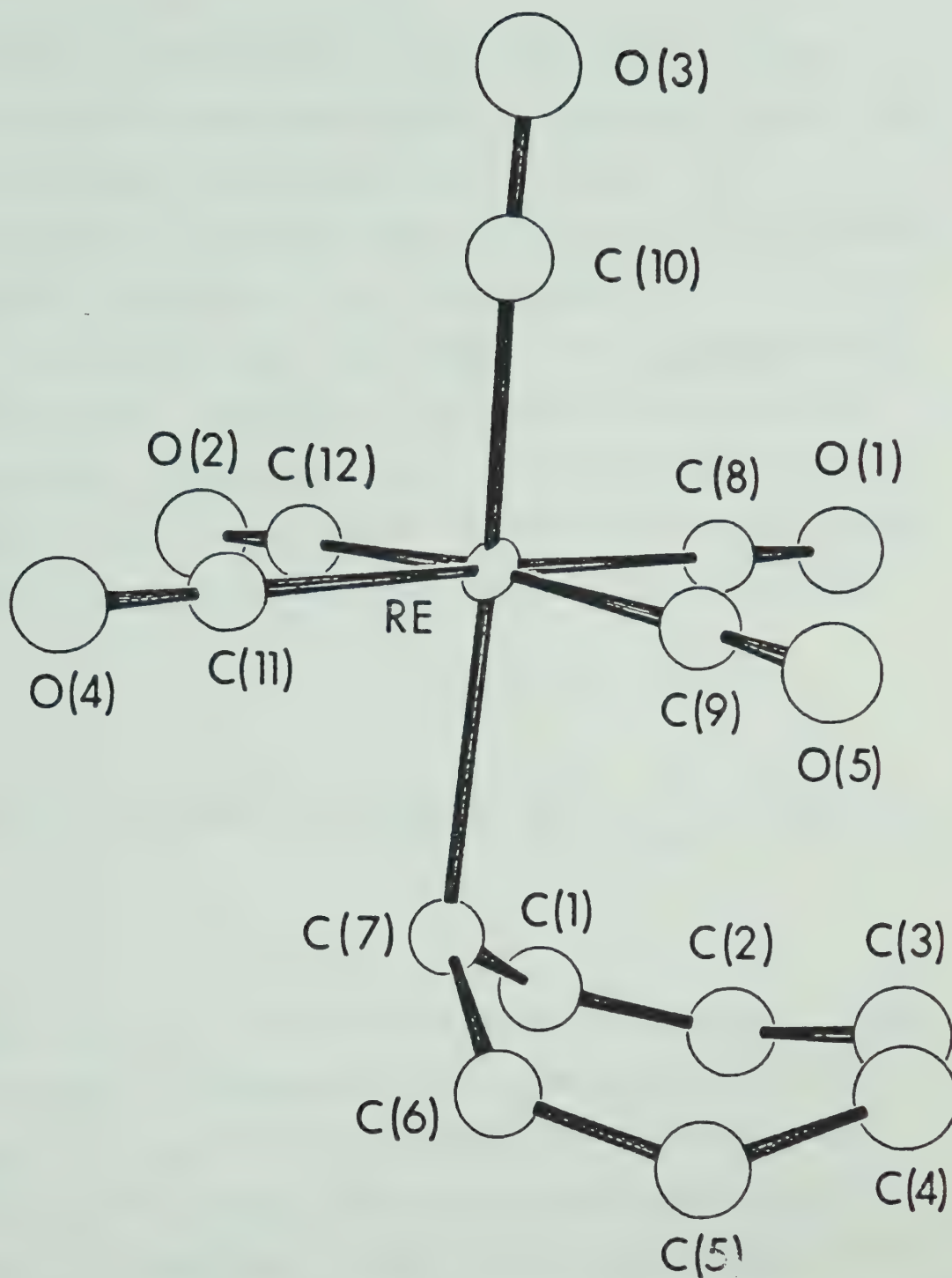
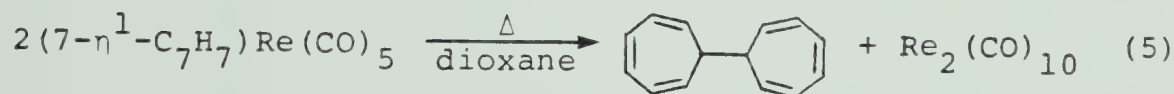


FIGURE V. The molecular structure of $(7-\eta^1-C_7H_7)Re(CO)_5$. Thermal ellipsoids are drawn at the 50% level.

electron diffraction.⁶⁰ To our knowledge no X-ray structure has been reported for a compound in which the $\text{Re}(\text{CO})_5$ group is bonded to an sp^3 carbon atom. A comparison of the solid state structures of 5 and another $\text{R-Re}(\text{CO})_5$ derivative would be interesting.

Since 5 is the first example of a monohaptocycloheptatrienyl compound of a transition metal, we were interested in making a quantitative measurement of the stability of this compound. Thermal decomposition of 5 gives $\text{Re}_2(\text{CO})_{10}$ and ditropyl (eq. 5) in a first order



reaction. Quantitative results were obtained by ^1H NMR monitoring in dioxane- d_8 (see Experimental section for details). Activation parameters calculated from an Eyring plot of data from three temperatures are $\Delta H^\ddagger = 30.4 \pm 0.3 \text{ kcal mol}^{-1}$; $\Delta S^\ddagger = 13 \pm 1 \text{ eu.}$; $\Delta G_{300}^\ddagger = 26.5 \pm 0.5 \text{ kcal mol}^{-1}$ (error limits correspond to one standard deviation).

As noted above, we had estimated a value for homolytic dissociation of the Re-C σ bond in 5 of about 27 kcal mol^{-1} , which is in good agreement with the observed activation

energy. As discussed in Chapter VII, this estimate of the M-C σ bond strength in 5 is important in establishing that the fluxional behaviour of this molecule does not arise from a dissociative process.

Section IV. Decarbonylation Reactions of $(\eta^1\text{-C}_7\text{H}_7)\text{Re}(\text{CO})_5$

The possibility of preparing rhenium analogs of $(\eta^3\text{-C}_7\text{H}_7)\text{Mn}(\text{CO})_4$ and $(\eta^5\text{-C}_7\text{H}_7)\text{Mn}(\text{CO})_3$ led us to consider decarbonylation reactions of 5. An obvious method to achieve this would be by further irradiation of 5, similar to the procedure employed for the manganese system. However, this approach might have yielded mixtures of various decarbonylation products requiring chromatographic separation, so an alternative method was sought.

The use of trimethylamine-N-oxide (Me_3NO) for decarbonylation of metal carbonyls is a well established reaction. This reaction is frequently used as an alternative to thermal or photochemical methods for replacing a metal bound CO with a ligand L ($\text{L} = \text{PR}_3, \text{P}(\text{OR})_3, \text{AsR}_3$, etc.). Advantages of this method are that milder conditions are required compared to thermal reactions, and that undesirable side reactions caused by photolysis are eliminated. For example, substituted group VI carbonyls $\text{L}_2\text{M}(\text{CO})_4$ and $\text{L}_3\text{M}(\text{CO})_3$ have been prepared using mild conditions.⁶¹

The remarkable acceleration of substitution by Me_3NO as compared to purely thermal reactions is demonstrated by the substitution of $\text{Ph-Mn}(\text{CO})_5$ by PPh_3 , (eq. 6)



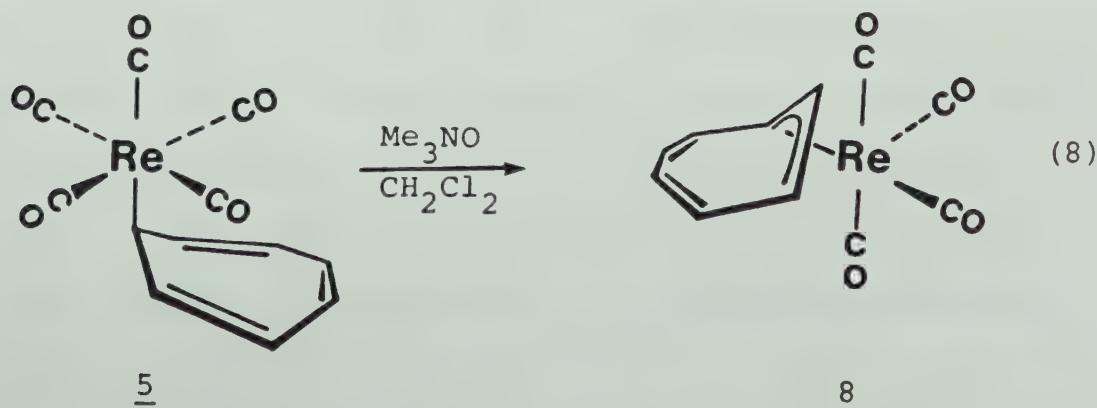
which gives a 64% yield after three days.⁶² Recent investigations by Brown and coworkers⁶³ have shown that this reaction is greatly accelerated in the presence of one equivalent of Me_3NO (88% isolated yield).

The mechanism of the promotion of CO loss is not entirely understood, but the reaction of Fe(CO)_5 with Me_3NO in the absence of added ligand has been shown to give a trimethylamine complex of iron (eq. 7), with



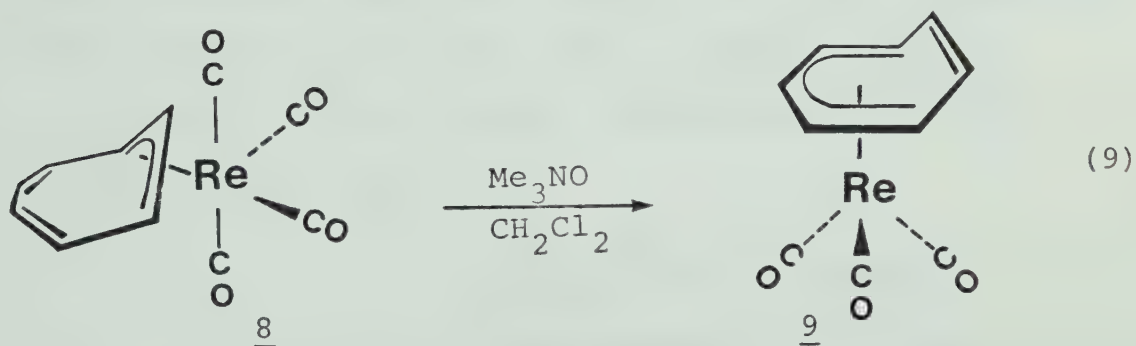
evolution of CO_2 .⁶⁴ These results suggest that the reaction proceeds via nucleophilic attack at carbonyl carbon, loss of CO_2 and subsequent complexation by Me_3N .

When 5 reacts with one equivalent of Me_3NO in CH_2Cl_2 , there is an immediate colour change from orange to deep wine red. $(\eta^3\text{-C}_7\text{H}_7)\text{Re(CO)}_4$ (8) can be isolated in 77% yield (eq. 8).



The infrared spectrum of 8 shows four ν_{CO} absorptions at 2089, 2006, 1980 and 1963 cm^{-1} (cyclohexane). This is very similar to the infrared spectrum reported for $(\eta^3\text{-C}_3\text{H}_5)\text{Re}(\text{CO})_4$: 2094, 1994, 1980, 1959 cm^{-1} (melt),⁴⁶ as well as that of $(\eta^3\text{-C}_7\text{H}_7)\text{Mn}(\text{CO})_4$ (see Figure II). The mass spectrum shows the molecular ion as well as successive loss of four CO's. ^1H and ^{13}C NMR studies have confirmed that the cycloheptatriene ring is bound to the metal in a trihapto fashion and that the compound exhibits fluxional behaviour via 1,2 shifts of the metal moiety around the ring. Detailed consideration of these NMR results will be found in Chapter VIII.

Further decarbonylation of (8) is readily effected, again using Me_3NO (eq. 9). In this reaction, the red

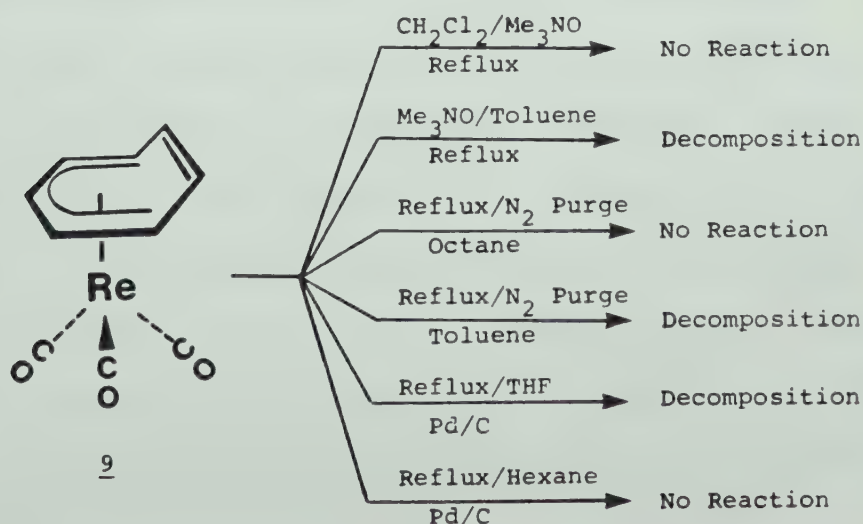


colour of (8) is replaced by the pale yellow colour of $(\eta^5\text{-C}_7\text{H}_7)\text{Re}(\text{CO})_3$ (9), initially identified by its infrared spectrum, which consists of three intense bands in the ν_{CO} region at 2034, 1963 and 1939 cm^{-1} (cylcohexane), a very similar spectrum to that observed for $(\eta^5\text{-C}_7\text{H}_7)\text{Mn}(\text{CO})_3$ (see Section II). Other spectroscopic

and analytical results are consistent with the formulation of 9 as a pentahapto cycloheptatrienyl complex. Once again, ^1H and ^{13}C NMR spectra show that the compound is fluxional, with the $\text{Re}(\text{CO})_3$ group migrating around the ring via 1,2 shifts. There is also a second fluxional process which scrambles the metal carbonyls. A detailed analysis of these processes is found in Chapter VIII.

As noted previously, Me_3NO promoted decarbonylation reactions are believed to proceed through an intermediate Me_3N complex. In our application of this method, the "ligand" which replaces CO is formally a double bond of a triene system which is already attached to the metal. Infrared monitoring of the reaction solutions gave no evidence for detectable concentrations of an intermediate. In these reactions, CO_2 loss could be followed immediately by coordination of two more carbon atoms of the ring.

Attempts to effect further decarbonylation of 9 initially were not successful.



The failure of 9 to decarbonylate in the presence of Me_3NO is perhaps not surprising in view of the requirement for nucleophilic attack on the coordinated CO group. The infrared spectrum of 9 shows that the carbonyl groups have lower ν_{CO} frequencies than in the tetracarbonyl compound 8 and thus have less positive charge at carbon. By comparison, $\text{CpMo}(\text{CO})_3\text{I}$ (ν_{CO} 2046, 1989, 1968 cm^{-1}) reacts rapidly with Me_3NO , but $\text{CpMo}(\text{CO})_3\text{-CH}_3$ (ν_{CO} 2018, 1950, 1946 cm^{-1}) does not react under the same conditions.⁶³ The infrared ν_{CO} frequencies of 9 fall between these two molybdenum compounds. Lower ν_{CO} frequencies indicate greater back bonding from the metal center into the $\text{CO}\pi^*$ orbitals and thus correlate with the observation of reduced susceptibility of the carbonyl carbon to attack by nucleophiles. Similar correlations have been observed for nucleophilic attack on coordinated carbonyl groups by organolithium compounds.⁶⁵

When decarbonylation of 9 using ultraviolet light (Hanovia 140 W lamp, quartz vessel) was attempted, no reaction was observed after 24 h. However, 9 was consumed when a more intense light source (450 W medium pressure Hg discharge) in an immersion well reactor cooled to -50°C was employed. Chromatographic work-up allowed isolation of a bright red crystalline material in ca. 1% yield (see Experimental section for details).

This product is soluble in CH_2Cl_2 or THF, but essentially insoluble in hydrocarbons. The ^1H NMR spectrum (CD_2Cl_2) at room temperature shows only one sharp singlet at δ 3.76 ppm ($\nu_{1/2} = 0.8$ Hz). The mass spectrum (see Figure VI) shows a molecular ion envelope at m/e 664-670 which matches the isotope pattern calculated for $\text{C}_{18}\text{H}_{14}\text{Re}_2\text{O}_4$. This cluster of ions corresponds to two $(\text{C}_7\text{H}_7)\text{Re}(\text{CO})_2$ units. Peaks corresponding to successive loss of four CO groups are also observed, as well as a peak at m/e 334 which has an isotope pattern consistent with $\text{C}_9\text{H}_7\text{ReO}_2$. These observations indicate that the product is best formulated as $[(\text{C}_7\text{H}_7)\text{Re}(\text{CO})_2]_2$ (10).

Structural possibilities for such a formulation are limited. One possibility is a dimer with a $\text{Re}=\text{Re}$ double bond. The very sharp single line observed in the



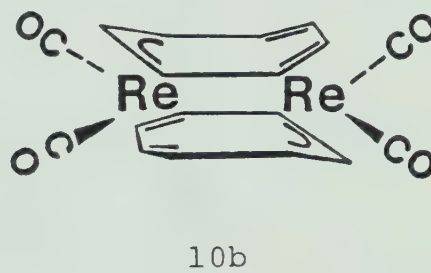
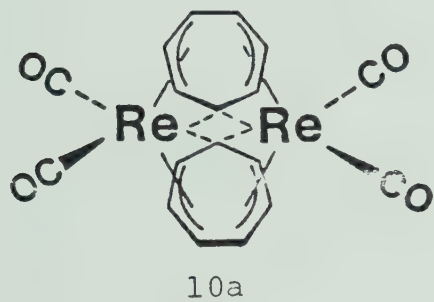
^1H NMR spectrum of 10 at room temperature is not consistent with this formulation. Pentahaptocycloheptatrienyl compounds are fluxional, but the barriers to metal migration observed are too high to give such a sharp line at ambient temperature (see Chapter VIII).

If $(\text{C}_7\text{H}_7)\text{Re}(\text{CO})_2$ satisfies the effective atomic number rule, other structural possibilities for a dimeric species require bridging ligands. The infrared spectrum



FIGURE VI. Mass spectrum of 10 (145°C, 70 eV).

of 10 (see Figure VII) consists of three ν_{CO} bands: 1981, 1951 and 1890 cm^{-1} (CH_2Cl_2 solution). The lowest frequency band is broad and slightly asymmetric, indicating the possibility of two absorptions which are incompletely resolved. Since there are no infrared bands due to bridging carbonyl groups, the bridging ligands must be cycloheptatrienyl groups. Two structural possibilities are:



Both of these structures have C_{2h} symmetry. Only two infrared active ν_{CO} bands would be expected for 10a or 10b. A possible explanation for the additional band(s) observed is that exact C_{2h} symmetry is not maintained in solution.

The bridging cycloheptatrienyl group is well documented in the literature. An example of a bonding mode analogous to 10b is provided by $\text{Fe}(\text{CO})_3(\text{C}_7\text{H}_7)\text{Rh}(\text{CO})_2$. The solid state structure⁶⁶ of this compound can be represented schematically:

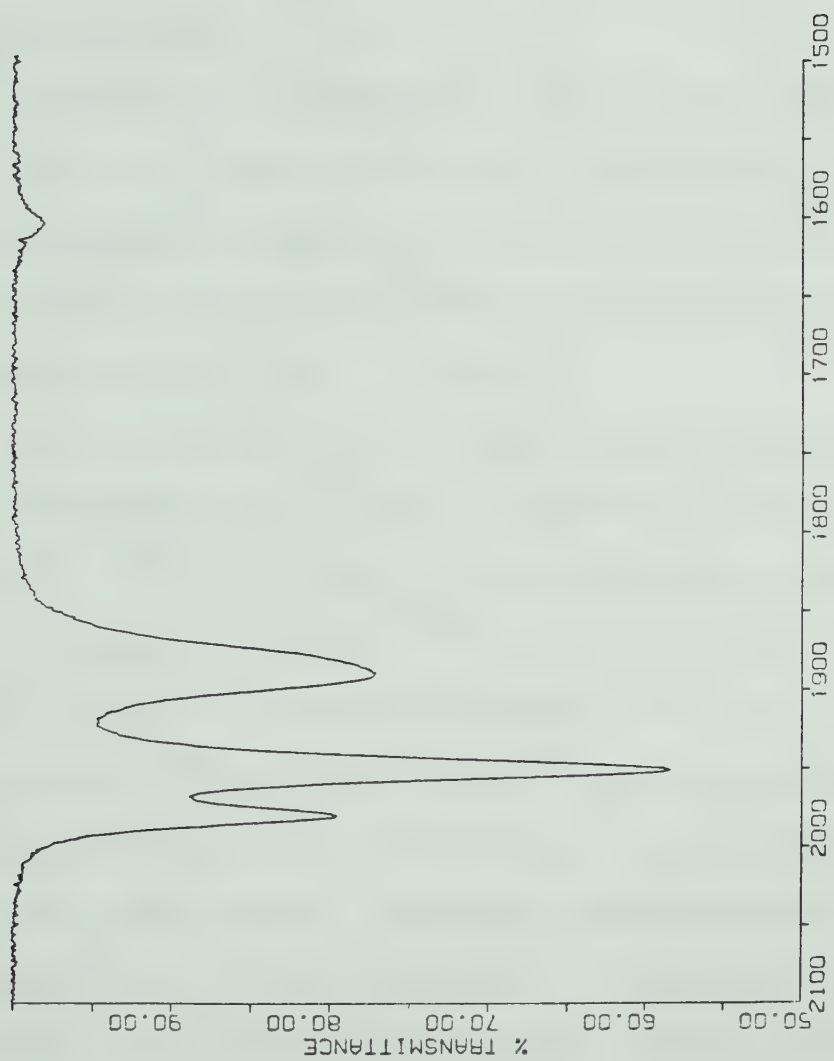
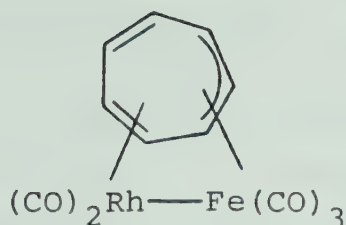


FIGURE VII. Infrared spectrum of 10, CH_2Cl_2 .

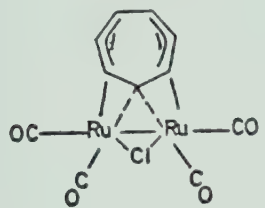
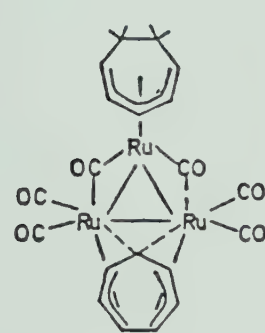


The ^1H NMR spectrum of this compounds shows a single line down to -160°C .

A geometry analogous to 10a has been demonstrated in the solid state for $\text{Ru}_3(\text{CO})_6(\text{C}_7\text{H}_7)(\text{C}_7\text{H}_9)$, in which the cycloheptatrienyl ring is equally bonded to two ruthenium atoms. The ^1H NMR spectrum of this ring shows a sharp singlet even at -100°C .

It is interesting to compare the properties of 10 to known neutral $(\eta^7\text{-C}_7\text{H}_7)$ compounds of the transition metals. $(\eta^7\text{-C}_7\text{H}_7)\text{V}(\text{CO})_3$ is a diamagnetic monomer,²⁷ as is $(\eta^5\text{-C}_5\text{H}_5)\text{Cr}(\eta^7\text{-C}_7\text{H}_7)$.⁶⁸ A paramagnetic vanadium analog of this chromium compound, $(\eta^5\text{-C}_5\text{H}_5)\text{V}(\eta^7\text{-C}_7\text{H}_7)$ is also known.⁶⁹ The structure of this compound was confirmed by X-ray crystallography.⁷⁰ The ^1H NMR spectra of some mononuclear, dinuclear and trinuclear $(\eta^7\text{-C}_7\text{H}_7)$ complexes are listed in Table I. The large variation in δ values and solvents make these results difficult to interpret but in general the mononuclear compounds exhibit resonances for the cycloheptatrienyl groups at lower field than the bridging derivatives. $[(\eta^7\text{-C}_7\text{H}_7)\text{Re}(\text{CO})_2]_2$ is typical of the bridging compounds at $\delta = 3.76$ ppm.

TABLE I. ^1H NMR Data for Some (C_7H_7) Compounds.

Compound	$\delta_{\text{C}_7\text{H}_7}$ (solvent)	Reference	
$(\eta^5\text{-C}_5\text{H}_5)\text{Cr}(\eta^7\text{-C}_7\text{H}_7)$	4.92 (C_6D_6)	68	
$(\eta^7\text{-C}_7\text{H}_7)\text{V}(\text{CO})_3$	4.64 (toluene- d_8)	27	
	4.11 (solvent ?)	67	
	3.14 (solvent ?)	67	
$\text{Fe}(\text{CO})_3(\text{C}_7\text{H}_7)\text{Rh}(\text{CO})_2$	4.16	$\left. \begin{array}{l} \\ \\ \end{array} \right\} (\text{CFHCl}_2:\text{CD}_2\text{Cl}_2)$ 4:1	66
$\text{Fe}(\text{CO})_3(\text{C}_7\text{H}_7)\text{Mn}(\text{CO})_3$	4.05		66
$\text{Fe}(\text{CO})_3(\text{C}_7\text{H}_7)\text{Re}(\text{CO})_3$	4.22		66
$[(\eta^7\text{-C}_7\text{H}_7)\text{Re}(\text{CO})_2]_2$ (<u>10</u>)	3.76 (CD_2Cl_2)	This work	

The ^1H NMR spectrum of 10 is thus indicative of the dimeric structure, in accord with the infrared and mass spectral results. However, the ^1H NMR spectrum does not distinguish between 10a and 10b as possible structures. An X-ray crystallographic study of 10 is currently under way.

Section V. Experimental

Rhenium carbonyl and manganese carbonyl were purchased from Strem Chemicals, Inc. The $\text{Mn}_2(\text{CO})_{10}$ was purified by sublimation before use. Tropylium tetrafluoroborate and $\text{Me}_3\text{NO}\cdot\text{H}_2\text{O}$ were obtained from Aldrich Chemicals. Dehydration of the $\text{Me}_3\text{NO}\cdot\text{H}_2\text{O}$ was effected by azeotropic distillation from toluene. 7-Cycloheptatrienylacetyl chloride was prepared by the method of Dewar and Pettit.⁷¹ An improved preparation of the carboxylic acid precursor developed by Betz was employed.⁷²

General Techniques

All reactions and manipulations were carried out under an atmosphere of purified nitrogen. Commercial nitrogen was purified by passing through a heated column (110°C) of BASF Cu-based catalyst (R3-11) to remove oxygen and a column of Mallinkrodt Aquasorb (P_2O_5 on an inert support) to remove water.

Solvents were distilled under nitrogen immediately prior to use. Drying agents employed were: pentanes, hexanes and benzene (CaH_2); CH_2Cl_2 (P_2O_5); acetone (Drierite); THF (potassium/benzophenone). Ether (anhydrous) was used as received from Mallinckrodt Chemical Works. In the case of preparations involving metal carbonyl anions prepared from Na/K, the THF solvent was transferred

directly from the drying agent in vacuo by cooling the reaction flask with liquid nitrogen.

Infrared spectra were recorded using a Nicolet MX-1 FT IR Spectrometer in 0.5 mm or 0.1 mm NaCl cells unless otherwise noted. Mass spectra were measured using an Associated Electronics Industries M5-12 Mass Spectrometer coupled with a Nova-3 computer employing D5-50 software. All NMR spectra were recorded using Bruker HFX-90, WP-200 or WH-400 FT NMR instruments. Details of operating parameters, temperature calibration and other experimental conditions used in obtaining NMR spectra are given in Chapters VII and VIII.

Melting points were determined using a Kofler hot stage microscope. Microanalyses were performed by the microanalytical laboratory of this department.

Preparation of $\text{C}_7\text{H}_7-\overset{\text{O}}{\underset{\parallel}{\text{C}}}-\text{Mn}(\text{CO})_5$ (1).

The procedure of Whitesides and Budnik³⁵ was followed, with slight modification. $\text{Mn}_2(\text{CO})_{10}$ (2.1 g, 5.4 mmol) was dissolved in 100 mL THF and stirred with excess 1% Na/Hg (20 mmol Na). After 2 h, excess amalgam was removed and the solution was filtered. 1.7 g (11 mmol, 1.3 mL) of $\text{C}_7\text{H}_7-\overset{\text{O}}{\underset{\parallel}{\text{C}}}-\text{Cl}$ ⁷¹ was added dropwise over one minute (the density of $\text{C}_7\text{H}_7-\overset{\text{O}}{\underset{\parallel}{\text{C}}}-\text{Cl}$ was determined as 1.32 g/mL). After one hour stirring, the solution was filtered to remove

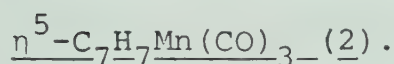
a pale yellow precipitate. The solution was taken to dryness on the Rotovap to give a red-orange crystalline residue. This residue was extracted with 10 x 25 mL of hexane. The combined extracts were filtered and cooled to -78°C to afford 1 as pale yellow needles, mp 84°C (darkens) lit. mp 83°C (dec).³⁵ Yield: 1.90 g, 56%. ^1H NMR in C_6D_6 identical with reported spectrum. For details of infrared spectrum, see discussion.

Photochemical decarbonylation of 1.

Compound 1, (990 mg, 3.15 mmol) was dissolved in 60 mL of N_2 saturated acetone and placed in an immersion well photochemical reactor. The lamp jacket was cooled with 50:50 ethylene glycol/water coolant recirculated and cooled to -25°C using a NESLAB RTE-8 refrigerated circulating bath. The entire apparatus was immersed in a dry ice-acetone bath maintained at -78°C . The temperature of the solution was ca. -50°C . A continuous N_2 purge was maintained throughout.

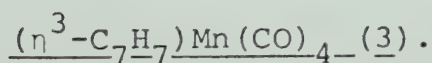
Infrared monitoring during photolysis indicated a rapid decrease in the intensity of the band at 2005 cm^{-1} due to the starting acyl. The photolysis was terminated after 19 minutes. The acetone was removed on the Rotovap to give a red oil. The oil was extracted with benzene and applied to a 5 cm x 10 cm column of silica gel

(Fisher Scientific Co., 28-200 mesh, grade 12). Elution with heptane gave a single orange band. The heptane solution was concentrated to ca. 5 mL, then applied to a second column consisting of 150 g Fluka Kieselgel G (TLC grade) slurried with heptane and packed under 12 psi N₂ to give a bed 3.5 cm x 14 cm. Elution with heptane gave Mn₂(CO)₁₀ followed by (η³-C₇H₇)Mn(CO)₄, and finally (η⁵-C₇H₇)Mn(CO)₃. Separation was complete.



The third fraction from the chromatography column was evaporated to give a bright yellow crystalline residue. Recrystallization from hexane afforded 2 as yellow needles (lit.:³⁵ orange) mp 64°C (lit.³⁵ mp 64°C) yield: 103 mg (14%). IR: (hexane, ν_{CO}, cm⁻¹) 2026s, 1964s, 1941s (lit. IR: (CS₂) 2025, 1951, 1930). ¹H NMR: (acetone-d₆, -50°C, 60 MHz, δ) 7.15 (t, 1H, H₃; J_{H₃-H₂} = 7.5 Hz), 5.40 (t, 2H, H_{2,4}), 4.70 (m, 2H, H_{6,7}), 3.53 (m, 2H, H_{1,5}).

Anal. Calcd for C₁₀H₇MnO₃: C, 52.20; H, 3.07. Found: C, 51.69; H, 3.14. λ_{max} (EtOH) 374 (ε 3450), 311 nm (ε 10350) Lit.³⁵: λ_{max} (EtOH) 307 (ε 4500), 262 nm (ε 10400).



The red band (second to elute, after Mn₂(CO)₁₀) was collected and evaporated to dryness to give a red

crystalline residue (150 mg) which was recrystallized from 15 mL hexane by cooling to -78°C . This procedure gave a mixture of red and white crystals. The ^1H NMR spectrum of a white crystal identified this material as ditropyl, which has identical solubility properties to 3. A second, slow recrystallization afforded 3 as deep red needles and ditropyl as large colourless plates. These were physically separated and the red material recrystallized once more to give pure 3 (60 mg, 7%) mp 66°C (gas evolved) IR (hexane, ν_{CO} , cm^{-1}) 2063m, 2001s, 1970s, 1960s (see Figure II). Mass spectrum: (14 eV, 80°C) M^+ , $\text{M}^+ - n \text{CO}$ ($n = 2-4$).

Anal. Calcd for $\text{C}_{11}\text{H}_7\text{MnO}_4$: C, 51.19; H, 2.74. Found: C, 51.09; H, 2.92. ^1H NMR (-90°C , $\text{THF}-d_8$, 400 MHz, δ) 3.48 (t, 1H, H_2 , $J_{1-2} = 7.2 \text{ Hz}$), 4.67 (m, 2H, $\text{H}_{1,3}$), 5.21 (m, 2H, $\text{H}_{5,6}$), 5.93 (m, 2H, $\text{H}_{4,7}$). λ_{max} (EtOH) 388 (ϵ 5150), 312 nm (ϵ 38700).

Preparation of $\text{C}_7\text{H}_7-\overset{\text{O}}{\underset{\parallel}{\text{C}}}-\text{Re}(\text{CO})_5$ (4).

A solution of $\text{C}_7\text{H}_7-\overset{\text{O}}{\underset{\parallel}{\text{C}}}-\text{Cl}$ (2.04 g, 13.2 mmol) in 15 mL THF was added at room temperature over 30 min to a solution of $\text{NaRe}(\text{CO})_5$ prepared from 4.32 g (6.6 mmol) $\text{Re}_2(\text{CO})_{10}$ by reaction with Na/Hg in 100 mL THF. After 30 min stirring, the volume of THF was reduced under vacuum to 20 mL; the solution was diluted with 200 mL

water and extracted with 5 x 30 mL hexane. The extracts were dried, filtered and cooled to -10°C . Further cooling to -78°C completed the crystallization, affording 4 as pale yellow crystals mp 98°C (4.1 g, 70%). IR (cyclohexane, cm^{-1} , ν_{CO} with intensity and assignment in C_{4v} symmetry) 2132 (w, A_1), 2061 (w, B_1), 2023 (s, E), 2014 (s, E), 199 (s, A_1), 1637, 1626 (w, acyl CO). ^1H NMR (methylcyclohexane- d_{14} , δ) 6.51 (m, 2H, $\text{H}_{3,4}$), 6.18 (m, 2H, $\text{H}_{2,5}$), 5.12 (m, 2H, $\text{H}_{1,6}$), 2.50 (t, H_7 , $^3\text{J}_{17} = 5.8$ Hz). ^{13}C NMR: (CDCl_3 , 25°C , δ) 71.6 (C_7), 109.4 ($\text{C}_{1,6}$), 125.8 ($\text{C}_{2,5}$), 129.5 ($\text{C}_{3,4}$), 181.0 (axial CO), 183.1 (equatorial CO), 243.7 (acyl CO).

Anal. Calcd for $\text{C}_{13}\text{H}_7\text{O}_6\text{Re}$: C, 35.04; H, 1.57. Found: C, 35.08; H, 1.70. Mass spectrum: (14 eV, 50°C). M^+ , $\text{M}^+ - n \text{ CO}$, $n = 1-4$. $\text{Re}(\text{CO})_6^+$ (base peak).

Preparation of $(7-\eta^1\text{-C}_7\text{H}_7)\text{Re}(\text{CO})_5$ (5).

Method (a). A sample of 4, (890 mg, 2 mmol) in 40 mL dry, oxygen-free acetone was placed in a quartz flask which was partly immersed in a dry ice/acetone bath and irradiated for 12 h using a Hanovia 140 W lamp. Acetone was removed in vacuum and the orange residue extracted with 4 x 15 mL hexane. Cooling to -78°C gave 5 contaminated slightly with 4. Two recrystallizations from hexane afforded pure 5 as orange needles mp 74°C (500 mg, 60%).

IR (cyclohexane, cm^{-1} , ν_{CO} with intensity and assignment in C_{4v} symmetry): 2120 (w, A_1), 2015 (s, E), 1983 (m, A_1). ^1H NMR (20°C , dioxane- d_8 , δ) 5.92 (m, 2H, $\text{H}_{3,4}$), 5.44 (m, 2H, $\text{H}_{1,6}$), 5.16 (m, 2H, $\text{H}_{2,5}$), 3.16 (tt, 1H, $^3J_{1-7} = 8.5$ Hz, $^4J_{17} = 1.0$ Hz). In methylcyclohexane- d_{14} : 5.96 (m, 2H, $\text{H}_{3,6}$), 5.44 (m, 2H, $\text{H}_{1,6}$), 5.24 (m, 2H, $\text{H}_{2,5}$), 3.16 (tt, 1H, H_7 , $^3J_{1-7} = 8.7$ Hz, $^4J_{2-7} = 1.0$ Hz). ^{13}C NMR (10°C , THF- d_8 , δ) 18.1 (C_7), 122.1 ($\text{C}_{2,5}$), 136.1 ($\text{C}_{3,4}$), 141.3 ($\text{C}_{1,6}$); 182.0 (axial CO), 187.3 (equatorial CO). In methylcyclohexane- d_{14} : 17.7 (C_7), 122.1 ($\text{C}_{2,5}$), 135.7 ($\text{C}_{3,4}$), 140.1 ($\text{C}_{1,6}$); 183.7 (axial CO), 186.4 (equatorial CO). UV-VIS (dioxane, λ_{max} , nm, ϵ): 278 (5200), 394 (2500).

Anal. Calcd for $\text{C}_{12}\text{H}_7\text{O}_5\text{Re}$: C, 34.52; H, 1.69. Found: C, 34.54; H, 1.78. Mass spectrum (16 eV, 35°C): M^+ , $\text{M}^+ - n \text{ CO}$ ($n = 2-5$); $\text{M}^+ - \text{C}_7\text{H}_7$, C_7H_7^+ (base peak).

Method (b). $\text{NaRe}(\text{CO})_5$ (10 mmol) in 100 mL THF was cooled to -78°C (a white precipitate formed) and solid $\text{C}_7\text{H}_7\text{BF}_4$ (1.78 g, 10 mmol) was added in one portion. The mixture was stirred at -78°C for 1 h, THF was removed under vacuum and the residue extracted with 3 x 20 mL hexane. Filtration and cooling of the hexane solution to -78°C affords 5 (3.8 g, 90%) identical to that of method (a).

Thermal decomposition of 5.

Samples of 5 (0.20 M) in dioxane- d_8 were freeze-thaw degassed in vacuum in NMR tubes which were then sealed off. ^1H NMR was used to monitor the first order disappearance of 5 at three temperatures: T, K: 54.3°C, $2.60 \times 10^{-5} \text{ sec}^{-1}$; 68.4°C, $2.00 \times 10^{-4} \text{ sec}^{-1}$; 83.4°C, $1.33 \times 10^{-3} \text{ sec}^{-1}$. Calculated activation parameters (error limits correspond to one standard deviation): $\Delta H^\ddagger = 30.4 \pm 0.3 \text{ kcal mol}^{-1}$; $\Delta S^\ddagger = 13 \pm 1 \text{ e.u.}$; $\Delta G_{300}^\ddagger = 26.5 \pm 0.5 \text{ kcal mol}^{-1}$. The major products of the thermal decomposition were $(\text{C}_7\text{H}_7)_2$ and $\text{Re}_2(\text{CO})_{10}$ with small amounts (1-5%) of C_7H_8 .

X-ray structure of 5.

The X-ray structure determination was performed by the crystallographic staff of Molecular Structure Corporation, College Station, Texas. All calculations were performed on a linked PDP-11/45-11/60 computation system using the Enraf-Nonius structure determination package⁷³ and private programs of Molecular Structure Corp.

A red prismatic crystal with dimensions ca. 0.12 x 0.12 x 0.10 mm was used for data collection. (Crystals were grown by slow sublimation in a sealed tube in a temperature gradient provided by the glowbar of a Perkin-Elmer 337 infrared spectrometer.) Details

of data collection are listed in Table I.

The structure was solved using the Patterson heavy-atom method which revealed the position of the Re atom. The remaining atoms were located in succeeding difference Fourier syntheses. Hydrogen atoms were not included in the calculations. The structure was refined in full-matrix least-squares where the function minimized was $\sum w(|F_o| - |F_c|)^2$ and the weight w is defined as $4F_o^2/\sigma^2(F_o^2)$. Only the 1487 reflections with $F_o > 3.0 \sigma(F_o)$ were used in refinement. The final cycle of refinement included 78 variable parameters and converged with $R_1 = \sum(|F_o| - |F_c|)/\sum|F_o| = 0.038$ and $R_2 = [\sum w(|F_o| - |F_c|)^2/\sum w|F_o|^2]^{1/2} = 0.049$. The highest peak in the final difference Fourier had a height of 0.52 e/\AA^3 . The structure of 5 is depicted in Figure I. Relevant bond lengths and bond angles are tabulated in Tables II and III. Positional and thermal parameters are listed in Table IV.

Preparation of $(\eta^3\text{-C}_7\text{H}_7)\text{Re(CO)}_4\text{-(8)}$.

210 mg (0.5 mmol) of 5 was dissolved in 20 mL CH_2Cl_2 . 38 mg (0.5 mmol) of Me_3NO was added. After 10 min stirring at room temperature, the CH_2Cl_2 was pumped off and the residue extracted with 3 x 10 mL of hexane. The solution was filtered and cooled to -10°C for 16 h. Cooling to

TABLE II. Crystal Data for $(7-\eta^1-C_7H_7)Re(CO)_5$

A. Cell Parameters at 23°C.^a

crystal system:	monoclinic	$a = 6.962(2) \text{ \AA}$
space group:	P_{2_1}/c	$b = 22.099(3) \text{ \AA}$
z	$z = 4$	$c = 8.955(1) \text{ \AA}$
fw	$fw = 417.39$	$\beta = 109.91(2)^\circ$
ρ (calcd)	$\rho (\text{calcd}) = 2.14 \text{ g/cm}^3$	$V = 1295.4 \text{ \AA}^3$

B. Collection of Intensity Data.

diffractometer: Enraf-Nonius CAD 4
 radiation: MoK_α ($\lambda = 0.71073 \text{ \AA}$)
 monochromator: graphite crystal, incident beam
 scan type: $\omega - \theta$
 scan rate: $2 - 20^\circ/\text{min}$ (in ω)
 scan width: $0.6 + 0.350 \tan \theta^\circ$
 max 2θ : 49.0°
 reflections collected: 2299 total, 2144 unique
 stds: 3 every 41 min, no measurable decay
 Absn. coeff: $\mu = 99.2 \text{ cm}^{-1}$
 corrections: Lorentz-polarization
 Empirical absorption^b

^aBased on 25 reflections in the range $6^\circ < \theta < 14^\circ$.

^bRelative transmission coefficients ranged from 0.89 to 1.00 with an average value of 0.95.

TABLE III. Bond Lengths (\AA).^a

Re -C(8)	1.980(12)	O(4)-C(11)	1.143(12)
Re -C(12)	1.959(12)	O(5)-C(9)	1.132(12)
Re -C(10)	1.919(13)	C(7)-C(6)	1.462(15)
Re -C(11)	1.966(11)	C(7)-C(1)	1.48(2)
Re -C(9)	1.981(11)	C(6)-C(5)	1.32(2)
Re -C(7)	2.348(11)	C(5)-C(4)	1.47(2)
O(1)-C(8)	1.129(12)	C(4)-C(3)	1.37(2)
O(2)-C(12)	1.156(13)	C(3)-C(2)	1.46(2)
O(3)-C(10)	1.171(14)	C(2)-C(1)	1.35(2)

^aNumbers in parentheses are estimated standard deviations in the least significant digits.

TABLE IV. Bond Angles (Degrees).^a

C(8) -Re-C(12)	88.8(5)	Re-C(8) -O(1)	179.(1)
C(8) -Re-C(10)	89.1(5)	Re-C(12) -O(2)	177.(1)
C(8) -Re-C(11)	178.4(4)	Re-C(10) -O(3)	178.(1)
C(8) -Re-C(9)	92.7(5)	Re-C(11) -O(4)	178.(1)
C(8) -Re-C(7)	92.3(4)	Re-C(9) -O(5)	178.(1)
C(12) -Re-C(10)	92.1(5)	Re-C(7) -C(6)	113.3(8)
C(12) -Re-C(11)	90.2(5)	Re-C(7) -C(1)	113.5(8)
C(12) -Re-C(9)	175.4(5)	C(6) -C(7) -C(1)	114.(1)
C(12) -Re-C(7)	84.6(4)	C(7) -C(6) -C(5)	127.(1)
C(10) -Re-C(11)	92.3(5)	C(6) -C(5) -C(4)	126.(1)
C(10) -Re-C(9)	92.2(5)	C(5) -C(4) -C(3)	124.(1)
C(10) -Re-C(7)	176.5(5)	C(4) -C(3) -C(2)	127.(2)
C(11) -Re-C(9)	88.2(4)	C(3) -C(2) -C(1)	124.(1)
C(11) -Re-C(7)	86.4(4)	C(7) -C(1) -C(2)	127.(1)
C(9) -Re-C(7)	91.0(4)		

^aNumbers in parentheses are estimated standard deviations in the least significant digits.

TABLE V. Positional and Thermal Parameters. a,b

Atom	\underline{x}	\underline{y}	\underline{z}	$\underline{\beta_{11}}$	$\underline{\beta_{22}}$	$\underline{\beta_{33}}$	$\underline{\beta_{12}}$	$\underline{\beta_{13}}$	$\underline{\beta_{23}}$
Re	0.20668(7)	0.09601(2)	0.28865(5)	0.02284(9)	0.00173(1)	0.01210(5)	0.00020(7)	0.0138(1)	0.00032(5)

Atom	\underline{x}	\underline{y}	\underline{z}	$\underline{B(A)}$	Atom	\underline{x}	\underline{y}	\underline{z}	$\underline{B(A)}$
O(1)	0.538(1)	0.0411(5)	0.167(1)	6.6(2)	C(9)	-0.017(2)	0.0710(6)	0.094(1)	4.3(2)
O(2)	0.549(2)	0.1482(5)	0.583(1)	7.4(3)	C(7)	0.227(2)	0.1908(6)	0.177(1)	4.3(3)
O(3)	0.189(2)	-0.0261(5)	0.452(1)	7.8(3)	C(6)	0.042(2)	0.2070(6)	0.046(1)	5.1(3)
O(4)	-0.125(1)	0.1532(4)	0.406(1)	5.5(2)	C(5)	-0.009(2)	0.1897(7)	-0.103(2)	6.0(3)
O(5)	-0.147(1)	0.0584(4)	-0.018(1)	5.8(2)	C(4)	0.109(3)	0.1494(8)	-0.169(2)	7.5(4)
C(8)	0.419(2)	0.0613(6)	0.213(1)	4.4(2)	C(3)	0.318(2)	0.1454(8)	-0.114(2)	7.7(4)
C(12)	0.424(2)	0.1274(6)	0.475(1)	4.7(3)	C(2)	0.459(2)	0.1806(8)	0.014(2)	6.8(4)
C(10)	0.197(2)	0.0207(7)	0.393(2)	5.4(3)	C(1)	0.418(2)	0.2000(7)	0.143(2)	6.0(3)
C(11)	-0.001(2)	0.1327(5)	0.364(1)	4.0(2)					

^aThe form of the anisotropic thermal parameter is

$$\exp[-(\beta_{11}^*h^2 + \beta_{22}^*k^2 + \beta_{33}^*l^2 + \beta_{12}^*hk + \beta_{13}^*hl + \beta_{23}^*kl)].$$

^bEstimated standard deviations in the least significant digits are shown in parentheses.

-78°C completed crystallization of (8) as deep red needles mp 84°C. Yield: 150 mg (77%) IR (cyclohexane, ν_{CO} , cm^{-1}) 2089 (m), 2006 (s), 1980 (s), 1963 (s). Mass spectrum: M^+ , $\text{M}^+ - n \text{CO}$ ($n = 1-3$).

Anal. Calcd for $\text{C}_{11}\text{H}_7\text{O}_4\text{Re}$: C, 33.91; H, 1.81. Found: C, 33.84; H, 1.86. ^1H NMR: (-70°C, methylcyclohexane- d_{14} , 200 MHz, δ) 2.90 (t, 1H, H_2 , $J_{1-2} = 7.4$ Hz), 4.10 (t, 2H, $\text{H}_{1,3}$), 4.50 (m, 2H, $\text{H}_{5,6}$), 5.27 (m, 2H, $\text{H}_{4,7}$) ^{13}C NMR (-40°C, methylcyclohexane- d_{14} , 50.3 MHz, δ) 55.8 (1C, C_2) 67.0 (2C, $\text{C}_{1,3}$), 120.1 (2C, $\text{C}_{5,6}$), 132.9 (2C, $\text{C}_{4,7}$), 190.0 (1C), 193.5 (1C) (axial carbonyls), 199.0 (2C) (equatorial carbonyls).

Preparation of $(\eta^5\text{-C}_7\text{H}_7)\text{Re}(\text{CO})_3$ (9).

390 mg (1 mmol) of (8) was dissolved in 30 mL CH_2Cl_2 . Me_3NO (80 mg, 1.07 mmol) was added. After two h stirring at room temperature, the CH_2Cl_2 was removed under vacuum and the residue extracted with 3 x 20 mL of hexane. The solution was filtered and cooled to -78°C for 16 h to yield 9 as bright yellow needles, mp 88°C. Yield: 264 mg, 73%. IR (cyclohexane, ν_{CO} , cm^{-1}) 2034, 1963, 1939. Mass spectrum: M^+ , $\text{M}^+ - \text{CO}$, $\text{M}^+ - 2\text{CO}$.

Anal. Calcd for $\text{C}_{10}\text{H}_7\text{O}_5\text{Re}$: C, 33.24; H, 1.95. Found: C, 33.38; H, 1.97. ^1H NMR: (-20°C, acetone- d_6 , 60 MHz δ) 3.90 (m, 2H, $\text{H}_{1,5}$), 5.00 (m, 2H, $\text{H}_{6,7}$), 5.86 (dd, 2H, $\text{H}_{2,4}$), 7.12 (tt, 1H, H_3). ^{13}C NMR (-90°C, acetone- d_6 ,

22.6 MHz, δ) 71.1 (2C, C_{1,5}), 93.6 (1C, C₃), 107.5 (2C, C_{2,4}), 130.0 (2C, C_{6,7}). Metal carbonyls: 191.2 (2C), 202.6 (1C).

Photolysis of (η^5 -C₇H₇)Re(CO)₃:

140 mg (0.39 mmol) of (η^5 -C₇H₇)Re(CO)₃ was dissolved in 225 mL of heptane in an immersion well photolysis reactor with N₂ purge. The lamp jacket was cooled to -25°C with continuously pumped glycol/H₂O coolant. The entire reactor was immersed in a dry ice-acetone bath (-78°C) in a large Dewar. The highest solution temperature during photolysis was -50°C. After 20 min photolysis a brown precipitate forms. Photolysis was terminated after 2.5 h, with about 50% of the starting material unreacted. The solution was filtered, concentrated to ca. 10 mL and applied to a 2 cm x 10 cm column of silica gel (Kieselgel G, Fluka AG, slurried in heptane and packed under 15 psi N₂). Elution with 200 mL heptane under pressure eluted all unreacted starting material. A very slow moving bright yellow-orange band had moved ca. 0.2 cm from the origin at this point. A further 2000 mL of heptane eluted this band ca. 4 cm. Elution was completed with 500 mL CH₂Cl₂/heptane (20:80). Evaporation of the solvents gave a red crystalline residue (3 mg). The product was soluble in CH₂Cl₂,

insoluble in hydrocarbons and could be recrystallized from CH_2Cl_2 /heptane. IR (CH_2Cl_2 , ν_{CO} , cm^{-1}) 1981 m, 1951 s, 1890 m (broad). ^1H NMR (CD_2Cl_2 , 25°C , 400 MHz): one sharp singlet at δ 3.76. Mass spectrum: (145°C , 70 eV) M^+ at m/e 664-670 matches isotope pattern calculated for $\text{C}_{18}\text{H}_{14}\text{Re}_2\text{O}_4$; $\text{M}^+ - n \text{ CO}$ ($n = 1-4$); m/e 334, m/e 306, m/e 91 (C_7H_7^+). The product is formulated as $[(\eta^7\text{-C}_7\text{H}_7)\text{Re}(\text{CO})_2]_2$ (see Discussion). Insufficient material was available for elemental analysis.

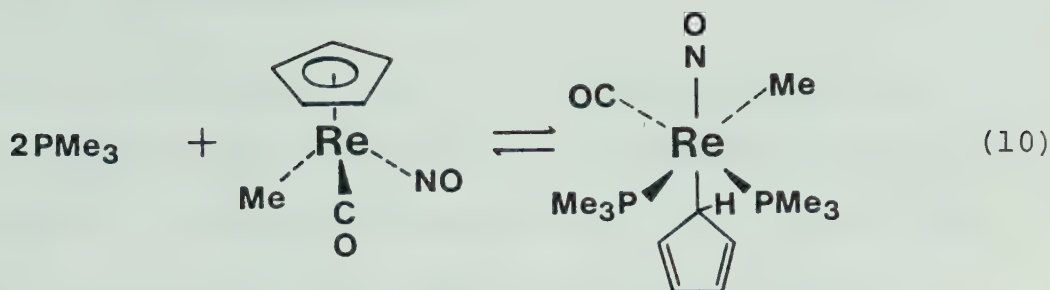
CHAPTER THREE

PHOSPHINE ADDITION REACTIONS

Section I. Introduction

The use of phosphines as ligands is widespread in transition metal organometallic chemistry. In metal carbonyls and their derivatives, replacement of CO by a phosphine often raises the melting point and increases the thermal stability of a compound. An example of this effect is the marked difference in stability between Me-Co(CO)_4 (decomp. at -35°C)⁷⁴ and $\text{Me-Co(CO)}_3(\text{PPh}_3)$ (decomp. at 20°C).⁷⁵

Triphenylphosphine is most commonly employed, probably due to convenience of handling compared to trialkylphosphines which are air sensitive liquids. Relatively few reports have appeared involving the use of PMe_3 , probably due to difficulties in handling this rather volatile, air sensitive liquid. Recently several reports of the use of PMe_3 as a ligand have appeared.⁷⁶ Particularly interesting is the work of C.P. Casey and W.D. Jones,⁷⁷ in which PMe_3 was found to reduce the hapticity of a cyclopentadienyl ligand from pentahapto to monohapto (eq. 10).

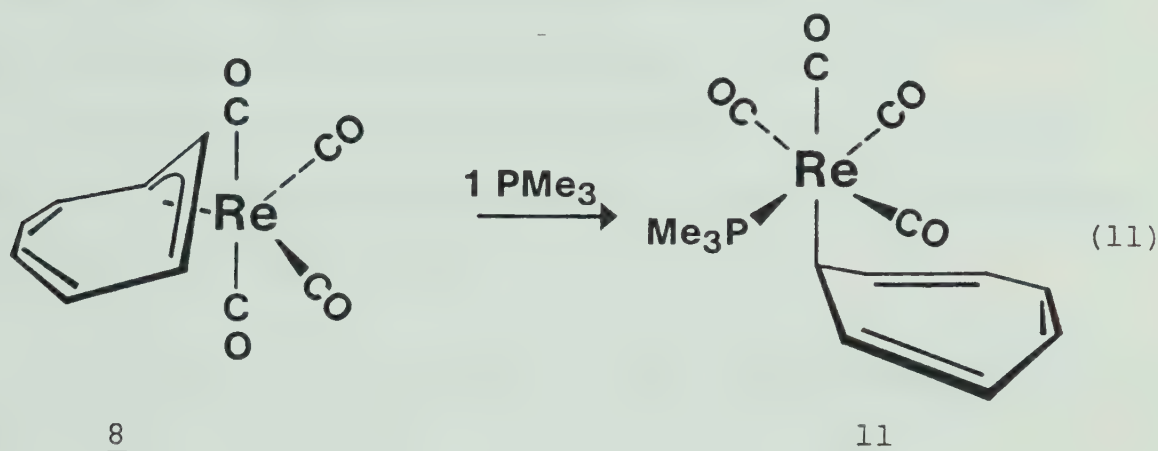


This reaction is associative (kinetic results show a linear dependence of rate on PMe_3 concentration) and reversible. Crystalline product was isolated from a reaction in hexane, from which the product crystallizes. The structure of the monohapto product was confirmed by X-ray crystallography.

This reaction is the first example of the conversion of a $(\eta^5\text{-C}_5\text{H}_5)$ ligand to a $(\eta^1\text{-C}_5\text{H}_5)$ ligand. Since trihapto and pentahapto derivatives of the cycloheptatrienyl ligand are relatively common and accessible, we sought to extend this hapticity reduction process to the synthesis of $(\eta^1\text{-C}_7\text{H}_7)$ compounds from the corresponding $(\eta^5\text{-C}_7\text{H}_7)$ and $(\eta^3\text{-C}_7\text{H}_7)$ complexes.

Section II. Rhenium Compounds

Since the stability of $(7-\eta^1\text{-C}_7\text{H}_7)\text{Re}(\text{CO})_5$ (5) has been established, and $(\eta^3\text{-C}_7\text{H}_7)\text{Re}(\text{CO})_4$ and $(\eta^5\text{-C}_7\text{H}_7)\text{Re}(\text{CO})_3$ are available via decarbonylation of 5, our initial goal was to prepare further monohapto alkyls of rhenium by phosphine addition reactions. The trihapto alkyl $(\eta^3\text{-C}_7\text{H}_7)\text{Re}(\text{CO})_4$, (8), was indeed found to react with one equivalent of PMe_3 to afford $(7-\eta^1\text{-C}_7\text{H}_7)\text{Re}(\text{CO})_4\text{PMe}_3$ (11) in 97% yield (eq. 11).



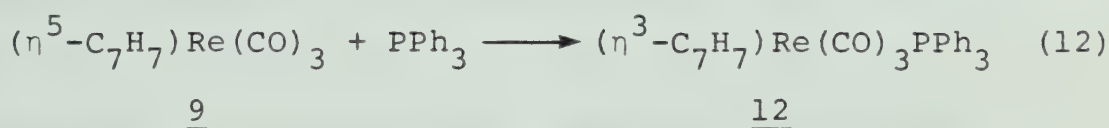
The ^1H NMR spectrum of 11 is consistent with the monohaptocycloheptatrienyl formulation. The resonance for H_7 is a quartet, due to equal coupling to $\text{H}_{1,6}$ and to P ($^3J_{1-7} = ^3J_{\text{H-P}} = 8.8$ Hz). As discussed in Chapter II, this value for the vicinal coupling constant indicates that the predominant conformation of 11 is the one shown in eq. 11.

The infrared spectrum, mass spectrum and elemental analysis are consistent with this formulation for 11.

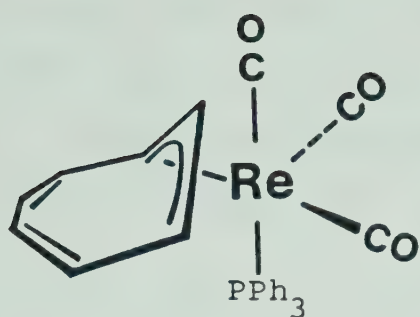
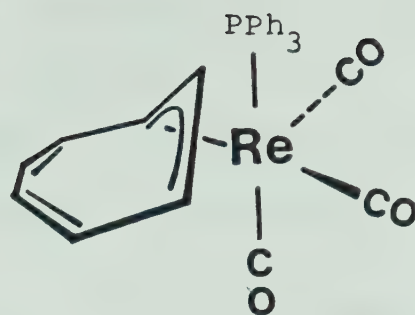
Solutions of 11 in cyclohexane-d₁₂ or benzene-d₆ show no detectable free PMe₃ after several days in solution, indicating that in the coordination of PMe₃ to this metal center, the equilibrium lies far to the side of complex formation.

The formation of 11 from 8 is accelerated when an excess of PMe₃ is employed. Although a quantitative kinetic study of this reaction has not been carried out, the reaction might reasonably be expected to be associative, as was observed by Casey and Jones in the reaction of PMe₃ with (η⁵-C₅H₅)Re(CO)(NO)CH₃⁷⁷ (eq. 10).

The reaction of (η⁵-C₇H₇)Re(CO)₃ with PPh₃ proceeds to give a trihaptocycloheptatrienyl compound incorporating one PPh₃ group (eq. 12).



Compound 12 has been fully characterized. The infrared spectrum in hexane solution shows three ν_{CO} bands of equal intensity at 2022, 1949 and 1914 cm⁻¹, consistent with expectations for the facial⁷⁸ isomer. The ¹H NMR spectrum (CD₂Cl₂, -70°C) is consistent with the trihapto-cycloheptatrienyl formulation. Two possible structures for 12 are shown as 12a and 12b. Since the PPh₃ group is quite sterically demanding,⁷⁹ structure 12a is probably preferred, since this would minimize interaction between

12a12b

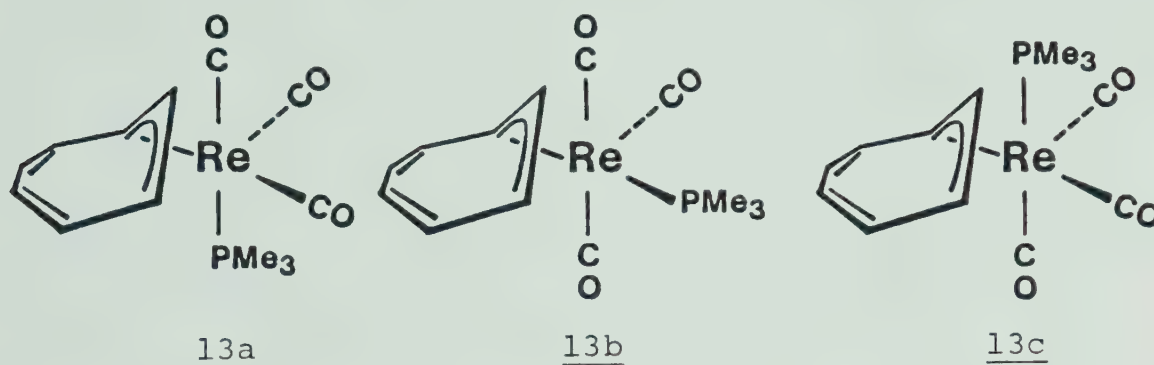
H_2 and the phosphine ligand. Attempts to grow crystals of crystallographic quality of 12 have so far not been successful.

The reactions of $(\eta^5\text{-C}_5\text{H}_5)\text{Re}(\text{CO})(\text{NO})\text{CH}_3$ with phosphines which were explored by Casey and Jones were limited to reactions with PMe_3 and dmpe . The more sterically demanding PBu_3 does not react under the same conditions. Although the reaction of PPh_3 was not investigated, it seems unlikely that PPh_3 would react with $(\eta^5\text{-C}_5\text{H}_5)\text{Re}(\text{CO})(\text{NO})\text{CH}_3$, since PPh_3 is even more sterically demanding than PBu_3 .⁷⁹ The formation of 12 demonstrates a considerable difference between $(\eta^5\text{-C}_5\text{H}_5)\text{Re}(\text{CO})(\text{NO})\text{CH}_3$ and 8 in reactivity toward phosphine substitution. No further reaction between 12 and excess PPh_3 could be detected.

When $(\eta^5\text{-C}_7\text{H}_7)\text{Re}(\text{CO})_3$ was combined with one equivalent of PMe_3 , a trihaptocycloheptatrienyl derivatives formulated as $(\eta^3\text{-C}_7\text{H}_7)\text{Re}(\text{CO})_3\text{PMe}_3$ (13) was formed. This formulation for 13 is consistent with the mass spectrum and the

elemental analysis. The infrared spectrum of 13 is quite complex, with six ν_{CO} bands (see Figure VIII).

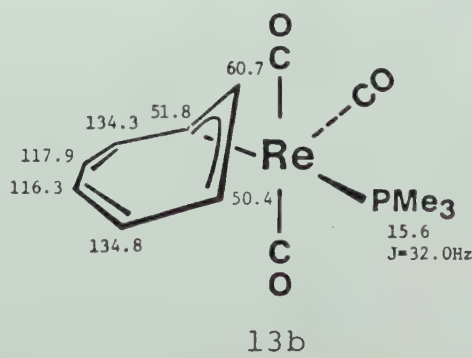
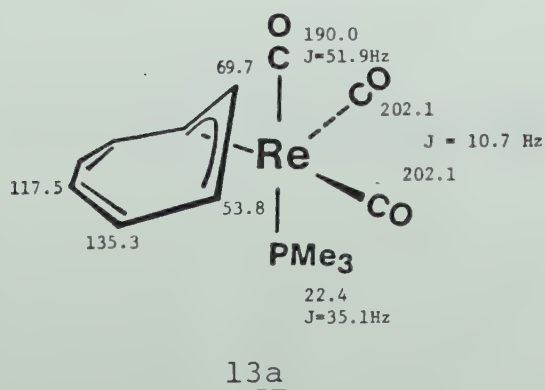
There are three possible geometric isomers of 13, as shown below. For the facial isomers 13a and 13c,



three ν_{CO} bands of equal intensity would be expected,⁷⁸ while meridional substitution as in 13b would give three ν_{CO} bands of unequal intensity.⁸⁰

The ^{13}C NMR spectrum indicates that two isomers are present in unequal amounts, with 13a the most likely formulation for the major isomer. The ^{13}C chemical shifts are listed below (chemical shifts are for a CD_2Cl_2 solution at -20°C , expressed in ppm, TMS = 0. J values refer to $J_{\text{C-P}}$).

$$3 \text{ CO's } \left\{ \begin{array}{l} 203.7 \text{ Low J} \\ 196.0 \text{ J}=11.3\text{Hz} \\ 191.4 \text{ J}=10.7\text{Hz} \end{array} \right. \text{ (1:1:1)}$$



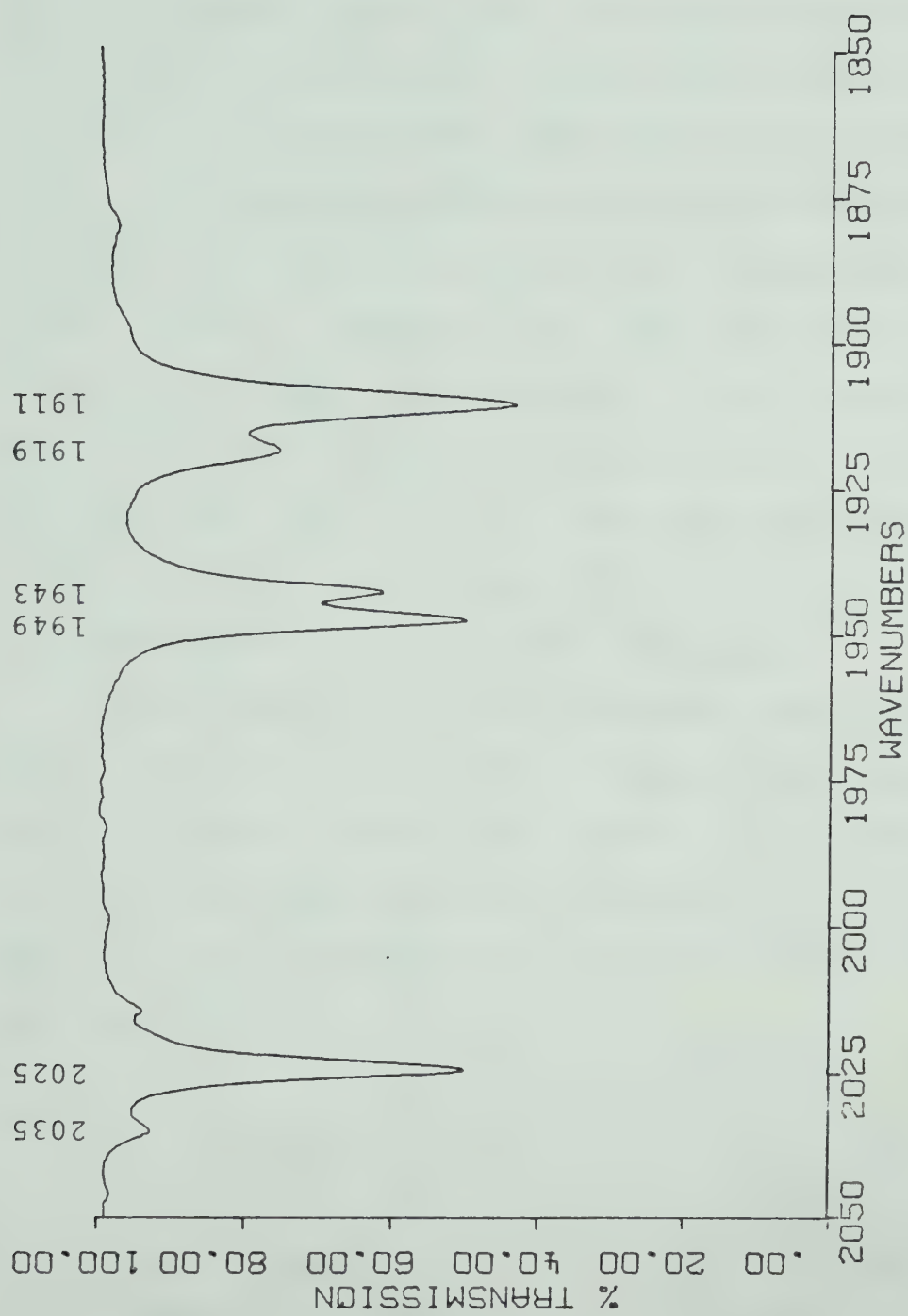
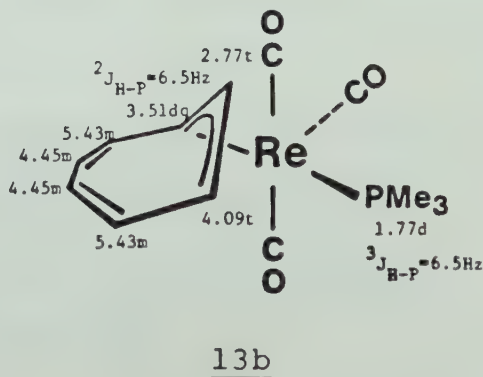
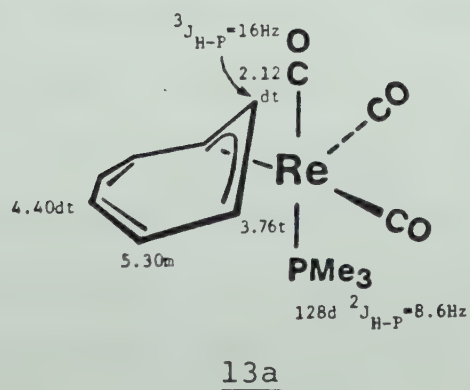


FIGURE VIII. Infrared spectrum of 13, hexane.

The observation of three carbonyl resonances in the ratio 1:1:1 is only consistent with 13b. A choice between 13a and 13c for the structure of the major isomer can be made by comparison to 12, where the more sterically demanding PPh_3 group makes 12a the most reasonable structure. The infrared spectrum of 13 can be resolved into the major and minor isomer components by assigning the three strong ν_{CO} bands at 2025, 1948 and 1911 cm^{-1} to the facial isomer 13a. This spectrum is very similar to that of 12 which shows 3 ν_{CO} bands of equal intensity at 2022, 1949 and 1914 cm^{-1} . The remaining three ν_{CO} bands in the spectrum of 13 (2035 w, 1943 s, 1919 m) are assigned to the meridional isomer 13b.

These observations are consistent with the observed ^1H NMR spectrum of 13, (-70°C , CD_2Cl_2) which shows two sets of signals for the two isomers. Integration of the PMe_3 signals gives a 13a:13b ratio of 88:12. The ^1H NMR data are summarized below (chemical shifts are in ppm from TMS = 0).

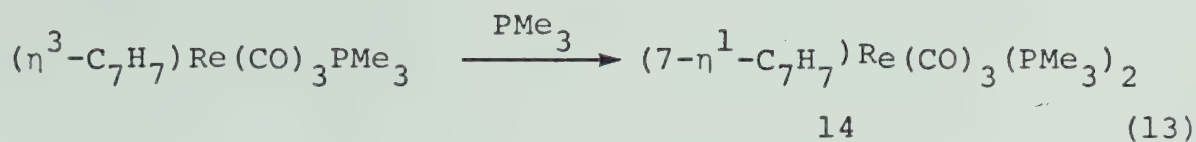


The ^1H NMR spectra of both isomers of 13 are very similar to that of $(\eta^3\text{-C}_7\text{H}_7)\text{Re}(\text{CO})_4$, with added complexity due to coupling to P. The spectrum of 13b should in principle show seven different signals for the cycloheptatrienyl group as was observed in the ^{13}C NMR spectrum. In fact, the chemical shift differences between the two sides of the ring were not fully resolved, and only five signals were observed. Some of the signals due to 13b may be obscured by the more intense signals due to 13a.

In the ^1H NMR spectra of both 12 and 13a, there is a large coupling between H_2 and P ($^3J_{\text{H-P}} = 16 \text{ Hz}$), but no observable coupling from P to $\text{H}_{1,3}$. If the proposed structures are correct, this large coupling is observed in the proton trans to the P ligand. In assigning the H_1 and H_3 signals of 13b, the signal at $\delta 3.51$ has $^3J_{\text{H-P}} = 6.5 \text{ Hz}$ and so is assigned to the proton trans to the PMe_3 group. The signal at $\delta 4.09$ does not show resolvable coupling to P, so it is assigned to the proton cis to the PMe_3 group.

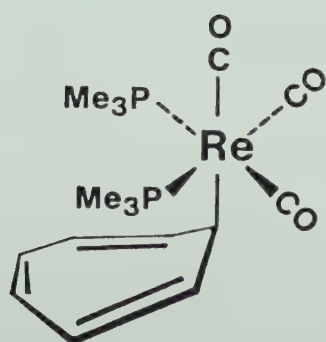
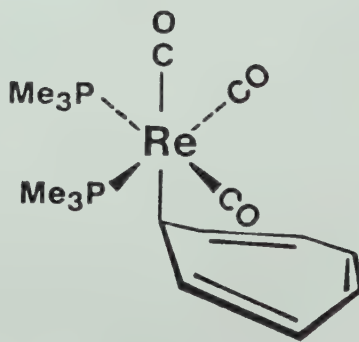
Both 12 and 13 show fluxional behaviour which has been investigated by ^1H NMR at various temperatures, as discussed in Chapter VIII.

In contrast to 12, which showed no reaction with a second equivalent of PPh_3 , compound 13 reacts readily with additional PMe_3 to give a disubstituted monohapto-cycloheptatrienyl compound, 14 (eq. 13).



Compound 14 can also be prepared by the reaction of $(\eta^5\text{-C}_7\text{H}_7)\text{Re}(\text{CO})_3$ with an excess of PMe_3 . The ^1H NMR spectrum of 14 is consistent with a monohapto formulation. This was confirmed by elemental analysis and mass spectroscopy. The infrared spectrum of 14 (cyclohexane solution) has three strong ν_{CO} bands at 2016, 1942 and 1893 cm^{-1} as well as two weaker bands at 2008 and 1925 cm^{-1} (see Figure IX).

The ^1H NMR spectrum of 14 shows only one set of resonances (in CD_2Cl_2 , benzene- d_6 or cyclohexane- d_{12}). The extra infrared bands are probably due to some isomerism in which isomer interconversion is rapid on the NMR time scale, but slow on the time scale of infrared spectroscopy. A tentative explanation for this could be the existence of rotomers about the Re-C_7 bond, as shown in 14a and 14b.

14a14b

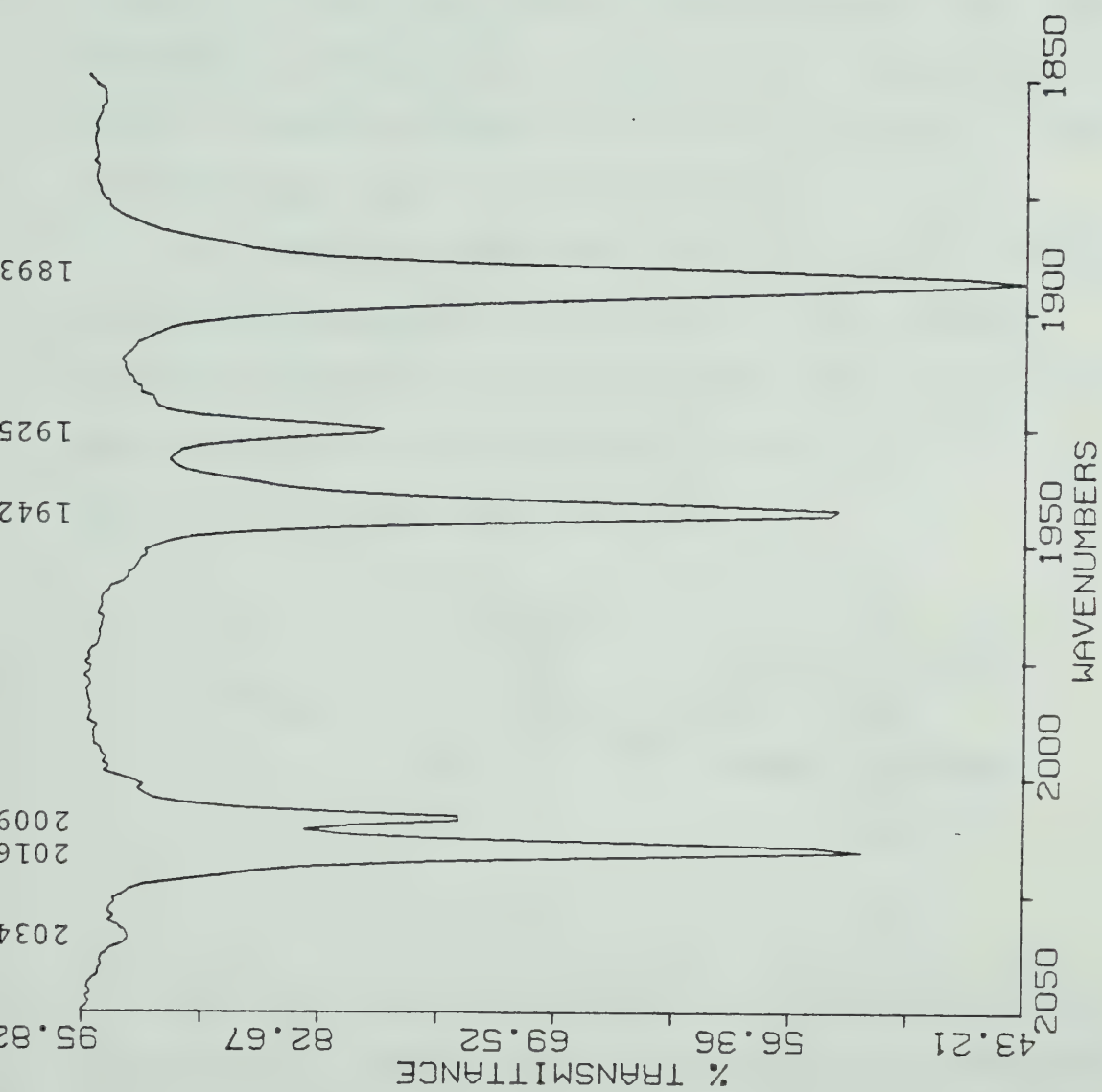
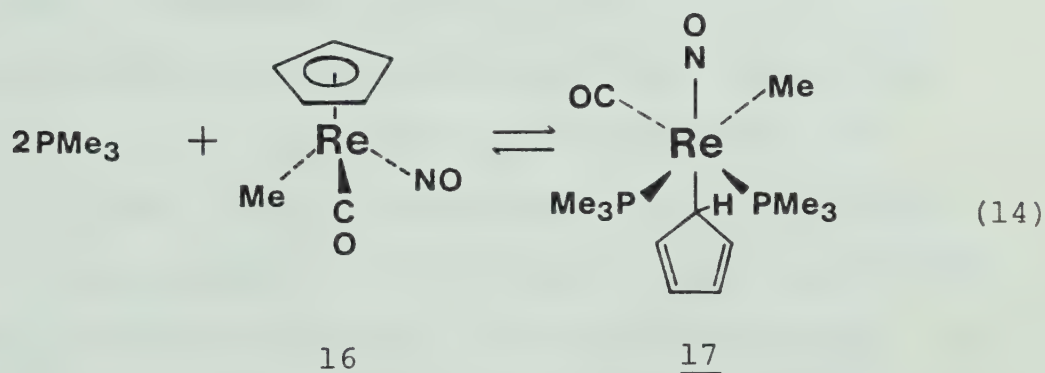


FIGURE IX. Infrared spectrum of $(7-\eta^1-\text{C}_7\text{H}_7)\text{Re}(\text{CO})_3(\text{PMe}_3)_2$, cyclohexane.

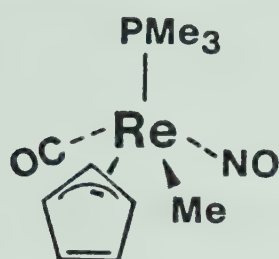
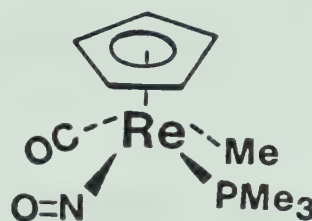
The reaction of $(\eta^5\text{-C}_7\text{H}_7)\text{Re}(\text{CO})_3$ with dmpe also affords a monohaptocycloheptatrienyl compound $(7\text{-}\eta^1\text{-C}_7\text{H}_7)\text{Re}(\text{CO})_3(\text{dmpe})$, (15). This compound has been fully characterized by mass spectroscopy, elemental analysis, ^1H NMR and infrared spectroscopy. The infrared spectrum is very similar to that of 14. The solubility of 15 in hexane and other hydrocarbon solvents is very limited, while 14 is slightly soluble.

The stepwise conversion of the pentahapto compound 8 to the monohapto 14 is analogous to the reaction reported by Casey and Jones in which $(\eta^5\text{-C}_5\text{H}_5)\text{Re}(\text{CO})(\text{NO})\text{CH}_3$ was converted by two equivalents of PMe_3 to $(\eta^1\text{-C}_5\text{H}_5)\text{Re}(\text{CO})(\text{NO})(\text{PMe}_3)_2\text{CH}_3$ (eq. 14)



This reaction was reversible and no intermediate monophosphine complex could be detected. In the formation of 14, (eq. 13), the equilibrium lies far to the right (no free PMe_3 was detected in solutions of 14) and the intermediate monosubstituted complex 13 is isolable. This is understandable since the trihapto coordination

mode of the cycloheptatrienyl group is quite stable. In the case of the cyclopentadienyl system, the presumed intermediate in the phosphine substitution reaction could be a compound containing a trihaptocyclopentadienyl group (16a) or a bent nitrosyl (16b). In either case, loss of PMe_3 to regenerate starting material or reaction with

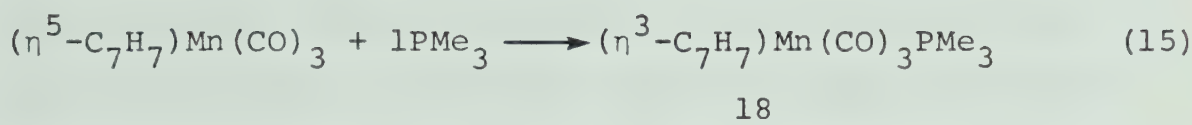
16a16b

further PMe_3 is apparently quite rapid.

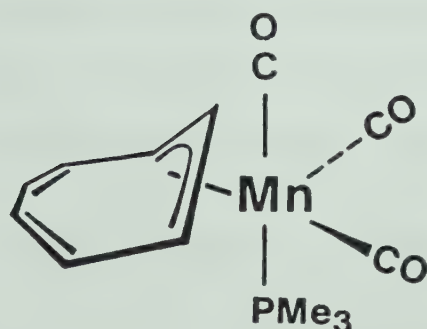
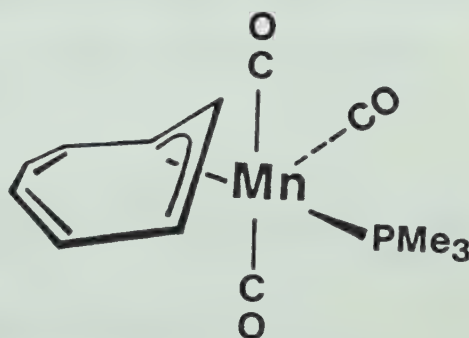
Two possible mechanisms for the first step in the conversion of 16 to 17 were suggested by Casey and Jones:⁷⁷ a) the $\eta^5\text{-C}_5\text{H}_5$ ligand could "slip" to form an η^1 or $\eta^3\text{-C}_5\text{H}_5$ species; b) the nitrosyl ligand could bend to change the electron count of the rhenium center. Our results are on a somewhat different system, but they clearly establish that a nitrosyl ligand is not a general requirement for these reactions to proceed.

Section III. Manganese Compounds

Since several new monohapto alkyls were obtained by phosphine addition reactions in rhenium systems, we next explored the extension of these reactions to manganese. Reaction of $(\eta^5\text{-C}_7\text{H}_7)\text{Mn}(\text{CO})_3$ with PMe_3 affords the trihaptocycloheptatrienyl complex 16 (eq. 15).



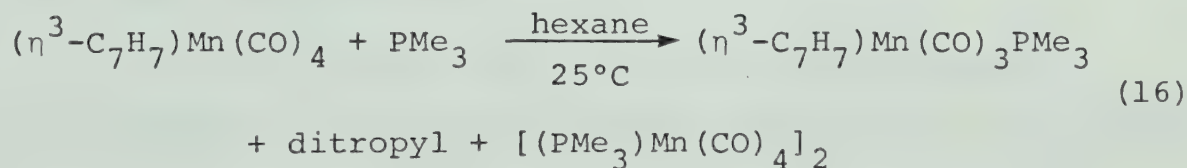
The infrared spectrum of 18 in cyclohexane solution shows ν_{CO} bands at 2006 s, 1944 s, 1937 m, 1918 w, 1901 s cm^{-1} . This is very similar to the spectrum observed for the rhenium analog 13, indicating the presence of facial and meridional isomers, shown below as 18a and 18b.

18a18b

The ^1H NMR spectrum (CD_2Cl_2 , -70°C) is consistent with 18a as the major isomer. The spectrum is very similar to that of 13a. Integration of the PMe_3 signals gives a ratio of 13a:13b of 100:1. Since the amount of

18b present is very small, the cycloheptatrienyl resonances for 18b were not detected. In the case of the rhenium analog 13, the 13a:13b ratio was 88:12. Another difference between 13 and 16 becomes apparent when the temperature of the solution is raised. The PMe_3 signals due to 18a and 18b broaden and coalesce at ca. -30°C , then sharpen again to give a single doublet at room temperature. These results indicate that the barrier for 18a \rightleftharpoons 18b interconversion is lower than that for 13a \rightleftharpoons 13b interconversion. Both 13 and 18 are fluxional, with the metal moiety migrating around the cycloheptatrienyl ring via 1,2 shifts. These results and the isomer interconversion process are examined in detail in Chapter VIII.

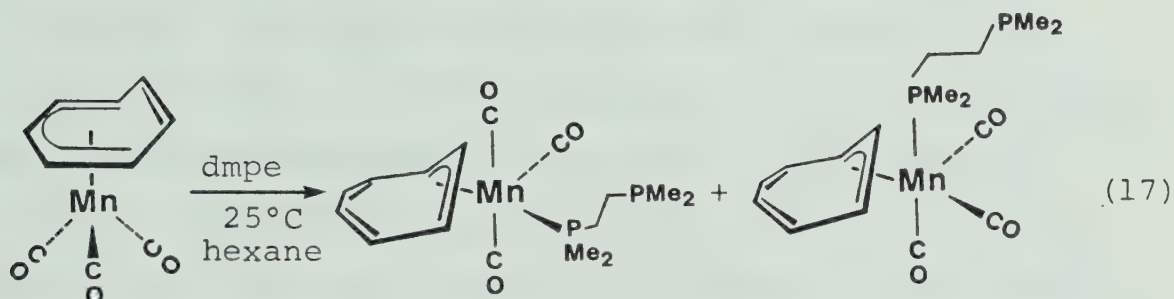
Having established that phosphine addition reactions will proceed in a manganese system, we next attempted to synthesize a manganese analog of 11 by the reaction of $(\eta^3\text{-C}_7\text{H}_7)\text{Mn}(\text{CO})_4$ with PMe_3 . The outcome of this reaction is shown in eq. 16.



As shown in eq. 16, this reaction does not follow the same course as with the rhenium analog. One of the products, $(\eta^3\text{-C}_7\text{H}_7)\text{Mn}(\text{CO})_3\text{PMe}_3$, demonstrates that PMe_3 displaces CO from the metal, which did not occur with

rhodium. The dimeric products $[(PMe_3)Mn(CO)_4]_2$ and ditropyl probably form via the homolytic cleavage of a weak Mn-C σ bond in an intermediate $(\eta^1-C_7H_7)Mn(CO)_4PMe_3$.

In hopes of spectroscopically identifying this intermediate, the reaction was carried out at low temperature in an NMR tube (CD_2Cl_2 , $-50^\circ C$ to $-10^\circ C$). The starting material was consumed to give only ditropyl and $[(PMe_3)Mn(CO)_4]_2$. A trace of $(\eta^3-C_7H_7)Mn(CO)_3PMe_3$ was also



observed. The CO displacement reaction is evidently reduced at lower temperatures.

The reaction of $(\eta^5-C_7H_7)Mn(CO)_3$ with dmpe was investigated in the hope that the presence of a chelating phosphine ligand would increase the stability of the product. When the reaction was carried out in hexane at room temperature, infrared spectroscopic evidence for a trihapto intermediate was obtained (eq. 17).

At room temperature, this intermediate quickly decomposed to give ditropyl (identified by NMR) and an insoluble precipitate.

When the reaction was repeated in an NMR tube (CD_2Cl_2 solvent) at low temperature (-50°C) the identity of the intermediate was confirmed by observation in the ^1H NMR spectrum of signals for a trihaptocycloheptatrienyl group, very similar to the ^1H NMR spectrum of 16. On increasing the temperature to -10°C , ditropyl was formed. There was no evidence for a monohaptocycloheptatrienyl species.

Our attempts to prepare monohapto alkyls of manganese have not been successful, in contrast to the rhenium analogs. This is probably due to the lower Mn-C σ bond strength for manganese compared to rhenium. When combined with the stabilization of the tropyli radical, the Mn-C σ bond strength is lowered to the point that homolytic bond cleavage to give ditropyl and metal dimers is very rapid. The arguments advanced in Chapter II regarding the instability of $(7-\eta^1\text{-C}_7\text{H}_7)\text{Mn}(\text{CO})_5$ apparently apply equally well to phosphine substituted derivatives.

Section IV. Experimental

PMe_3 was purchased from Strem Chemicals, Inc. PPh_3 was purchased from Aldrich Chemical Co. The manganese and rhenium precursors were prepared by the methods described in Chapter II.

Preparation of $(7-\eta^1\text{-C}_7\text{H}_7)\text{Re}(\text{CO})_4(\text{PMe}_3)$ (11)

$(\eta^3\text{-C}_7\text{H}_7)\text{Re}(\text{CO})_4$, (39 mg, .1 mmol) was dissolved in 20 mL hexane. PMe_3 (11 μL , .11 mmol) was added. After 2 h. stirring, the solution was filtered and cooled to -78°C , depositing orange crystals of 11, mp 105°C . Yield: 45 mg (97%). IR (cyclohexane, ν_{CO} , cm^{-1}) 2074 w, 1995 m, 1912 s, 1935 m. ^1H NMR (cyclohexane- d_{12} , 25°C , δ) 1.57 (d, 9H, PMe_3 , $^2J_{\text{H-P}} = 8.4$ Hz), 2.48 (quart., 1H, H_7 , $^3J_{7-1} = ^3J_{\text{H-P}} = 8.8$ Hz), 5.12 (m, 2H, $\text{H}_{2,3}$), 5.30 (t, 2H, $\text{H}_{1,6}$), 5.89 (m, 2H, $\text{H}_{3,4}$). Anal: calc. for $\text{C}_{14}\text{H}_{16}\text{ReO}_4\text{P}$: C, 36.12; H, 3.46. Found: C, 35.87; H, 3.59. Mass spectrum (16 ev, 90°C) M^+ , M^+-2CO , M^+-3CO , $\text{M}^+-\text{C}_7\text{H}_7$, C_7H_7^+ (base peak). The formation of 11 was accelerated when an excess of PMe_3 was used.

Preparation of $(\eta^3\text{-C}_7\text{H}_7)\text{Re}(\text{CO})_3 \text{PPh}_3$

$(\eta^5\text{-C}_7\text{H}_7)\text{Re}(\text{CO})_3$, (150 mg, .41 mmol) was dissolved in 15 mL CH_2Cl_2 . PPh_3 (65 mg, .25 mmol) was added. After 8 h.

stirring, the CH_2Cl_2 was removed under vacuum and the residue washed with 10 mL pentane at 0°C . The residue was extracted with 3×10 mL ether at room temperature. The combined extracts were filtered and reduced in volume to 10 mL. An equal volume of pentane was added. A red precipitate formed. Cooling to -10°C completed crystallization of the product. A second recrystallization from ether/pentane afforded 12 as red microcrystals, mp 98°C (dec). Yield: 60 mg (39%). IR (hexane, ν_{CO} , cm^{-1}) 2022, 1949, 1914. ^1H NMR (CD_2Cl_2 , -40°C , δ) 2.05 (dt, 1H, H_2 , $^3J_{\text{H-P}} = 16$ Hz), 3.28 (t, 2H, $\text{H}_{1,3}$), 4.40 (dd, 2H, $\text{H}_{5,6}$), 5.22 (m, 2H, $\text{H}_{4,7}$), 7.2-7.6 (br mult, 16 H, Ph). Anal: Calc. for $\text{C}_{28}\text{H}_{22}\text{ReO}_3\text{P}$: C, 53.89; H, 3.55. Found: C, 53.82; H, 3.95. A mass spectrum could not be obtained. Several attempts gave only a mass spectrum for PPh_3 .

When 12 was stirred in CH_2Cl_2 with excess PPh_3 for 24 h., no reaction was detected. The procedure reported here for the preparation of 12 employs a deficiency of PPh_3 in order to avoid the difficult separation of 12 from PPh_3 .

Preparation of $(\eta^3\text{-C}_7\text{H}_7)\text{Re}(\text{CO})_3\text{PMe}_3$

$(\eta^5\text{-C}_7\text{H}_7)\text{Re}(\text{CO})_3$, (72 mg, .2 mmol) was dissolved in 20 mL of hexane. PMe_3 , (20 μl , .2 mmol) was added. After 6 h. stirring at room temperature, infrared spectroscopy

indicated that ca. 20% starting material remained. The solution was filtered, reduced in volume to 10 mL, and cooled to -10°C . A red precipitate was collected. The precipitate was recrystallized from 5 mL hexane by cooling to -10°C to afford 13 as red needles, mp 111°C . Yield: 45 mg (52%). IR (hexane, ν_{CO} , cm^{-1}) 2035 w, 2024 s, 1948 s, 1943 m, 1914 w, 1911 s (see discussion). Anal: Calc. for $\text{C}_{13}\text{H}_{16}\text{ReO}_3\text{P}$: C, 35.67; H, 3.69. Found: C, 35.80; H, 3.66. Mass spectrum (16 ev, 100°C) M^+ , M^+-CO , M^+-2CO (base peak), M^+-3CO , $\text{M}^+-(\text{CO} + \text{PMe}_3)$, C_7H_8^+ , C_7H_7^+ . For ^1H and ^{13}C NMR spectral results, see discussion.

Preparation of $(7\text{-}\eta^1\text{-C}_7\text{H}_7)\text{Re}(\text{CO})_3(\text{PMe}_3)_2$ (14)

Method (a). $(\eta^5\text{-C}_7\text{H}_7)\text{Re}(\text{CO})_3$, (72 mg, .2 mmol) was dissolved in 20 mL hexane to give a pale yellow solution. PMe_3 (100 μl , 5 \times excess) was added. The solution turned red immediately. After 2 h., the colour of the solution was yellow. The solution was evaporated to a yellow residue which was dissolved in 15 mL hexane, filtered and cooled to -78°C . 14 was collected as yellow needles, mp 92°C . Yield: 94 mg (91%). IR (cyclohexane, ν_{CO} , cm^{-1}) 2034 vw, 2016 s, 2009 w, 1942 s, 1925 w, 1893 s. ^1H NMR (CD_2Cl_2 , 25°C , δ) 5.85 (m, 2H, $\text{H}_{3,4}$), 5.26 (br t, 2H, $\text{H}_{1,6}$), 5.06 (m, 2H, $\text{H}_{2,5}$), 1.88 (quint, 1H, H_7 , $^3\text{J}_{1-7} = ^3\text{J}_{\text{H-P}} = 9\text{ Hz}$), 1.55

(lines of an $H_9PP'H_9$ system, $20H$, PMe_3). Anal: calc. for $C_{16}H_{25}ReP_2O_3$: C, 37.42; H, 4.91. Found: C, 37.32; H, 4.96. Mass spectrum (70 ev, $70^\circ C$) M^+ , M^+-CO , M^+-PMe_3 .

Method (b). ($\eta^3-C_7H_7$) $Re(CO)_3PMe_3$, (11 mg, .025 mmol) was dissolved in 5 mL hexane. PMe_3 (5 μl , $2\times$ excess) was added. After 2 h. at room temperature, the solution was filtered and cooled to $-10^\circ C$. Compound 14, (10 mg, 78%), was collected by filtration. The product is identical to that obtained by method (a).

Preparation of ($7-\eta^1-C_7H_7$) $Re(CO)_3(dmpe)$ (15)

($\eta^5-C_7H_7$) $Re(CO)_3$, (36 mg, .1 mmol) was dissolved in 100 mL hexane. $Dmpe$ (20 μl , ca. .2 mmol) was added. After 6 h. stirring at room temperature, no starting material remained (IR) and a fine orange precipitate had formed. The solution was cooled to $5^\circ C$ overnight, the supernatant was syringed off, and the product washed with 2×10 mL pentane. The product forms orange microcrystals, mp $130^\circ C$. Yield: 45 mg (88%). IR (hexane, ν_{CO} , cm^{-1}) 2016 s, 2009 w, 1949 s, 1932 w, 1892 s. 1H NMR (CD_2Cl_2 , $25^\circ C$, δ) 5.92 (m, 2H, $H_{3,4}$), 5.21 (br t, 2H, $H_{1,6}$), 5.10 (m, 2H, $H_{2,5}$), 1.69 (d, $^3J_{H-P} = 9$ Hz, ca. 6H, PMe), 1.49 (d, $^3J_{H-P} = 10$ Hz, 6H, PMe), 1.6-1.8 (v. complex mult., ca. 6H, $P-CH_2$). H_7 was located at $\delta 1.70$ by decoupling $H_{1,6}$ which causes a slight change in

a complex group of signals. Decoupling at $\delta 1.70$ caused $H_{1,6}$ to collapse to a doublet. The 1H NMR spectrum is simplified in benzene- d_6 : δ 6.39 (m, 2H, $H_{3,4}$), 5.64 (m, 2H, $H_{2,5}$), 5.32 (brt, 2H, $H_{1,6}$), 1.45 (quintet, 1H, H_7 , $^3J_{H-P} = 8.8$ Hz), 0.76-0.86 (complex mult., 4H, P- CH_2). Anal: calc. for $C_{16}H_{23}ReP_2O_3$: C, 37.55; H, 4.53. Found: C, 37.07; H, 4.49. Mass spectrum (70 ev, $100^\circ C$) M^+ , $M^+ - 2CO$, $M^+ - C_7H_7$ (base peak) $C_7H_7^+$ (also dmpe fragmentation).

Preparation of $Mn(CO)_3PMe_3(\eta^3-C_7H_7)$ (18)

$(\eta^5-C_7H_7)Mn(CO)_3$, (6.6 mg, .028 mmol) was dissolved in 5 mL hexane. PMe_3 , (3 μl , ca. .03 mmol) was added. The pale yellow colour of the starting material darkened to a red-orange colour after 5 minutes. After 45 min., infrared spectra show that no starting material remains. The solvent was pumped off to leave a red-orange crystalline residue. The residue was dissolved in 2 mL pentane, filtered and cooled to $-10^\circ C$, to afford 18 as shiny red needles, mp $108^\circ C$. Yield: 5.8 mg (66%). IR (cyclohexane, ν_{CO} , cm^{-1}) 2006 s, 1944 s, 1937 m, 1918 w, 1901 s. 1H NMR ($-70^\circ C$, CD_2Cl_2 , δ) 5.74 (m, 2H, $H_{5,6}$), 4.92 (dd, 2H, $H_{4,7}$), 3.76 (t, 2H, $H_{1,3}$, $^3J_{1-2} = 7.3$ Hz), 1.74 (dt, 1H, H_2 , $^3J_{H-P} = 15.9$ Hz), 1.20 (d, 9H, PMe_3 , $^2J_{H-P} = 8.6$ Hz). An additional doublet signal due to the PMe_3 group of the minor isomer is

observed at $\delta 1.50$ ($^2J_{H-P} = 9.2$ Hz). Integration of the two PMe_3 signals gives a ratio of ca. 100:1 for the major:minor isomers. Mass spectrum (16 ev, $75^\circ C$) M^+ , M^+-3CO (base peak), $M^+-(3CO + PMe_3)$. Anal: calc. for $C_{13}H_{16}MnO_3P$: C, 51.00; H, 5.27. Found: C, 50.08; H, 5.24.

Reaction of $(\eta^3-C_7H_7)Mn(CO)_4$ with PMe_3

5.0 mg of $(\eta^3-C_7H_7)Mn(CO)_4$ were dissolved in 5 mL hexane. 5 μl of PMe_3 was added. All the starting material was consumed after two hours. The products are $(\eta^3-C_7H_7)Mn(CO)_3PMe_3$ and a new species having 2 ν_{CO} bands at 1905 and 1950 cm^{-1} . The solution was pumped dry, then extracted with 3 mL cold pentane. This solution was filtered and cooled to $-10^\circ C$ to give a yellow crystalline material. IR (hexane, ν_{CO} , cm^{-1}) 2034 w, 1946 s, 1905 m. 1H NMR ($CDCl_3$, $25^\circ C$) lines of an $H_9PP'H_9$ system at $\delta 1.60$. Mass spectrum (14 ev, $85^\circ C$). $Mn_2(CO)_5(PMe_3)_2^+$, $Mn(CO)_4PMe_3^+$, $Mn(CO)_4^+$ (base peak). Insufficient material for analysis. This product is tentatively identified as $[(PMe_3)Mn(CO)_4]_2$. When this reaction was carried out in THF- d_8 or CD_2Cl_2 in a sealed NMR tube (at $-10^\circ C$ to $-50^\circ C$), products identified were ditropyl, $(\eta^3-C_7H_7)Mn(CO)_3PMe_3$ and $[(PMe_3)Mn(CO)_4]_2$. There was no evidence for a monohaptocycloheptatrienyl manganese compound. Less

$(\eta^3\text{-C}_7\text{H}_7)\text{Mn}(\text{CO})_3\text{PMe}_3$ was formed at the lower temperatures.

Reaction of $(\eta^5\text{-C}_7\text{H}_7)\text{Mn}(\text{CO})_3$ with dmpe

$(\eta^5\text{C}_7\text{H}_7)\text{Mn}(\text{CO})_3$, (12 mg, .05 mmol) was dissolved in 10 mL hexane to give a pale yellow solution. dmpe (10 μl , ca. .1 mmol) was added. The solution rapidly turned red and a tan precipitate formed. Infrared bands at 2007 s, 1944 s, 1937 m, 1903 s cm^{-1} for the product were very similar to the spectrum observed for 16. On further standing at room temperature, the amount of precipitate increased, the solution became colourless and no ν_{CO} bands were observed in the infrared spectrum. The supernatant was syringed off, evaporated to dryness, and taken up in CD_2Cl_2 . The ^1H NMR spectrum shows ditropyl and dmpe.

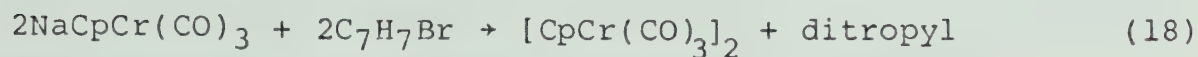
When this reaction was carried out in an NMR tube, (CD_2Cl_2 , -50°C) the identity of the intermediate species was confirmed by observation in the ^1H NMR spectrum of signals for a trihaptocycloheptatrienyl complex. The methyl and methylene regions of the spectrum were extremely complex. On warming to -10°C , the trihapto intermediate is slowly consumed, and ditropyl was the only new product observed. There was no evidence for a monohapto species.

CHAPTER IV

COMPOUNDS OF CHROMIUM, MOLYBDENUM AND TUNGSTEN

Section I. Introduction

The reaction of NaCpCr(CO)_3 with the tropylium cation (eq. 18) was first reported by E.O. Fisher and H.P. Fritz in 1958.²⁵



Apparently this was an attempt to prepare $(\eta^5\text{-C}_5\text{H}_5)\text{Cr}(\eta^7\text{-C}_7\text{H}_7)$ (later prepared by a quite different route⁸¹). To quote E.O. Fischer²⁵: "it was found that the great sensitivity of tropylium bromide to reduction, coupled with the strong reducing power of the carbonyl hydrides militated against success."

This reaction is actually a very convenient method for the preparation of $[\text{CpCr(CO)}_3]_2$. A 1963 report in *Inorganic Syntheses* made use of the reaction of NaCpCr(CO)_3 with tropylium bromide or allyl chloride to prepare $[\text{CpCr(CO)}_3]_2$ in 37% yield.⁸² The failure of these reactions to yield stable alkyl compounds such as $\text{CpCr(CO)}_3(\eta^1\text{-C}_7\text{H}_7)$ or $\text{CpCr(CO)}_3(\sigma\text{-allyl})$ is perhaps not surprising in view of the reported thermal instability of $\text{CpCr(CO)}_3\text{-CH}_3$ ¹², which is

the only chromium alkyl of this type reported.

In the classic paper of 1956 by Piper and Wilkinson¹², the reaction of the anions $\text{CpM}(\text{CO})_3^-$ ($\text{M} = \text{Cr}, \text{Mo}, \text{W}$) with methyl iodide was explored. $\text{CpMo}(\text{CO})_3\text{-CH}_3$ decomposes at 124°C while $\text{CpW}(\text{CO})_3\text{-CH}_3$ melts at 145°C . Both were prepared in 80% yield. In contrast, the Cr analog was characterized only by infrared spectroscopy since the yield was only 1-3%. A purification of $\text{CpCr}(\text{CO})_3\text{-CH}_3$ by vacuum distillation was subsequently reported by Wilkinson in 1963⁸³, but it is not clear that the compound was actually isolated. More recently, $\text{CpCr}(\text{CO})_3\text{-CH}_3$ was isolated as yellow crystals from the reaction of $\text{NaCpCr}(\text{CO})_3$ with MeI at -20°C in THF, followed by a pentane extraction workup and crystallization at -78°C .⁸⁴ No melting point or analytical data were reported, but the compound seems to be a stable solid at room temperature, since it was employed in further reactions.

Similar results have been reported for compounds of the type $\text{CpM}(\text{CO})_3(\sigma\text{-allyl})$. For $\text{M} = \text{Cr}$, this compound is unknown, apparently due to thermal instability. For $\text{M} = \text{Mo}$, Green and Cousins have reported decomposition at 60°C and mp ca. -5°C .⁸⁵ For $\text{M} = \text{W}$, there is no reported decomposition temperature (mp $24\text{-}26^\circ\text{C}$).²⁶

These and other results indicate that the thermal and

oxidative stability of alkyls of this type increases on descending the group (for further data, cf. the review by Barnett and Sloan⁸⁷). It seemed likely that the extension of reaction 18 to Mo and W could yield stable alkyls of the type $\text{CpM}(\text{CO})_3(7-\eta^1\text{-C}_7\text{H}_7)$.

In addition to the direct reactions of tropylium with metal carbonyl anions, indirect synthetic routes to monohaptocycloheptatrienyl alkyls have also been explored. These include decarbonylation reactions of acyl compounds and addition of PMe_3 to trihaptocycloheptatrienyl compounds.

Section II. Reactions of Metal Carbonyl Anions with Tropylium

The reactions of the anions $\text{CpM}(\text{CO})_3^-$ ($\text{M} = \text{Mo}, \text{W}$) with tropylium tetrafluoroborate were carried out at -78°C in THF (eq. 19)

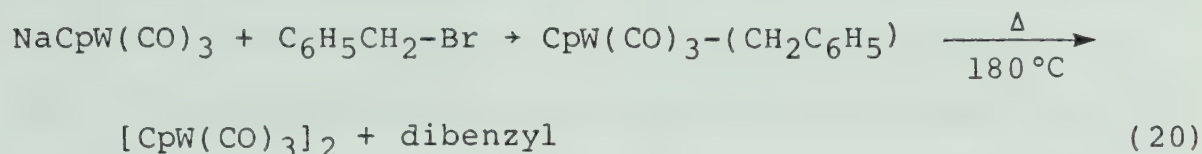


$\text{M} = \text{Mo}, \text{W}$

In the case of tungsten, the potassium salt of the anion was also prepared and reacted with tropylium, with the same results. Yields of the dimers are 85% (W) and 86% (Mo). Separation of the more soluble ditropylium is readily accomplished by recrystallization from CH_2Cl_2 /heptane since the metal dimers are only slightly soluble in hydrocarbon solvents.

These reactions may have some synthetic utility. The first preparation of these Mo and W dimers was reported by Wilkinson in 1954, employing a high temperature vapor phase reaction of $\text{M}(\text{CO})_6$ with cyclopentadiene, to give a yield of 30% in both cases.⁸⁸ An improved route (50% yield) to $[\text{CpMo}(\text{CO})_3]_2$ involving oxidation of $\text{CpMo}(\text{CO})_3\text{-H}$ was reported in 1963.⁸² According to Wrighton and coworkers, attempts to extend this procedure to the tungsten dimer gave yields of

only 10%.⁸⁹ The best preparation currently available for the tungsten dimer is a two step method involving the thermal decomposition of $\text{CpW}(\text{CO})_3-(\text{CH}_2\text{C}_6\text{H}_5)$ (eq. 20)



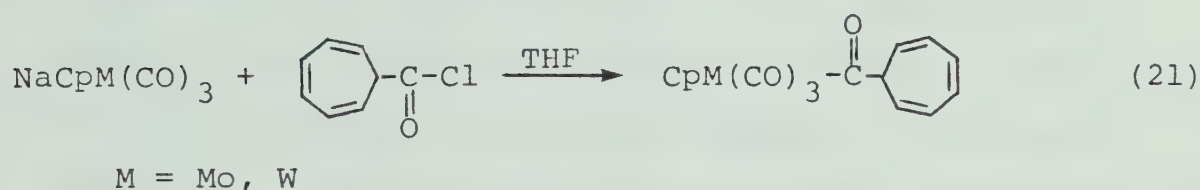
An overall yield of >90% after a chromatographic workup was claimed for this procedure.⁸⁹

Although it was not our intention to develop new synthetic methods for these dimers, it seems clear that the tropylium reactions provide a simple one-step preparation which is comparable in yield in the case of tungsten and superior in the case of molybdenum, to alternative routes currently available.

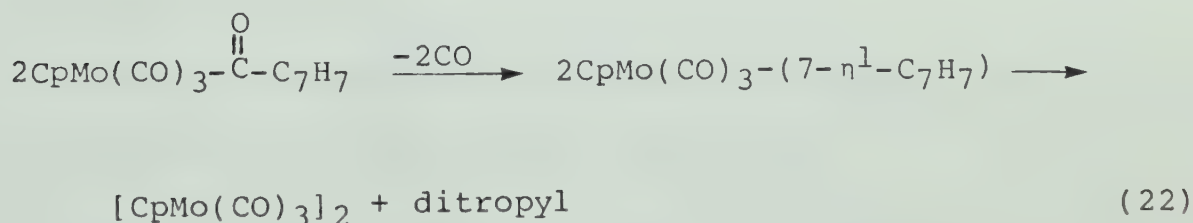
The failure of these reactions to yield the desired alkyl compounds does not necessarily mean that such compounds are all inherently unstable. As mentioned in the introduction, there is also the possibility of electron transfer from the anions to the tropylium cation to give radical species, followed by coupling to give the observed dimeric products. There is some potential for success if an indirect synthetic route could be employed.

Section III. Indirect Synthetic Routes

Since the direct synthetic route had failed, the same approach initially used for the $\text{Re}(\text{CO})_5$ system was next employed. The formation of an acyl compound which could then be decarbonylated to a σ alkyl was envisaged (eq. 21).



In the case of $\text{CpMo}(\text{CO})_3\text{C}(=\text{O})\text{C}_7\text{H}_7$, the product is very unstable, decomposing rapidly to give $[\text{CpMo}(\text{CO})_3]_2$, presumably via loss of CO to give the σ alkyl, followed by homolytic cleavage of the Mo-C σ bond (eq. 22).

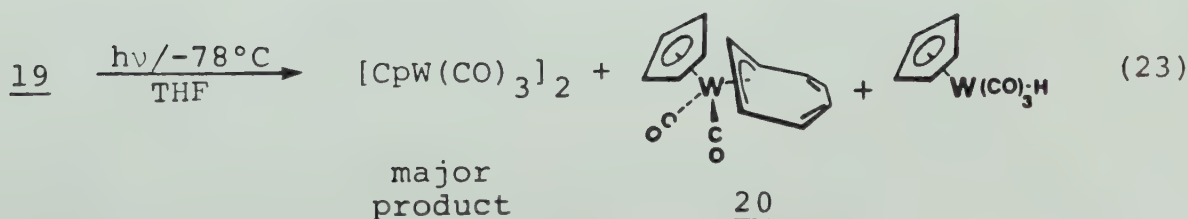


The tungsten analog, $\text{CpW}(\text{CO})_3\text{C}(=\text{O})\text{C}_7\text{H}_7$ (19), is more stable and can be isolated with some difficulty as a pale yellow crystalline solid, which has been fully characterized.

The physical properties of 19 are similar to those reported for $\text{CpW(CO)}_3\text{-}\overset{\text{O}}{\parallel}\text{C-CH}_2\text{CH}_3$, which was described as a waxy orange solid, mp 5°C .⁹⁰ The infrared spectrum of this material has only one acyl stretching band at 1640 cm^{-1} (CCl_4 solution). The infrared spectrum of 19 shows two acyl stretching bonds at 1643 and 1619 cm^{-1} (see figure X). This is probably due to the existence of two rotamers with respect to the carbon-carbon bond in the acyl group, as was described in Chapter II for the compounds $\text{C}_7\text{H}_7\text{-}\overset{\text{O}}{\parallel}\text{C-M(CO)}_5$ ($\text{M}=\text{Mn, Re}$). A similar doubling of the acyl stretching mode was observed in $\text{CpW(CO)}_3\text{-}\overset{\text{O}}{\parallel}\text{C-CH=CH}_2$, where frequencies of 1630 and 1623 cm^{-1} (Nujol) were reported.⁹¹

The mass spectrum of 19 does not show a molecular ion. The highest observed m/e values correspond to M^+-CO . The observation of this ion in the mass spectrometer is perhaps encouraging for the success of the photochemical decarbonylation of 19.

The low temperature photochemical decarbonylation of 19 was carried out in THF at -78°C (eq. 23).



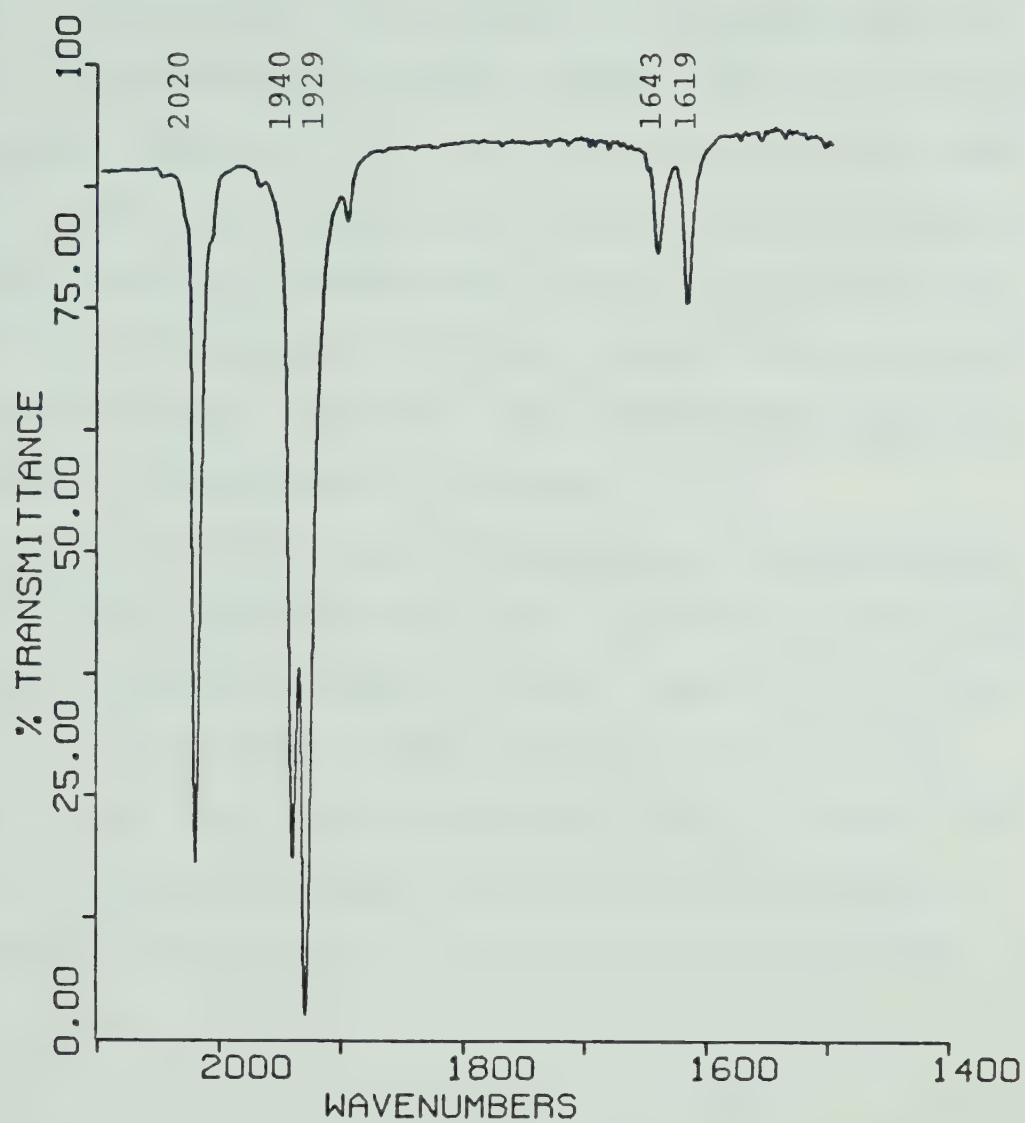
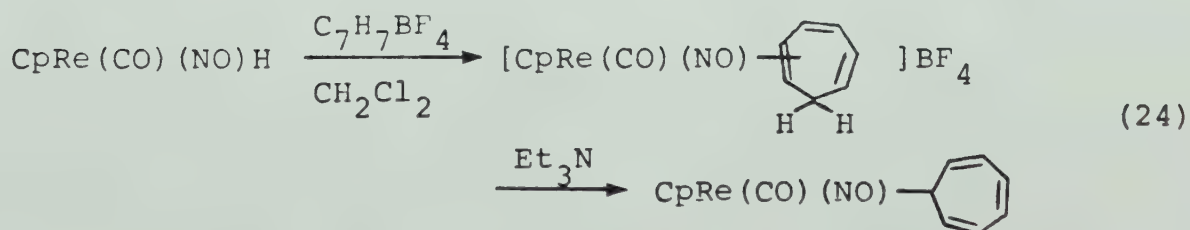


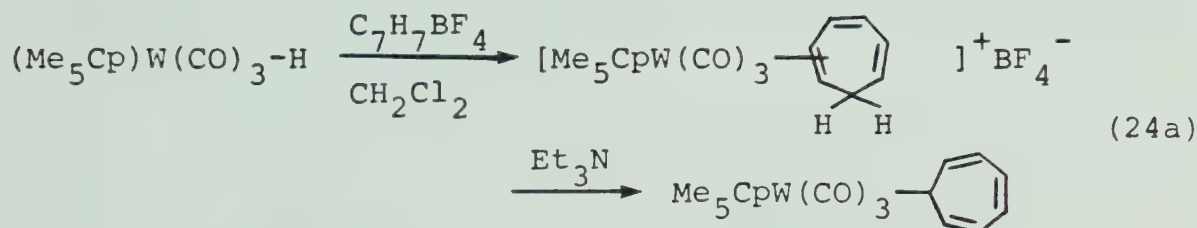
FIGURE X. Infrared spectrum of 19, cyclohexane

$\text{CpW}(\text{CO})_2(\eta^3\text{-C}_7\text{H}_7)$, (20) and $\text{CpW}(\text{CO})_3\text{H}$ were formed in approximately equal amounts. The $[\text{CpW}(\text{CO})_3]_2$ may be formed by homolytic cleavage of the metal-carbon σ bond in the possible intermediate $\text{CpW}(\text{CO})_3(7\text{-}\eta^1\text{-C}_7\text{H}_7)$; $\text{CpW}(\text{CO})_3\text{H}$ could be the result of hydrogen abstraction from the solvent by $\text{CpW}(\text{CO})_3\cdot$. The results are consistent with, but do not require, the intermediacy of $\text{CpW}(\text{CO})_3(7\text{-}\eta^1\text{-C}_7\text{H}_7)$ as the first step in the decarbonylation reaction. This intermediate would be thermally or photochemically unstable.

Another indirect route to monohaptocycloheptatrienyl alkyls of this group which has been explored is the hydride abstraction method developed by Sweet and Graham.⁹² This reaction employs hydride abstraction by C_7H_7^+ to form cationic metal complexes containing $\eta^2\text{-C}_7\text{H}_8$ moieties. The acidity of cycloheptatriene is considerably enhanced by coordination to the metal, allowing ready deprotonation to give a σ alkyl (eq. 24).

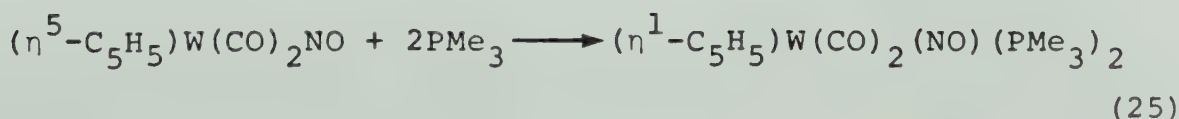


The tungsten hydride $(\text{Me}_5\text{Cp})\text{W}(\text{CO})_3\text{-H}$ was prepared by the method of King and Fronzaglia.⁹³ The proposed reaction is shown in eq. 24a

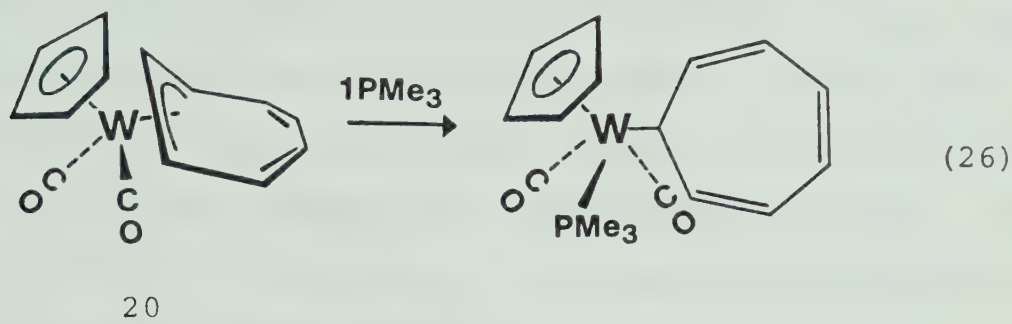


Infrared spectra indicated that a cation was formed, but attempts to precipitate the cation from CH_2Cl_2 by addition of ether or to deprotonate with triethylamine led to displacement of the coordinated cycloheptatriene. For reasons not yet clearly understood, the binding of cycloheptatriene to this metal center is quite weak.

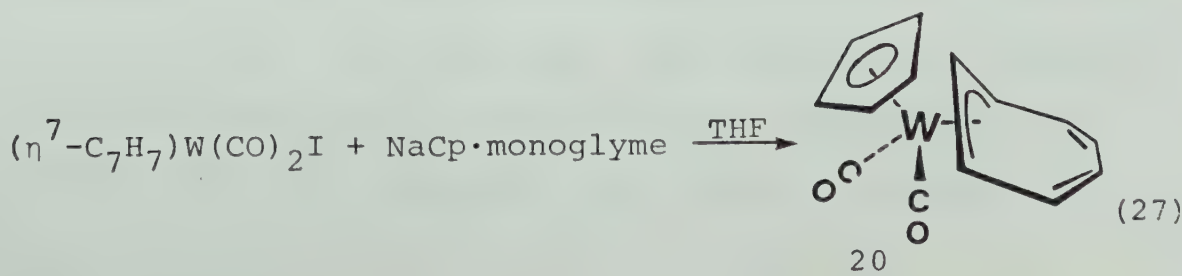
Another indirect approach to the problem was suggested by the success of the trihapto \rightarrow monohapto conversion carried out using the reaction of PMe_3 with $(\eta^3\text{-C}_7\text{H}_7)\text{Re}(\text{CO})_4$ (see Chapter III, section II). Recent results reported by Casey and coworkers suggested that such a hapticity reduction reaction might also be applicable to tungsten systems (eq. 25).⁹⁴



The compound $\text{CpW(CO)}_2(\eta^3\text{-C}_7\text{H}_7)$ (20), mentioned above as a by-product of the decarbonylation of 19 is structurally quite similar to the tungsten nitrosyl compound which was found by Casey to be quite reactive towards PMe_3 . Thus the reaction of eq. 26 was planned as an indirect synthesis of the elusive monohapto alkyl.



The literature method for the preparation of compound 20 gives only a 16.5% yield after a chromatographic workup.⁹³ It was found that this yield could be increased to 71% by the simple expedient of using a carefully prepared salt of the cyclopentadienide anion (which was crystalline) rather than an in situ preparation of NaCp as employed previously (see experimental section for details). The reaction used is shown in eq. 27.



When 20 was combined with excess PMe_3 at room temperature in a variety of solvents (THF, benzene, hexane), there was no reaction detectable by infrared spectroscopy. Refluxing for 24 hours in hexane produced no reaction. Although this lack of reactivity toward PMe_3 on the part of 20 is disappointing, it is very interesting in terms of the mechanism of these phosphine addition reactions. Casey has shown that the mechanism of the PMe_3 addition in the case of $\text{CpRe}(\text{CO})(\text{NO})\text{CH}_3$ ⁷⁷ and $\text{CpW}(\text{CO})_2\text{NO}$ ⁹⁴ is associative (i.e. rate depends on $[\text{P}]$ and $[\text{substrate}]$). Since both of these compounds contain an NO group, it is tempting to postulate a shift in nitrosyl bonding mode from linear to bent as a key part of the reaction mechanism. However, our results with Re and Mn compounds (see Chapter III) which do not contain NO groups indicated that the NO ligand is not required for phosphine addition to occur. A more likely explanation is that the metal center in $\text{CpW}(\text{CO})_2(\eta^3\text{-C}_7\text{H}_7)$ is more electron rich than in $\text{CpW}(\text{CO})_2\text{NO}$ and thus less susceptible to attack by an entering nucleophile. This difference in electron density at the metal is perhaps best illustrated by a comparison of MCO stretching frequencies in the infrared spectra of the two compounds. The reported ν_{CO} frequencies for $\text{CpW}(\text{CO})_2\text{NO}$ are 2011 and 1934 cm^{-1} (hexane solution).⁹⁵ $\text{CpW}(\text{CO})_2(\eta^3\text{-C}_7\text{H}_7)$ exhibits a more complex infrared spectrum

since the presence of two isomers gives a total of four ν_{CO} bands at 1966, 1955, 1907 and 1891 cm^{-1} .⁹⁶ In spite of this complication, it is clear that the CO stretching frequencies are observed at substantially higher frequencies in the tungsten nitrosyl compound, in accord with the greater reactivity of this compound towards PMe_3 .

All the currently available synthetic routes for monohapto cycloheptatrienyl compounds have now been exhausted in our attempts to prepare Mo and W derivatives. Possibilities which remain unexplored include variations on the carbonyl anion reactions such as the use of $\text{CpW(CO)}_2(\text{PEt}_3)^-$ anion.⁹⁷ This may form an alkyl $\text{CpW(CO)}_2(\text{PEt}_3)(\eta^1\text{-C}_7\text{H}_7)$ in which the presence of the phosphine ligand should increase the thermal stability of the product. (This is a general observation in compounds of this type, cf. ref. 87.)

Section IV. Experimental

$W(CO)_6$, $[CpMo(CO)_3]_2$ and PMe_3 were purchased from Strem Chemicals, Inc.

$NaCpMo(CO)_3 + C_7H_7BF_4$

A solution of 10 mmol of $NaCpMo(CO)_3$ in 100 mL THF was prepared from $[CpMo(CO)_3]_2$ with excess 1% Na/Hg according to the method of Hayter.⁹⁸ After removal of the excess amalgam, the solution was filtered into a Schlenk tube and cooled to $-78^\circ C$. $C_7H_7BF_4$ (1.78 g, 10 mmol) was added over 2 h. The colour of the solution changed from straw yellow to deep red immediately on addition of the first portion of $C_7H_7BF_4$. IR monitoring indicated that the dimer was the only product. The THF was pumped off and the residue extracted with CH_2Cl_2 . The product was recrystallized twice from CH_2Cl_2 /heptane to give $[CpMo(CO)_3]_2$ as wine-red crystals mp $205-210^\circ C$ (lit.⁸⁸ mp $215-217^\circ C$). Yield: 2.1 g (86%). IR (hexane, ν_{CO} , cm^{-1}) 1962, 1917. (lit.⁸⁹ IR; iso-octane: 1960, 1915).

Preparation of $NaCpW(CO)_3$

1.36 g NaCp (15.5 mmol) prepared from excess Na sand at room temperature in THF was dissolved in 300 mL THF with 11 g of $W(CO)_6$ (31 mmol). After 85 h. reflux, the THF was

pumped off and the excess $W(CO)_6$ was sublimed out onto a water cooled probe by warming the flask to $60^\circ C$. The residue is a slightly off-white solid which is quite air sensitive.

Preparation of $KCpW(CO)_3$

A sample of KCp was prepared from 391 mg (10 mmol) of K and 5 mL of cyclopentadiene in 50 mL dry ether at $0^\circ C$. When all the potassium metal had been consumed, the ether and excess cyclopentadiene were pumped off to give a white solid. 3.86 g (11 mmol) of $W(CO)_6$ was added, followed by 100 mL THF. The mixture was refluxed for 120 h. The THF was pumped off to give a pale yellow crystalline residue. The excess $W(CO)_6$ was sublimed out as before. The same reaction can be achieved in 12-24 hours in diglyme but the difficulty encountered in pumping off diglyme makes it necessary to use the resulting solution directly.

Preparation of $CpW(CO)_3-\overset{O}{\parallel}C-C_7H_7$ (19)

1.2 g (3.4 mmol) of $NaCpW(CO)_3$ was dissolved in 50 mL THF. $C_7H_7-\overset{O}{\parallel}C-Cl$ (.40 mL, 3.4 mmol) was added. After four hours stirring at room temperature, the THF was pumped off to give a dark brown residue which was extracted with 3×25 mL of hexane. The solution was filtered and cooled to $-10^\circ C$

overnight, then filtered again and cooled to -78°C for ca. 1 hour. An orange precipitate forms. The supernatant was syringed off. The precipitate oils on warming, but solidifies after a few minutes pumping. The precipitate was dissolved in 25 mL hexane, filtered and cooled slowly to -10°C over 24 hours. This procedure was repeated twice to afford 19 as yellow crystals, mp 42°C . Yield: 410 mg (27%). IR (cyclohexane, ν_{CO} , cm^{-1}) 2020 s, 1940 s, 1929 vs, 1643 w, 1619 w. ^1H NMR: (benzene- d_6 , 25°C , δ) 2.72 (t, 1H, H_7 , $^3\text{J}_{7-1} = 5.1$ Hz), 4.25 (m, 2H, $\text{H}_{1,6}$), 6.06-6.20 (m, 4H, $\text{H}_{3,4}$ and $\text{H}_{2,5}$), 4.68 (s, 4.5H, Cp); Mass spectrum: (90°C , 16 ev) $\text{M}^+ - \text{CO}$, $\text{M}^+ - 2\text{CO}$, $\text{M}^+ - 3\text{CO}$, C_7H_7^+ (base peak). Anal.: calcd. for $\text{C}_{16}\text{H}_{12}\text{WO}_4$: C, 42.48; H, 2.65. Found: C, 42.48; H, 2.74.

Photolysis of 19

30 mg of the acyl compound was dissolved in THF, transferred to a quartz irradiation vessel and the solution cooled to -78°C . The solution was irradiated with a 140 W Hanovia lamp. Infrared monitoring indicated that starting material was consumed and that the major product was $[\text{CpW}(\text{CO})_3]_2$ (bands at 1953 and 1904 cm^{-1}). Photolysis was terminated after three hours and the THF was pumped off. The red residue was extracted with hexane, which left most

of the dimer undissolved. The infrared spectrum of the hexane extract indicated the presence of $\text{CpW(CO)}_2(\eta^3\text{-C}_7\text{H}_7)$ and $\text{CpW(CO)}_2\text{-H}$. Various attempts to carry out this irradiation in pyrex or in hydrocarbon solvents gave similar results. No evidence for $\text{CpW(CO)}_3(\eta^1\text{-C}_7\text{H}_7)$ was obtained.

$\text{KCpW(CO)}_3 + \text{C}_7\text{H}_7\text{BF}_4$

10 mmol of KCpW(CO)_3 in 150 mL THF was cooled to -78°C (some white ppt. forms). 1.78 g (10 mmol) of $\text{C}_7\text{H}_7\text{BF}_4$ was added over 15 min. The solution instantly turned dark red. Infrared monitoring indicated quantitative conversion to $[\text{CpW(CO)}_3]_2$. After one hour stirring at -78°C , the solution was warmed to room temperature and the THF pumped off to give a red semi-crystalline residue. The residue was extracted with CH_2Cl_2 and recrystallized twice from CH_2Cl_2 /heptane. Yield: 2.81 g (85%). IR (heptane, ν_{CO} , cm^{-1}) 1960, 1912 (lit.⁸⁹ 1958, 1910 cm^{-1} , iso-octane). Similar results were obtained using NaCpW(CO)_3 .

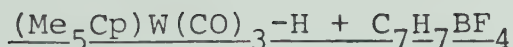
Preparation of $\text{CpW(CO)}_2(\eta^3\text{-C}_7\text{H}_7)$ (20)

$(\eta^7\text{-C}_7\text{H}_7)\text{W(CO)}_2\text{I}$ was prepared by the literature method.⁹³ 93 mg (.2 mmol) of $(\eta^7\text{-C}_7\text{H}_7)\text{W(CO)}_2\text{I}$ was dissolved in 10 mL THF. This solution was added to a solution of 75 mg (.42 mmol) of $\text{NaCp}\cdot\text{monoglyme}$ (prepared by the method of

Mink⁹⁹) in 10 mL THF. The initially colourless NaCp solution turned bright red-orange instantly as the deep green solution of the iodide was added. An infrared spectrum taken after 5 min. showed no starting material remaining and two new bands at 1941 and 1871 cm^{-1} . The THF was pumped off to leave an orange oily residue. The residue was extracted with 10 mL hexane. The solution was filtered and cooled to -78°C to afford 56 mg (71%) of $\text{CpW}(\text{CO})_2(\eta^3\text{-C}_7\text{H}_7)$ as orange crystals, mp 135°C (dec) (lit.⁹³ mp 137°C dec.). IR (hexane, ν_{CO} , cm^{-1}) 1966, 1955, 1907, 1891 (lit.⁹³ infrared: 1967, 1958, 1908, 1892 cm^{-1} (cyclohexane)). Reference 93 gives a 16.5% yield of product mp $111\text{--}117^{\circ}\text{C}$ after chromatography. Purer product, mp 137°C was obtained by sublimation, but the recovery of sublimed product was only ca. 10%.

Reaction of $\text{CpW}(\text{CO})_2(\eta^3\text{-C}_7\text{H}_7)$ with PMe_3

$\text{CpW}(\text{CO})_2(\eta^3\text{-C}_7\text{H}_7)$ was combined with excess (tenfold to hundredfold) PMe_3 in THF, benzene or hexane. No reaction was detected by infrared spectroscopy after 24 hours at room temperature. Refluxing for 24 hours in hexane produced no reaction.



$(\text{Me}_5\text{Cp})\text{W}(\text{CO})_3\text{H}^{93}$, (78 mg, .2 mmol) was dissolved in 20 mL CH_2Cl_2 to give a pale yellow solution. The infrared spectrum showed two ν_{CO} bands at 2007 and 1910 cm^{-1} . Addition of $\text{C}_7\text{H}_7\text{BF}_4$ (35 mg, .2 mmol) caused the solution to turn deep red. Infrared spectra indicated that no starting material remained. There were 2 new ν_{CO} bands at 2052 and 1958 cm^{-1} . The solution was divided into two parts. The first part was treated with ca. 4 volumes of ether in an attempt to precipitate the cation. No precipitate formed. All solvent was removed under vacuum and the red crystalline residue was redissolved in CH_2Cl_2 . The infrared spectrum had 2 ν_{CO} bands at 2042 and 1951 cm^{-1} . The second part of the solution was treated with several drops of Et_3N . There was an immediate colour change to orange-red. The infrared spectrum showed 2 ν_{CO} bands at 2020 and 1918 cm^{-1} . A portion of this sample was evaporated and gave an orange red oil which was dissolved in CD_2Cl_2 . The ^1H NMR spectrum showed several resonances in the Me_5Cp region and free C_7H_8 . There was no evidence for a monohapto-cycloheptatrienyl compound or for ditropyl formation.

CHAPTER V

CYCLOHEPTATRIENYL COMPOUNDS OF IRON AND RUTHENIUM

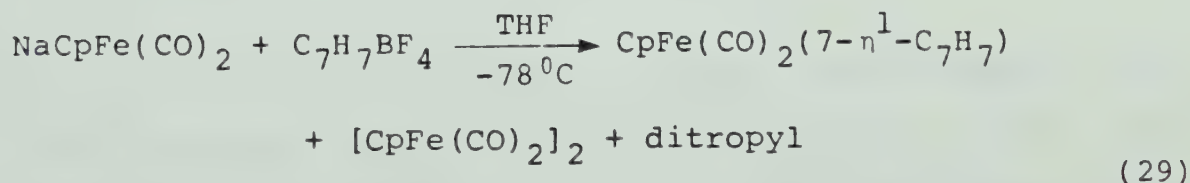
Section I. Introduction

The first reaction of an iron carbonyl anion with the tropylium cation was reported by Wilkinson and coworkers in 1958²⁶ (eq. 28)



(both in low yield)

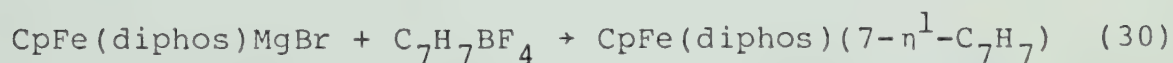
It is not clear what product was actually expected from this reaction, but a more recent report by Rosenblum and Ciappenelli¹⁰⁰ was clearly an attempt to prepare a monohaptocycloheptatrienyl alkyl of iron (eq. 29).



The compound, which was thought to be $\text{CpFe(CO)}_2(7-\eta^1-\text{C}_7\text{H}_7)$, was obtained in only 4% yield. The major products of the reaction are ditropyl and $[\text{CpFe(CO)}_2]_2$.

Further examination of the properties of compound 20 led to reformulation as $\text{CpFe(CO)(}\eta^3\text{-C}_7\text{H}_7\text{)}$, which presumably arises from decarbonylation of a dicarbonyl intermediate. This observation indicates that the synthesis of a monohaptocycloheptatrienyl compound of iron might be possible if decarbonylation to a trihapto species could be prevented. In the present work, the reaction of NaCpFe(CO)_2 with $\text{C}_7\text{H}_7\text{BF}_4$ has been reinvestigated.

The reaction of CpFe(diphos)Br with magnesium to give CpFe(diphos)MgBr was reported by Felkin in 1974.¹⁰² Reactions of this material with alkyl halides were subsequently reported to give alkyls of the type CpFe(diphos)R .¹⁰³ A possible route to a monohapto alkyl is shown in eq. 30. Formation of a trihapto species would be unlikely in this case.

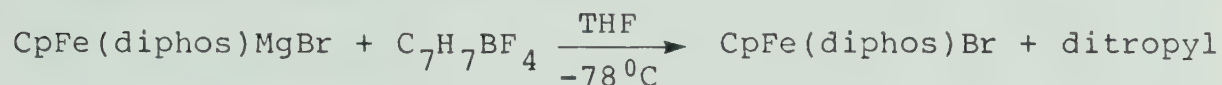


Reactions of carbonyl anions of ruthenium have also been explored and will be described in this chapter. The reaction of KCpRu(CO)_2 , NaCpRu(CO)_2 and $\text{KMe}_5\text{CpRu(CO)}_2$ with tropylium gives results which shed light on the mechanism of the reaction of metal carbonyl anions, particularly with respect to the involvement of radicals as intermediates.

Alkyls of the type $\text{CpM}(\text{CO})(\text{PR}_3)(\text{R})$ ($\text{M} = \text{Fe}, \text{Ru}$) have a pseudo-tetrahedral metal center with four different ligands. Compounds of this type exist as two different enantiomers. Synthesis of monohaptocycloheptatrienyl derivatives of these metal centers would allow the stereochemistry of the metal center during the course of the metal migration to be investigated. Synthetic routes to compounds of this type are discussed in Section IV.

Section II. Iron Compounds

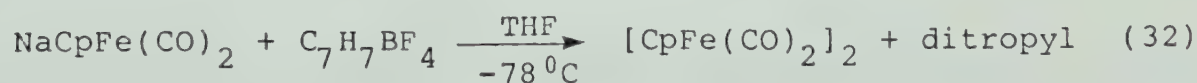
The reaction of $\text{CpFe(diphos)MgBr}^{103}$ with $\text{C}_7\text{H}_7\text{BF}_4$ at -78°C in THF gave only ditropyl and CpFe(diphos)Br (eq. 31).



(31)

This outcome indicated that even in a system where decarbonylation cannot occur, the monohapto alkyl species is probably unstable. This result is in contrast to the stability of the closely related benzyl derivative of this iron system, $\text{CpFe(diphos)-CH}_2\text{Ph}^{103}$, possibly due to metal-carbon bond weakening caused by the stability of the tropyl radical.

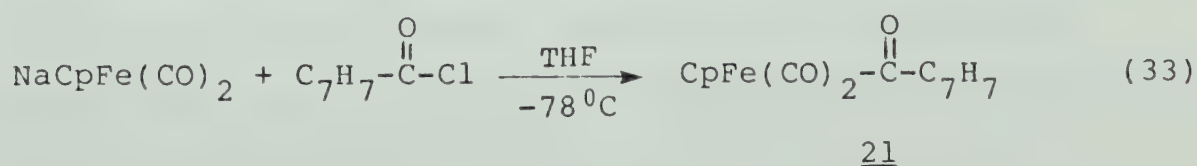
The reaction of NaCpFe(CO)_2 with $\text{C}_7\text{H}_7\text{BF}_4$ was reinvestigated. In our hands, the only products of this reaction were ditropyl and $[\text{CpFe(CO)}_2]_2$ (eq. 32).



There was no evidence for the formation of $\text{CpFe(CO)}(\eta^3\text{-C}_7\text{H}_7)$. Variations of this reaction were also attempted.

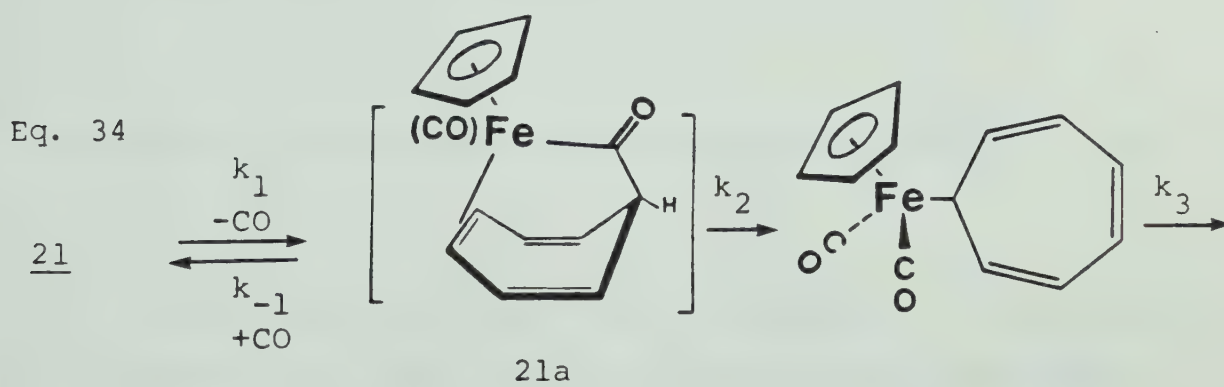
KCpFe(CO)₂ and KMe₅CpFe(CO)₂ were reacted with C₇H₇BF₄ in THF at -78°C, with the same results. The failure of these reactions to give any CpFe(CO)(η³-C₇H₇) or (Me₅Cp)Fe(CO)(η³-C₇H₇) led us to investigate the exact experimental conditions used in the published preparation. Perusal of the Ph.D. thesis of D.J. Ciappenelli showed that the best yield of CpFe(CO)(η³-C₇H₇) obtained in a large number of experiments was 4%.¹⁰⁴ It is also noted in this thesis that when the CpFe(CO)₂⁻ anion was prepared from recrystallized [CpFe(CO)₂]₂, the reaction with C₇H₇BF₄ failed to give any CpFe(CO)(η³-C₇H₇).¹⁰⁵ When crude dimer was used, low yields of the trihapto species were obtained. We conclude that an unknown species in the impure dimer starting material is essential to success in this reaction, so that our failure to reproduce the reported results is not surprising.

The indirect approach using an acyl intermediate which was successful for rhenium was next attempted. The reaction of NaCpFe(CO)₂ with C₇H₇- $\overset{\text{O}}{\parallel}$ C-Cl gives an acyl species (eq. 33).



Infrared spectra of the reaction solution showed two

terminal ν_{CO} bands at 2020 and 1956 cm^{-1} and a less intense acyl band at 1652 cm^{-1} . Attempts to work up the mixture led to complete decomposition to $[\text{CpFe}(\text{CO})_2]_2$. Reduction in volume of the solution under vacuum at -78°C caused rapid decomposition. The instability of 21 is in marked contrast to the high thermal stability of other $\text{CpFe}(\text{CO})_2-\overset{\text{O}}{\parallel}\text{C}-\text{R}$ compounds. For example, $\text{CpFe}(\text{CO})_2-\overset{\text{O}}{\parallel}\text{C}-\text{CH}_3$ can be sublimed at $70-90^\circ\text{C}$ (0.3 mm) and recovered unchanged.¹⁰⁶ The decarbonylation of 21 may be proceeding via a chelating acyl intermediate, as suggested by Whitesides and Budnik for $\text{C}_7\text{H}_7-\overset{\text{O}}{\parallel}\text{C}-\text{Mn}(\text{CO})_5$ ³⁵ (see Chapter II). A possible reaction sequence for decomposition of 21 is shown in eq. 34.



The ν_{CO} frequencies of 21 do not suggest unusual lability of the CO ligands. However, the rate of the reverse reaction (k_{-1}) could be substantially reduced by the

formation of 21a, which is coordinatively saturated. The C-C bond broken in the second step (k_2) is a relatively weak bond, so k_2 is probably greater than the rates for normal alkyl migration reactions. Since the σ bonded alkyl is probably very unstable, k_3 is large and dimer formation would be rapid. The overall rate of the reaction under these conditions ($k_2 \gg k_{-1}$) is determined by the rate of initial CO loss (k_1). A possible explanation for the thermal instability of 21 consistent with this scheme is that CO loss is accelerated by the coordination of the double bond to the metal during the formation of 21a.

In an attempt to prepare a more stable acyl derivative, the pentamethylcyclopentadiene analog of 21 was prepared (eq. 35).



Compound 22 was isolated with some difficulty. It is a pale yellow crystalline solid which gave satisfactory elemental analysis and spectroscopic data (see experimental section). Like the cyclopentadienyl analog 21, compound 22 is unstable towards decarbonylation, decomposing rapidly in solution to give $[(\text{Me}_5\text{Cp})\text{Fe}(\text{CO})_2]_2$ and ditropyl. This reaction occurs slowly even at -78°C , as indicated by the colour of the reaction mixture and monitoring by infrared

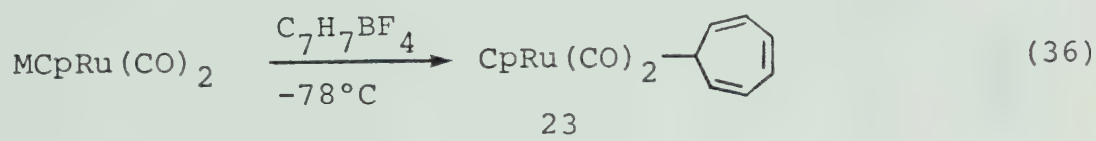
spectroscopy. When the acyl chloride is added to the solution of $\text{K}(\text{Me}_5\text{C}_5)\text{Fe}(\text{CO})_2$, the red colour of the anion is discharged and replaced by the pale yellow colour of the acyl 22. On pumping at -78°C , the yellow colour darkens to red, due to formation of $[\text{Me}_5\text{CpFe}(\text{CO})_2]_2$, which ultimately is also observable by infrared spectroscopy.

Irradiation of 22 at -78°C in pentane or in THF gave only $[\text{Me}_5\text{CpFe}(\text{CO})_2]_2$ and ditropyl. There was no evidence for $\text{Me}_5\text{CpFe}(\text{CO})(\eta^3\text{-C}_7\text{H}_7)$, a compound similar to the previously reported $\text{CpFe}(\text{CO})(\eta^3\text{-C}_7\text{H}_7)$. This result indicates that $\text{Me}_5\text{CpFe}(\text{CO})_2(7\text{-}\eta^1\text{-C}_7\text{H}_7)$, the presumed intermediate in the photolysis, has such low stability that its lifetime is too short to allow further decarbonylation before homolytic cleavage with dimer formation occurs.

Although quantitative data on Fe-C σ bond strengths is not available, the results obtained indicate that such bonds are not strong enough to overcome the stabilization of the troyl radical.

Section III. Ruthenium Compounds

Since the iron compounds that we had intended to prepare seemed to be very unstable, the analogous ruthenium species were chosen as the next synthetic objective. In marked contrast to the iron case, the reaction of $\text{KCpRu}(\text{CO})_2$ or $\text{NaCpRu}(\text{CO})_2$ with $\text{C}_7\text{H}_7\text{BF}_4$ gives quantitative formation of a monohaptocycloheptatrienyl compound (eq. 36)



M = K, Na

Infrared monitoring of the reaction shows quantitative formation of 23 (see Figure XI). Isolated yields were 50-70%. Compound 23 is extremely soluble in hydrocarbons, so complete crystallization is difficult, even at -78°C .

Thermal instability of 23 is also a problem, leading to continuous production of $[\text{CpRu}(\text{CO})_2]_2$ and ditropyl.

Quantitative measurements have not been made, but qualitative observations indicate that 23 is slightly less thermally stable than $(7-\eta^1\text{-C}_7\text{H}_7)\text{Re}(\text{CO})_5$. A half-life of ca. 36 h. at ambient temperature in C_6D_6 was observed for 23.

The ^1H NMR spectrum of 23 shows a triplet for H_7 at δ

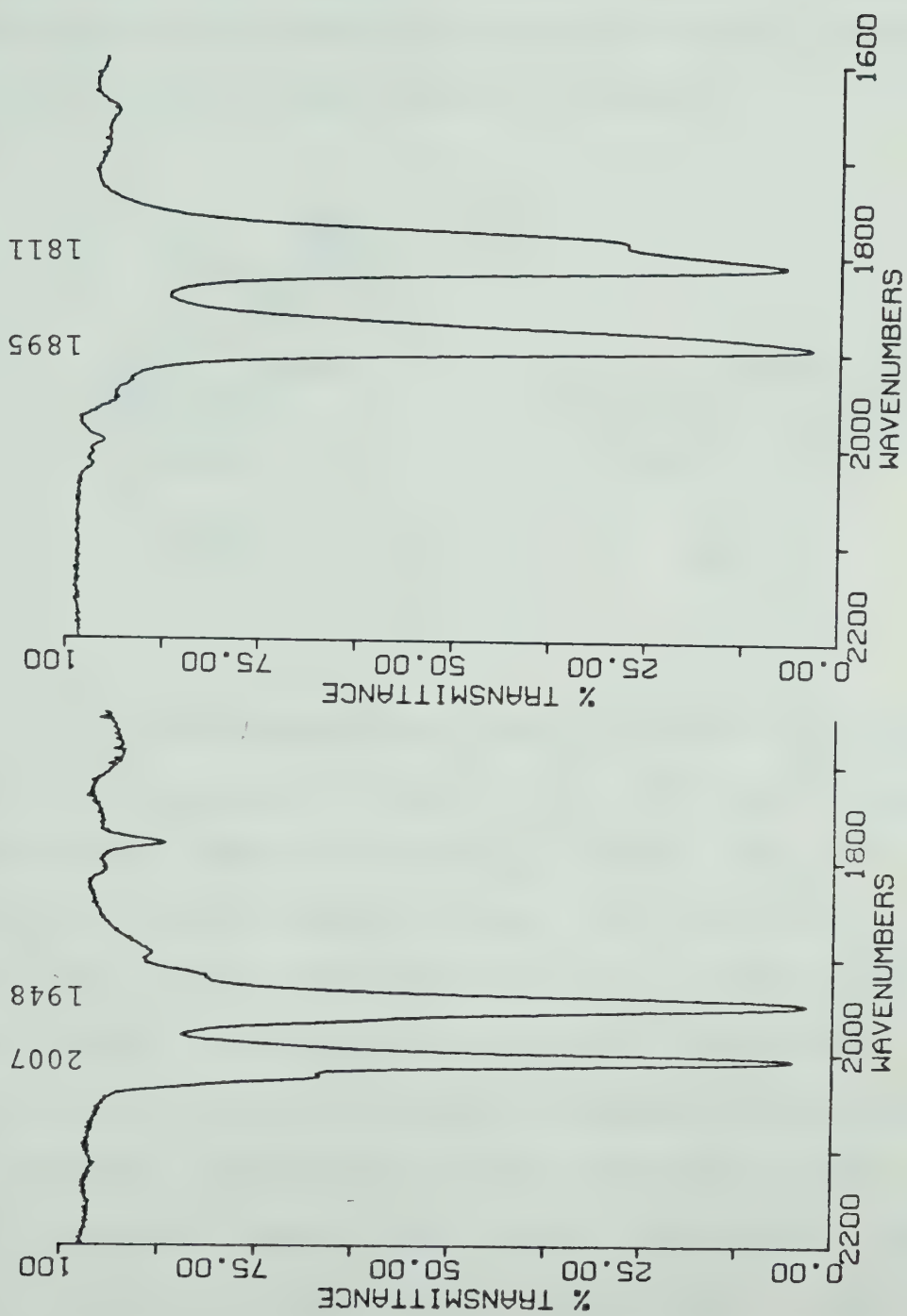
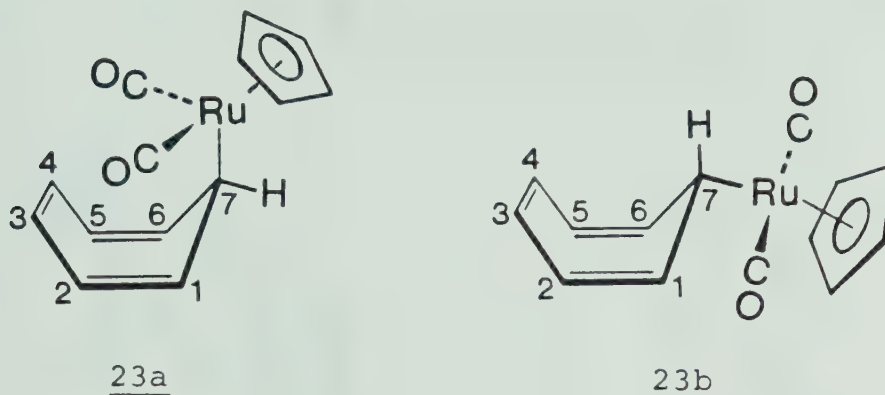


FIGURE XI. Infrared spectra of $\text{KCpRu}(\text{CO})_2$ in THF (right). After addition of $\text{C}_7\text{H}_7\text{BF}_4$ (left).

4.02 (see Figure XII). The value for $^3J_{1-7}$ is 7.8 Hz, indicating that conformer 23a predominates in solution (see Chapter II for a complete discussion of the structural implications of this coupling constant).



The infrared spectrum of 23 in cyclohexane solution shows 2 ν_{CO} bands at 2013 and 1957 cm^{-1} (see Figure XIII), similar to those of $\text{CpRu}(\text{CO})_2\text{Me}$ (2028, 1960 cm^{-1} in CS_2).¹⁰⁷ Closer examination of the spectrum of 23 reveals a shoulder on the lower frequency band. This feature is real and not due to an impurity since the position and intensity of this peak are unaffected by repeated recrystallization. A possible explanation for this phenomenon is the existence of rotational isomers with respect to the $\text{Ru}-\text{C}_7$ bond. The two rotamers are represented schematically as 23c and 23d. An example of such isomerism causing extra bands in an

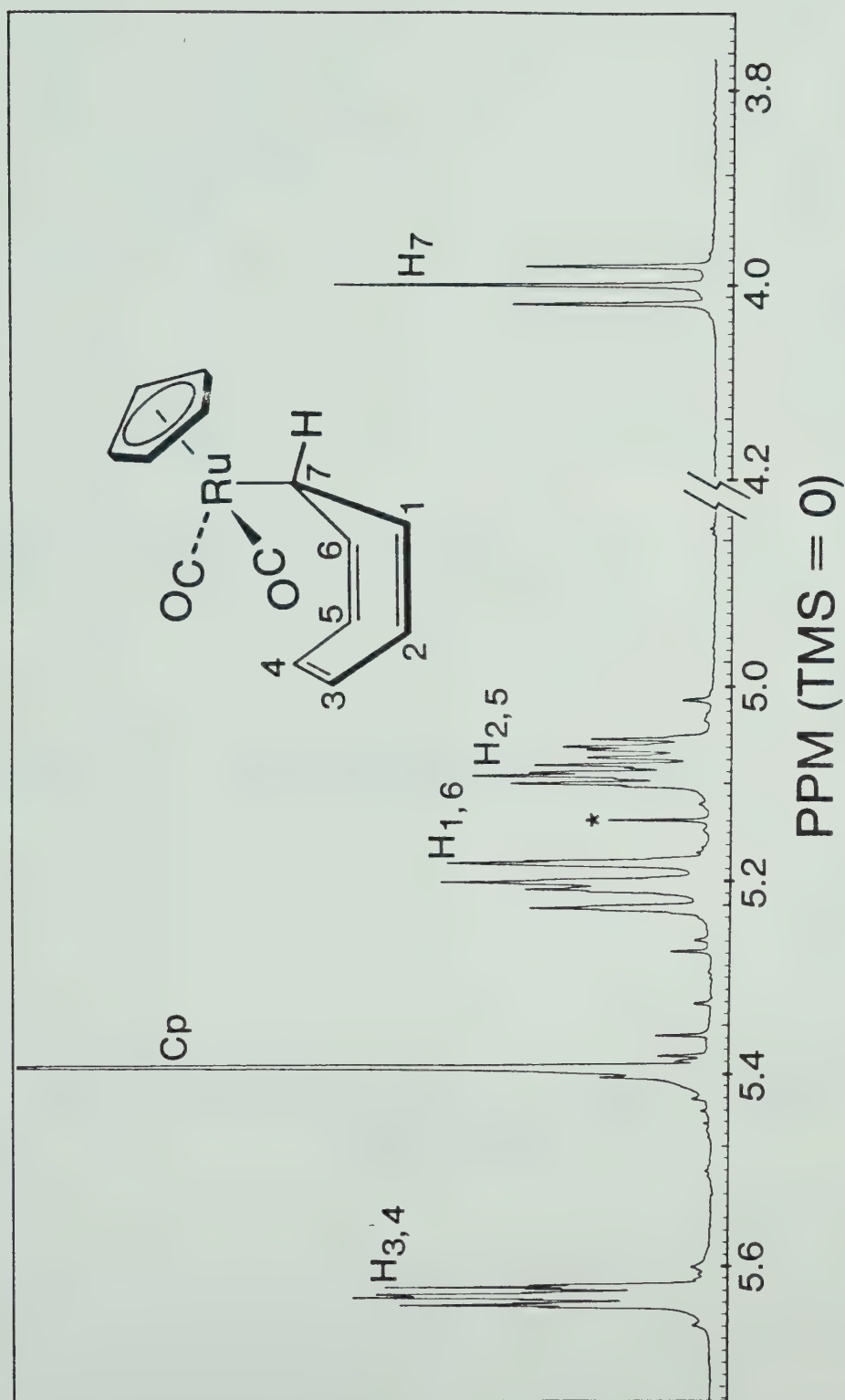


FIGURE XII. ^1H NMR spectrum of $\text{CpRu(CO)}_2(7\text{-}\eta^1\text{-C}_7\text{H}_7)$, cyclohexane- d_{12} (* = $[\text{CpRu(CO)}_2]_2$).

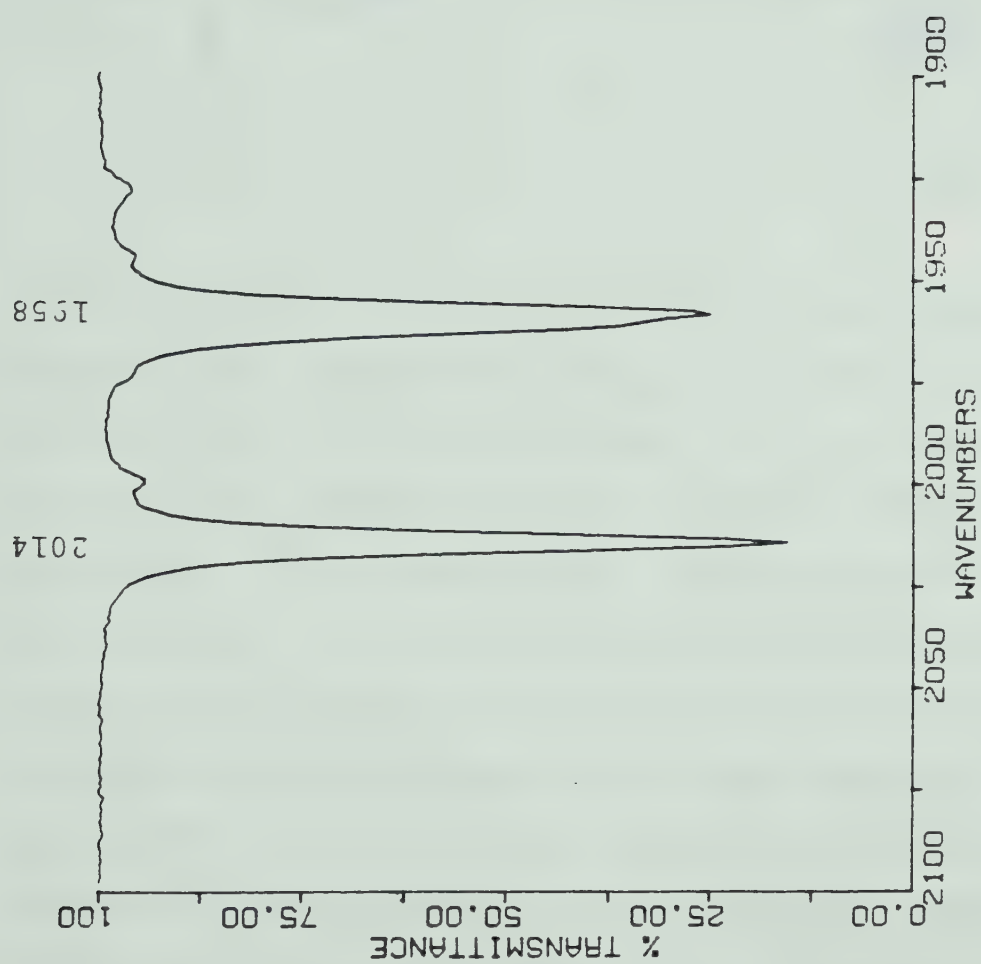
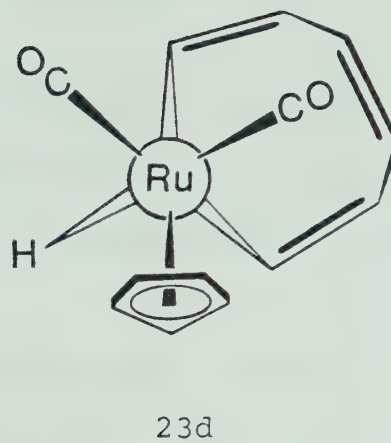
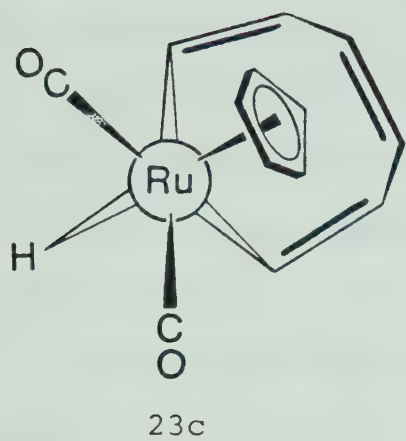


FIGURE XIII. Infrared spectrum of 23, cyclohexane.



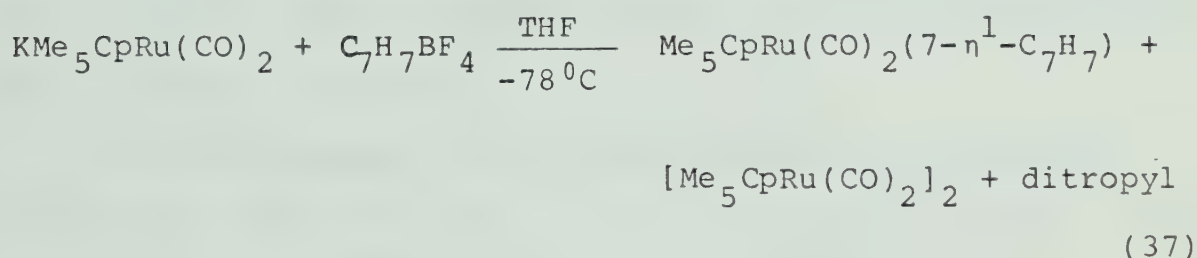
infrared spectrum is provided by the closely related alkyl compound $(\eta^5\text{-C}_5\text{H}_5)\text{Ru}(\text{CO})_2(\eta^1\text{-C}_5\text{H}_5)$, which has four ν_{CO} bands at 2030, 2023, 1976 and 1969 cm^{-1} (cyclohexane solution).¹⁰⁸ In this example, a constant difference of 7 wavenumbers is observed between the band positions of the two rotomers. This situation does not always prevail, and unequal splittings of the high and low energy bonds have been observed in compounds of the type $\text{CpFe}(\text{CO})_2\text{-SnCl}_2\text{Ph}$.¹⁰⁹ In 23, the low energy band splitting is ca. 2-3 wavenumbers, while the high energy band is unaffected, indicating a splitting of less than one wavenumber.

Further confirmation of the monohapto coordination of the cycloheptatrienyl group is provided by the mass spectrum of 23, which exhibits a molecular ion envelope at m/e 308-317 with a pattern of intensities consistent with the

composition $C_{14}H_{12}RuO_2$. Peaks due to M^+-2CO and $C_7H_7^+$ are also observed.

Compound 23 exhibits remarkable fluxional behaviour, with the metal moiety migrating around the ring by both (1,2) and (1,4) shifts. These results are discussed in Chapter VII.

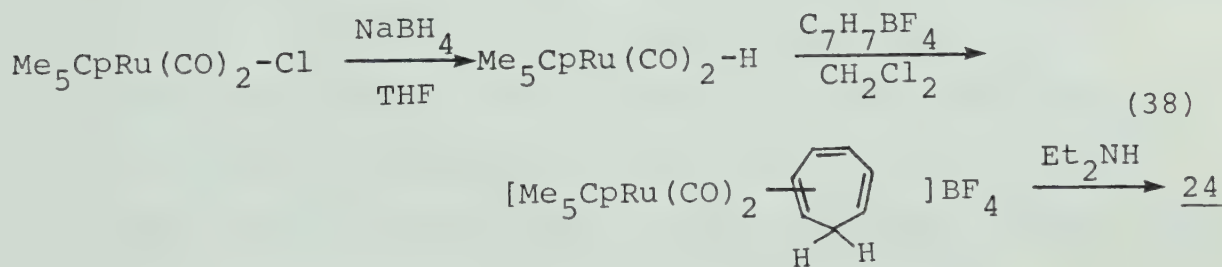
A similar reaction of $KMe_5CpRu(CO)_2$ with $C_7H_7BF_4$ affords a low yield (8%) of $Me_5CpRu(CO)_2(7-\eta^1-C_7H_7)$ (eq. 37).



Compound 24 has been fully characterized by NMR, infrared, mass spectroscopy and elemental analysis. Interestingly, the infrared spectrum of 24 shows only two ν_{CO} bands at 1997 and 1944 cm^{-1} (cyclohexane). There is no evidence for the presence of more than one rotational isomer. This is probably the result of the steric bulk of the pentamethylcyclopentadienyl group, which renders only one rotamer (perhaps analogous to 23d) energetically accessible.

The ^1H NMR spectrum of 24 is very similar to that of the cyclopentadienyl analog 23, but there are also some interesting differences. The H_7 resonance is found at δ 3.04, which is ca. 1 ppm upfield from the position of the H_7 resonance in 23. This is consistent with the electron donating ability of the five methyl groups in 24 causing greater shielding of H_7 . Slight differences in the geometry of the seven-membered ring are indicated by the value of $^3\text{J}_{1-7} = 7.4$ Hz for 24, and the resolution of $^4\text{J}_{2-7} = 1.0$ Hz. In 23, H_7 gave a simple triplet with $^3\text{J}_{1-7} = 7.8$ Hz and $^4\text{J}_{2-7}$ was not resolved.

An improved yield of 24 was achieved by an indirect route (eq. 38).



Separation of 24 from large quantities of ditropyl was avoided by using this preparative route. As discussed in Chapter IV, hydride abstraction by tropylium followed by deprotonation of the intermediate cycloheptatriene cation was employed by Sweet and Graham to prepare $\text{CpRe}(\text{CO})(\text{NO})(7\text{-}\eta^1\text{-C}_7\text{H}_7)$.⁹² The same method has been employed by Graham and Hoyano to prepare osmium analogs of 23 and 24.¹¹⁰ In this case the yield of 24 was 19% (based on $\text{Me}_5\text{CpRu}(\text{CO})_2\text{Cl}$).

Section IV. Mechanistic Considerations

It is instructive to consider the reason for the poor yield of 24 in the reaction of $\text{KMe}_5\text{CpRu}(\text{CO})_2$ with $\text{C}_7\text{H}_7\text{BF}_4$. Monitoring of this reaction by infrared spectroscopy showed substantial formation of $[\text{Me}_5\text{CpRu}(\text{CO})_2]_2$, (ca. 50%) along with 24. The amount of dimer formed may actually be higher, since its low solubility in cold THF will cause some of the dimer to precipitate from solution. The actual isolated yield of 24 was reduced by the necessity for multiple recrystallization to separate 24 from the large amount of ditropyl which is formed.

This result contrasts sharply with the nearly quantitative formation of alkyl 23 which was observed in the reaction of $\text{KCpRu}(\text{CO})_2$ with $\text{C}_7\text{H}_7\text{BF}_4$ (see Figure XI). Although quantitative results have not been obtained, qualitative observations indicate that 23 and 24 have similar thermal stabilities, so the difference in the course of these reactions must be otherwise explained.

It should be pointed out that all the isolable monohaptocycloheptatrienyl compounds that are discussed in this thesis are only kinetically stable. The products of thermodynamic equilibrium are ditropyl and M-M dimer. All isolable compounds depend for their limited stability on a low rate of M-C bond homolysis.

The mechanism of the reaction of metal carbonyl anions with the tropylium cation is not entirely understood. San Fillipo and Krusic have shown that the reaction of NaCpFe(CO)_2 with the more reactive alkyl halides proceeds via a mixture of $\text{S}_{\text{N}}2$ substitution and electron transfer to give radicals, which then combine to give metal alkyls.^{111,112}

In the case of reactions with tropylium cation, a wide variety of metal carbonyl anions including NaCpFe(CO)_2 , NaMn(CO)_5 , NaCpMo(CO)_3 and NaCo(CO)_4 were found to give rise to tropyl radicals (detected by ESR spectroscopy). These observations could not be quantified, so the relative importance of $\text{S}_{\text{N}}2$ versus electron transfer reaction is not known. A further uncertainty in the interpretation of these results arises when the instability of the expected alkyl products is considered. The observed tropyl radicals may arise from rapid homolytic cleavage of very unstable $\text{M}-(\eta^1\text{-C}_7\text{H}_7)$ alkyls. The reaction of NaCpFe(CO)_2 under the same conditions with benzyl bromide and allyl bromide gave rise to strong spectra of benzyl and allyl radicals, respectively. In these reactions, the iron alkyl products formed are known to be stable, so the observed radicals must be the product of an electron transfer from the carbonyl anion. Since benzyl bromide is less readily reduced than

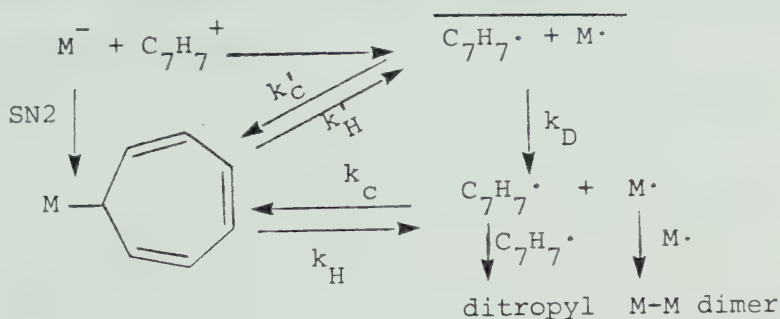
tropylium cation¹¹³, the troyl radicals observed in the ESR experiments are probably the result of electron transfer. Again, it must be emphasized that the relative importance of this pathway compared to the direct substitution reaction is not known.

The infrared spectrum of $\text{KCpRu}(\text{CO})_2$ in THF consists of two ν_{CO} bands at 1895 and 1811 cm^{-1} . The spectrum of the sodium analog is similar, with two bands at 1905 and 1824 cm^{-1} . Some difference in anion-cation interaction is indicated, but the difference between these two salts does not seem to affect the outcome of their reaction with $\text{C}_7\text{H}_7\text{BF}_4$, since both are converted quantitatively to the alkyl 23. The infrared spectrum of $\text{KMe}_5\text{CpRu}(\text{CO})_2$ in THF is more complex, with four ν_{CO} bands at 1876, 1792, 1866 and 1768 cm^{-1} . Similar observation of more than the two ν_{CO} bands expected in the case of $\text{NaCpFe}(\text{CO})_2$, in conjunction with other data, was interpreted in terms of tight ion pairs and solvent separated ion pairs.¹¹⁴

Two explanations for the different reactivities of these two ruthenium carbonyl anions are possible. If the reaction with tropylium cation is predominantly a substitution reaction, the ion pairing indicated by infrared spectroscopy in solutions of $\text{KMe}_5\text{CpRu}(\text{CO})_2$ may reduce the rate of this substitution reaction. The large amounts of

ditropyl and dimer could be formed from radicals generated by electron transfer. An alternative explanation is that both reactions occur primarily by electron transfer, perhaps via initial formation of a solvent caged radical pair. Less efficient productive radical recombination in this solvent cage and greater diffusion out of the cage could account for the low yield of 24. These possible reactions are summarized in Scheme I.

SCHEME I



k_D = rate of diffusion out of the solvent cage to give free radicals.

k'_C = rate of productive combination in the solvent cage.

k'_H = rate of M-C bond homolysis to give radicals in a solvent cage.

k_C = rate of productive combination of free radicals.

k_H = rate of homolysis to free radicals.

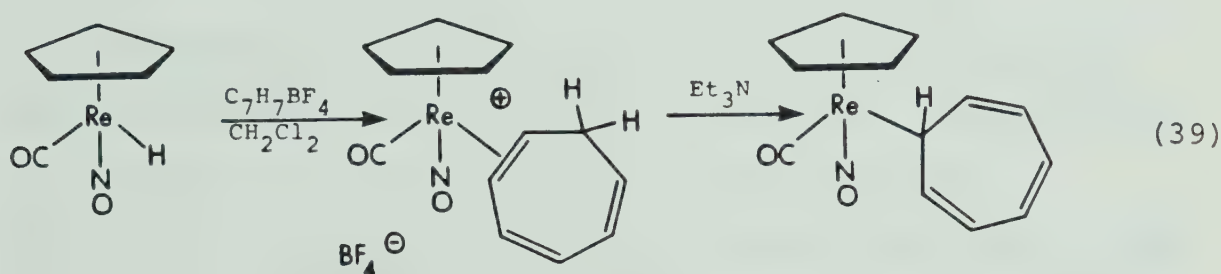
There is no evidence to decide which of these pathways is predominant, but two facts are clear from a consideration

of this scheme:

- 1) the large amounts of ditropyl and dimer observed in the reaction of $\text{KMe}_5\text{CpRu}(\text{CO})_2$ with $\text{C}_7\text{H}_7\text{BF}_4$ are not explicable in terms of an exclusive $\text{S}_\text{N}2$ reaction.
- 2) any alkyl $\text{M}-(7-\eta^1-\text{C}_7\text{H}_7)$ which is isolable, should be obtainable by the direct reaction of the appropriate metal carbonyl anion with tropylium. If this reaction fails, indirect methods are unlikely to succeed, since k_H (or k_H') is probably quite large, due to low metal-carbon bond strength.

Section V. Preparation of Monohaptocycloheptatrienyl Alkyls
With Asymmetric Metal Centers

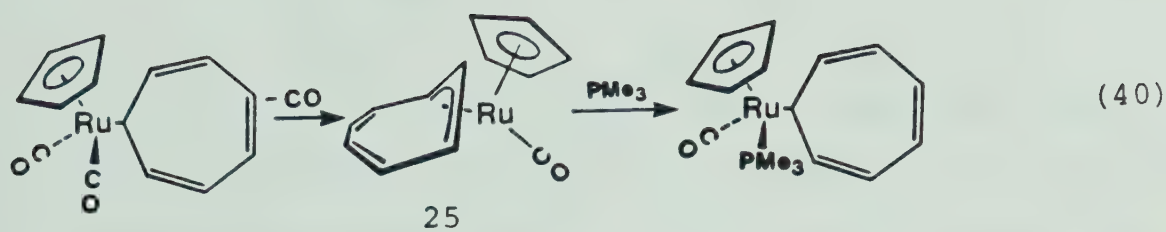
In order to investigate the stereochemistry of the metal migrations observed in the monohaptocycloheptatrienyl alkyl compounds, a probe of optical activity at the metal center is required. A compound of this type has been reported by Sweet and Graham⁹² (eq. 39).



This compound shows excellent thermal and oxidative stability. Unfortunately, it exhibits no fluxional behaviour, even at elevated temperatures.

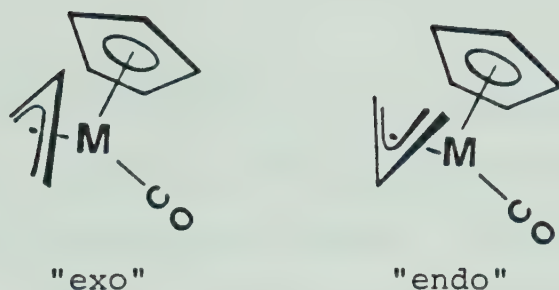
In view of the established stability of the alkyls of ruthenium described in the previous section and the pseudo-tetrahedral nature of the metal center, compounds of the type $\text{CpRu}(\text{CO})(\text{P})(7-\eta^1\text{-C}_7\text{H}_7)$ were our initial synthetic objective ($\text{P} = \text{PMe}_3$ or PMe_2Ph).

Since we were successful in converting trihapto rhenium complexes to monohapto alkyls using PMe_3 (as described in Chapter III), the reaction scheme outlined in eq. 40 extending this reaction to ruthenium seems reasonable.

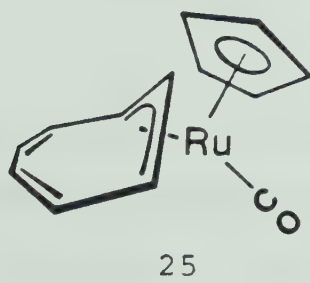


Compound 25 was prepared by photochemical or Me_3NO induced decarbonylation of 23, and was fully characterized by infrared, NMR, mass spectroscopy and elemental analysis. The infrared spectrum exhibits only one ν_{CO} band at 1971 cm^{-1} (cyclohexane). The reported infrared spectrum of $\text{CpFe}(\text{CO})(\eta^3\text{-C}_7\text{H}_7)$ consists of a single ν_{CO} band at 1959 cm^{-1} (cyclohexane).¹⁰¹

Both the iron and ruthenium compounds could exist as two conformational isomers. Such isomerism has been reported for $\text{CpFe}(\text{CO})(\eta^3\text{-C}_3\text{H}_5)$ ¹¹⁵ and $\text{CpRu}(\text{CO})(\eta^3\text{-C}_3\text{H}_5)$ ⁴⁴ which both have two ν_{CO} absorptions in their infrared spectra and two sets of ^1H NMR resonances. The two isomers involved differ only in orientation of the allyl groups.



For $M = \text{Fe}$, the equilibrium between these two isomers has been studied for the simple allyl compound and a variety of substituted derivatives.¹¹⁵ In all cases studied, the "exo" isomer is more stable. From steric considerations, the most likely structure of 25 is the exo isomer:

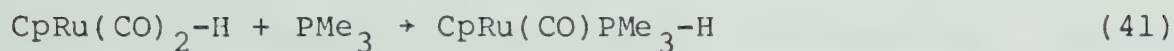


The ^1H NMR spectrum (-20°C , $\text{THF-}d_8$) of 25 shows only one Cp resonance and the four resonances expected for the trihaptocycloheptatrienyl group (see experimental section for details). Compound 25 is fluxional, with the metal group migrating around the ring via (1,2) shifts. This process is discussed in more detail in Chapter VIII.

When compound 25 was combined with excess PMe_3 in hexane, no reaction was observed, even after 24 hours refluxing in hexane. This result is in marked contrast to the ready reactivity of compounds such as $(\eta^3\text{-C}_7\text{H}_7)\text{Re}(\text{CO})_4$,

which are easily converted to the monohapto species.

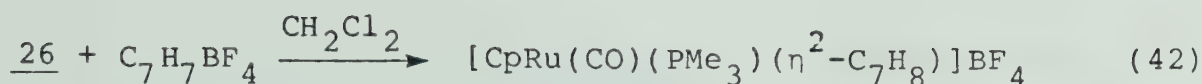
The next synthetic route explored was to approach the problem via a substituted hydride. The reaction of $\text{CpRu}(\text{CO})_2\text{-H}$ with PPh_3 to give $\text{CpRu}(\text{CO})(\text{PPh}_3)\text{-H}$ was reported by Knox and Humphries in 1975.¹¹⁶ When a similar reaction was carried out using PMe_3 , an analogous monocarbonyl hydride was obtained (eq. 41).



26

This hydride has been fully characterized. In the infrared spectrum of a cyclohexane solution of 26, a single ν_{CO} at 1931 cm^{-1} with a shoulder at ca. 1940 cm^{-1} was observed. The reported infrared spectrum of $\text{CpRu}(\text{CO})\text{PPh}_3\text{-H}$ (hexane solution) consists of a single broad peak at 1937 cm^{-1} .¹¹⁶ The shoulder at 1940 cm^{-1} in the spectrum of 26 persists after recrystallization or sublimation of the product. This feature was ultimately identified as the Ru-H stretch by the observation of a strong band at 1943 cm^{-1} in the Raman spectrum of 26.

When 26 was reacted with $\text{C}_7\text{H}_7\text{BF}_4$, hydride abstraction occurred to give a $\eta^2\text{-C}_7\text{H}_8$ cation 27 (eq. 42).



Cation formation was indicated by the appearance of a new ν_{CO} band at 1997 cm^{-1} . Attempts to isolate this cation by precipitation with ether led to displacement of cycloheptatriene. When a concentrated solution of 27 in CD_2Cl_2 (ca. 100 mg/mL) was stored at -78°C for 7 days, a yellow precipitate was deposited. ^1H NMR spectra of the supernatant showed increased amounts of free C_7H_8 . Analysis (C,H) of the precipitate was not consistent with the formulation of 27. Free C_7H_8 could arise by formation of a BF_4 complex, $\text{CpRu}(\text{CO})(\text{PMe}_3)\text{BF}_4$. The carbon content of the precipitate was intermediate between the value expected for 27 and the value calculated for $\text{CpRu}(\text{CO})(\text{PMe}_3)\text{BF}_4$ (see Experimental section).

Support for the proposed structure of 27 is provided by the ^1H NMR spectrum (see Figure XIV). There are two singlets of equal intensity due to $(\eta^5\text{-C}_5\text{H}_5)$ groups at δ 5.295 and 5.382 ppm. Similarly, two doublets due to PMe_3 groups are observed at 1.716 and 1.591 ppm ($^2J_{\text{H-P}} = 10.7$ and 10.4 Hz, respectively). The sixteen signals expected for the cycloheptatriene protons of the two diastereomers 27a and 27b were not completely resolved. Only nine signals

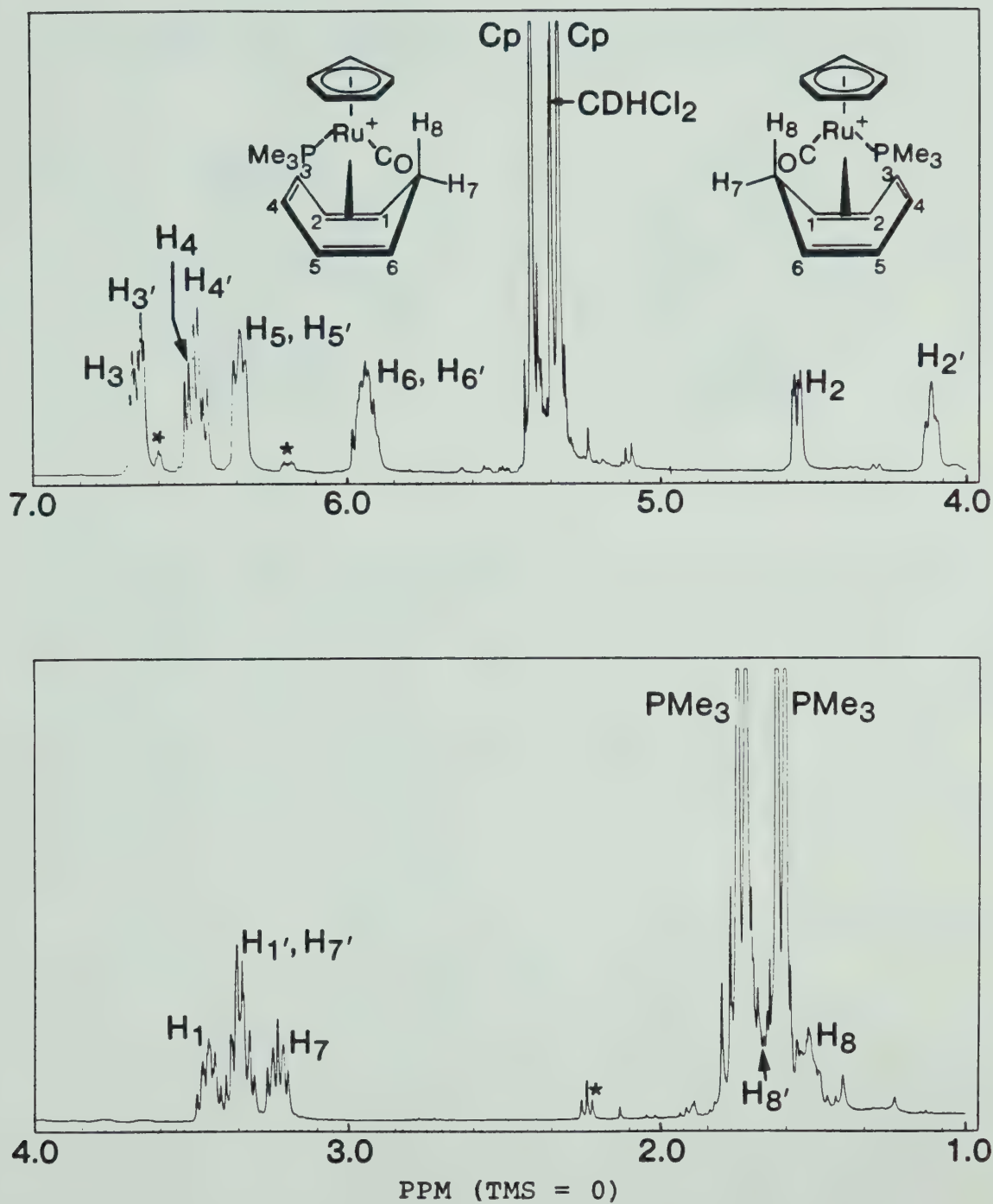
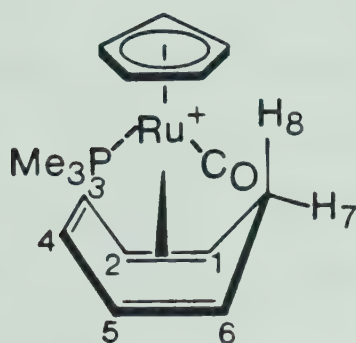
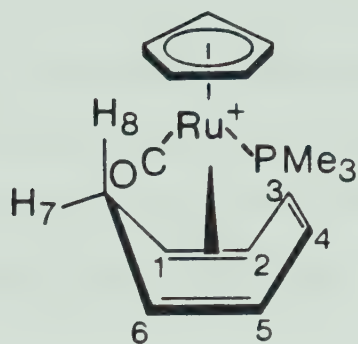


FIGURE XIV. ^1H NMR spectrum of $\text{CpRu}(\text{CO})(\text{PMe}_3)(1,2-\eta^2-\text{C}_7\text{H}_8)$, CD_2Cl_2 (* = free C_7H_8).

were observed.* Two more (H_8 and H_8') were located



27a



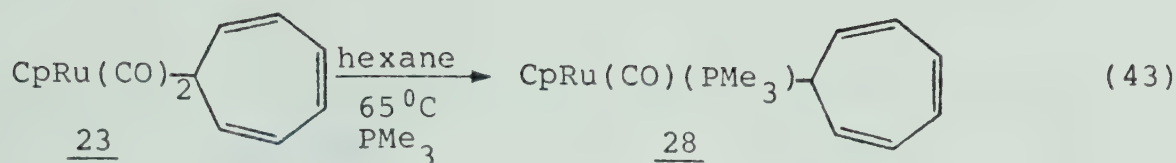
27b

underneath the PMe_3 signals be decoupling experiments. Other signals are obscured by coincidental overlap and small diastereotopic shifts. The assignments shown in the figure are based on eleven decoupling experiments. The NMR spectrum of 27 is similar to that reported by Sweet for $CpRe(CO)(NO)(\eta^2-C_7H_8)BF_4$.¹¹⁷

Attempts to deprotonate 27 with a variety of bases did not afford an alkyl compound. Instead, free cycloheptatriene was formed (detected by 1H NMR).

The phosphine substituted alkyl derivatives were ultimately obtained by a simple thermal substitution reaction of the dicarbonyl compound 23 (eq. 43).

* Only one enantiomer of each diastereomer is shown.



Compound 28 was identified by a single ν_{CO} band at 1920 cm^{-1} . This phosphine substitution reaction does not proceed via a trihapto intermediate since it has been shown that $\text{CpRu(CO)(}\eta^3\text{-C}_7\text{H}_7\text{)}$ does not react with PMe_3 under similar conditions.

Similar results were obtained when PMe_2Ph was employed, to afford $\text{CpRu(CO)(PMe}_2\text{Ph)(7-}\eta^1\text{-C}_7\text{H}_7\text{)}$ (29). Both 28 and 29 exhibit diastereotopic shifts of the C_7H_7 ring protons in the ^1H NMR spectra. The methyl groups of the PMe_2Ph ligand in 29 are also diastereotopic. The partial 400 MHz ^1H NMR spectrum of 29 (cyclohexane- d_{12}) is shown in Figure XV. The olefinic protons were assigned by decoupling experiments. The assignment of H_1 or H_6 is arbitrary, but once this choice is made, all other assignments are sequential around the ring. The magnitude of the chemical shift differences between diastereotopic proton pairs in both 28 and 29:

$|\delta \text{H}_1 - \delta \text{H}_6| > |\delta \text{H}_3 - \delta \text{H}_4| > |\delta \text{H}_2 - \delta \text{H}_5|$. These results are consistent with the observations of Sweet and Graham for $\text{CpRe(CO)(NO)(7-}\eta^1\text{-C}_7\text{H}_7\text{)}$.⁹²

The value for the vicinal coupling constant $^3\text{J}_{1-7}$ in 28 is 7.5 Hz ($^3\text{J}_{1-7} = 7.2 \text{ Hz}$ in 29). As discussed in Chapter

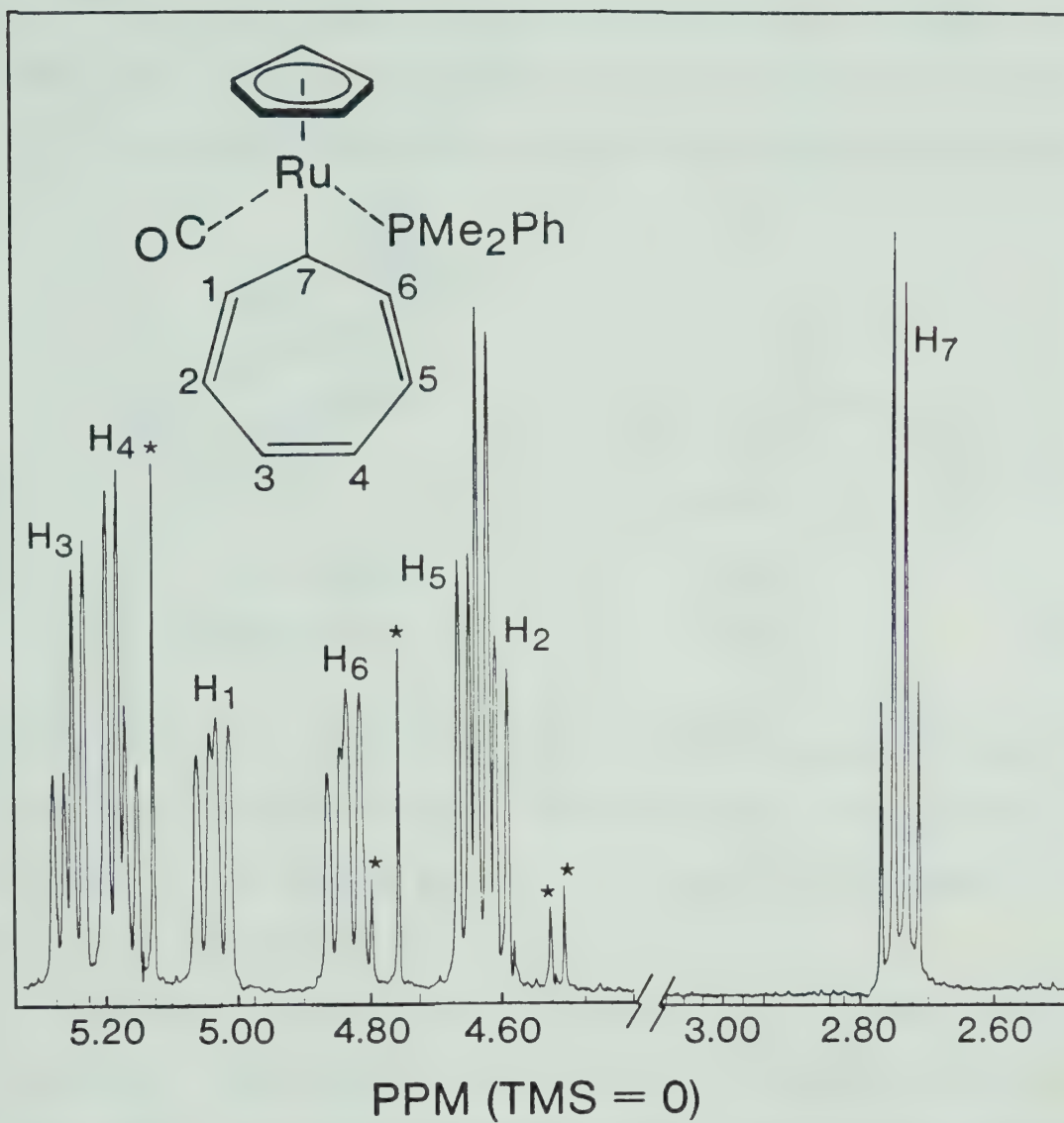
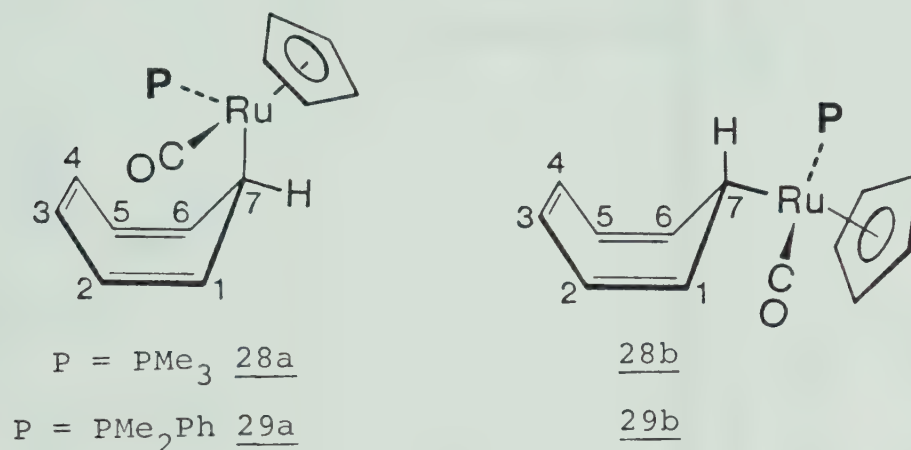


FIGURE XV. Partial ^1H NMR spectrum of $\text{CpRu(CO)(PMe}_2\text{Ph)-(7-}\eta^1\text{-C}_7\text{H}_7\text{)}$, cyclohexane- d_{12} (* = Cp resonances due to impurities).

II, this large value for the vicinal coupling constant indicates that one conformer (28a or 29a) predominates. This conclusion is consistent with the observed chemical



shift differences between pairs of diastereotopic protons. The closer the protons are to the chiral metal center, the greater is the difference in the magnetic environment on the two sides of the ring.

Similar effects are observed in the ^{13}C NMR spectra of 28 and 29. The olefinic region of the ^{13}C NMR spectrum of 28 (100.6 MHz) is shown in Figure XVI. Assignments are based on selective proton decoupling experiments. In the case of C_2 and C_5 , it was not possible to decouple H_2 without affecting H_5 , due to the small chemical shift difference between these protons. The assignment was made by carrying out ten different selective proton decoupling experiments, stepping the decoupler position through the H_2 and H_5

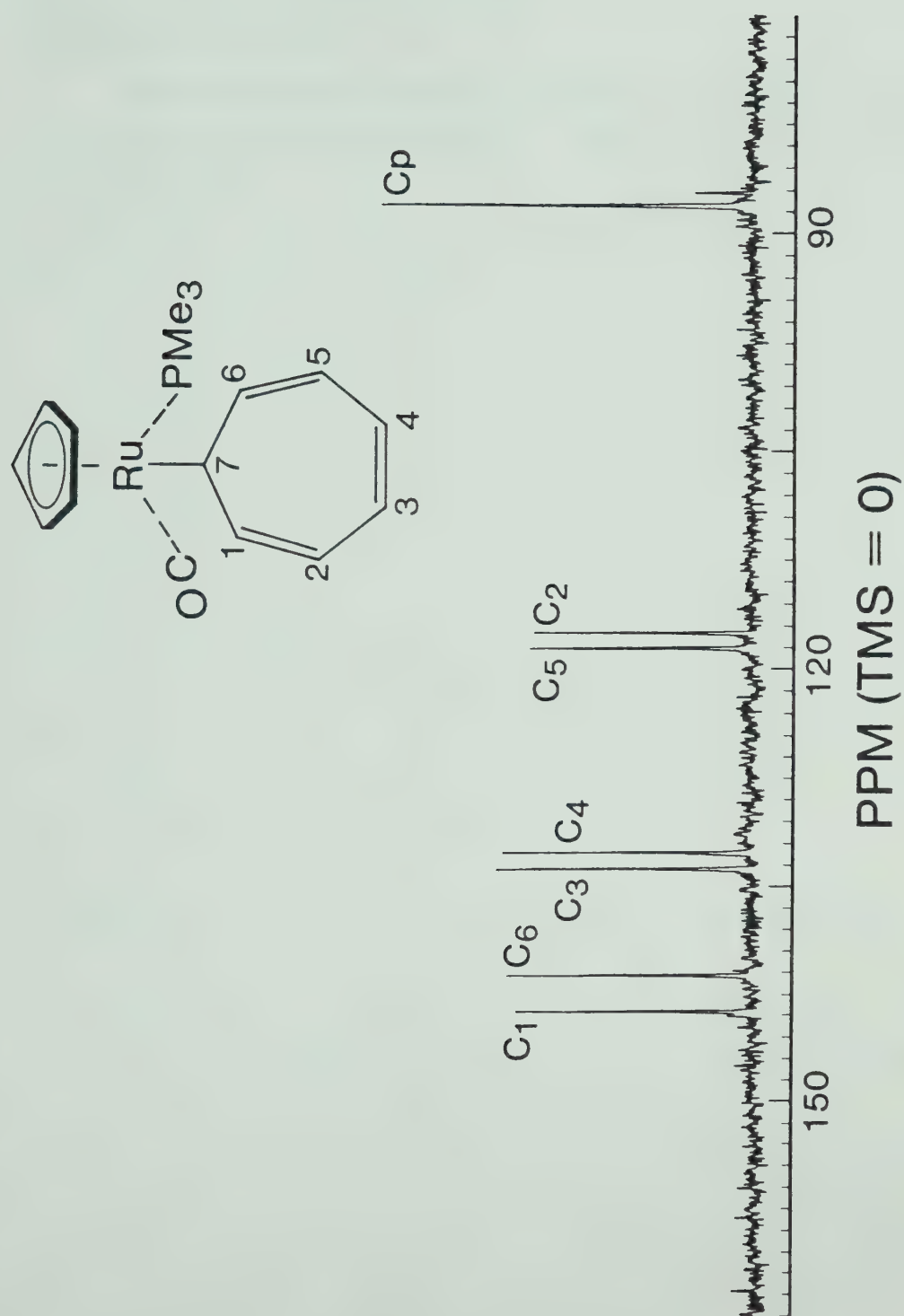


FIGURE XVI. Partial ^{13}C NMR spectrum of $\text{CpRu(CO)(PMe}_3\text{)(7-}\eta^1\text{-C}_7\text{H}_7\text{)}$, cyclohexane- d_{12} .

resonances. Similar procedures were used to assign the ^{13}C spectrum of 29.

{ The fluxional behaviour of 29 has been investigated by ^{13}C and ^1H NMR experiments. These results are discussed in Chapter VII.

Section VI. Experimental

$\text{Fe}(\text{CO})_5$, $[\text{CpFe}(\text{CO})_2]_2$, PMe_3 , PMe_2Ph , diphos and pentamethylcyclopentadiene were purchased from Strem Chemicals. $\text{C}_7\text{H}_7\text{BF}_4$ was purchased from Aldrich Chemicals. $\text{CpFe}(\text{CO})_2\text{Br}$ was prepared from the dimer by the method of Pauson and Hallam.¹¹⁸ $\text{CpFe}(\text{diphos})\text{Br}$ was prepared from the dicarbonyl using the procedure of King et al.¹¹⁹ $[\text{Me}_5\text{CpFe}(\text{CO})_2]_2$ was prepared from $\text{Fe}(\text{CO})_5$ by the method of King.¹²⁰ $\text{Ru}_3(\text{CO})_{12}$ was prepared by the Pomeroy modification¹²¹ of the Inorganic Syntheses method¹²² or purchased from Strem Chemicals. $[\text{CpRu}(\text{CO})_2]_2$ was prepared according to the procedure of Knox and Humphries.¹¹⁶ Na/K (20:80) was prepared by melting the metals together in a Schlenk tube under nitrogen.

Reaction of $\text{CpFe}(\text{diphos})\text{MgBr} \cdot 2\text{THF}$ with $\text{C}_7\text{H}_7\text{BF}_4$

$\text{CpFe}(\text{diphos})\text{MgBr} \cdot 2\text{THF}$ (300 mg, 0.40 mmol) prepared by the method of Meunier et al.¹⁰³ was dissolved in 15 mL THF. The red solution was cooled to -78°C . $\text{C}_7\text{H}_7\text{BF}_4$ (72 mg, .40 mmol) was added. After 2 h. stirring at -78°C , the solution had turned black. Removal of the solvent at -10°C gave a black residue, identified by ^1H NMR as a mixture of ditropyl and $\text{CpFe}(\text{diphos})\text{Br}$.

Preparation of $[\text{Me}_5\text{CpRu}(\text{CO})_2]_2$

$\text{Ru}_3(\text{CO})_{12}$ (1.28 g, 2 mmol) was dissolved in 200 mL of n-octane. Me_5CpH (2 mL, 10 mmol) was added. After 16 h. reflux, the solution was cooled to room temperature, depositing large orange crystals, which were isolated by syringing off the supernatant, then washing with 3×5 mL THF, then 3×5 mL pentane. Yield: 550 mg. The supernatant solution was refluxed for a further 8 hours. The same procedure allowed recovery of a further 500 mg of product from this solution. Overall yield 1.05 g (60%). Analysis: Calcd. for $\text{C}_{24}\text{H}_{30}\text{Ru}_2\text{O}_4$: C, 49.31; H, 5.17. Found: C, 49.49; H, 5.08. The literature procedure afforded a 32% yield after chromatography.¹²³

Preparation of $\text{Me}_5\text{CpRu}(\text{CO})_2\text{-Cl}$

$[\text{Me}_5\text{CpRu}(\text{CO})_2]_2$, (175 mg, 0.3 mmol) was dissolved in 100 mL of CCl_4 . The solution was stirred under ambient fluorescent light for 24 h. After removal of CCl_4 , the brown residue was chromatographed on Florisil (2 cm \times 5 cm column) with CH_2Cl_2 as eluant. The product was recrystallized from CH_2Cl_2 /heptane to afford the chloride as a bright yellow crystalline solid, mp 120°C (dec). Yield: 150 mg (76%). IR: (cyclohexane, ν_{CO} , cm^{-1}) 2033, 1984. ^1H NMR (cyclohexane- d_{12} , 25°C, δ) 1.86 s. Anal.: Calcd. for

$C_{12}H_{15}RuO_2Cl$: C, 43.97; H, 4.61. Found: C, 43.86; H, 4.59.

Preparation of $Me_5CpRu(CO)_2-H$

Method (a). The supernatant solution from the preparation of $[Me_5CpRu(CO)_2]_2$ was evaporated to give a deep red oil which was chromatographed on Florisil (3 cm \times 15 cm) with heptane elution to give a fraction containing Me_5CpH followed by a fraction containing the hydride. Evaporation of heptane followed by sublimation at 65°C (0.1 mm) onto a water cooled probe afforded $Me_5CpRu(CO)_2H$ as a colourless crystalline solid, mp 41°C (75 mg). IR (cyclohexane, ν_{CO} , cm^{-1}): 2013, 1954. 1H NMR (cyclohexane d_{12} , 25°C, δ): 2.01 (s, 15H, Me_5Cp), -10.6 (s, 1H, Ru-H). Anal: Calcd. for $C_{12}H_{16}RuO_2$: C, 49.14; H, 5.50. Found: C, 49.38; H, 5.15.

Method (b). $Me_5CpRu(CO)_2-Cl$ (130 mg, 0.4 mmol) was dissolved in 25 mL THF. $NaBH_4$ (40 mg, 1 mmol) was added, followed by 1 mL of water. The mixture was stirred for 6 h., then pumped dry to give an off-white residue. Sublimation at 60°C onto a water cooled probe afforded 95 mg of $Me_5CpRu(CO)_2H$ (81%) identical to the product of method (a).

Preparation of $\text{CpFe(CO)}_2\text{-}\overset{\text{O}}{\parallel}\text{C-C}_7\text{H}_7\text{-}$ (21)

$[\text{CpFe(CO)}_2]_2$ (345 mg, 1 mmol) in 50 mL THF was reduced (2 h.) with 25% excess 1% Na/Hg, filtered and cooled to -78°C . $\text{C}_7\text{H}_7\text{-}\overset{\text{O}}{\parallel}\text{C-Cl}$ (308 mg, 2 mmol) was added. The red colour of the anion was discharged immediately to give a yellow solution. The infrared spectrum had ν_{CO} bands at 2020, 1956 and 1652 cm^{-1} . On warming or pumping to reduce the volume of THF, the solution turned dark red, and the infrared spectrum indicated formation of $[\text{CpFe(CO)}_2]_2$. Attempts to form this acyl compound and photochemically decarbonylate it in situ at -78°C gave only $[\text{CpFe(CO)}_2]_2$. There was no evidence for formation of $\text{CpFe(CO)}(\eta^3\text{-C}_7\text{H}_7)$.

Preparation of $\text{Me}_5\text{CpFe(CO)}_2\text{-}\overset{\text{O}}{\parallel}\text{C-C}_7\text{H}_7\text{-}$ (22)

$[\text{Me}_5\text{CpFe(CO)}_2]_2$ (50 mg, .1 mmol) was stirred in 25 mL THF with .1 mL (80 mg) of Na/K for 3 h. The deep red anion solution was filtered and cooled to -78°C . 31 mg (.2 mmol) of $\text{C}_7\text{H}_7\text{-}\overset{\text{O}}{\parallel}\text{C-Cl}$ was added. The solution immediately turned yellow. The THF was pumped off at -78°C over 24 h. The residue was extracted at -78°C with 10 mL of pentane saturated with CO. The yellow solution was filtered and concentrated by pumping at -78°C to ca. 2 mL. A yellow precipitate was deposited. Yield: 8 mg (21%). IR (pentane, ν_{CO} , cm^{-1}): 2008, 1953, 1656. Mass spectrum: (14 ev, 55°C) highest m/e corresponds to M^+-3CO . Anal:

calcd. for $C_{20}H_{22}FeO_3$: C, 65.69; H, 6.06. Found: C, 66.78; H, 6.56. Attempts to prepare $Me_5CpFe(CO)(\eta^3C_7H_7)$ by UV irradiation of this acyl compound at $-78^\circ C$ were not successful. Only $[Me_5CpFe(CO)_2]_2$ was formed.

Reactions of iron anions with $C_7H_7BF_4$

Reaction of $NaCpFe(CO)_2$, $NaMe_5CpFe(CO)_2$ or $KMe_5CpFe(CO)_2$ with $C_7H_7BF_4$ in THF at $-78^\circ C$ gave only the respective dimers and ditropyl. The reactions were worked up by pumping off the THF below $-50^\circ C$, then extracting the residues at $-50^\circ C$ with pentane. Only the dimers were found in the pentane extracts, even though more soluble mononuclear compounds such as $CpFe(CO)(\eta^3-C_7H_7)$ should be extracted preferentially. 1H NMR of the pentane extracts showed only ditropyl and dimer. (NMR samples were prepared by evaporation to dryness, then dissolving the residue in CD_2Cl_2 at room temperature. Spectra were taken immediately.)

Preparation of $CpRu(CO)_2(7-\eta^1-C_7H_7)$ (23)

$[CpRu(CO)_2]_2$, (222 mg, 0.5 mmol) in 50 mL THF was stirred vigorously with excess 1% Na/Hg for 4 h.¹²⁴ The solution was filtered and cooled to $-78^\circ C$. $C_7H_7BF_4$ (178 mg, 1 mmol) was added. The solution was stirred for 30 min at

-78°C. The THF was pumped off at 0°C. The residue was extracted with 2 × 15 mL pentane and the extracts were filtered and cooled to -78°C to afford an orange precipitate, mp 47°C. Yield: 180 mg (57%). IR (cyclohexane, ν_{CO} , cm^{-1}): 2013 s, 1960 sh, 1957 s. Anal: calcd. for $\text{C}_{14}\text{H}_{12}\text{RuO}_2$: C, 53.67; H, 3.86. Found: C, 53.63; H, 3.86. Mass spectrum (14 eV, 25°C): M^+ , $\text{M}^+ - \text{CO}$, $\text{M}^+ - 2\text{CO}$, C_7H_7^+ (base peak). ^1H NMR (cyclohexane- d_{12} , 20°C, δ): 5.40 (s, 5H, Cp), 5.64 (m, 2H, $\text{H}_{3,4}$), 5.22 (m, 2H, $\text{H}_{1,6}$), 5.10 (m, $\text{H}_{2,5}$), 4.02 (t, H_7 , $^3\text{J}_{\text{H}_1-\text{H}_7} = 7.8$ Hz); ^{13}C NMR: (THF- d_8 , 20°C, δ): 202.7 (CO), 140.8 (2C, $\text{C}_{1,6}$), 135.0 (2C, $\text{C}_{3,4}$), 122.9 (2C, $\text{C}_{2,5}$), 89.9 (5C, Cp), 19.5 (1C, C_7). Similar results were obtained using $\text{KCpRu}(\text{CO})_2$ from the reduction of the dimer with Na/K. In both cases, infrared monitoring of the reaction mixtures indicated near quantitative formation of the alkyl. Yields of isolated material varied from 50-70%.

Preparation of $\text{Me}_5\text{CpRu}(\text{CO})_2(1,2-\eta^2-\text{C}_7\text{H}_8)\text{BF}_4$

$\text{Me}_5\text{CpRu}(\text{CO})_2\text{-H}$, (60 mg, .2 mmol) dissolved in 5 mL CH_2Cl_2 was added over 1 h. to 40 mg (22 mmol) of $\text{C}_7\text{H}_7\text{BF}_4$ suspended in 10 mL CH_2Cl_2 . After a further hour stirring, the solution was filtered and the volume reduced to ca. 3 mL. Ether (25 mL) was added with stirring and the yellow

precipitate which formed was dissolved in 5 mL CH_2Cl_2 and recrystallized by addition of 25 mL Et_2O . Yield: 40 mg (42%). IR (CH_2Cl_2 , ν_{CO} , cm^{-1}): 2063, 2022. ^1H NMR (CD_2Cl_2 , 25°C , δ): 1.45 (m, 1H, H_7 or H_8), 1.94 (s, 14H, Me_5Cp), 2.40 (quint, 1H, H_7 or H_8), 2.57 (quart, 1H, H_1), 3.34 (br d, 1H, H_2) 5.94 (br quart, 1H, H_6), 6.44 (m, 1H, H_5), 6.70 (m, 2H, $\text{H}_{3,4}$). Anal: calcd. for $\text{C}_{19}\text{H}_{23}\text{RuO}_2\text{BF}_4$: C, 48.43; H, 4.92. Found: C, 48.21; H, 4.95.

Preparation of $\text{Me}_5\text{CpRu}(\text{CO})_2(7\text{-}\eta^1\text{-C}_7\text{H}_7)$ (24)

(a) Anion method: $[\text{Me}_5\text{CpRu}(\text{CO})_2]_2$, (292 mg, .5 mmol) was dissolved in 50 mL THF over 0.25 mL (200 mg) of Na/K. After 16 h. stirring, the mixture was filtered to give a clear yellow-orange solution. The infrared spectrum showed four ν_{CO} at 1876, 1866, 1792 and 1768 cm^{-1} . After cooling to -78°C , 178 mg (1 mmol) of $\text{C}_7\text{H}_7\text{BF}_4$ was added. After 1 h. stirring, the infrared spectrum showed that the anion had reacted to give 24 and the starting dimer in about equal amounts. (The low solubility of this dimer in THF at -78°C probably means that the amount of dimer formed is greater than 50%.) The THF was pumped off at 0°C . The residue was extracted with 3×20 mL of pentane at 0°C , filtered, and cooled to -78°C . An orange precipitate formed which was identified as $[\text{Me}_5\text{CpRu}(\text{CO})_2]_2$. The supernatant was pumped

dry to give a red-orange crystalline residue which was recrystallized twice from pentane (10 mL) to afford 24 as an orange crystalline solid, mp 108°C (dec). Yield: 30 mg (8%). IR (cyclohexane, ν_{CO} , cm^{-1}): 1997, 1944. Anal: calcd. for $\text{C}_{19}\text{H}_{22}\text{RuO}_2$: C, 59.52; H, 5.78. Found: C, 59.26; H, 6.23. Mass spectrum (14 eV, 70°C): M^+ , $\text{M}^+ - \text{CO}$, $\text{M}^+ - 2\text{CO}$, $\text{M}^+ - \text{C}_7\text{H}_7$, Me_5CpH^+ , C_7H_7^+ (base peak). ^1H NMR (cyclohexane- d_{12} , 20°C, δ): 3.04 (tt, 1H, H_7 , $^3\text{J}_{1-7} = 7.5$ Hz, $^4\text{J}_{2-7} = 1.0$ Hz), 5.20, 5.25 (m, 4H, $\text{H}_{2,5}$ and $\text{H}_{1,6}$), 5.88 (m, 2H, $\text{H}_{3,4}$), 1.84 (s, 16H, Me_5Cp).

(b) Deprotonation method: $\text{Me}_5\text{CpRu}(\text{CO})_2(\text{n}^2\text{C}_7\text{H}_8)\text{BF}_4$, (24 mg, .05 mmol) was dissolved in 10 mL CH_2Cl_2 and Et_2NH (3 drops) was added. After 1 h. stirring at room temperature, the CH_2Cl_2 was pumped off and the orange residue extracted with 2×5 mL of pentane. Filtration and concentration to ca. 3 mL total volume followed by cooling to -78°C afforded 15 mg of 24 (78%), identical with the product obtained from the anion reaction. When the deprotonation route was used without isolation of intermediates, a 19% overall yield starting from $\text{Me}_5\text{CpRu}(\text{CO})_2\text{-Cl}$ was obtained. This route has the advantage over method (a) that separation of product from ditropyl is not required.

Preparation of $\text{CpRu}(\text{CO})(\eta^3\text{-C}_7\text{H}_7)$ (25)

$\text{CpRu}(\text{CO})_2(7\text{-}\eta^1\text{-C}_7\text{H}_7)$, (190 mg, .60 mmol) was dissolved in 10 mL CH_2Cl_2 . Me_3NO (100 mg, 1.3 mmol) was added. After 8 h stirring, solvent was removed under vacuum to leave a black residue. After extraction for 16 h with 20 mL pentane, an orange solution was obtained. After filtration and reduction in volume to ca. 5 mL, cooling to -10°C afforded a red precipitate. Recrystallization from 5 mL pentane gave large red-orange needles, mp 133°C . Yield: 55 mg (32%). The same product can be obtained in ca. 10% yield by photochemical decarbonylation of 23. IR

(cyclohexane, ν_{CO} , cm^{-1}): 1971. Mass spectrum (16 ev, 105°C): M^+ , $\text{M}^+ - \text{CO}$ (base peak). Anal: calcd. for

$\text{C}_{13}\text{H}_{12}\text{RuO}$: C, 54.57; H, 4.51. Found: C, 54.21; H, 4.40.

^1H NMR (-20°C , THF d_8 , δ): 2.60 (t, 2H, H_2 , $^3\text{J}_{1-2} = 7.5$ Hz), 4.68 (6, 2H, $\text{H}_{1,3}$), 4.98 (m, 2H, $\text{H}_{5,6}$), 5.88 (m, 2H, $\text{H}_{4,7}$), 5.03 (s, 5H, Cp).

Preparation of $\text{CpRu}(\text{CO})\text{PMe}_3\text{-H}$ (26)

A procedure similar to that used by Knox and Humphries for the preparation of $\text{CpRu}(\text{CO})\text{PMe}_3\text{-H}^6$ was employed. A solution of 0.51 mmol $\text{CpRu}(\text{CO})_2\text{-H}$ was generated by refluxing $\text{Ru}_3(\text{CO})_{12}$ (1.10 g, 0.17 mmol) with CpH (2 mL) in 200 mL heptane for 3 h. PMe_3 (.5 mL, 5 mmol) was added. After 5 min. reflux, IR monitoring indicated complete consumption of

the starting hydride. The solution was reduced in volume to ca. 50 mL. An orange precipitate of $[\text{Me}_5\text{CpRu}(\text{CO})_2]_2$ formed which was filtered off to give a yellow filtrate.

Evaporation of this filtrate to dryness afforded a pale yellow precipitate which was recrystallized from 30 mL hexane by cooling to -78°C . Yield: 1.15 g (83%) mp 79°C . Colourless material was obtained by sublimation at 55°C (0.1 mm) onto a water-cooled probe. IR (cyclohexane, ν_{CO} , cm^{-1}): 1931. ^1H NMR (CD_2Cl_2 , 25°C , δ): 4.99 (s, 5H, Cp), 1.49 (d, 9H, PMe_3 , $^2\text{J}_{\text{H-P}} = 9.8$ Hz), -12.63 (d, 1H, Ru-H, $^2\text{J}_{\text{H-P}} = 35.4$ Hz). Raman (solid state, HeNe laser): 1943 cm^{-1} . Anal: calcd. for $\text{C}_9\text{H}_{15}\text{RuOP}$: C, 39.84; H, 5.57. Found: C, 40.09; H, 5.57.

Preparation of $[\text{CpRu}(\text{CO})\text{PMe}_3(1,2\text{-n}^2\text{-C}_7\text{H}_8)]\text{BF}_4$ (27)

$\text{CpRu}(\text{CO})\text{PMe}_3\text{-H}$ (54 mg, .2 mmol) in 5 mL CH_2Cl_2 was added dropwise over 1 h. to a rapidly stirred suspension of $\text{C}_7\text{H}_7\text{BF}_4$ (50 mg, .28 mmol) in 5 mL CH_2Cl_2 . Infrared spectra showed that the single ν_{CO} band of the starting hydride (1909 cm^{-1}) had been replaced by one at 1997 cm^{-1} . Attempts to precipitate the cation by addition of ether caused displacement of C_7H_8 (^1H NMR). When a concentrated solution of 27 in CD_2Cl_2 was stored at -78°C for 7 days, a yellow precipitate formed slowly. Analysis: calcd. for 27,

$C_{16}H_{22}RuOPBF_4$: C, 42.78; H, 4.94. Found: C, 35.28; H, 4.20. 1H NMR spectra indicated large amounts of free C_7H_8 in the supernatant. The precipitate did not redissolve in dichloromethane.

The identification of 27 as a cycloheptatriene cation is consistent with the 1H NMR spectrum (400 MHz, CD_2Cl_2 , $0^\circ C$). Due to the presence of two diastereomers, the spectrum is very complex (see Figure XIV and discussion in section V). Attempts to deprotonate the cation in situ with a variety of bases (Et_3N , $NaN(SiMe_3)_2$ or 1,8 bis-(dimethylamino)-naphthalene) did not give an alkyl product. Rapid formation of free cycloheptatriene was detected by 1H NMR.

Preparation of $CpRu(CO)PMe_3(7-\eta^1-C_7H_7)$ (28)

$CpRu(CO)_2(7-\eta^1-C_7H_7)$, (250 mg, .80 mmol) was dissolved in 20 mL hexane, and PMe_3 (5 mmol) was added. The solution was heated to $65^\circ C$ for 10 min, cooled to room temperature, filtered, and evaporated to afford a red oil. After 1 h under vacuum, the oil was dissolved in 10 mL pentane. When this solution was filtered and cooled to $-78^\circ C$, an orange-red crystalline precipitate formed. The supernatant was syringed off and the precipitate pumped dry at $-78^\circ C$. On warming, the precipitate melts to a red oil at ca. $0^\circ C$.

Repeated attempts to crystallize this oil from hydrocarbon solvents have not been successful. IR (cyclohexane, ν_{CO} , cm^{-1}): 1920. ^1H NMR (cyclohexane d_{12} , 25°C , δ): 1.36 (d, 9H, PMe_3 , $^2J_{\text{H-P}} = 9.2$ Hz), 2.84 (q, 1H, H_7 , $^3J_{7-1} = ^3J_{\text{HP}} = 7.5$ Hz), 4.65 (dd, 1H, H_2), 4.68 (dd, 1H, H_5), 4.87 (br dd, 1H, H_6), 5.06 (br dd, H_1), 5.19 (br dd, 1H, H_4), 5.27 (br dd, 1H, H_3), 5.48 (s, 5H, Cp). ^{13}C NMR (cyclohexane- d_{12} , 5°C , δ): 21.55 (d, 3C, PMe_3 , $^1J_{\text{C-P}} = 29$ Hz), 23.22 (d, 1C, C_7 , $^2J_{\text{C-P}} = 7$ Hz), 88.21 (s, 3.5C, Cp), 117.58 (s, 1C, C_2), 118.61 (s, 1C, C_5), 132.76 (s, 1C, C_4), 133.88 (s, 1C, C_3), 141.28 (s, 1C, C_6), 143.84 (s, 1C, C_1), 205.3 (d, .2C, CO, $J_{\text{C-P}} = 20$ Hz).

Preparation of $\text{CpRu}(\text{CO})\text{PMe}_2\text{Ph}(7\text{-}\eta^1\text{-C}_7\text{H}_7)$ (29)

$\text{CpRu}(\text{CO})_2(7\text{-}\eta^1\text{-C}_7\text{H}_7)$, (228 mg, .73 mmol) was dissolved in 10 mL hexane. PMe_2Ph (100 μL , 85 mg, .61 mmol) was added. The solution was warmed to 65°C for 5 min. After cooling to room temperature, 10 mg of silica gel was added (Fisher, 28-200 mesh). The mixture was stirred for 10 minutes, then filtered, reduced in volume to 5 mL and cooled to -10°C . A red oily precipitate formed overnight. The supernatant was syringed off. ^1H NMR showed that the supernatant contained ditropyl, 29 and ca. 20% free PMe_2Ph . The supernatant was discarded. The red oil was

dissolved in 5 mL hexane, filtered and cooled to -10°C . A red oil separated. The supernatant was syringed off. The oil did not solidify even after several hours pumping. IR (cyclohexane, ν_{CO} , cm^{-1}): 1922. ^1H NMR (cyclohexane- d_{12} , 20°C , δ): 1.60 (d, 3H, PMe, $^2J_{\text{H-P}} = 8.8$ Hz), 1.68 (d, 3H, PMe, $^2J_{\text{H-P}} = 8.8$ Hz), 2.74 (q, 1H, H_7 , $^3J_{\text{H-P}} = ^3J_{1-7} = 7.2$ Hz), 4.64 (dd, 1H, H_2), 4.68 (dd, 1H, H_5), 4.86 (dd, 1H, H_6), 5.05 (dd, 1H, H_1), 5.18 (dd, 1H, H_4), 5.27 (dd, 1H, H_3), 5.43 (s, 4H, Cp), 7.24–7.32 (m, 3H, m + p), 7.58–7.66 (m, 2H, ortho). ^{13}C NMR (cyclohexane- d_{12} , 20°C , δ): 20.3 (t, 2C, PMe_2 , $^1J_{\text{C-P}} = 30$ Hz), 23.10 (1C, C_7 , $^2J_{\text{C-P}} = 4.6$ Hz), 88.58 (s, 3.5 C, Cp), 118.00 (s, 1C, C_2), 118.77 (s, 1C, C_5), 133.04 (s, 1C, C_4), 133.91 (s, 1C, C_3), 141.67 (s, 1C, C_6), 143.80 (s, 1C, C_1), 206.25 (d, .2C, CO, $^2J_{\text{C-P}} = 21.4$ Hz). Aromatic carbon atoms of the phosphine ligand were assigned based on comparison to the free ligand and the size of $J_{\text{C-P}}$: 130.49 (d, 2C, $J_{\text{C-P}} = 10.8$ Hz, ortho), 128.73 (d, 2C, $J_{\text{C-P}} = 7.6$ Hz, meta), 126.28 (d, 1C, $J_{\text{C-P}} = 4.5$ Hz, para). The carbon atom directly attached to P was not located. An inverse gated decoupling spectrum of the free ligand located the resonance for this carbon atom at δ 143.7 ppm. This signal is relatively weak even in the absence of NOE effects, presumably due to a long T_1 .

CHAPTER VI

DINUCLEAR RUTHENIUM COMPOUNDS

Section I. Introduction

Metal dimers containing η^5 cyclopentadienyl groups and carbonyl ligands have been intensively studied in recent years.¹²⁵ Particularly interesting compounds are the cyclopentadienyl dicarbonyl dimers of the iron triad, $[\text{CpM}(\text{CO})_2]_2$ ($\text{M} = \text{Fe}, \text{Ru}, \text{Os}$). The iron dimer has been the subject of infrared and NMR studies which have led to a detailed understanding of the structures of the various isomers and the processes by which they are interconverted.¹²⁶ The ruthenium analog has also been investigated by ^1H NMR¹²⁷ and infrared spectroscopy.¹²⁸

The chemical reactivity of the iron dimer has been extensively investigated, including studies of ligand substitution reactions where a carbonyl ligand is replaced by another ligand L such as a phosphine, phosphite or isonitrile group. Many unsuccessful attempts to prepare disubstituted dimers have been reported. Typical of these results is the reaction of $[\text{CpFe}(\text{CO})_2]_2$ with various phosphines and phosphites, which gave only monosubstituted products $\text{CpFe}(\text{CO})(\text{L})\text{-CpFe}(\text{CO})_2$.¹²⁹ Disubstitution can be

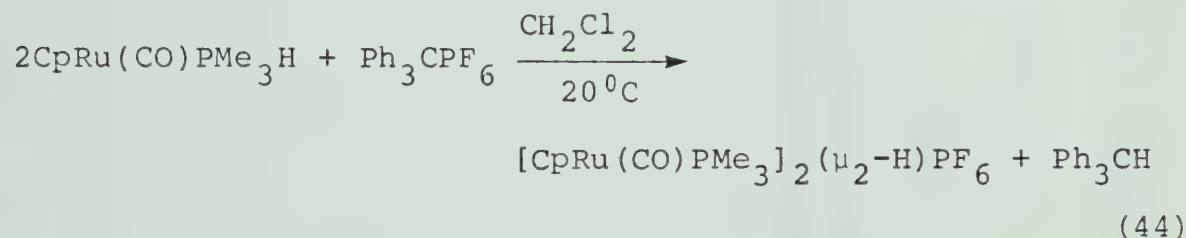
achieved by employing bridging ligands. Compounds of the type $\text{CpFe(CO)Ph}_2\text{P-(CH}_2)_n\text{-PPh}_2\text{(CO)FeCp}$ ($n = 1-3$) have been reported.¹³⁰ The novel ligand $\text{PF}_2\text{N(CH}_2\text{CH}_3)_2$ was employed by R.B. King and coworkers to prepare

$[\text{CpFe(CO)PF}_2\text{N(CH}_2\text{CH}_3)_2]_2$, the only disubstituted dimer with monodentate ligands reported to date.¹³¹

Previous workers have employed the direct thermal or photochemical reaction of a ligand with the tetracarbonyl dimer. It is not surprising that in most cases only monosubstitution was observed, since the replacement of one carbonyl group with a ligand which is a better σ donor and less capable π acceptor than CO will reduce the lability of the remaining CO groups. In this chapter, indirect methods for the synthesis of disubstituted dimers which allow this problem to be avoided are described.

Section II. Preparation of [CpRu(CO)PMe₃]₂

The instability of [CpRu(CO)(PMe₃)(η^2 -C₇H₈)]BF₄, 27, with respect to loss of cycloheptatriene was described in Chapter V (Section E). In the presence of CpRu(CO)(PMe₃)-H, 27 is rapidly consumed to give a new species. ¹H NMR spectra show two new (η^5 -C₅H₅) singlets and two PMe₃ doublets. This new species was identified as a dinuclear compound by an independent synthesis using the hydride abstraction method developed by Sweet for the synthesis of [CpRe(CO)(NO)]₂(μ_2 -H)PF₆¹¹⁷ (eq. 44).



The reaction was carried out by adding a solution of Ph₃CPF₆ in CH₂Cl₂ to a solution of 26 in the same solvent. Compound 30 precipitates from solution upon addition of diethyl ether.

The ¹H NMR spectrum of 30 in CD₂Cl₂ has two Cp singlets at δ 5.154 and 5.162. Doublets due to PMe₃ groups are observed at δ 1.635 and 1.653 (²J_{H-P} = 9.6 and 10.4 Hz respectively). Two triplets are observed at δ -20.26 and -21.70 ppm (see Figure XVII). These hydride resonances are

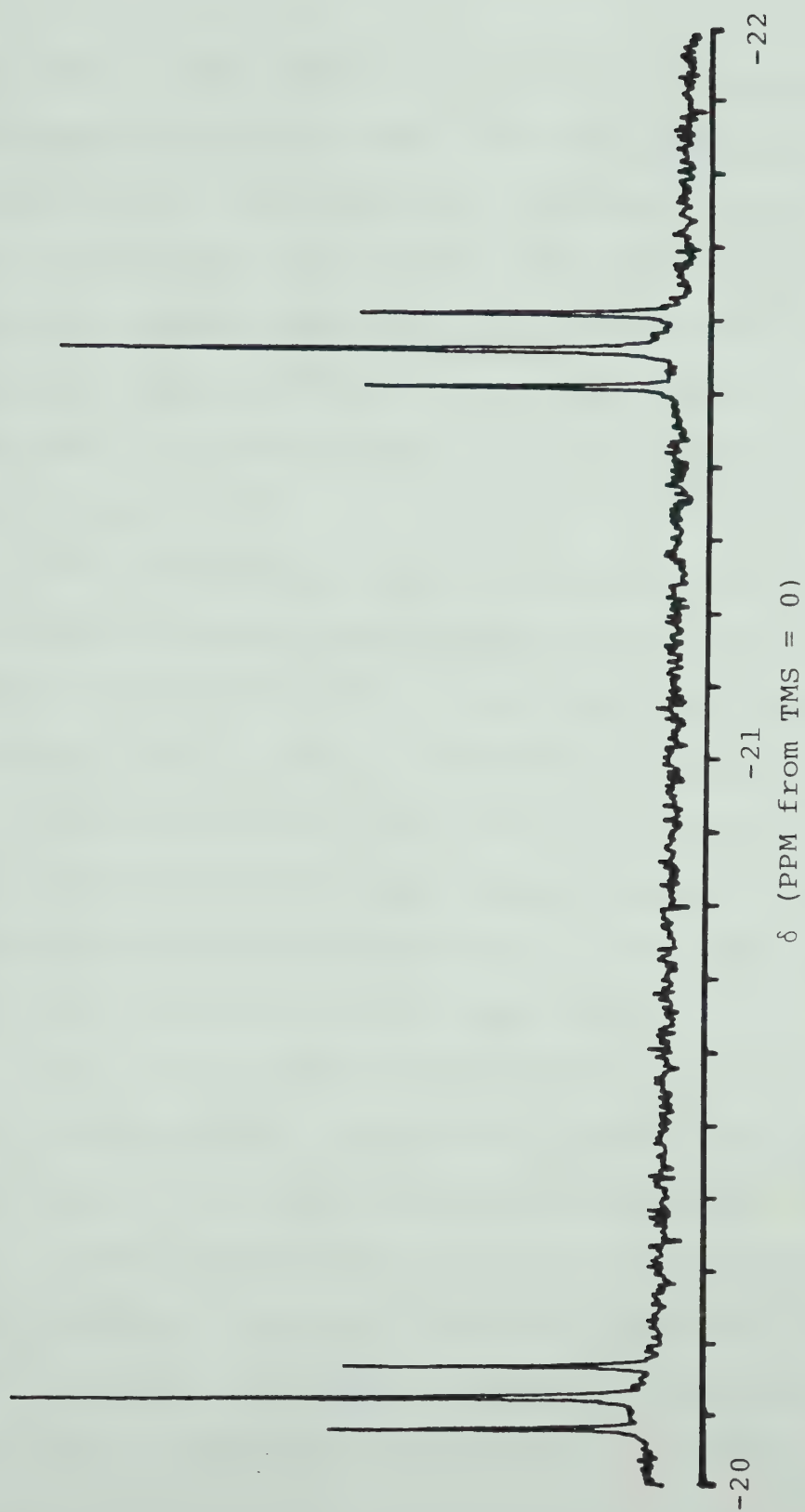


FIGURE XVII. Hydride region of the ^1H NMR spectrum of 30, CD_2Cl_2 .

observed at much higher field than in the mononuclear precursor 26 (δ -12.6 ppm). The observation of triplets for these signals indicates equal coupling to two P nuclei. Previous reports indicate that the NMR resonance of a bridging hydride occurs at higher field than that of a terminal hydride.^{132,133} A shift upfield of ca. 7 ppm was reported for $[\text{CpRe}(\text{CO})(\text{NO})]_2(\mu_2\text{-H})\text{PF}_6$ compared to $\text{CpRe}(\text{CO})(\text{NO})\text{-H}$.¹¹⁷

The two complete sets of NMR resonances observed for 30 (a similar situation was observed in the ^{13}C NMR spectrum) occur in the ratio 52:48. (The same ratio is obtained by comparing the Cp, PMe_3 or hydride resonances.) This ratio is independent of solvent (THF-d_8 or CD_2Cl_2). These observations indicate that $[\text{CpRu}(\text{CO})(\text{PMe}_3)]_2(\mu_2\text{-H})\text{PF}_6$ exists in solution as two diastereomers, rather than as two geometric isomers (i.e. cis and trans).

The infrared spectrum of 30 lends further support to this interpretation. Only two ν_{CO} bands are observed (see Figure XVIII) and their position and relative intensity are only slightly affected by changing the solvent (CH_2Cl_2 , CH_3CN or THF). The most probable structures for 30 are the sterically less demanding trans structures (only one enantiomer of the RR/SS diastereomer is shown).

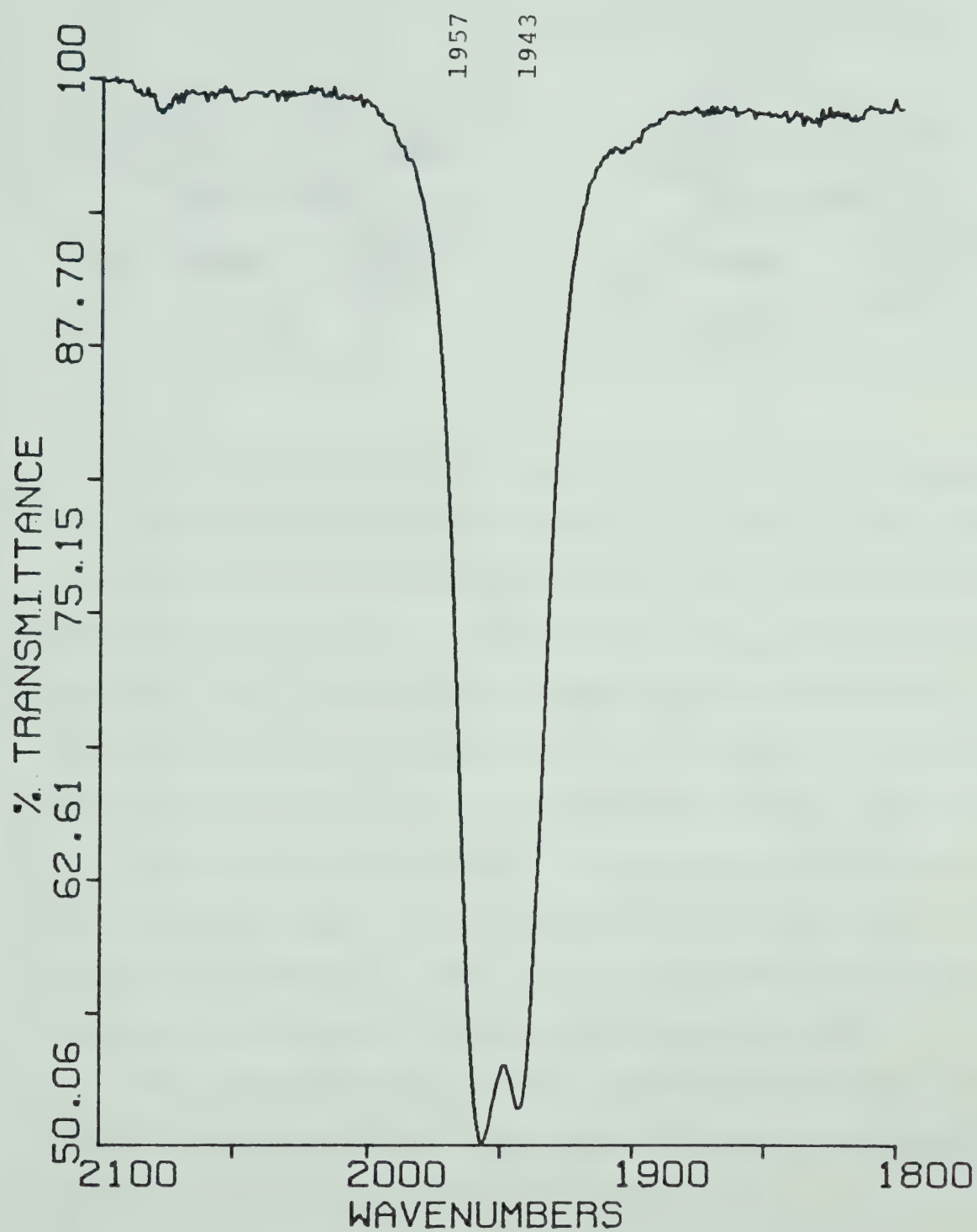
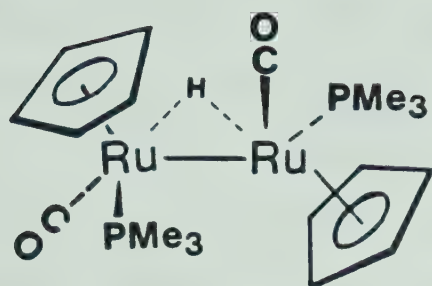
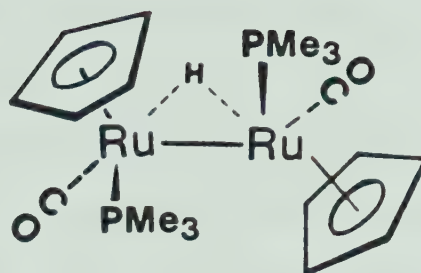


FIGURE XVIII. Infrared spectrum of 30, CH_3CN .

30-RS30-RR

The number of infrared bands expected for 30 depends on the location of the hydride ligand. If the hydride ligand of 30-RS were located exactly between the Ru atoms, the molecule would have C_i symmetry and one ν_{CO} band would be expected. With the hydride ligand off-center as shown in the structure, the symmetry would be C_1 and two ν_{CO} bands would be predicted. Thus the observed infrared spectrum could be accounted for by only one of the diastereomers. Alternatively, the two ν_{CO} bands observed could each be due to one diastereomer. Very similar spectroscopic data were reported by Sweet for $[\text{CpRe}(\text{CO})(\text{NO})]_2(\mu_2\text{-H})\text{PF}_6$.¹¹⁷

The protonated form of the unsubstituted dimer, i.e. $[\text{CpRu}(\text{CO})_2]_2(\mu_2\text{-H})^+$, has been observed spectroscopically¹³⁴ and the iron analog has been isolated as a hexafluorophosphate salt.¹³⁵ Protonation of $\text{Cp}_2\text{Fe}_2(\text{CO})_3(\text{P}(\text{OMe})_3)$ was reported to give a hydride bridged

cation.¹³⁴ In all of these cases, the bridging carbonyl groups present in the parent dimer are replaced by a bridging hydride ligand in the cation.

A typical reaction of hydride bridged metal dimer cations is facile deprotonation to give the corresponding neutral dimers. For example, $[\text{CpRe}(\text{CO})(\text{NO})]_2(\mu_2\text{-H})\text{PF}_6$ ¹¹⁷ and $[\text{CpFe}(\text{CO})]_2(\mu_2\text{-H})(\mu_2\text{-diphos})\text{BF}_4$ ¹³⁶ are both deprotonated by Et_3N .

Compound 30 does not react with Et_3N , Et_2NH or 1,8-bis-(dimethylamino)naphthalene. With excess $\text{NaN}(\text{SiMe}_3)_2$ in THF, a bright red crystalline compound (31) was isolated in low yield. The compound has very limited solubility in THF. It reacts with CH_2Cl_2 to give $\text{CpRu}(\text{CO})\text{PMe}_3\text{-Cl}$, identified by comparison of infrared spectra with an authentic sample. The infrared spectrum in THF shows only one ν_{CO} band at 1645 cm^{-1} . This band is broad and slightly asymmetric.

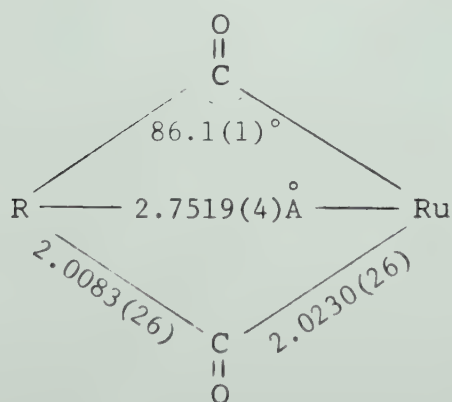
A ^1H NMR spectrum of 31 in THF-d_8 was obtained by grinding the crystalline material and stirring in THF-d_8 . Only one Cp singlet at δ 4.69 and one PMe_3 doublet at δ 1.33 ppm ($^2J_{\text{H-P}} = 13.2\text{ Hz}$) were observed. Aside from small shifts in peak positions, the spectrum was unchanged on cooling to -100°C .

Compound 31 melts with decomposition at 240°C and gives a mass spectrum (70 ev, 220°C) with a molecular ion envelope

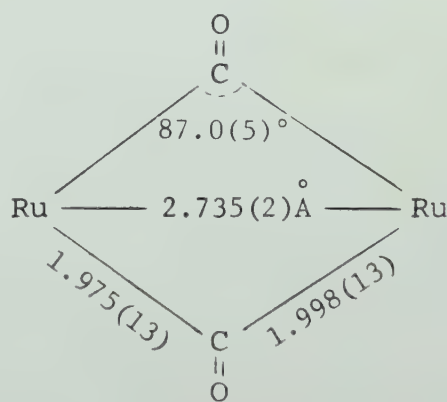
at m/e 533-547 having an intensity pattern consistent with the formulation $[\text{CpRu}(\text{CO})(\text{PMe}_3)]_2$.

The structure of 31 was confirmed by an x-ray crystal structure determination carried out by Dr. Richard Ball of this department. Details of the data collection and refinement procedure as well as tables of structural parameters, bond lengths and bond angles will be found in the experimental section. The structure in the solid state is the trans configuration with bridging carbonyl groups (see Figure XIX). This structure is consistent with the spectroscopic observations in solution. The lack of terminal ν_{CO} bands in the infrared spectrum and the single Cp resonance in the ^1H NMR spectrum (ie lack of evidence for diastereomers expected for a non-bridged structure) indicates that the solution structure is probably the same as that found in the solid state.

The structure of 31 is very similar to that previously reported for the tetracarbonyl dimer, $[\text{CpRu}(\text{CO})_2]_2$.¹³⁷ This



31



$[\text{CpRu}(\text{CO})_2]_2$

compound also has a carbonyl bridged centrosymmetric structure in the solid state. The central core of the two compounds show essentially the same structural features. The metal-metal distance in 31 is only slightly longer than in $[\text{CpRu}(\text{CO})_2]_2$.

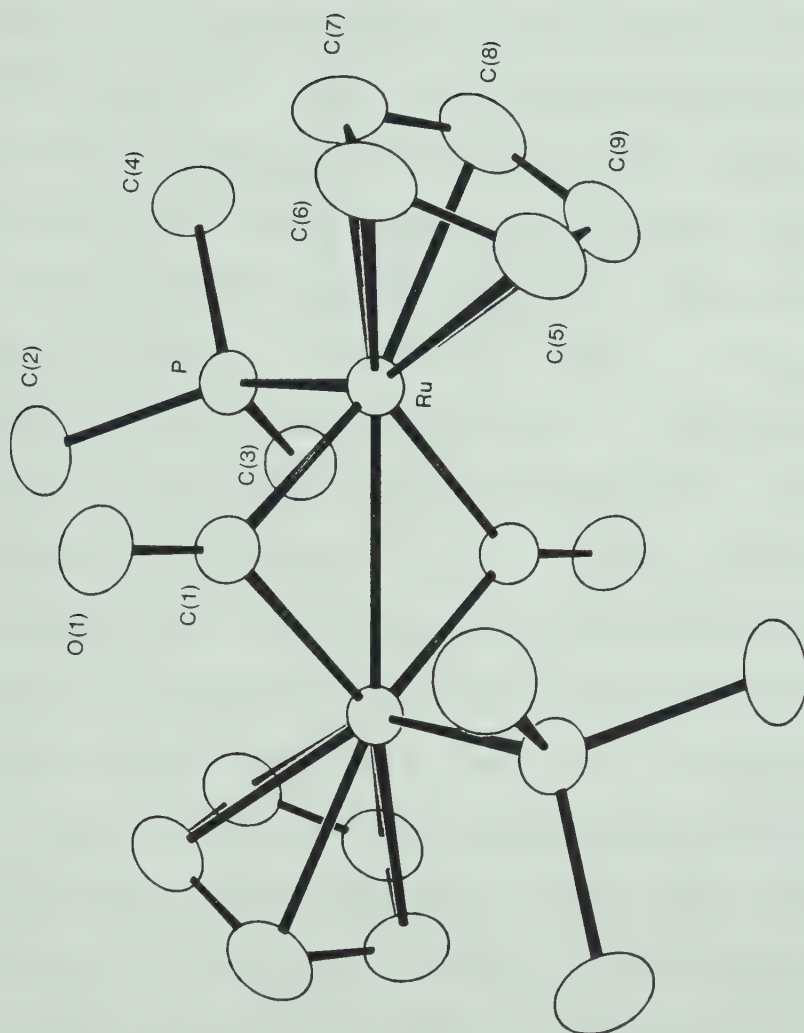


FIGURE XIX. Molecular structure of 31. Thermal ellipsoids are drawn at the 50% level.

Section III. Preparation of $[\text{CpRu}(\text{CO})(\text{PMe}_2\text{Ph})]_2$

The preparation of $\text{CpRu}(\text{CO})(\text{PMe}_2\text{Ph})(7-\eta^1\text{-C}_7\text{H}_7)$ (29) was described in Chapter V. All monohaptocycloheptatrienyl alkyls so far investigated show varying degrees of thermal instability, decomposing to give ditropyl and a metal-metal bonded dimer. In the case of 29, heating a homogeneous solution in methylcyclohexane to 90°C for 15 min caused the deposition of a fine orange precipitate (32).

The infrared spectrum of 32 in THF solution shows a single ν_{CO} band at 1697 cm^{-1} . The ^1H NMR spectrum (THF-d_8), in addition to aromatic protons of the ligand, has one singlet Cp resonance at δ 4.45 ppm and a doublet due to PMe_2 groups at δ 1.52 ppm ($^2J_{\text{H-P}} = 8.5\text{ Hz}$). Analytical data are consistent with the formulation $[\text{CpRu}(\text{CO})(\text{PMe}_2\text{Ph})]_2$. The similarity of the spectroscopic results for 31 and 32 suggests that these two dimers are isostructural.

The synthetic methods described here for the preparation of novel dimeric species are capable of extension to the other metals in the iron group. Although σ cycloheptatrienyl compounds of iron appear to be very unstable, substituted hydrides such as $\text{CpFe}(\text{CO})(\text{PMe}_3)\text{-H}$ are known.¹³⁸ In the case of osmium, $\text{CpOs}(\text{CO})_2(7-\eta^1\text{-C}_7\text{H}_7)$ and $\text{CpOs}(\text{CO})_2\text{-H}$ have recently been prepared by Hoyano and Graham¹³⁹, so suitable starting materials are available for

this metal. It would be very interesting to prepare $[\text{CpOs}(\text{CO})(\text{P})]_2$, since the parent tetracarbonyl dimer is known to adopt a non-bridged structure in solution. Possibly phosphine substitution would force the compound into a carbonyl bridged structure analogous to 31 and 32.

Section IV. Experimental

Ph_3CPF_6 was purchased from Aldrich Chemical Co.

Preparation of $[\text{CpRu}(\text{CO})(\text{PMe}_3)]_2(\mu_2\text{-H})\text{PF}_6$ (30)

$\text{CpRu}(\text{CO})\text{PMe}_3\text{-H}$ (400 mg, 1.48 mmol) was dissolved in 5 mL CH_2Cl_2 . Ph_3CPF_6 (272 mg, 0.7 mmol) in 5 mL CH_2Cl_2 was added over 0.5 h. The solution was stirred for 0.5 h. The product was precipitated by addition of 20 mL ether. Recrystallization was effected by dissolving the precipitate in 5 mL CH_2Cl_2 and adding 10 mL ether to afford 30 as an orange powder. Yield: 390 mg (81%). IR (CH_3CN , ν_{CO} , cm^{-1}): 1957, 1943. ^1H NMR (CD_2Cl_2 , 400 MHz, 25°C , δ): 1.635 (d, 9H, PMe_3 , $^2J_{\text{H-P}} = 9.6$ Hz), 1.653 (d, 9H, PMe_3 , $^2J_{\text{H-P}} = 10.4$ Hz), 5.154 (s, 4H, Cp), 5.162 (s, 4H, Cp), -20.26 (t, 1H, $^2J_{\text{H-P}} = 19.7$ Hz), -21.70 (t, 1H, $^2J_{\text{H-P}} = 17.6$ Hz). ^{13}C NMR (CD_2Cl_2 , 100.6 MHz, 5°C , δ): 23.15 (d, 3C, PMe_3 , $^1J_{\text{C-P}} = 33.5$ Hz), 23.42 (d, 3C, $^1J_{\text{C-P}} = 35.1$ Hz), 85.19 (s, 5C, Cp), 86.07 (s, 5C, Cp), 202.88 (d, .2C, CO, $^2J_{\text{C-P}} = 19.8$ Hz), 203.20 (d, .2C, CO, $^2J_{\text{C-P}} = 19.8$ Hz). The ^{13}C spectrum was also run at 50 MHz in order to distinguish P couplings from chemical shift differences between the two diastereomers. Analysis: calcd. for $\text{C}_{18}\text{H}_{29}\text{Ru}_2\text{O}_2\text{P}_3\text{F}_6$: C, 31.49, H, 4.26. Found: C, 31.47; H, 4.27.

Preparation of [CpRu(CO)(PMe₃)]₂ (31)

Compound 30 (4.4 mg, .0064 mmol), NaN(SiMe₃)₂ (10 mmol) and 0.8 mL THF were combined and thoroughly mixed to give a homogeneous red solution. Cooling the solution to 5°C for 48 h caused the crystallization of 31 as deep red crystals. The supernatant was syringed off and the crystals washed 3 times with THF. Yield: 0.975 mg (28%). IR (THF, ν_{CO} , cm⁻¹): 1645. ¹H NMR (THF-d₈, 20°C, δ): 1.33 (d, PMe₃, ²J_{H-P} = 13.2 Hz), 4.69 (s, Cp). Mass spectrum (70 ev, 220°C): M⁺, M⁺/2, and many fragment ions.

Preparation of [CpRu(CO)(PMe₂Ph)]₂ (32)

CpRu(CO)(PMe₂Ph)(7- η^1 -C₇H₇), (25 mg, .059 mmol) was dissolved in 10 mL methylcyclohexane and heated to 90°C for 15 min. A precipitate formed. On cooling, an orange microcrystalline precipitate was collected by syringing off the supernatant and washing the crystalline residue with 3 x 5 mL pentane. Yield: 15 mg (77%). IR (THF, ν_{CO} , cm⁻¹): 1697. ¹H NMR (THF-d₈, 25°C, δ): 1.52 (d, PMe₂, ²J_{H-P} = 8.5 Hz), 4.45 (s, Cp), 7.26-7.38 (m, o & p), 7.72-7.78 (m, meta). Anal: calcd. for C₂₈H₃₂Ru₂O₂P₂: C, 50.59; H, 4.85. Found: C, 49.10; H, 4.88.

X-ray Structure of $\underline{31}$ ¹⁴⁰

A deep red parallelepiped crystal with dimensions ca. 0.02 x 0.01 x 0.02 mm was used for data collection. Details of the data collection procedure are listed in Table VI.

The structure was solved using the Patterson heavy-atom method, which revealed the position of the Ru atom. The remaining non-hydrogen atoms were located by the usual combination of least-squares refinement and difference Fourier Synthesis. The molecule is constrained to be centrosymmetric by virtue of its position in the cell thus only half of the atoms need be located to completely define the molecule.

The structure was refined in full-matrix least-squares where the function minimized was $\sum w(|F_O| - |F_C|)^2$ and the weight w is defined as $4F_O^2/\sigma^2(F_O^2)$. The final cycle of refinement included 109 parameters and 1911 observations having $I > 3 \sigma(I)$ and converged with $R_1 = \sum |F_O| - |F_C| / \sum |F_O| = 0.036$ and $R_2 = [\sum w(|F_O| - |F_C|)^2 / \sum w |F_O|^2]^{1/2} = 0.060$. The highest peak in the final difference Fourier was 0.9(2) e/Å. The structure of 31 is depicted in Figure XIX. Bond lengths and bond angles are tabulated in Tables VII and VIII. Positional and thermal parameters are listed in Table IX.

Table VI. Crystal data for $[\text{CpRu}(\text{CO})\text{PMe}_3]_2$

A. Cell parameters (room temperature)^a

Crystal system: monoclinic	$a = 8.080 (1) \text{ \AA}$
space group $P2_1/c$	$b = 8.107 (1) \text{ \AA}$
$Z = 2$	$c = 15.058 (2) \text{ \AA}$
f.w. = 540.51	$\beta = 91.73 (1)^\circ$
ρ (calcd.) = 1.82 g/cm^3	$V = 985.82 \text{ \AA}^3$

B. Collection of Intensity Data^b

diffractometer: Enraf-Nonius CAD4
 radiation: $\text{MoK}\alpha$ ($\lambda = 0.71073 \text{ \AA}$)
 monochromator: graphite crystal, incident beam
 scan type: ω - θ
 scan rate: $0.6 - 10^\circ/\text{min}$ (in ω)
 scan width: $0.65 + 0.35 \tan \theta^\circ$
 max. 2θ : 27.5°
 reflections collected: 2265 unique, 1911 with $I > 3 \sigma$
 absorption coeff.: $\mu = 16.65 \text{ cm}^{-1}$
 corrections: none

^a Based on 25 reflections in the range $71^\circ < \theta < 181^\circ$.

^b Computer programs used include the Enraf-Nonius Structure Determination package and several locally written or modified programs.

TABLE VII. Bond Lengths (\AA)^a

Ru	Ru'	2.7519(4)
Ru	P	2.2804(7)
Ru	C(1)	2.0230(26)
Ru	C(1)'	2.0083(26)
Ru	C(5)	2.2933(27)
Ru	C(6)	2.2745(28)
Ru	C(7)	2.2395(29)
Ru	C(8)	2.2663(32)
Ru	C(9)	2.2822(29)
P	C(2)	1.8261(32)
P	C(3)	1.8096(31)
P	C(4)	1.8330(33)
C(1)	O(1)	1.1837(32)
C(5)	C(6)	1.4083(55)
C(5)	C(9)	1.3860(45)
C(6)	C(7)	1.3848(47)
C(7)	C(8)	1.4086(49)
C(8)	C(9)	1.4052(49)

^aNumbers in parentheses are estimated standard deviations in the least significant digits.

TABLE VIII. Bond Angles (Degrees)^a

C (1)	Ru	C (1)	93.9 (1)
C (2)	P	C (3)	104.68 (16)
C (2)	P	C (4)	99.55 (16)
C (3)	P	C (4)	99.23 (16)
Ru	C (1)	Ru'	86.1 (1)
C (6)	C (5)	C (9)	108.35 (30)
C (5)	C (6)	C (7)	107.82 (30)
C (6)	C (7)	C (8)	108.32 (31)
C (7)	C (8)	C (9)	107.45 (29)
C (5)	C (9)	C (8)	108.04 (30)

^aNumbers in parentheses are estimated standard deviations in the least significant digits.

TABLE IX. Positional and Thermal Parameters. a,b

Atom	x	y	z	β_{11}	β_{22}	β_{33}	β_{12}	β_{13}	β_{23}
Ru(1)	0.13128(3)	-0.08864(3)	0.03550(2)	0.00819(5)	0.00725(5)	0.00191(1)	-0.00105(4)	-0.00043(4)	0.00032(3)

Atom	x	y	z	β_{11}	β_{22}	β_{33}	β_{12}	β_{13}	β_{23}
P(1)	0.1710(1)	-0.2371(1)	-0.09071(7)	0.0106(1)	0.0085(1)	0.00238(4)	-0.0006(2)	0.0008(1)	-0.0009(1)
O(1)	0.2078(4)	0.2293(4)	-0.0555(3)	0.0112(4)	0.0103(4)	0.0068(2)	-0.0054(7)	0.0028(5)	0.0050(5)
C(1)	0.1143(5)	0.1275(5)	-0.0176(3)	0.0092(5)	0.0080(4)	0.0028(2)	-0.0013(9)	0.0000(5)	0.0012(5)
C(2)	0.0057(6)	0.6238(6)	-0.1286(3)	0.0176(8)	0.0124(6)	0.0041(2)	-0.0083(13)	-0.0010(7)	-0.0056(6)
C(3)	0.2285(6)	0.8739(6)	-0.1894(3)	0.0145(7)	0.0159(7)	0.0030(2)	-0.0021(13)	0.0038(4)	0.0014(7)
C(4)	0.6566(7)	0.3839(6)	0.0832(4)	0.0164(8)	0.0130(6)	0.0045(2)	0.0111(12)	0.0008(7)	-0.0018(7)
C(5)	0.3159(6)	0.4825(7)	0.3190(3)	0.0.61(7)	0.0174(7)	0.0022(2)	-0.0013(14)	-0.0037(4)	0.0015(6)
C(6)	0.3436(6)	0.3112(7)	0.3236(3)	0.0158(7)	0.0181(8)	0.0022(2)	0.0002(14)	-0.0034(4)	-0.0037(6)
C(7)	0.2212(6)	0.2431(6)	0.3746(3)	0.0173(8)	0.0143(7)	0.0030(2)	-0.0078(12)	-0.0038(4)	-0.0020(6)
C(8)	0.1145(6)	0.3706(7)	0.4005(3)	0.0120(7)	0.0194(8)	0.0034(2)	0.0019(14)	-0.0030(4)	0.0001(8)
C(9)	0.1765(5)	0.5190(4)	0.3666(3)	0.0118(6)	0.0152(7)	0.0034(2)	0.0041(12)	-0.0036(6)	0.0011(7)

^aThe form of the anisotropic thermal parameter is

$$\exp[-(\beta_{11}^*h^2 + \beta_{22}^*k^2 + \beta_{33}^*l^2 + \beta_{12}^*hk + \beta_{13}^*hl + \beta_{23}^*kl)].$$

^bEstimated standard deviations in the least significant digits are shown in parentheses.

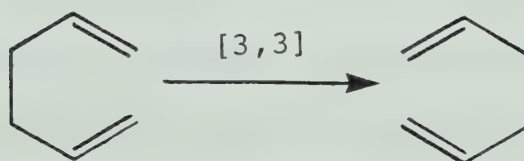
CHAPTER VII

FLUXIONAL BEHAVIOUR OF MONOHAPTOCYCLOHEPTATRIENYL COMPOUNDS

Section I. Introduction

A. Application of Orbital Symmetry Criteria to Sigmatropic Shifts

Woodward and Hoffman³² defined a sigmatropic shift of order $[i,j]$ as the migration of a σ bond, flanked by one or more π electron systems, to a new position whose termini are $i-1$ and $j-1$ atoms removed from the original bonded loci, in an uncatalyzed intramolecular process. An example illustrating the system of notation is provided by the rearrangement of 1,5 hexadienes (Cope rearrangement). This rearrangement is an example of a $[3,3]$ sigmatropic shift.



It is important to note that in the designations $[1,3]$ and $[1,5]$, commonly used in describing sigmatropic migrations, 3

and 5 refer to the number of the carbon atom which is the migration terminus. The designation 1 does not refer to the migration origin. This number specifies that in both reactant and product bonding is to the same atom in the migrating group.

The basic principle of the theory proposed by Woodward and Hoffmann is that reactions occur readily when the symmetry properties of molecular orbitals in the reactant and the product allow for maximum favorable (bonding) overlap throughout the reaction (an allowed reaction). When this condition is not met, the reactions proceed only with difficulty (a forbidden reaction). Thus orbital symmetry is conserved in concerted reactions.³³

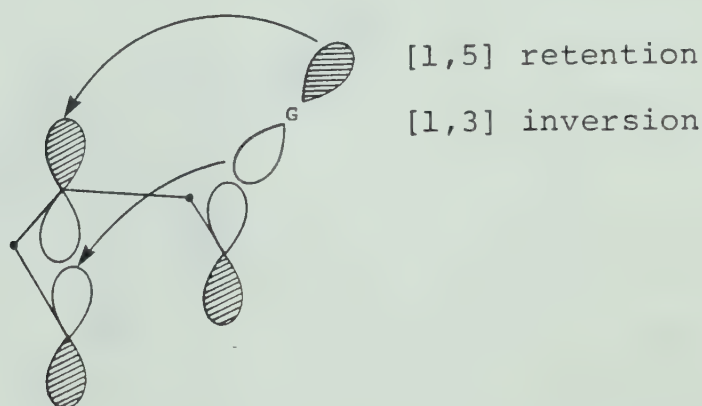
The fundamental simplicity of this hypothesis has been obscured by a lack of a clear understanding of the definition of a concerted reaction. The mistaken supposition has arisen that all allowed reactions are concerted, and all forbidden reactions are non-concerted. As was pointed out by Andrist, this reasoning would render the theory irrefutable, since a failure to observe the outcome predicted from orbital symmetry constraints in a particular reaction could be interpreted as either a violation of the theory or as a non-concerted reaction.¹⁴¹

In the context of sigmatropic shifts, an acceptable

definition for concertedness is that there is an equal amount of bond breaking and bond formation at all times during the migration.¹⁴² This definition does not exclude the formation of an intermediate. The concertedness of bond breaking and bond formation processes assures orbital symmetry control of the outcome, regardless of the existence or lifetime of the intermediate. In previous studies of sigmatropic migration reactions, it has been considered adequate to establish that the reaction is intramolecular, since concertedness or a lack thereof is not subject to experimental verification. It has been argued that the observation of a negative entropy of activation, a previously accepted criterion for concertedness in sigmatropic shifts, is inadequate for this purpose.¹⁴³ In the absence of solvation effects, negative entropy of activation is indicative of bond formation during the rate determining step¹⁴⁴, but does not establish that a bond is broken concurrently. Since a dissociative reaction occurs with an increase in entropy¹⁴⁵, the entropy criterion is a useful method to distinguish between dissociative and non-dissociative rearrangements.

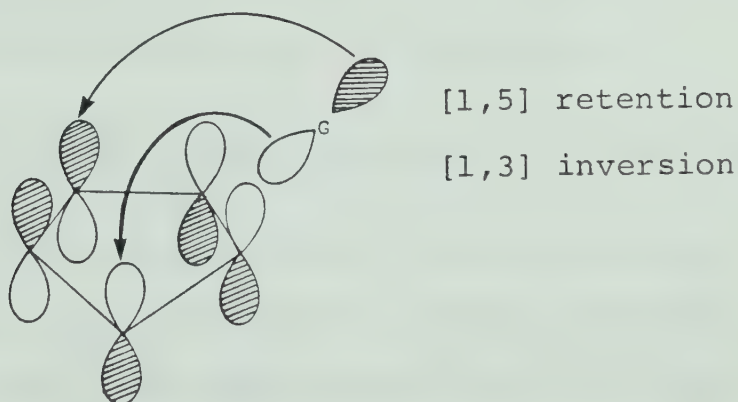
As mentioned in the introduction, fluxional rearrangements observed in σ -cyclopolyenyl metal compounds can be considered as a series of sigmatropic migrations. Before

considering the cyclic systems, it is instructive to clarify the concepts and terminology employed using acyclic polyenyl systems and a migrating group (G) having only a p type orbital available for bonding. The highest occupied molecular orbital (HOMO) of the polyenyl fragment can be used to predict which carbon atoms will have favorable (bonding) interactions with the migrating group, and the stereochemical consequences. Only suprafacial shifts are considered, since antarafacial shifts are considered to be impossible in small and medium sized cyclic systems.¹⁴⁶ The predicted shifts for a pentadienyl system are [1,5] with retention and [1,3] with inversion.



As was pointed out by Anastassiou¹⁴⁷, predictions based on acyclic polyenyl systems cannot be directly generalized to the cyclic systems since the cyclic π interaction due to the development of a p orbital at the migration origin is

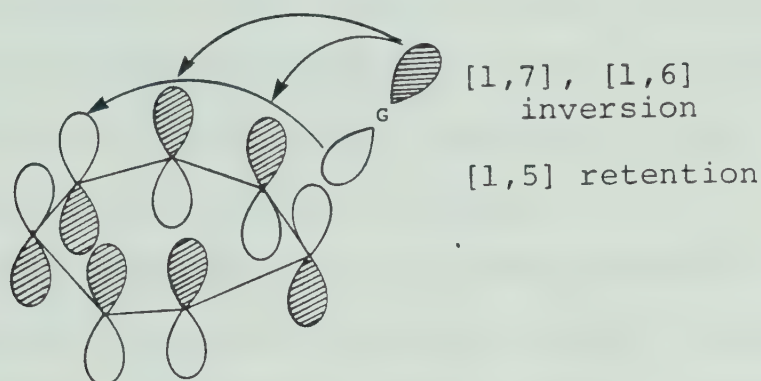
not accounted for. In a cyclic system, the HOMO must be chosen from an energetically degenerate pair of molecular orbitals. A procedure for choosing the correct MO has been outlined by Salem, based on the use of simple perturbation theory.¹⁴⁸ The predicted pathways of sigmatropic shifts in various cyclopolyenyl systems have been summarized in a review by McKinney and Haworth.¹⁴⁹ The result for a σ -cyclopentadienyl system is that [1,5] sigmatropic migrations are allowed if the stereochemistry of the migrating group is unchanged, while [1,3] shifts with inversion are also allowed.



The migration to the adjacent carbon with retention of stereochemistry is conventionally termed a [1,5] shift, in keeping with the acyclic nomenclature. Of course in this cyclic system a [1,5] shift is equivalent to a [1,2] shift.

The same consideration of the symmetry properties of

the HOMO leads to the conclusion that there are three allowed pathways for sigmatropic shifts in a cycloheptatrienyl compound. Once again the nomenclature



used here is consistent with the acyclic notation. Equally correct terminology would be [1,2] or [1,3] shifts with inversion and [1,4] shifts with retention.

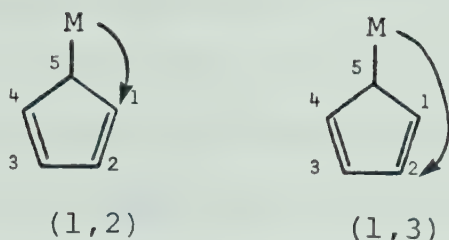
B. σ -cyclopolyenyl Metal Complexes: Previous Results

There are a large number of σ -cyclopolyenyl complexes of the main group and transition metals and their fluxional properties have been intensively studied by many investigators. Cyclopentadienyl compounds are by far the most numerous group. As noted in Chapter I, the first example of fluxional behaviour in a compound of this type was reported by Piper and Wilkinson in 1956.¹² The compound $(C_5H_5)_2Fe(CO)_2$ was prepared and a structure containing one pentahapto and one monohapto ring was proposed, based on

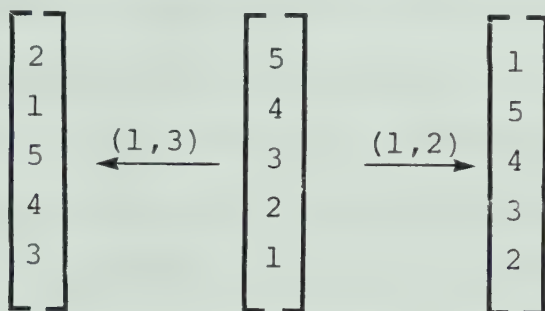
infrared spectroscopic evidence which indicated the presence of a σ -bonded cyclopentadienyl ring. However, the room temperature ^1H NMR spectrum of this compound showed only two singlet resonances. This observation was interpreted by these authors as the consequence of rapid migration of the metal around the σ bonded ring, which led to time averaging of the signals expected for this group*.

Subsequent analysis of the ^1H NMR spectrum at various temperatures by Cotton and coworkers showed that the expected AA'BB'X spectrum for the monohapto ring was observed at -80°C .¹⁵³ On warming, these signals broadened and ultimately coalesced to give a single resonance, confirming the earlier observation. Confirmation of the proposed structure was provided by an x-ray structure determination. Careful examination of the olefinic region of the ^1H NMR spectra revealed that the collapse of these signals was not symmetric. This result indicated that the pathway of metal migration is not random. The two possible non-random pathways are (1,2) and (1,3) shifts of the metal. A simple system of matrix notation (attributed to

*The theoretical basis for NMR line broadening by exchange processes is an extension of the Bloch equations to include exchange terms.^{150,151} The derivation of the necessary equations has been summarized.¹⁵²



J.W. Faller^{*}) was employed to predict the effect of these two different pathways on the observed line broadening of the olefinic ^1H resonances. In the (1,2) shift pathway



the $\text{H}_{2,3}$ protons are exchanged only half as often as the $\text{H}_{1,4}$ protons, so this resonance is expected to be less broadened. Once the olefinic resonances have been assigned, a choice of pathway can be made. This methodology is widely applicable to the determination of the pathway of site

^{*}See ref. 154 for an anecdotal account of the early development of this field.

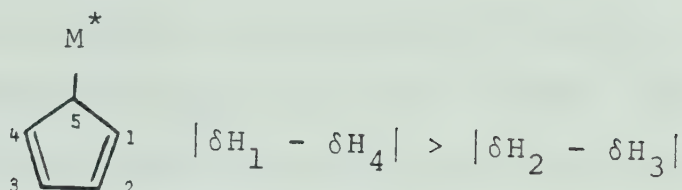
exchange. In every case examined to date, a (1,2) metal migration has been observed.^{155,31}

Studies of this type can reveal the pathway of site exchange, but further information is required for the deduction of the mechanism of the process. In cases where the metal has an isotope of appropriate nuclear spin, coupling between the hydrogen (or ^{13}C) nuclei of the cyclopentadienyl group and the metal which is retained in the high temperature limiting spectrum is evidence for an intramolecular process. For example, the intramolecular nature of the metal migration in $(\eta^1\text{-C}_5\text{H}_5)\text{Pt}(\text{CH}_3)(\text{COD})$ ¹⁵⁶ has been demonstrated by this method.

Compounds in which the metal center is asymmetric allow the stereochemistry of the migration process to be investigated. The metal migration in $(\eta^5\text{-C}_5\text{H}_5)\text{-(ON)[S}_2\text{CN(n-Bu)}_2\text{]Mo}(\eta^1\text{-C}_5\text{H}_5)$ was shown to occur via (1,2) shifts with retention of the configuration of the migrating metal group.¹⁵⁷ Asymmetry at the metal center has the further benefit of simplifying the problem of assignment of the olefinic resonances in the ^1H NMR spectrum. The chemical shift differences between diastereotopic proton (or ^{13}C) pairs increases with proximity to the asymmetric metal center*. Retention of configuration during a (1,2) metal

* This generalization can only be verified by decoupling experiments which are sometimes inconclusive. To date, no exceptions have been reported.

migration has also been demonstrated in $(\eta^5\text{-C}_5\text{H}_5)\text{-Re}(\text{CO})(\text{NO})(\eta^1\text{-C}_5\text{H}_5)$.¹¹⁷



Asymmetric migrating groups have been employed in the study of silyl group migrations in organosilanes such as $(\eta^1\text{-C}_5\text{H}_5)\text{SiHCl}(\text{n-Bu})$, (33), which was found to undergo silyl group migration with retention of configuration. On the basis of this result, it was claimed that "the fluxional process in 33 (and perhaps in all related monohaptocyclopentadienyl metal compounds) is correctly termed a concerted [1,5] metallatropic rearrangement with conservation of orbital symmetry."¹⁵⁸ No evidence for concertedness or intramolecularity was presented.

As mentioned in Chapter I, fluxional behaviour was observed in $(7\text{-}\eta^1\text{-C}_7\text{H}_7)\text{SnPh}_3$. A (1,4) shift pathway was observed²⁰ and later confirmed⁵⁶ in this compound. The intramolecular nature of this rearrangement was established by a determination of the activation energy for Sn-C bond homolysis, which is substantially higher than the activation

energy for the metal migration.²⁰ If this migration is concerted then this process is an example of a [1,5] sigmatropic shift. Similar [1,5] proton migrations have been observed in cycloheptatriene itself¹⁵⁹ and 7-substituted derivatives C_7H_7R ($R = Ph^{160}, Me^{161}, OMe^{162}$, etc.). A [1,5] methyl group migration was observed in 3,7,7-trimethyl-1,3,5-cycloheptatriene.¹⁶³

C. Scope of the Present Studies

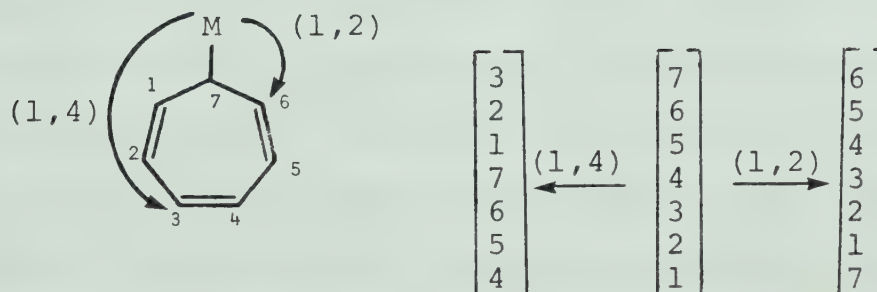
Currently available results for main group and transition metal σ -polyenyl compounds are all in accord with expectations based on the conservation of orbital symmetry expected in concerted sigmatropic migrations. The objective of the investigations presented in this chapter is to extend the available data to include monohaptocycloheptatrienyl compounds of the transition metals, with a view to understanding the mechanism of metal migration reactions in which the migrating group possesses molecular orbitals of substantial d character at accessible energy levels. Although such cases were not dealt with explicitly in the original formulation of the principles of orbital symmetry conservation, this principle is of course applicable to these systems, provided that the symmetry properties of the orbitals are taken into account.

Since there is no evidence to the contrary, it will be assumed throughout that the observed rearrangements are concerted sigmatropic migrations. This assumption is reasonable, but unfortunately it is not subject to experimental verification.

Section II. Fluxional Processes in $(7-\eta^1-C_7H_7)Re(CO)_5$ (5)

A. The Pathway of Metal Migration

The 1H and ^{13}C NMR spectra of 5 (see Figures III and IV) at ambient temperature show no evidence of line broadening indicative of site exchange. The 1H NMR spectrum of 5 at $90^\circ C$ (dioxane- d_8 , 400 MHz), shows substantial line broadening of all resonances, with the $H_{3,4}$ resonance least affected ($\nu_{1/2} = 20$ Hz for $H_{3,4}$, $\nu_{1/2} = 40$ Hz for $H_{1,6}$ and $H_{2,5}$). Using a matrix representation of the seven sites of the cycloheptatriene ring, the effects of (1,2) versus (1,4)



metal migration on the linewidths of the olefinic resonances can be predicted. The (1,4) shift pathway exchanges the 2,5 positions only half as often as the other olefinic sites. The (1,2) pathway exchanges the 3,4 site less rapidly than

the 2,5 or 1,6 sites and is thus consistent with the observed linewidths.

Since 5 is thermally unstable, temperatures which allow the observation of line broadening also cause rapid decomposition of the compound to ditropyl and $\text{Re}_2(\text{CO})_{10}$. The olefinic resonances of ditropyl partially obscure the signals due to 5. The qualitative observation that (1,2) metal migration is occurring can be made, but reliable quantitative data regarding the rate of this process could not be obtained.

Exchange processes which occur too slowly to cause NMR line broadening can be studied using techniques such as isotopic labelling.¹⁵⁹ Recent improvements in NMR instrumentation have allowed the use of a double resonance technique known as spin saturation transfer to obtain similar information. This method is applicable in cases where the rate of exchange is comparable to the rate of longitudinal relaxation of the nucleus used for observation (as expressed by the spin-lattice relaxation time T_1). In these cases, two sites linked by an exchange process can be identified by saturation of one site and observation of an intensity decrease at the site with which it is exchanging. The decrease in intensity results from the partial transfer of saturation to the new site effected by

the exchange process.

The theoretical basis for quantitative determination of rate constants from experiments of this type is the modification of the Bloch equations due to McConnell.¹⁵¹ The first experiments in this area were carried out by Forsén and Hoffmann.¹⁶⁴ Subsequently this technique has been applied to a wide variety of problems. A readable general account of the method with applications and examples is available.¹⁶⁵

In the case of compound 5, qualitative confirmation of the pathway of site exchange is readily obtained by saturating the resonance due to H_7 with a second RF field. The intensity of the $H_{1,6}$ resonance decreases, indicating that these two sites are exchanging with H_7 via a (1,2) shift pathway. The decrease in signal intensity at the $H_{1,6}$ site can be quantitatively measured by using a difference spectrum (see Figure XX). In this procedure, a normal spectrum of 5 is taken with the saturating field on, but not centered on H_7 . A spectrum is then taken with saturation of H_7 and the two FID's are subtracted to give a difference FID, which is then Fourier transformed to give a difference spectrum. This allows the intensity decrease to be quantitatively evaluated by integration against an internal standard.

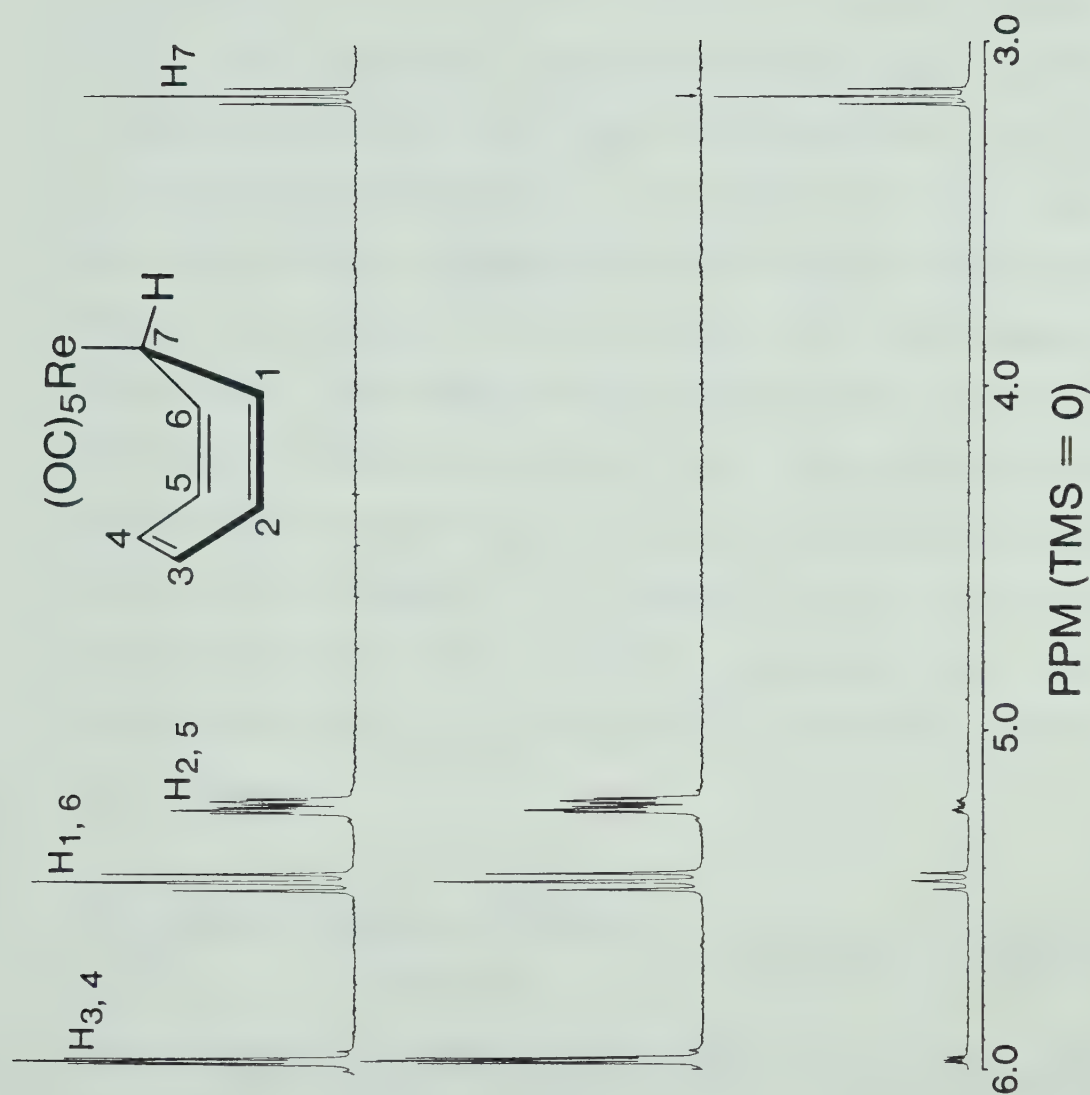


FIGURE XX. ^1H SST difference experiment on $(7-\eta^1\text{-C}_7\text{H}_7)\text{Re}(\text{CO})_5$ in methylcyclohexane- d_{14} , 298.2°K. Top: normal spectrum. Middle: saturation of H_7 . Bottom: difference spectrum.

Rate constants are readily derived from the size of the decrease in signal intensity and a knowledge of the T_1 values for each proton in the molecule (it is not necessary to determine the T_1 of the nucleus being saturated). Since three metal migration pathways are possible, three rate constants (k_{12} , k_{13} and k_{14}) are considered (k is defined as a one-way rate constant*). The parameter which must be measured is the z component of the equilibrium magnetization (M_z) at each site, in the presence (M_z^∞) and absence (M_z^0) of saturation. The equilibrium magnetization is proportional to signal intensity, provided that full relaxation can occur between observation pulses. This condition is met by using a delay of at least $5 \times T_1$ between pulses. For the 1,6 site, with saturation of the H_7 resonance, the time dependence of $M_{z(1,6)}$ is given by a modified Bloch equation (eq. 45).

$$\frac{dM_{z(1,6)}^\infty}{dt} = \frac{M_{z(1,6)}^0 - M_{z(1,6)}^\infty}{T_1(1,6)} + k_{12}M_{z(2,5)}^\infty + k_{13}M_{z(3,4)}^\infty + k_{14}(M_{z(2,5)}^\infty + M_{z(3,4)}^\infty) - (2k_{12} + k_{13} + 2k_{14})M_{z(1,6)}^\infty \quad (45)$$

*The total rate at which the metal leaves site 7 by (1,2) shifts is given by $2k_{12}$.

Similar equations apply for $M_{Z(2,3)}$ and $M_{Z(3,4)}$. At equilibrium, $dM_Z^\infty/dt = 0$. With $M_{Z(1,6)}^\infty$ arbitrarily defined as 1, this equation can be simplified and rearranged to give equation 46.

$$k_{12} = \frac{1}{2} \left[\frac{1 - M_{Z(1,6)}^\infty}{M_{Z(1,6)}^\infty} \right] \frac{1}{T_{1(1,6)}} + \frac{\frac{1}{2}k_{12}M_{Z(2,5)}^\infty}{M_{Z(1,6)}^\infty} + \frac{\frac{1}{2}k_{13}M_{Z(3,4)}^\infty}{M_{Z(1,6)}^\infty} + \frac{\frac{1}{2}k_{14}(M_{Z(2,5)}^\infty + M_{Z(3,4)}^\infty)}{M_{Z(1,6)}^\infty} - (\frac{1}{2}k_{13} + k_{14}) \quad (46)$$

A set of three equations with three unknown rate constants describes this system. Input of measured M_Z^∞ values allows all the rate constants to be determined. The details of the derivation and solution of these equations are given in the Appendix.

A study of the (1,2) metal migration in 5 at various temperatures in dioxane- d_8 has been carried out (see Figure XXI). The results at the lower temperatures show that the saturation of H_7 leads to an intensity decrease at $H_{1,6}$. The higher temperature experiments show the effect of successive (1,2) shifts, which are manifested by intensity decreases at the 2,5 site and to a lesser extent at the 3,4 site. Solution of the set of three equations describing $M_{Z(1,6)}^\infty$, $M_{Z(2,5)}^\infty$ and $M_{Z(3,4)}^\infty$ gives values for the rate constants k_{12} , k_{13} and k_{14} at each temperature. The results



FIGURE XXI. ^1H SST difference spectra (H_7 saturated) at various temperatures (dioxane- d_8).

of this process, along with the M_2^∞ and T_1 values used in the calculations, are tabulated in Table X. The rate constants k_{13} and k_{14} were not significantly different from zero.

Rate constants were also calculated using the results of the SST experiment depicted in Figure XX. A value of $k_{12} = 2.84 \times 10^{-2} \text{sec}^{-1}$ for 5 in methylcyclohexane- d_{14} at 298.2 K was obtained. This is 10% higher than the value obtained in dioxane- d_8 at the same temperature. Thus it can be concluded that the rate of metal migration is not substantially affected by this change in solvent.

The precision of these values for k_{12} is affected by a number of sources of error. There is uncertainty in the temperature, in the determination of relaxation times (T_1 's) and in the evaluation of M_2^∞ for each site in the ring. As outlined in the experimental section of this chapter, the probe temperature was carefully determined with a calibrated thermistor and is accurate to $\pm 0.1^\circ\text{C}$. The probe temperature varies less than $\pm 0.1^\circ\text{C}$ under the experimental conditions.

Relaxation times were measured using the conventional $(\pi - \tau - \frac{\pi}{2} - 5 \times T_1)$ pulse sequence. The precision of this procedure was estimated to be $\pm 5\%$ (2 standard deviations) by Levy and coworkers.¹⁶⁶ Due to superior field homogeneity of the superconducting magnet used in our experiments, the

TABLE X. ^1H Spin Saturation Transfer Data for $(7\text{-}\eta^1\text{-C}_7\text{H}_7)\text{Re}(\text{CO})_5$.

T, K	$M_z(3,4)$	$M_z(2,5)$	$M_z(1,6)$	$T_1(3,4)$	$T_1(2,5)$	$T_1(1,6)$	$10^2 \times k_{12} (\text{s}^{-1})$	$10^2 \times k_{13}$	$10^2 \times k_{14}$
298.2	.976	.970	.881	7.26	7.10	6.34	2.46	0.28	0.20
301.1	.965	.942	.820	7.64	7.39	6.73	4.01	0.27	0.39
304.0	.943	.901	.759	8.02	7.69	7.09	5.87	0.26	0.77
306.9	.903	.875	.702	8.39	7.98	7.46	8.21	0.78	0.28
309.9	.866	.831	.628	8.78	8.29	7.84	12.1	1.06	-0.27
312.9	.836	.780	.601	9.17	8.59	8.21	12.8	0.67	1.19
315.8	.769	.733	.559	9.43	8.79	8.49	15.6	1.72	0.83

precision may be improved, but no systematic investigation of the precision achieved in the T_1 determinations has been carried out. An indication of the precision of these results is that the relative order $T_{1(2,5)} < T_{1(3,4)}$ is maintained at all temperatures studied, although the two values differ by only ca. 5%. The T_1 's show a linear dependence on the temperature except at the upper limits of the temperature range, where averaging due to the exchange process causes some deviations. The values listed in Table X are the result of a linear regression analysis of data from 288.4 K to 312.9 K.

Evaluation of M_Z^∞ depends on precise integration of difference spectra. With the proviso that phase anomalies are avoided and that an adequate signal:noise ratio is obtained, integration of the difference signal is believed to be precise to $\pm 5\%$. These integrals are evaluated by comparison to an internal standard provided by the signal which is saturated.

The uncertainty in the rate constants determined by the solution of the three simultaneous equations can be roughly calculated by varying the inputs accordingly. The worst case in which a 5% error in the T_1 and a 5% error in the integral reinforce each other leads to an 11% change in k_{12} .

Activation parameters for the (1,2) metal migration in

5 were obtained from an Eyring plot of the data of Table X (see Figure XXII). Values obtained were $\Delta H^\ddagger = 18.0 \pm 0.7$ kcal mol⁻¹, $\Delta S^\ddagger = -5.0 \pm 3.2$ e.u. and $\Delta G_{300}^\ddagger = 19.5 \pm 1.0$ kcal mol⁻¹. The uncertainty limits correspond to one standard deviation in the slope based on a linear regression analysis employing program ACTEN. This program accepts errors in both k and T and propagates these errors through to the calculation of the slope. In this case, the inputs were $k_{12} \pm 10\%$ and $T \pm 0.2^\circ\text{C}$. Although the ΔG^\ddagger value is probably fairly reliable, the entropy of activation is very approximate, since the data cover a narrow temperature range and the ΔS^\ddagger value is derived from an intercept which is the result of a very long extrapolation.

There are two potential sources of error in this experiment which arise from using ¹H, which has 99% natural abundance, as the nucleus of observation. The protons involved are in close physical proximity and highly coupled to each other. When the resonance due to H₇ is saturated, there is a possibility of spurious intensity enhancement at H_{1,6} due to the nuclear Overhauser effect (NOE)¹⁶⁷, as well as the possibility of propagation of demagnetization to other ring protons via spin-spin interactions.¹⁶⁸ It is experimentally impossible to distinguish NOE effects from spin saturation transfer due to chemical exchange if both

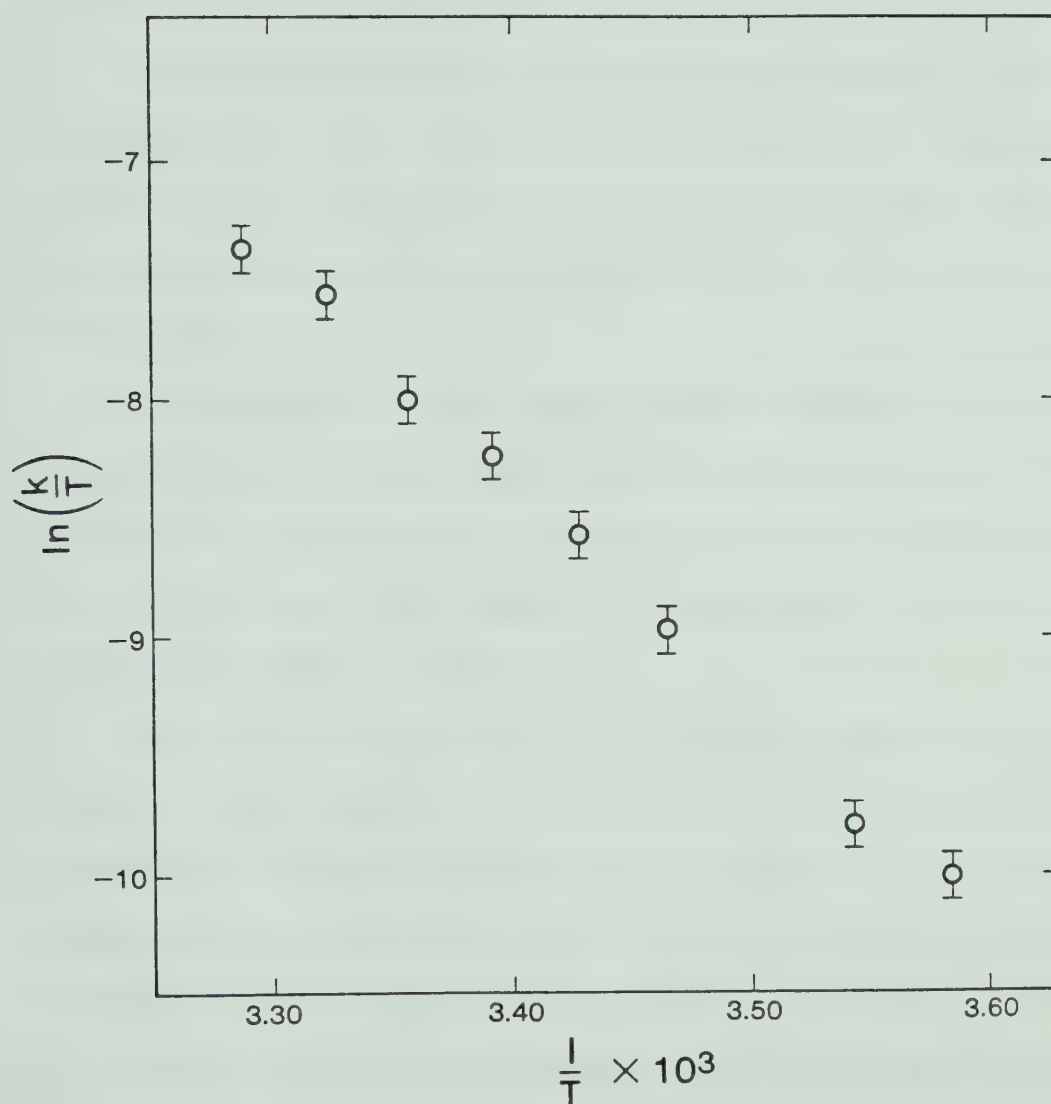


FIGURE XXII. Eyring plot of ^1H rate data for $(7\text{-}\eta^1\text{-C}_7\text{H}_7)\text{Re}(\text{CO})_5$ (Error bars indicate $k \pm 10\%$).

are occurring. In the absence of exchange, NOE effects can be detected. In the case of 5, there was no observable NOE effect and no chemical exchange effects at 288.4 K.

The possibility of NOE effects between H_7 and $H_{1,6}$ in compounds of this type cannot be dismissed, since such effects were observed in $(7-\eta^1-C_7H_7)Re(CO)_4PMe_3$ and other phosphine substituted derivatives of 5 (see Section III of this chapter).

The potential problems can be avoided by using a magnetically dilute observation nucleus, such as ^{13}C . Fluxional processes in 5 were studied by ^{13}C NMR at 100.6 MHz in THF- d_8 . (The complete temperature range used was not accessible using dioxane- d_8 .)

The determination of ^{13}C T_1 's in 5 was complicated by the fact that the T_1 of C_7 is quite short (ca. 0.5 sec) compared to those of the olefinic carbons. The exchange process causes the observed T_1 of $C_{1,6}$ and $C_{2,5}$ to be reduced at the higher temperatures (see Figure XXIII). The T_1 values show a linear dependence on temperature in the range 275.8 K to 291.7 K. A linear regression analysis of this data was used to obtain the T_1 's at higher temperatures.

Decoupling of ^{13}C was achieved by using an external frequency synthesizer (see Experimental Section). Probe

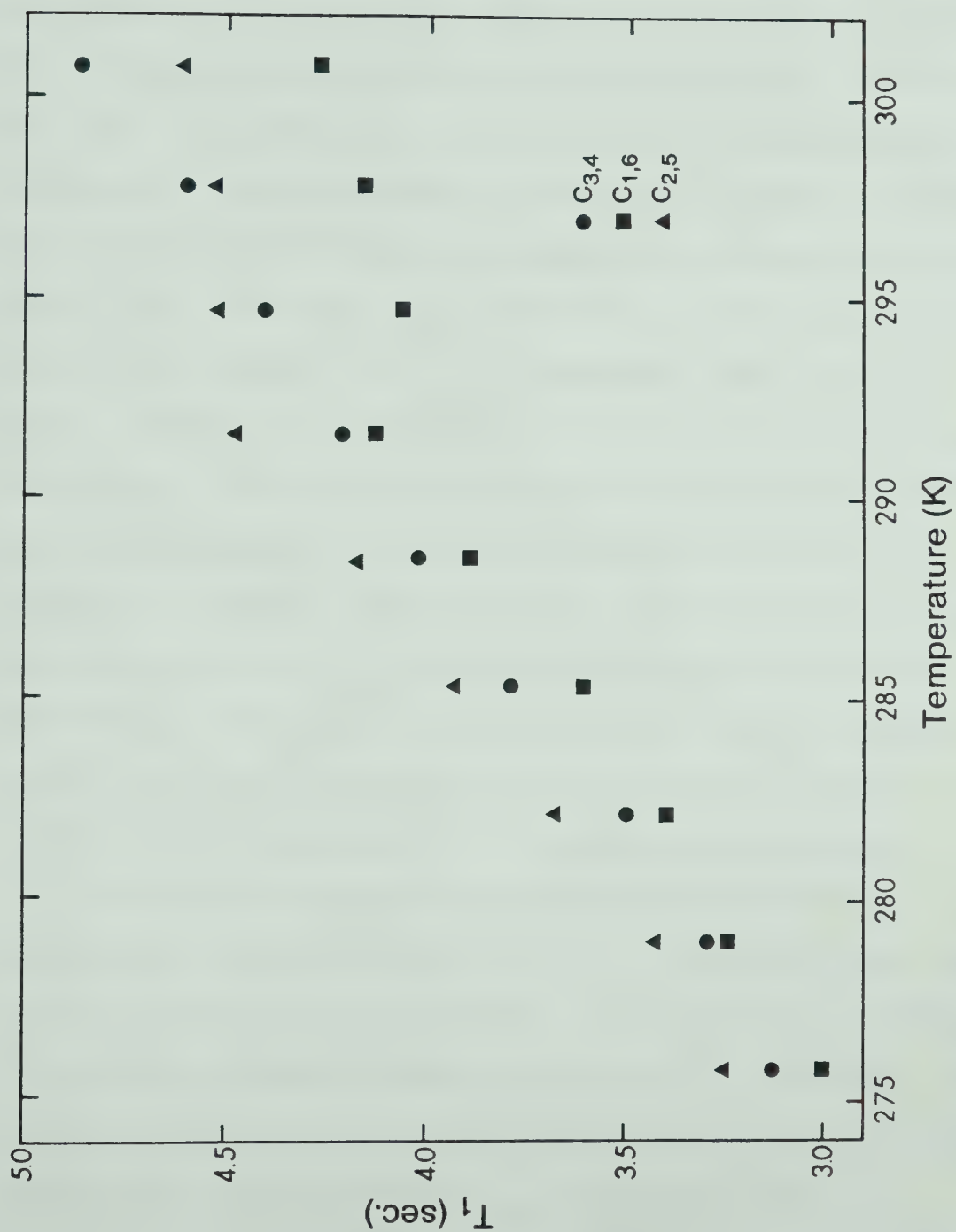


FIGURE XXIII. Plot of ^{13}C T_1 's of $(7-\eta^1\text{-C}_7\text{H}_7)\text{Re}(\text{CO})_5$ as a function of temperature.

temperatures were calibrated as in the case of the ^1H probe, and are constant to $\pm 0.1^\circ\text{C}$. Saturation transfer effects were detected by recording difference spectra, as described in the preceeding section for ^1H experiments. Any one of the four ^{13}C resonances due to the ring carbons can be saturated. An example of a saturation transfer experiment with saturation of the $\text{C}_{3,4}$ resonance is shown in Figure XXIV. The difference spectrum clearly shows that there is saturation transfer to $\text{C}_{2,5}$, consistent with a (1,2) shift. There is no decrease in the intensity of the $\text{C}_{1,6}$ resonance. The effectiveness of the subtraction procedure is demonstrated by the lack of residual signal at the $\text{C}_{1,6}$ position. Another important point to note is that complete saturation of the $\text{C}_{3,4}$ resonance was achieved (middle spectrum). Since the difference signal due to $\text{C}_{3,4}$ is used as the internal intensity standard, complete saturation is crucial to the accuracy of the quantitative results.

A series of difference spectra were recorded at various temperatures with saturation of C_7 . A selection of these spectra are shown in Figure XXV. As expected, the largest intensity decrease is observed at the $\text{C}_{1,6}$ position. The intensity decrease caused by two successive (1,2) shifts is smaller and the effect at $\text{C}_{3,4}$ is smaller still.

The values for M_2^∞ , T_1 's and the rate constants

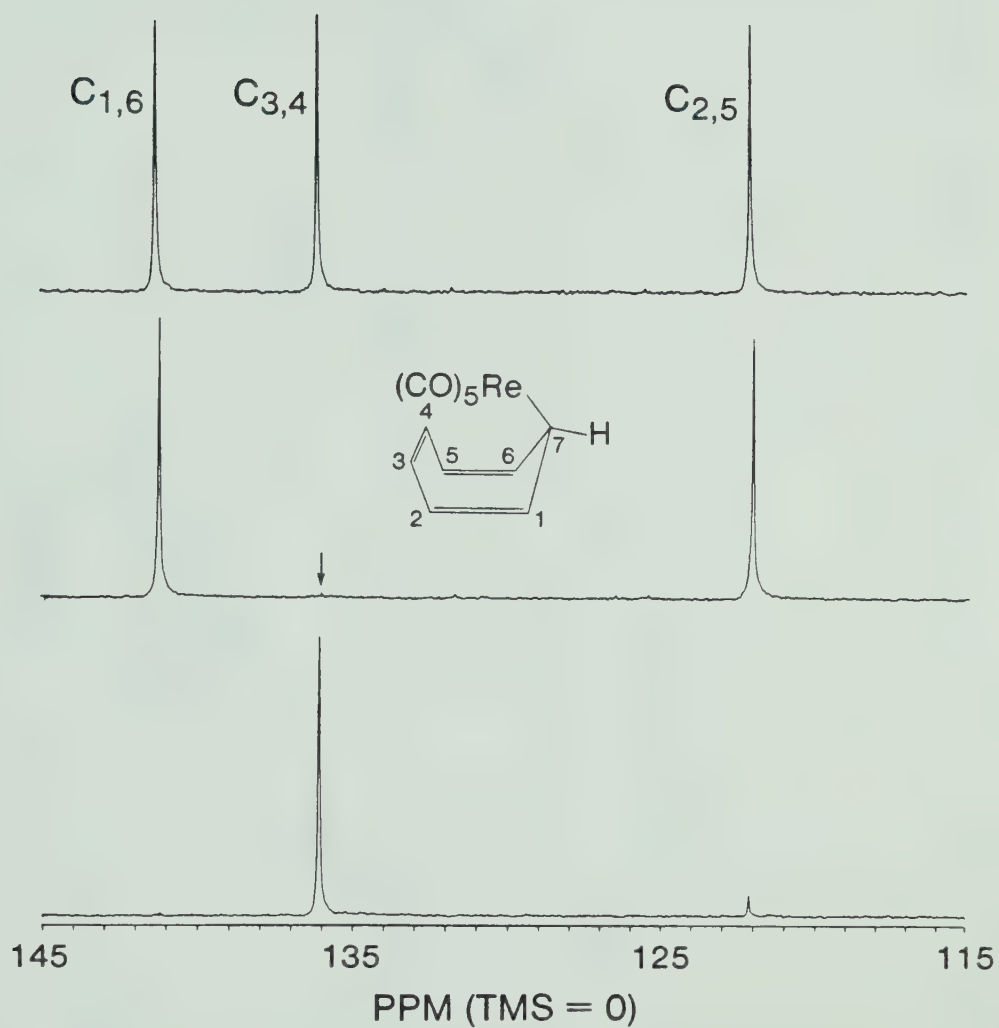


FIGURE XXIV. ^{13}C SST difference experiment on $(7-\eta^1\text{-C}_7\text{H}_7)\text{Re}(\text{CO})_5$ in THF. Top: normal spectrum. Middle: saturation of $\text{C}_{3,4}$. Bottom: difference spectrum.

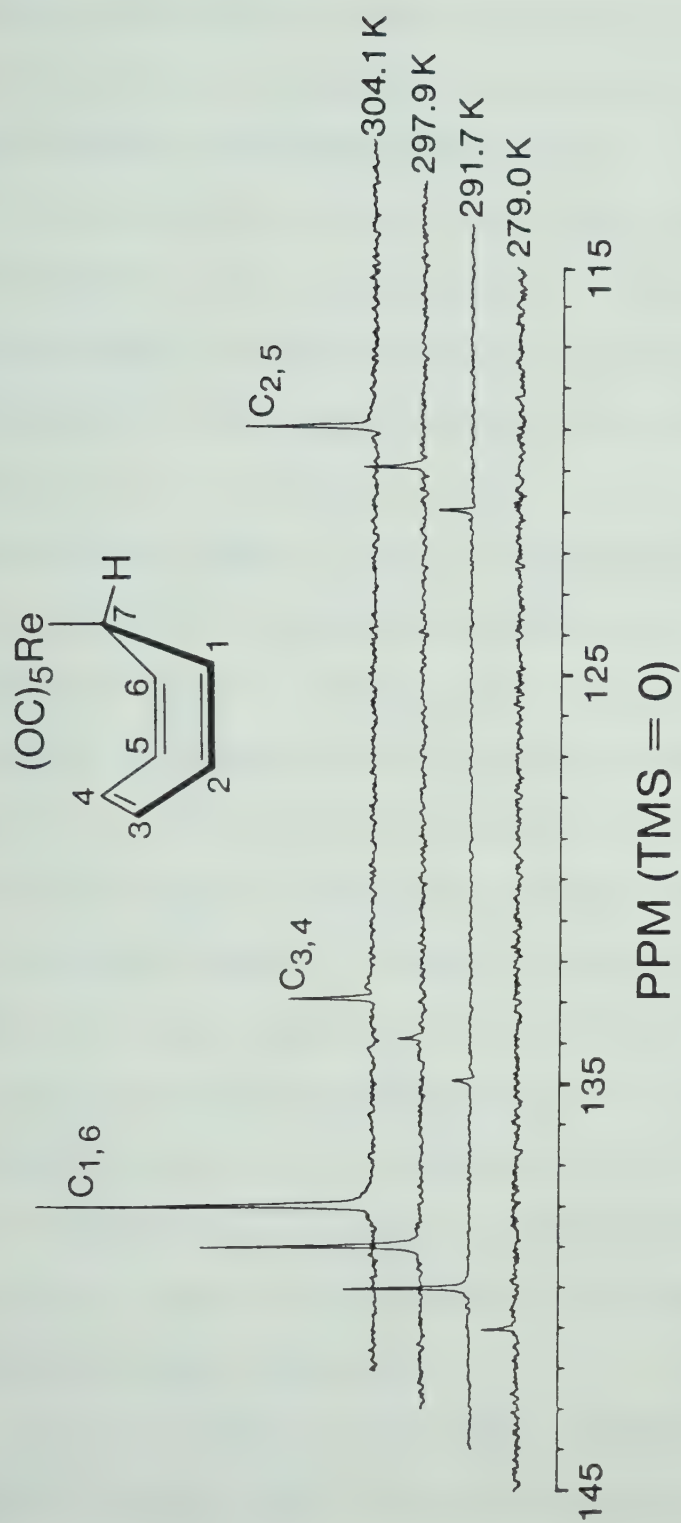


FIGURE XXV. ^{13}C SST difference spectra for $(7-\eta^1\text{-C}_7\text{H}_7)\text{Re(CO)}_5$ at various temperatures (saturation of C_7 , THF-d_8).

obtained from these experiments are listed in Table XI. As in the case of the proton results, k_{13} and k_{14} were not significantly different from zero.

The sources of error which were discussed for the ^1H measurements also apply to the ^{13}C experiments. NOE effects and spin-spin interactions are eliminated. There is one difference in the experimental conditions which may have an effect on the accuracy of the results. As noted in the experimental section, the ^{13}C decoupling field was generated by an external frequency synthesizer, not subject to direct computer control. Manual switching of the decoupler frequency between the on and off resonance modes was required. In the proton experiments this task is automated, so the saturating field was switched from on resonance to off resonance every 4 scans to minimize problems due to field drift and temperature variation. In the ^{13}C spectra, the decoupler was switched only once, at the halfway point in accumulations of 100-300 scans (1-3 hours). In some of the ^{13}C experiments, poorly phased difference spectra were obtained. These results were disregarded and the experiments were repeated.

An Eyring plot of the rate constants from Table XI is shown in Figure XXVI. The activation parameters were obtained as previously discussed. Input uncertainties were

TABLE XI. ^{13}C Spin Saturation Transfer Data for $(7\text{-}\eta^1\text{-C}_7\text{H}_7)\text{Re}(\text{CO})_5$.

T, k	$M_z^{\infty}(3,4)$	$M_z^{\infty}(2,5)$	$M_z^{\infty}(1,6)$	$T_{1(3,4)}$	$T_{1(2,5)}$	$T_{1(1,6)}$	$10^2 \times k_{12}(\text{s}^{-1})$	$10^2 \times k_{13}$	$10^2 \times k_{14}$
279.0	1	1	.963	3.32	3.45	3.20	1.25	0.002	-0.05
282.2	1	1	.951	3.54	3.69	3.43	1.58	0.004	-0.08
288.6	1	1	.889	3.98	4.18	3.84	3.67	0.04	-0.41
291.7	1	.977	.841	4.19	4.42	4.05	5.51	-0.09	-0.09
294.8	.994	.958	.791	4.40	4.66	4.26	7.77	-0.10	-0.11
297.9	.975	.939	.751	4.61	4.90	4.46	9.95	0.23	-0.34
300.9	.949	.900	.688	4.82	5.13	4.66	14.2	0.44	-0.54
304.1	.928	.870	.630	5.04	5.37	4.88	19.2	0.70	-0.15

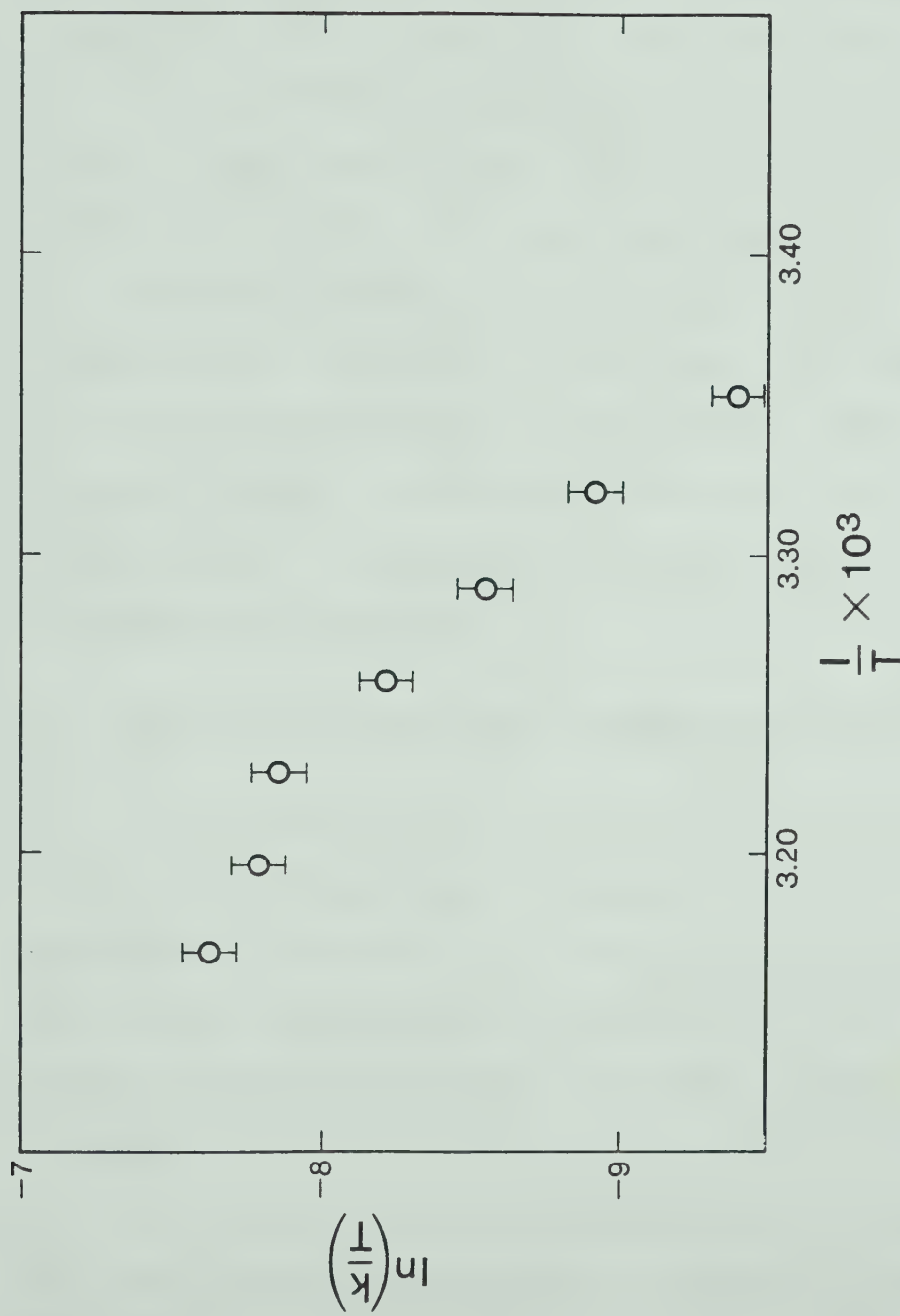


FIGURE XXVI. Eyring plot of ^{13}C rate constant data for $(7-\eta^1-C_7H_7)Re(CO)_5$ (Error bars indicate $k \pm 10\%$).

$k_{12} \pm 10\%$ and $T \pm 0.2^\circ$. The activation parameters obtained for the (1,2) metal migration in 5 are $\Delta G_{300}^\ddagger = 18.8 \pm 0.6$ kcal mol⁻¹, $\Delta H^\ddagger = 18.1 \pm 0.5$ kcal mol⁻¹ and $\Delta S^\ddagger = -2.4 \pm 1.5$ eu. The activation parameters for this process obtained from ¹H experiments were: $\Delta G_{300}^\ddagger = 19.5 \pm 1.0$ kcal mol⁻¹, $\Delta H^\ddagger = 18.0 \pm 0.7$ kcal mol⁻¹ and $\Delta S^\ddagger = -5.0 \pm 3.2$ eu. The free energy of activation obtained from the ¹³C measurements is slightly lower than the result obtained from the proton experiments. Since the ¹³C experiments cover a slightly greater temperature range and are based on observation of a magnetically dilute nucleus, they are probably more reliable.

B. Carbonyl Exchange and the Mechanism of Metal Migration

As pointed out in the introduction to this Chapter, information concerning the pathway of metal migration can be obtained by observation of the pattern of site exchange. No information regarding the mechanism of the rearrangement process can be obtained in this way. Further data is needed.

The activation energy for homolysis of the Re-C₇ σ bond in 5 was determined to be 26.5 kcal mol⁻¹ (Chapter II). This value is substantially greater than the measured activation energy of 19.5 kcal mol⁻¹ for the (1,2) metal

migration. Thus a dissociative mechanism can be ruled out. Similar arguments were advanced by Larrabee²⁰ to establish that the fluxional behaviour of $\text{Ph}_3\text{Sn}(7-\eta^1-\text{C}_7\text{H}_7)$ was the result of an intramolecular process.

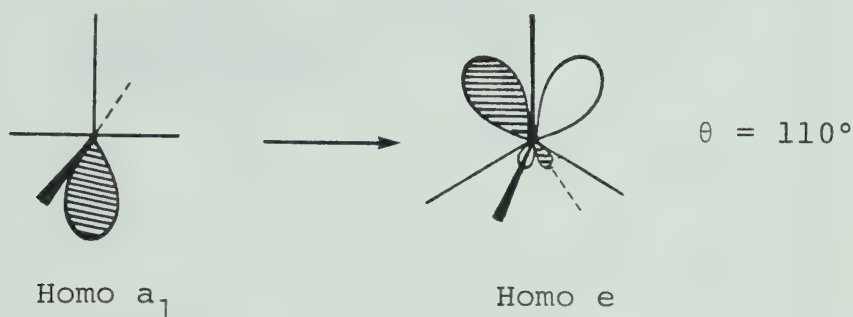
Since the metal migration in 5 is intramolecular, it will be assumed that it is also a concerted reaction and that orbital symmetry restrictions should apply. On this basis a [1,5] metal migration, as observed in $\text{Ph}_3\text{Sn}(7-\eta^1-\text{C}_7\text{H}_7)$, would be expected. The similarity in solid-state and solution structures between 5 and this tin compound were pointed out in Chapter II. There is no geometric constraint on a [1,5] metal migration in 5. The observed [1,7] metal migration in 5 is not consistent with expectations based on participation of a single invariant σ orbital of the $\text{Re}(\text{CO})_5$ group. The observed migration must involve orbitals of the $\text{Re}(\text{CO})_5$ group of other than σ symmetry. The energy ordering of molecular orbitals for molecular fragments of the type $\text{M}(\text{CO})_n$ have been the subject of theoretical study by Elian and Hoffmann.¹⁶⁹ In the case of the $\text{Mn}(\text{CO})_5$ fragment, the HOMO is an a_1 orbital of σ symmetry (predominantly d_z^2).



These calculations are equally applicable to $\text{Re}(\text{CO})_5$

fragments.¹⁷⁰

The involvement of e type orbitals (d_{xz} and d_{yz} hybrids) in the transition state for metal migration would seem reasonable, since calculations show that a slight distortion of the $\text{Re}(\text{CO})_5$ fragment could render these orbitals energetically similar to the a_1 orbital. An increase in θ to approximately 110° is required to



equalize the energy of the a_1 and e orbitals. The interaction with the HOMO of the C_7H_7 fragment is depicted in Figure XXVII. Such a process would render the observed [1,7] shift symmetry allowed, and it would also exchange the axial CO group with one of the equatorial CO groups. This exchange process should be occurring at the same rate as the metal migration, and should be detectable by a ^{13}C SST experiment. Such an experiment has been carried out.

The saturation of the ^{13}C resonance due to the axial carbonyl group of 5 causes a decrease in the intensity of the signal for the equatorial carbonyls. The rate of

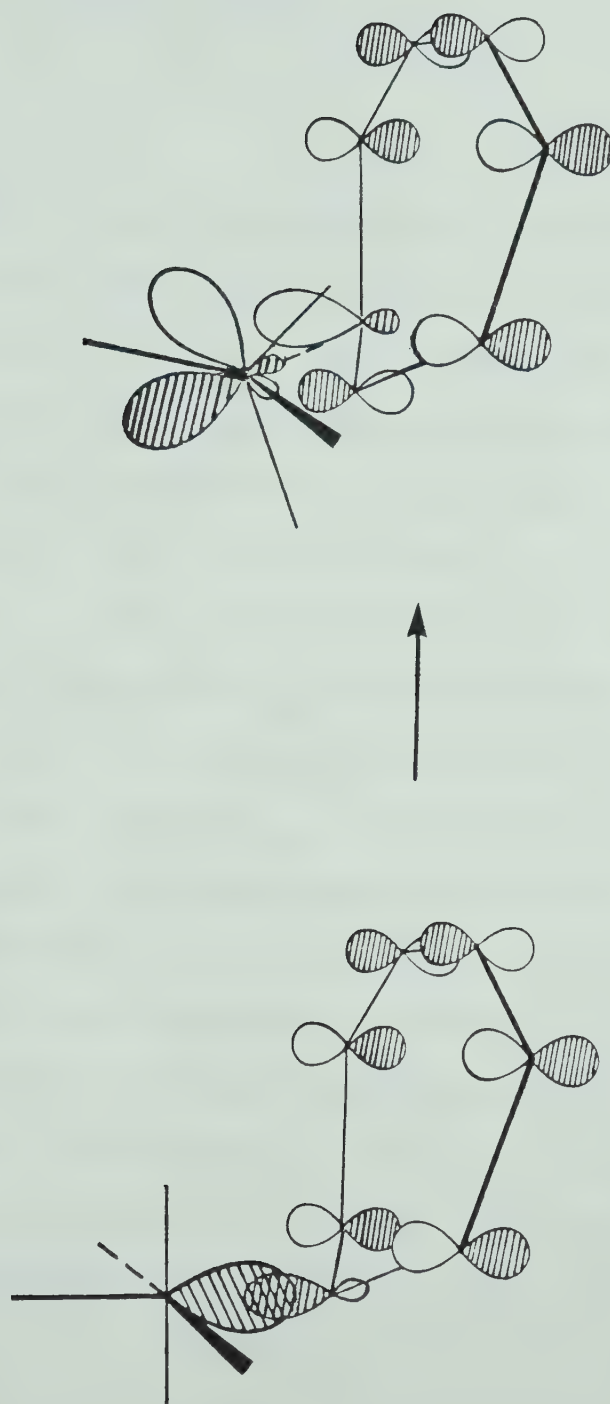


FIGURE XXVII. Proposed transition state geometry for the metal migration process in $(7-\eta^1\text{-C}_7\text{H}_7)\text{Re}(\text{CO})_5$.

exchange was calculated using the formula:

$$k_{\text{ex}} = 4 \left[\frac{M_{\text{Z}(\text{eq})}^{\text{O}} - M_{\text{Z}(\text{eq})}^{\infty}}{M_{\text{Z}(\text{eq})}^{\infty}} \right] \cdot \frac{1}{T_1(\text{eq})}$$

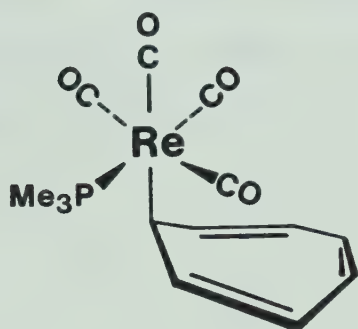
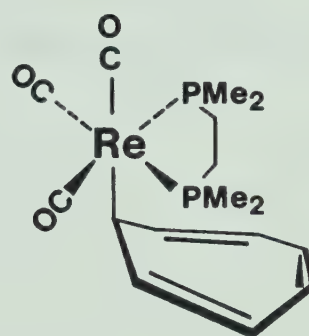
The equilibrium magnetization of the ^{13}C nuclei in the equatorial positions is designated $M_{\text{Z}(\text{eq})}^{\text{O}}$ in the absence of saturation and $M_{\text{Z}(\text{eq})}^{\infty}$ with saturation. The factor of four allows for the population difference between these two sites. This definition of the rate of exchange, k_{ex} , is consistent with the definition of k_{12} as a one-way rate constant. Since metal migration in either direction causes carbonyl exchange, k_{ex} should be twice k_{12} .

At 304.1 K, the T_1 of the equatorial carbonyl cation is 3.7 sec, giving $k_{\text{ex}} = 0.23 \text{ sec}^{-1}$. The expected value for k_{ex} at this temperature is 0.38 sec^{-1} . When the same ^{13}C SST experiment was carried out using $\text{CH}_3\text{-Re}(\text{CO})_5$, no SST effect was detected at 308 K.

Thus we conclude that the observed carbonyl scrambling in 5 is a consequence of the metal migration. The proposed mechanism for the [1,7] shift in 5 is in accord with orbital symmetry predictions and with the experimental observations.

Section III. Spin Saturation Transfer Experiments on
Phosphine Substituted Derivatives of (η^1 -
 $C_7H_7Re(CO)_5$

Two phosphine substituted derivatives of 5 have been studied by 1H NMR SST experiments. These are the trimethylphosphine substituted tetracarbonyl 11 and the dmpe derivative 15.

1115

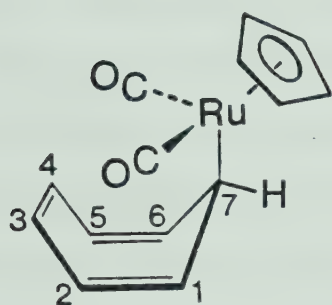
Saturation of the H_7 resonance of 11 or 15 at 297 K led to an increase in the intensity of the $H_{1,6}$ signal, presumably due to an NOE effect.¹⁶⁷ There was no evidence for an SST effect at the $H_{2,5}$ or $H_{3,4}$ resonances. Since NOE enhancement of signal intensities depends on dipole-dipole (ie 1H - 1H) interaction, the effect is critically dependent on the distance (r) between nuclei. The size of the effect is proportional to $\frac{1}{r^6}$.¹⁶⁷ Replacement of one or more

carbonyl groups in 5 with phosphines presumably causes some slight change in the conformation of the cycloheptatrienyl ring, leading to a smaller separation between H₇ and H_{1,6}.

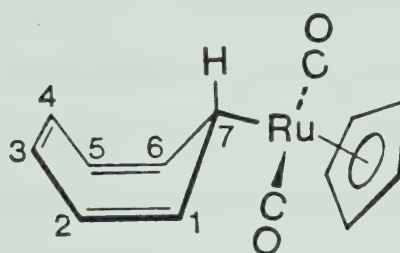
The lack of observable SST effects exhibited by the H_{2,5} and H_{3,4} resonances indicates that metal migration is quite slow at these temperatures. Phosphine substitution seems to have increased the activation energy for metal migration. More definitive information could be obtained by employing ¹³C as the observation nucleus. Since the quantities of 11 and 15 available are limited, this has not yet been investigated.

Section IV. Metal Migration in $\text{CpRu}(\text{CO})_2(7-\eta^1\text{-C}_7\text{H}_7)$ (23)

Although no crystallographic data is available for this compound, the value of 7.8 Hz for the vicinal coupling constant $^3J_{1-7}$ is consistent with 23a. The structure of 23



23a



23b

may be a rapidly exchanging mixture of 23a and 23b, with 23a predominating. As was the case with 5, there are no geometric constraints on the pathway of metal migration.

The ^1H NMR spectrum of 23 is shown in Figure XII. Saturation of the resonance due to H_7 (298 K) causes an intensity decrease at $\text{H}_{1,6}$, $\text{H}_{2,5}$ and $\text{H}_{3,4}$. The size of the effect at $\text{H}_{3,4}$ is not consistent with a (1,2) shift alone. Due to the potential problems with NOE effects, further experiments were confined to the use of magnetically dilute ^{13}C for observation.

The ^{13}C NMR spectrum of 23 is very similar to that

observed for 5. The results of an SST experiment with saturation of C_7 are shown in Figure XXVIII. The difference spectrum shows that the largest intensity decrease is at $C_{1,6}$. There is also an effect at $C_{2,5}$ and $C_{3,4}$. It is clear on comparing this result to those obtained for 5 that some pathway in addition to the (1,2) shift observed in 5 must be exchanging C_7 with $C_{2,5}$ and $C_{3,4}$.

Analysis of a series of spectra at various temperatures showed similar effects (see Figure XXIX). The observed intensity changes are tabulated in Table XII. The measurement of T_1 's in 23 was hampered by exchange averaging at higher temperatures. As observed in 5, T_1 for C_7 is much shorter than the others, leading to a deviation from linearity at the higher temperatures. The T_1 's listed in Table XII are the result of a least squares fit of data from 260.5 K to 285.4 K (8 points). Values for higher temperatures were extrapolated.

The calculation of rate constants for the metal migration was carried out as described for compound 5. Three rate constants k_{12} , k_{13} and k_{14} were considered. The solution of the three equations describing the magnetization transfer gave non-zero values for k_{12} and k_{14} at all temperatures. The values for k_{13} were not significantly different from zero (see Table XII).

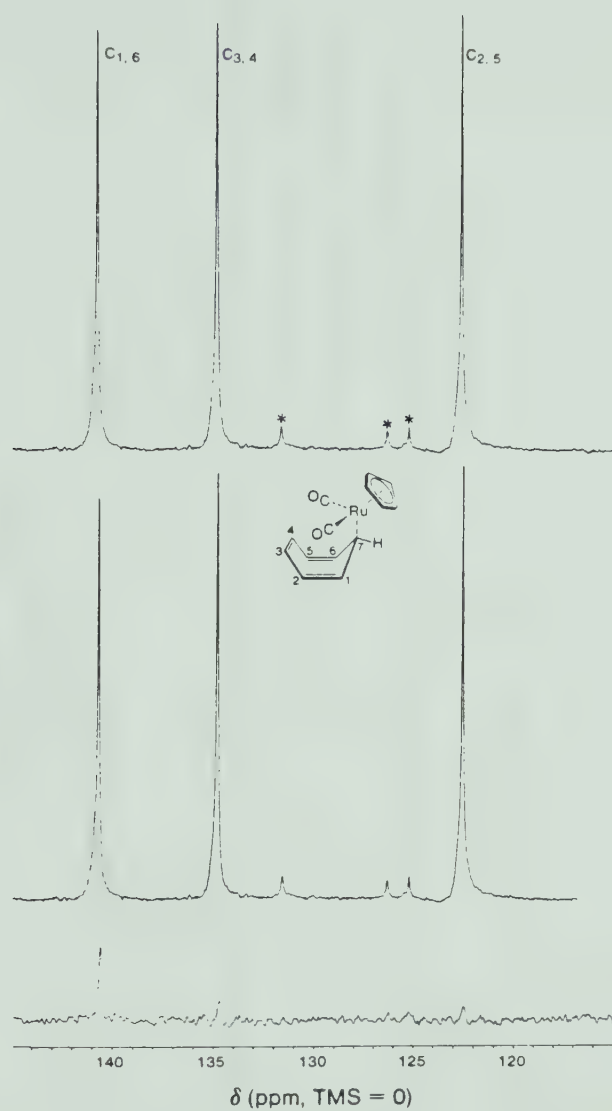


FIGURE XXVIII. ^{13}C SST difference experiment on $\text{CpRu}(\text{CO})_2(7-\eta^1\text{-C}_7\text{H}_7)$ (THF-d_8 , 279.0 K). Top: normal spectrum. Middle: saturation of C_7 . Bottom: difference spectrum (* = 2% ditropyl impurity).

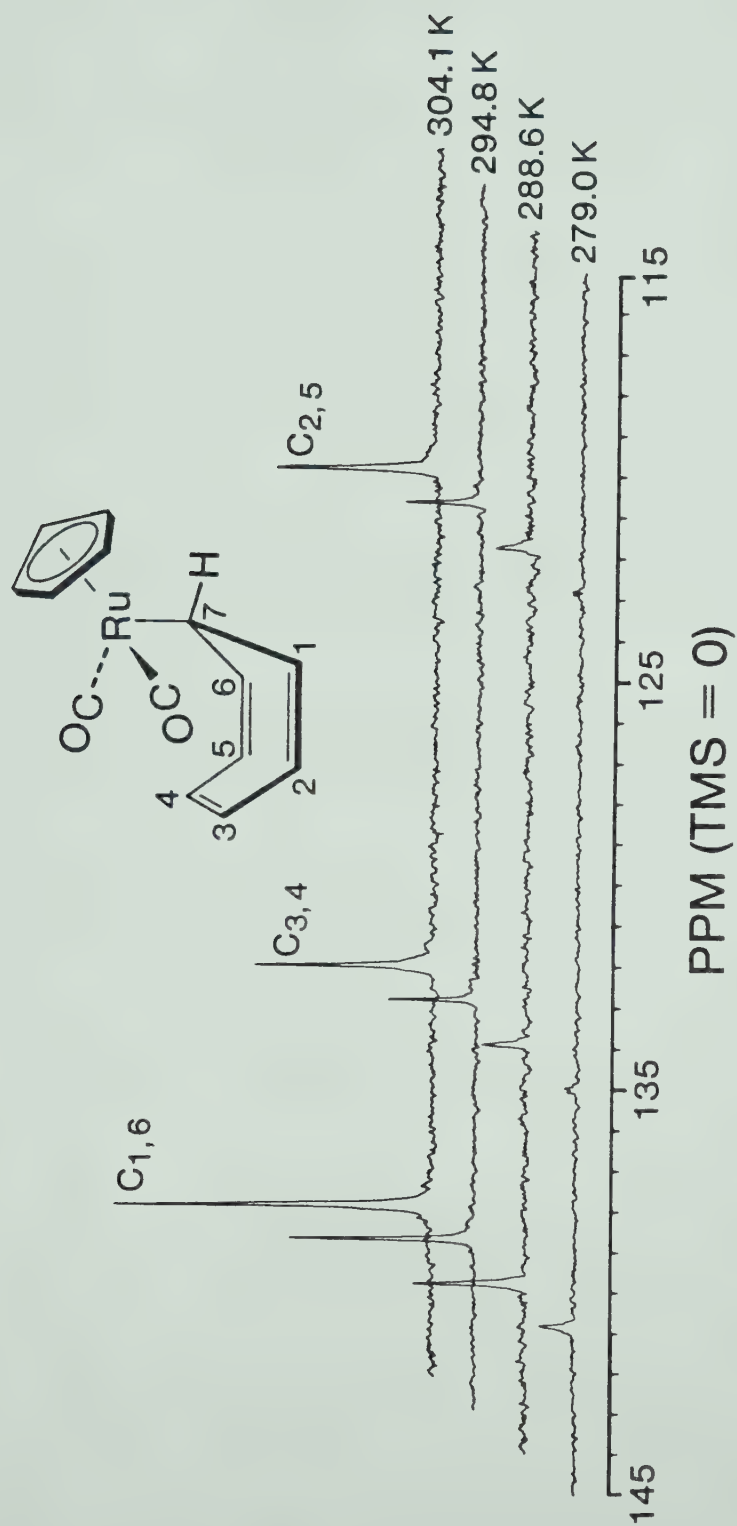


FIGURE XXIX. ^{13}C difference spectra for $\text{CpRu(CO)}_2(7\text{-}\eta^1\text{-C}_7\text{H}_7)$ at various temperatures (saturation of C_7 , THF-d_8).

TABLE XII. ^{13}C Spin Saturation Transfer Data for $\text{CpRu}(\text{CO})_2(7\text{-}\eta^1\text{-C}_7\text{H}_7)$.

T, K	$M_z(3,4)^\infty$	$M_z(2,5)^\infty$	$M_z(1,6)^\infty$	$T_{1(3,4)}$	$T_{1(2,5)}$	$T_{1(1,6)}$	$10^2 \times k_{12}(\text{s}^{-1})$	$10^2 \times k_{13}$	$10^2 \times k_{14}$
279.0	.990	.994	.952	3.23	3.16	3.11	1.73	0.31	+0.1
282.2	.962	.968	.921	3.45	3.38	3.34	2.85	1.09	+0.7
288.6	.930	.935	.832	3.89	3.81	3.79	6.67	1.71	+0.9
291.7	.927	.936	.801	4.10	4.02	4.01	8.17	1.74	+0.2
294.8	.883	.890	.721	4.31	4.23	4.23	13.5	2.73	-0.3
297.9	.821	.836	.661	4.52	4.43	4.44	18.5	4.42	-0.7
300.9	.746	.768	.567	4.73	4.64	4.66	30.9	9.26	-0.4
304.1	.682	.732	.521	4.95	4.85	4.87	40.3	11.3	-0.9

An Eyring plot of the rate constant data is shown in Figure XXX. The plot of $\ln\left(\frac{k_{12}}{T}\right)$ as a function of $1/T$ is linear. The analogous plot for k_{14} is somewhat more erratic, but only one point (282.2 K, marked with an asterisk in Figure XXX), was considered to deviate far enough from a linear relationship to warrant omission from the calculation of the slope. Activation parameters calculated for the (1,2) metal migration are $\Delta G_{300}^{\ddagger} = 18.4 \pm 0.5 \text{ kcal mol}^{-1}$, $\Delta H^{\ddagger} = 20.5 \pm 0.4 \text{ kcal mol}^{-1}$ and $\Delta S^{\ddagger} = 9.0 \pm 1.4 \text{ eu}$. For the (1,4) shift, $\Delta G_{300}^{\ddagger} = 19.1 \pm 0.6 \text{ kcal mol}^{-1}$, $\Delta H^{\ddagger} = 21.8 \pm 0.4 \text{ kcal mol}^{-1}$, $\Delta S^{\ddagger} = 9.0 \pm 1.4 \text{ eu}$. The uncertainty inputs for this calculation were $k \pm 10\%$ and $T \pm 0.2^{\circ}\text{C}$. This estimate of the uncertainty in k is based on the assumptions outlined in Section II, i.e. $T_1 \pm 5\%$ and a similar uncertainty in the integral of the difference spectra. As noted in the case of 5, the ΔG^{\ddagger} values quoted here are probably accurate, but the ΔS^{\ddagger} values are not reliable. The $\Delta G_{300}^{\ddagger}$ values for the two metal migration pathways are sufficiently similar that there is some doubt that the difference between them is significant. The Eyring plot (Figure XXX) shows clearly that the rate constants for these two processes are significantly different. The set of data available is not large enough or precise enough to allow calculation of activation parameters with sufficient precision to make this distinction.

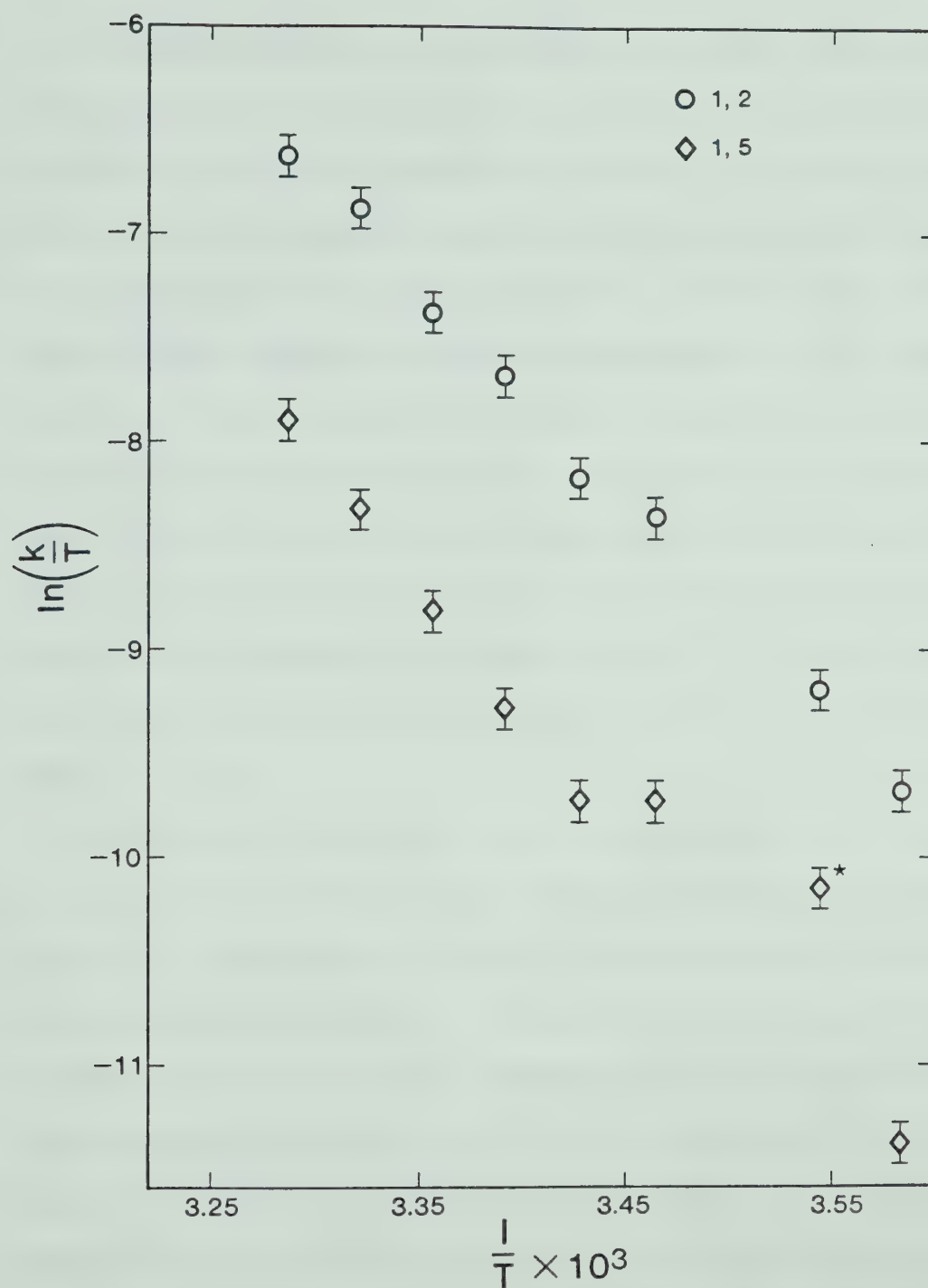


FIGURE XXX. Eyring plot of ^{13}C rate constant data for $\text{CpRu}(\text{CO})_2(7-\eta^1\text{-C}_7\text{H}_7)$. Point marked with * was not included in calculation of the slope. Error bars indicate $k \pm 10\%$.

The observation of two distinct metal migration pathways in 23 illustrates the power and discriminating ability of the spin saturation method. To detect a second, smaller metal migration pathway by analysis of lineshape data alone would be very difficult, if not impossible. An example of a similar problem is provided by $(\eta^6\text{-C}_8\text{H}_8)\text{-Cr(CO)}_3$. Spin saturation transfer experiments using ^{13}C for observation showed that both a (1,2) and (1,3) shift were involved in the metal migration around the cyclooctatetraene ring.¹⁷¹ Previous studies of ^1H NMR line broadening in this molecule had suggested random shifts.¹⁷⁸ A (1,3) shift mechanism was also proposed based on the same lineshape data.³⁵

Once again assuming that the observed metal migrations in 23 are the result of concerted processes, the observation of a [1,5] sigmatropic shift is in accord with orbital symmetry considerations. The activation energy for this process is $3.3 \text{ kcal mol}^{-1}$ greater than the most reliable value reported for the [1,5] metal migration in $\text{Ph}_3\text{Sn}(\eta^1\text{-C}_7\text{H}_7)$.⁵⁶ The more interesting observation is that this symmetry allowed process is not the lowest energy pathway for metal migration. The [1,7] shift occurs with a lower activation energy. This result is explicable in two different ways. It is possible that the migrating metal

group undergoes an inversion of configuration, which would render the [1,7] shift allowed. An alternative explanation is that there is involvement of metal d orbitals in the transition state, allowing orbitals of suitable symmetry to become available for bonding.

The molecular orbital energies in $\text{CpFe}(\text{CO})_2\text{R}$ compounds have been calculated using the extended Hückel method.¹⁷³ Studies of compounds of the type $\text{CpM}(\text{CO})_2\text{R}$ ($\text{M} = \text{Fe}, \text{Ru}$) by photoelectron spectroscopy have shown that the orbital energy levels are very similar for Fe and Ru compounds.¹⁷⁴ The HOMO in compounds of this type is an a_1 orbital of σ symmetry which has considerable d_{z^2} character.¹⁷³ Using this orbital alone, the observed [1,7] shift in 23 would be forbidden.

Photoelectron spectra of compounds with double bonds allylic to the metal center, such as $\text{CpFe}(\text{CO})_2(\eta^1\text{-C}_3\text{H}_5)$ have been reported. It was found that the presence of allylic double bonds reduces the ionization potential of the Fe d orbitals, compared to alkyls such as $\text{CpFe}(\text{CO})_2\text{-CH}_3$. Extended Hückel calculations were employed to interpret these results in terms of mixing of the olefin π orbitals with metal d orbitals.¹⁷⁵

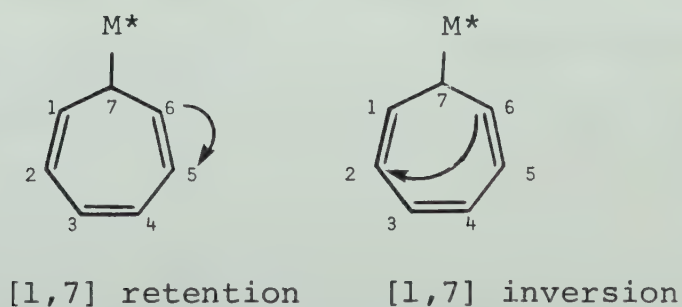
Further data is needed to decide which of the two possibilities mentioned above applies to 23. Specifically,

a probe of the stereochemistry at the metal center would allow the detection of inversion or retention of configuration during the [1,7] metal migration.

Section V. Stereochemistry of Metal Migration in
 $\text{CpRu}(\text{CO})(\text{PMe}_2\text{Ph})(7-\eta^1\text{-C}_7\text{H}_7)$ (29)

Two phosphine substituted derivatives of 23 have been prepared. These are $\text{CpRu}(\text{CO})(\text{PMe}_3)(7-\eta^1\text{-C}_7\text{H}_7)$ (28) and $\text{CpRu}(\text{CO})(\text{PMe}_2\text{Ph})(7-\eta^1\text{-C}_7\text{H}_7)$ (29). Both compounds show diastereotopic splitting of the cycloheptatrienyl ring nuclei, (^1H or ^{13}C) such that seven separate resonances are observed in both cases (see Figure XV for the ^1H NMR spectrum of 29 and Figure XVI for the ^{13}C NMR spectrum of 28). Compound 29 has the additional advantage of having two diastereotopic methyl groups on the phosphine ligand, so study has been concentrated on this compound.

In principle, it is possible to determine the pathway and stereochemistry of metal migration in 28 or 29 with an SST experiment. The occurrence of [1,7] shifts with inversion or retention of configuration have quite different consequences for the pattern of spin saturation transfer. If the configuration at the metal is unchanged during the



shift, saturation transfer will occur to the same side of the ring. If inversion accompanies metal migration, saturation will be transferred to the opposite side of the ring.

This experiment has been carried out. Saturation of the C_6 resonance in 29 led to an intensity decrease at the resonance assigned to C_5 (see Figure XXXI), indicating that the metal migration is a [1,7] shift with retention of configuration.* This conclusion rests upon the correctness of the assignment of C_2 versus C_5 , which is based on selective proton decoupling of the two carbon resonances. The proton resonances involved (H_2 and H_5) differ in chemical shift by only ca. 12 Hz (at 400 MHz). Since reversal of this assignment would reverse the conclusion of the experiment, we sought to verify this result by an independent method.

The diastereotopic methyl groups in 29 should remain distinct even at high rates of metal migration if the conclusion reached above is correct. If the metal migration proceeds with inversion, the two different methyl resonances should coalesce, given a sufficiently rapid rate of metal

* Assignment of C_1 versus C_6 is arbitrary, but once this choice is made, all other assignments follow sequentially around the ring (see Chapter V, Section V).

migration.

The rate of metal migration at 308 K was calculated from the ^{13}C SST experiment shown in Figure XXXI. Saturation of C_6 led to an intensity decrease at C_5 which is related to the rate of metal migration by the two-site formula:*

$$k_{12} = \left[\frac{M_z^0(5) - M_z^\infty(5)}{M_z^\infty(5)} \right] \cdot \frac{1}{T_1(5)}$$

The T_1 of C_5 at this temperature is 1.46 sec, giving $k_{12} = 9.3 \times 10^{-2} \text{ sec}^{-1}$. Data for the rate of metal migration at higher temperatures was obtained from computer simulations of the lineshape of the partial ^1H NMR spectrum of 29 using the program DNMR3.† The ^1H spectra were measured at 90 MHz with ^{31}P decoupling. Under these conditions, the H_7 resonance is a triplet ($^3J_{7-1} = 7.8 \text{ Hz}$) and the two diastereotopic methyl groups of 29 give two singlet resonances.

* This is a simplification of eq. 45 from Section II in which terms for multiple shifts are neglected.

† DNMR3 is the third revised version of a program for the computation of exchange-broadened NMR line shapes originally developed by Binsch.¹⁷⁶ The program was obtained from QCPE and established at the University of Alberta by R.G. Cavell. The general complex matrix inversion routine CMINVS was supplied by R.E.D. McClung.

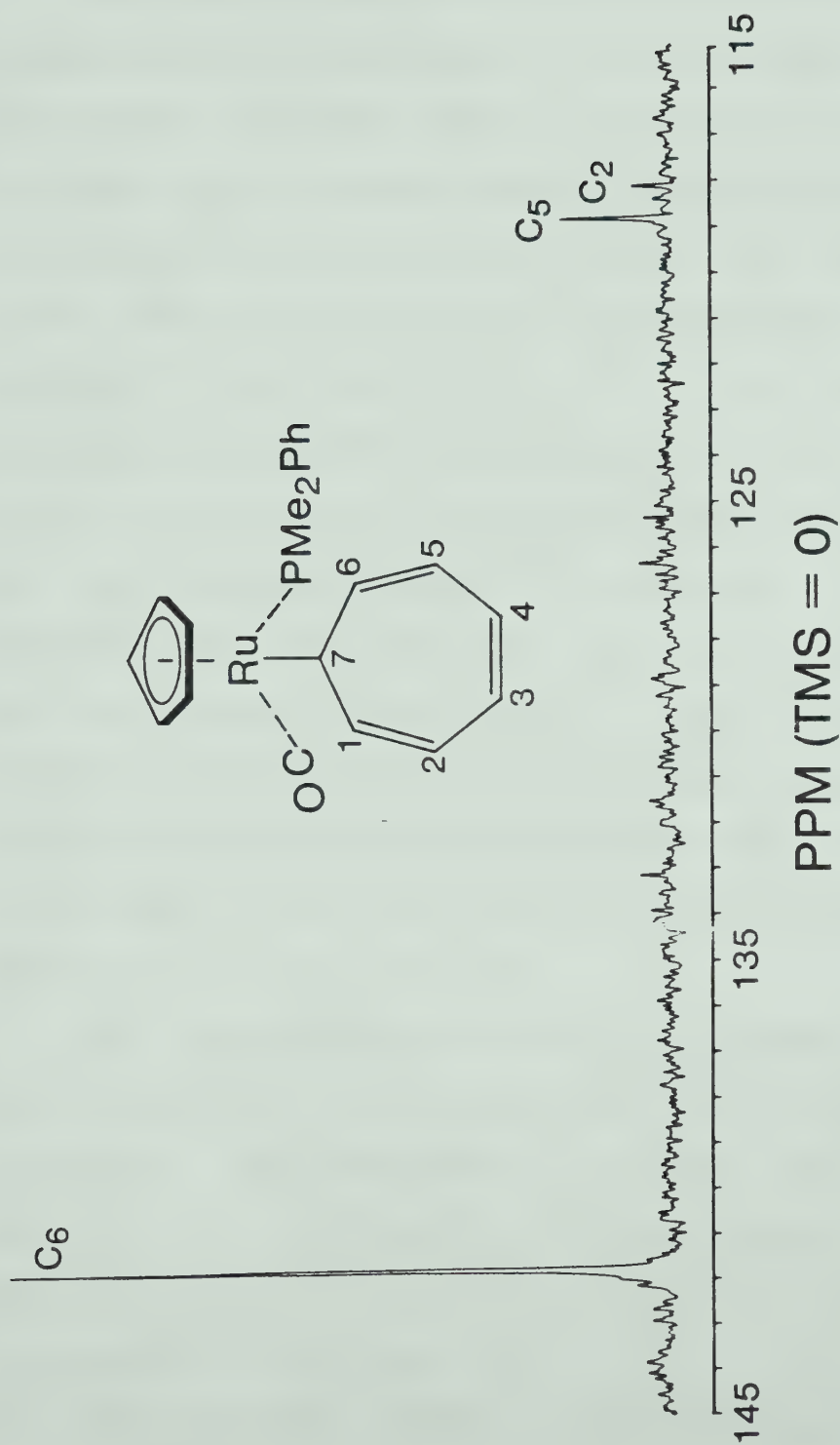


FIGURE XXXI. ^{13}C SST difference spectrum of $\text{CpRu(CO)(PMe}_2\text{Ph)(7-}\eta^1\text{-C}_7\text{H}_7\text{)}$ with saturation of C_6 (THF-d_8 , 308.0 K).

The rate of metal migration was estimated at various temperatures by comparison of the broadening of the H₇ triplet to calculated spectra (see Figure XXXII). Rate constants k_{12} are again defined as one-way rate constants, consistent with the practise adopted for calculation of rates from SST experiments. An Eyring plot of this data in addition to the value of $k_{12} = 9.3 \times 10^{-2} \text{ sec}^{-1}$ at 308 K obtained from the ^{13}C SST experiment allowed approximate activation parameters to be calculated. An uncertainty in the rate constant from the ^{13}C experiment of $\pm 10\%$ was assumed. The rate constants from the lineshape comparisons were assigned an uncertainty of $\pm 20\%$. The quality of the spectra is poor due to extensive sample decomposition. The activation parameters calculated from the Eyring equation where $\Delta G_{300}^{\pm} = 19.5 \pm 0.3 \text{ kcal mol}^{-1}$, $\Delta H^{\pm} = 19.4 \pm 0.2 \text{ kcal mol}^{-1}$ and $\Delta S^{\pm} = -0.3 \pm 0.7 \text{ eu}$.

The qualitative observation can be made that phosphine substitution has slightly reduced the rate of metal migration. The rate constant for metal migration in 29 at 308 K is $9.3 \times 10^{-2} \text{ sec}^{-1}$. Similar values of k_{12} in the dicarbonyl derivative 23 were observed at much lower temperatures (see Table XII).

The appearance of the two methyl singlets will be affected by the metal migration process if the migration is

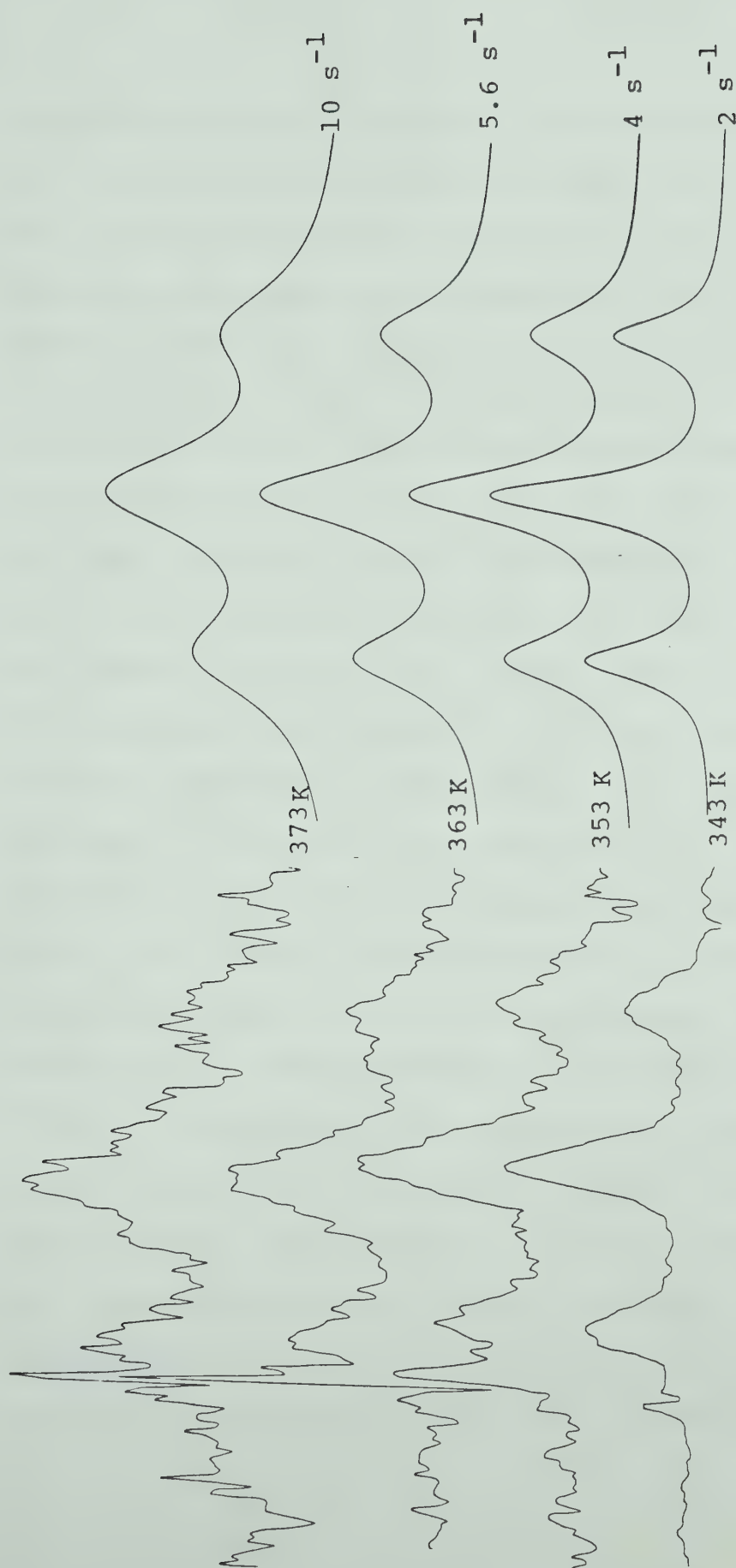


FIGURE XXXII. Left: Observed ^1H NMR spectra (90 MHz, $\{^3\text{P}\})$ of the H_7 resonance of 29 in methylcyclohexane- d_{14} . Right: Calculated spectra for various rates of metal migration.

accompanied by an inversion of configuration. Using the definition of the rate of metal migration, k_{12} , as a one-way, pseudo first order rate constant, the rate of metal inversion at a particular temperature will be twice k_{12} , assuming that every migration is accompanied by inversion. ^1H NMR spectra of the two methyl singlets at various temperatures along with the calculated lineshapes based on the assumption of inversion occurring with each migration are shown in Figure XXXIII. The observed lineshapes are clearly not consistent with the occurrence of inversion of configuration at the metal center. There is a small amount of line broadening observed at 90°C , but this is attributed to field inhomogeneity broadening. The cyclopentadienyl resonance of 29 shows a similar amount of broadening at this temperature. The thermal decomposition products of 29 (see Chapter VI) include $[\text{CpRu}(\text{CO})(\text{PMe}_2\text{Ph})]_2$, which forms an orange precipitate from methylcyclohexane, even at high temperatures. The broadening of the lines observed in the ^1H NMR is attributed to the presence of this solid suspended in the sample. Further evidence against coalescence of the diastereotopic methyl signals is provided by the observation of a constant separation between the lines. If the observed broadening were due to coalescence of these two signals, a reduction in separation would also be observed.



FIGURE XXXIII. Left: Observed ^1H NMR spectra (90 MHz, $\{^{31}\text{P}\}$) of the methyl resonance of 29 in methylcyclohexane- d_{14} . Right: Calculated spectra assume methyl group exchange with each metal migration at rates listed, which are equal to twice the one-way rate constant for migration at each temperature.

It is concluded that the metal migration in 29 occurs with retention of configuration at the migrating group. The same mechanism may be operative in the observed [1,7] Ru migration observed in the dicarbonyl 23. Both of these observations are explicable in terms of conservation of orbital symmetry provided that d orbital participation in the transition state is postulated. As mentioned in Section IV, a theoretical study of the molecular orbital energy levels of CpFe(CO)_2 systems has been carried out.¹⁷³ The observed stereochemistry of the metal migration is readily explained in terms of the available molecular orbitals. The HOMO is a $3a'$ orbital of σ symmetry, but there is available at similar energy a filled a'' orbital of suitable symmetry to facilitate the formally forbidden [1,7] metal migration. The effects of interaction with the π system of the cycloheptatrienyl ring could shift the relative energy of these orbitals, as was observed in $\text{CpFe(CO)}_2(\eta^1\text{-C}_5\text{H}_5)$ by Labinger.¹⁷⁵

Section VI. Conclusions.

The stereochemistry as well as the pathway of certain metal migrations has been elucidated. All of the experimental observations are consistent with the principle of conservation of orbital symmetry. In some cases, a consideration of the energy and symmetry of the molecular orbitals of the metal fragment has led to an understanding of the metal migration process in terms of orbital symmetry.

The availability of d orbitals renders the unexpected [1,7] pathway allowed and in the case of $\text{CpRu}(\text{CO})_2(7-\eta^1\text{-C}_7\text{H}_7)$ the activation energy for this process is lower than that for the allowed [1,5] shift employing only σ type orbitals. Stereochemical studies of the phosphine substituted derivatives of this compound show that the [1,7] shift occurs with retention of configuration, strongly implying that d orbitals are involved in the transition state.

The results obtained for $(7-\eta^1\text{-C}_7\text{H}_7)\text{Re}(\text{CO})_5$ demonstrate the predictive power of molecular orbital calculations. The metal migration mechanism suggested by the calculated energies of the molecular orbitals of the $\text{M}(\text{CO})_5$ fragment implied a distortion of the metal fragment during migration. The carbonyl group scrambling predicted on the basis of this distortion was subsequently observed.

Section VII. Experimental

A. General

$\text{CH}_3\text{Re}(\text{CO})_5$ was prepared by the method of Hieber.¹⁷⁷ All other compounds were prepared according to the synthetic procedures outlined in previous Chapters. Samples for SST experiments were prepared by vacuum transfer of dried, degassed solvents into 5 or 10 mm NMR tubes. After three cycles of freeze-thaw degassing, the tubes were sealed off under vacuum.

B. Instrumentation and Methodology

^1H SST experiments were carried out using a Bruker WH-400 spectrometer (400 MHz). ^{13}C experiments at 100.6 MHz employed the same instrument. The field drift of this particular instrument is quite low (ca. 40 Hz/day). Direct computer control of the second RF field used for proton SST experiments is possible using this instrument, allowing the difference spectra to be collected using rapid switching (every 4 scans) between on and off resonance decoupling. This pulse sequence can be automated using a simple microprogram sequence:

Command	Comment
1 ZE	zero memory
2 02	select decoupler frequency

3	HG	turn on decoupler
4	D2	time for saturation ($5 \times T_1$)
5	DO	turn off decoupler
6	D3	settling delay
7	GO=3	apply observation pulse and collect FID
8	NM	invert memory
9	LO TO 2, TIMES:8	loop to 2, 8 times
10	EXIT	terminate

The result of this sequence is that n scans are collected with saturation of the resonance of interest and subtracted from n scans with the saturating field applied at some point off the resonance of interest. The resulting FID is processed normally. In the case of ^{13}C SST experiments, the second RF field for ^{13}C spin saturation was generated using a PTS-160 frequency synthesizer (Programmed Test Sources Inc.), then tripled and modulated by a Bruker BSV 3BX decoupler unit. This synthesizer is not subject to automated frequency control, so a slightly different microprogram sequence was employed. The frequency of the saturating field was manually changed from on resonance to off resonance halfway through the experiment.

1	ZE	
2	HG	
3	D2	
4	DO	
5	D3	
6	GO=2	
7	NM	+ switch decoupler to off resonance
8	HG	
9	D2	
10	DO	


```

11  D3
12  GO=8
13  EXIT

```

The settings used were:

```

PTS-160:      Level:  off
               Standard: External
BSV 3BX:      Internal: Comp  22-30 dB
               attenuation
13C-13C Decoupling selector switch:  ON
1H Decoupling:  BB 20W 07 dB attenuation

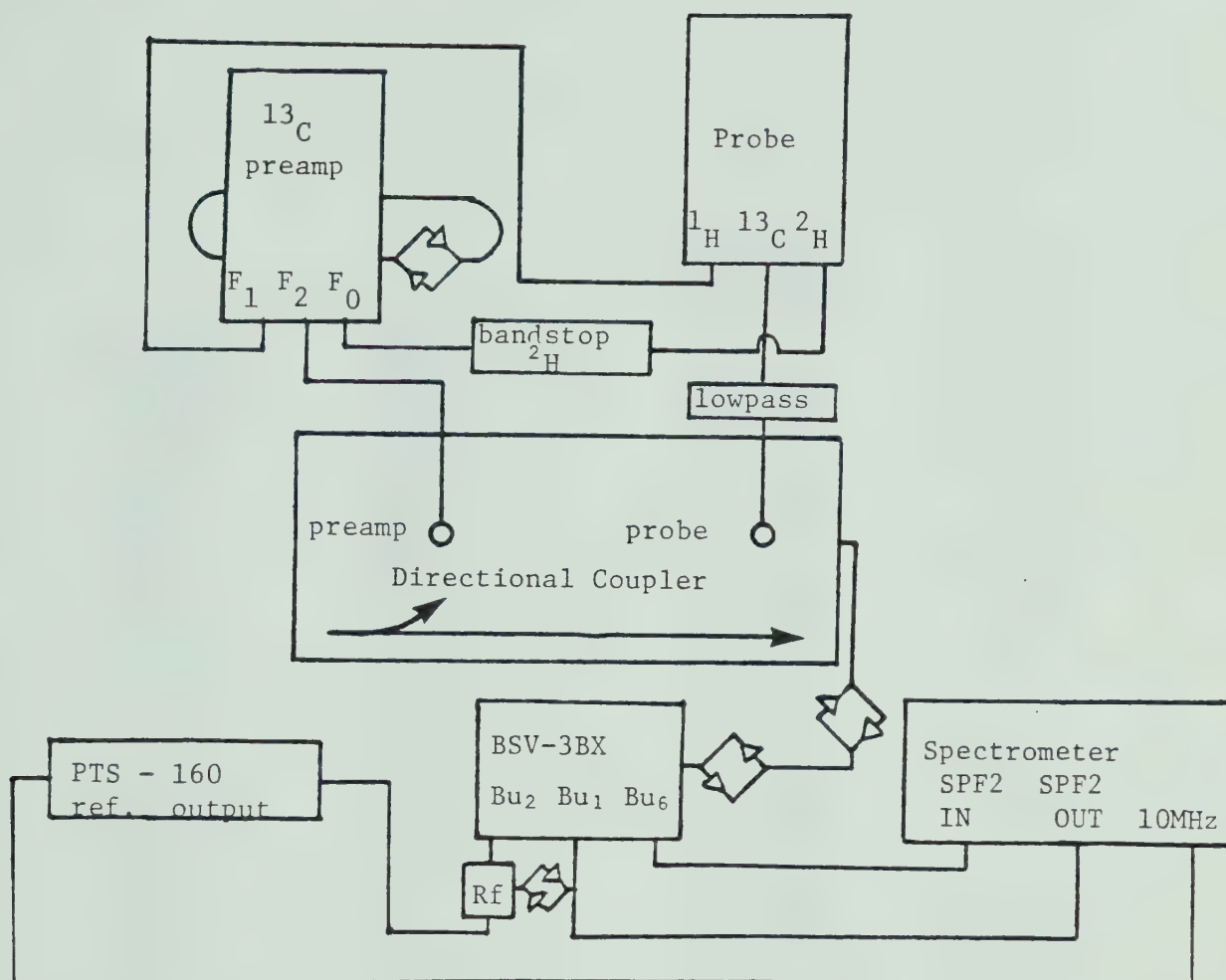
```

The experimental setup is non-standard, so a schematic diagram is included on the following page.

Spin lattice relaxation times (T_1 's) were measured using the standard π , τ , $\frac{\pi}{2}$, $5 \times T_1$ pulse sequence. The T_1 values were calculated using the program T1CAL (T. Nakashima).

C. Temperature Control and Calibration

The BVT-1000 temperature control unit will maintain a constant temperature to $\pm 0.1^\circ\text{C}$, but the dial reading is not the true probe temperature. Probe temperatures were measured with a calibrated thermocouple (Doric 400 Type Cu Con). The thermocouple wire was placed in a 5 mm NMR tube



with ca. 1 mL of THF. This assembly was lowered into the probe and temperatures read to $\pm 0.1^\circ\text{C}$ after allowing 15 min for equilibration. For the ^{13}C probe (10 mm), broad-band proton decoupling conditions must be used since the decoupling power levels employed causes substantial heating of the sample. The thermocouple wire acts as a RF receiver, so meaningful temperature readings could only be obtained with

5 mm

10 mm

dial	true	dial	true
		258.000	260.45
		259.000	261.48
		260.000	262.52
		261.000	263.56
		262.000	264.60
		263.000	265.64
		264.000	266.68
		265.000	267.71
		266.000	268.75
		267.000	269.79
		268.000	270.83
		269.000	271.87
		270.000	272.91
		271.000	273.94
		272.000	274.98
		273.000	276.02
		274.000	277.06
		275.000	278.10
		276.000	279.14
		277.000	280.17
		278.000	281.21
		279.000	282.25
		280.000	283.29
		281.000	284.33
		282.000	285.37
		283.000	286.40
		284.000	287.44
		285.000	288.48
		286.000	289.52
		287.000	290.56
		288.000	291.60
		289.000	292.63
		290.000	293.67
		291.000	294.71
		292.000	295.75
		293.000	296.79
		294.000	297.83
		295.000	298.86
		296.000	299.90
		297.000	300.94
		298.000	301.98
		299.000	303.02
		300.000	304.06
		301.000	305.09
		302.000	306.13
		303.000	307.17
280.000	281.65		
281.000	282.63		
282.000	283.60		
283.000	284.57		
284.000	285.55		
285.000	286.52		
286.000	287.50		
287.000	288.47		
288.000	289.44		
289.000	290.42		
290.000	291.39		
291.000	292.37		
292.000	293.34		
293.000	294.31		
294.000	295.29		
295.000	296.26		
296.000	297.24		
297.000	298.21		
298.000	299.19		
299.000	300.16		
300.000	301.13		
301.000	302.11		
302.000	303.08		
303.000	304.06		
304.000	305.03		
305.000	306.00		
306.000	306.98		
307.000	307.95		
308.000	308.93		
309.000	309.90		
310.000	310.88		
311.000	311.85		
312.000	312.82		
313.000	313.80		
314.000	314.77		
315.000	315.75		
316.000	316.72		
317.000	317.69		
318.000	318.67		
319.000	319.64		
320.000	320.62		

the decoupler switched off. This problem was avoided by allowing 15 minutes for equilibration, then turning off the decoupler and immediately reading the temperature.

The correction to be applied is not constant, but in both cases (5 mm and 10 mm), a linear relationship between true probe temperature and the dial reading was observed. Regression analysis fit the data to a straight line, allowing intermediate temperatures to be interpolated.

D. Field Homogeneity and Probe Tuning

For both ^1H and ^{13}C SST experiments, it is critical to success that the field homogeneity be carefully optimized at each temperature used. For ^{13}C , the probehead must be carefully tuned. The standard procedure outlined in the Bruker operating manual was employed. If these precautions are not carefully followed, poorly phased difference spectra are obtained, which cannot be integrated accurately.

E. Integrals

The integrals of the difference spectra were normalized based on $\text{C}_7(\text{H}_7) = 1$. This procedure depends on knowledge of the integral ratios of the olefinic nuclei versus the aliphatic one. These integrals were measured at only one temperature (the lowest in the range). Conditions for these

experiments were the same as those used for the SST experiments (ie $5 \times T_1$ between pulses).

	$H_{3,4}$	$H_{2,5}$	$H_{1,6}$	H_7	solvent
$(7-\eta^1-C_7H_7)Re(CO)_5$	1.97	1.95	1.94	1.00	methylocyclohexane- d_{14}
	2.02	2.05	2.03	1.00	dioxane- d_8
	$C_{3,4}$	$C_{2,5}$	$C_{1,6}$	C_7	
$CpRu(CO)_2(7-\eta^1-C_7H_7)$	2.05	2.12	2.08	1.00	THF- d_8
$(7-\eta^1-C_7H_7)Re(CO)_5$	2.03	2.02	1.94	1.00	THF- d_8

CHAPTER VIII

FLUXIONAL BEHAVIOUR OF TRIHAPTO AND PENTAHAPTO CYCLOHEPTATRIENYL COMPOUNDS

Section I. Introduction

The fluxional processes considered in this chapter involve metal migrations around trihapto and pentahapto-cycloheptatrienyl ring systems. The bonding of the metal to the organic group in these cases has both a σ and π component. The rearrangements observed are not sigmatropic shifts.

There are a large number of examples of trihaptocycloheptatrienyl compounds of various transition metals. All those reported show fluxional behaviour. In every case where the pathway of metal migration has been determined, a (1,2) metal migration pathway was found.³¹

The occurrence of pentahapto coordination of cycloheptatriene is less common. Five compounds of this type are known. The first reported example was $(\eta^5\text{-C}_7\text{H}_7)\text{Fe}(\text{CO})_3^+$, prepared by Pettit in 1964.¹⁷⁸ $(\eta^5\text{-C}_7\text{H}_7)\text{Mn}(\text{CO})_3$ was reported by Whitesides and Budnik in 1971.³⁵ Other examples of this type of coordination are $(\eta^5\text{-C}_7\text{H}_7)\text{Fe}(\eta^5\text{-C}_7\text{H}_9)$ ^{179,180} and $(\eta^5\text{-C}_7\text{H}_7)\text{Ru}(\eta^5\text{-C}_7\text{H}_9)$.¹⁸¹

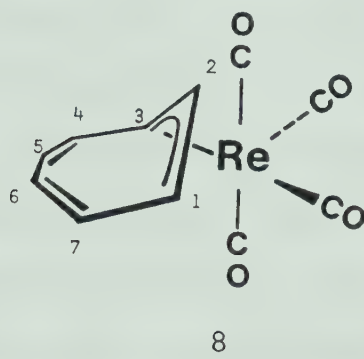
All of these compounds exhibit fluxional behaviour, with metal migration around the pentahapto ring via a series of (1,2) shifts.

The preparation of $(\eta^5\text{-C}_7\text{H}_7)\text{Fe}(\text{CO})_2\text{SnPh}_3$ was described by Reuvers.¹⁸² The metal migration around the pentahaptocycloheptatrienyl ring in this compound has been tentatively attributed to a (1,3) metal migration pathway.¹⁸³

Section II. Fluxionality in $(\eta^3\text{-C}_7\text{H}_7)\text{M}(\text{CO})_4$ ($\text{M} = \text{Mn}, \text{Re}$)
and Phosphine Substituted Derivatives

A. $(\eta^3\text{-C}_7\text{H}_7)\text{Re}(\text{CO})_4$ and $(\eta^3\text{-C}_7\text{H}_7)\text{Mn}(\text{CO})_4$

The fluxional behaviour of compound 8 has been thoroughly investigated by both ^1H and ^{13}C NMR. The ^1H NMR



spectrum at ambient temperature consists of a single broad resonance at δ 4.90. Cooling the sample to -50°C (90 MHz) gave the expected low temperature limiting spectrum for a trihapto-cycloheptatrienyl complex. The resonance of the central proton (H_2) in a trihapto ring appears at highest field¹⁰¹ (δ 2.90 in this case). This situation is reversed in the event of pentahapto coordination (see Section III).

The pathway of metal migration in 8 was readily determined by observing the pattern of collapse of the ^1H

resonances as the sample temperature was increased. The resonance due to $H_{5,6}$ was least affected by line broadening, consistent with a (1,2) metal migration pathway.

Quantitative data on the rate of this fluxional process was obtained by recording the ^{13}C NMR spectrum (50 MHz, ^1H decoupled) of 8 in methylcyclohexane- d_{14} at various temperatures. The low temperature limiting chemical shifts were obtained at 223° K. The chemical shifts are unchanged in the temperature range 223° K to 243° K. Rate constants were obtained at five temperatures between 264.5° K and 310.7° K by fitting the observed spectrum to spectra calculated using program DNMR3. The minimum signal:noise ratio in the intermediate exchange region was 10:1. The estimated uncertainty in the rate constants derived from this procedure is $\pm 10\%$. The rate data is tabulated in Table XIII. The probe temperature was calibrated by a similar procedure to the one outlined in Chapter VIII (see Experimental Section). The temperature control unit maintains the probe temperature constant to $\pm 0.5^\circ\text{C}$. Activation parameters were calculated using program ACTEN. Inputs were $k \pm 10\%$ and $T \pm 0.5^\circ$. The activation parameters for the (1,2) Re migration in 8 are $\Delta H^\ddagger = 14.6 \pm 0.2 \text{ kcal mol}^{-1}$, $\Delta S^\ddagger = 7.4 \pm 0.8 \text{ eu}$ and $\Delta G_{300}^\ddagger = 12.4 \pm 0.3 \text{ kcal mol}^{-1}$.

TABLE XIII. Rate Constants for (1,2) Re Migration in 8.

T, K	k_{12} (sec ⁻¹)*
264.5	200
273.7	500
283.0	1,200
292.2	3,000
310.7	14,000

*Consistent with the definition previously adopted, the rate constant k is defined as a one-way rate constant.

Another important observation from the ¹³C NMR spectra is that the carbonyl carbon resonances of 8 remained sharp at all temperatures studied. This result indicates that the carbonyl groups of 8 remain distinct and are not exchanged during the metal migration. This observation is consistent with the activation energy of 26.5 kcal mol⁻¹ determined for the axial-equatorial carbonyl scrambling process in the related compound (η^3 -C₃H₅)Re(CO)₄.¹⁸⁴

The fluxional behaviour of (η^3 -C₇H₇)Mn(CO)₄ (3) is similar to that observed for 8. The ¹H NMR spectrum of 3 at room temperature (CD₂Cl₂, 400 MHz) consists of a single resonance at δ 4.90. A low temperature limiting spectrum

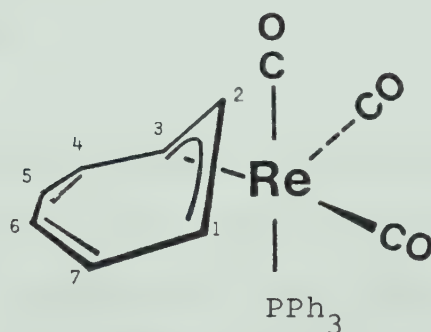
very similar to that of 8 was observed at -80°C (400 MHz). On warming the sample, all the resonances broaden, with $\text{H}_{5,6}$ least affected, consistent with a (1,2) pathway for metal migration. The only difference between the fluxional behaviour of 8 and 3 is that 3 has a lower activation energy for the (1,2) shift process.

Insufficient quantities of 3 were available for ^{13}C NMR studies. The available program (DNMR3) is not capable of fully simulating the ^1H spectrum of 3. An approximate value for the rate constant for exchange can be obtained from the ^1H spectrum of 3 at 213 K (THF-d_8) using a simulated spectrum calculated with program DNMR3. At this temperature, the lines are broad ($\nu_{1/2} = \text{ca. } 80\text{--}100 \text{ Hz}$), rendering unimportant the contributions to the linewidth due to coupling. The low temperature limiting linewidth was simulated by using $T_2 = 0.2 \text{ sec}$. On this basis, the rate constant k_{12} at 213 K is ca. 40 sec^{-1} . A value of $\Delta G_{213}^{\ddagger} = 10.7 \text{ kcal mol}^{-1}$ was calculated from this rate. This value is lower than the more precisely determined value of $\Delta G_{213}^{\ddagger} = 13.0 \text{ kcal mol}^{-1}$ for 8. Due to the uncertainty of the ΔG^{\ddagger} value determined for 3, it is not clear that this difference is significant. The qualitative observation that metal migration is occurring more rapidly in 3 than in 8 can be made by comparing the ^1H NMR spectra of the two

compounds. The chemical shift differences among the cycloheptatrienyl protons in the two compounds are very similar. The low temperature limiting spectrum of 8 was obtained at -50°C (90 MHz) while a temperature of -80°C and higher field (400 MHz) was required to observe the low temperature limiting spectrum of 3.

B. Phosphine Substituted Derivatives

The triphenylphosphine substituted derivative of 8, $(\eta^3\text{-C}_7\text{H}_7)\text{Re}(\text{CO})_3\text{PPh}_3$, (12), also exhibits fluxional behaviour. As observed for 8 and 3, the $\text{H}_{5,6}$ resonance in

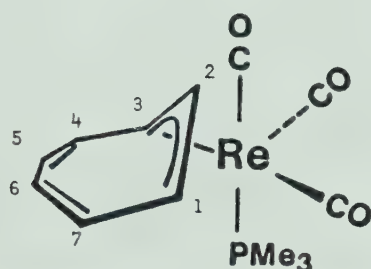


12

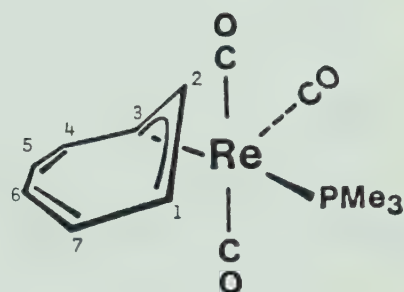
the ^1H NMR spectrum of 12 was least affected by line broadening in the intermediate exchange region, indicating a (1,2) shift pathway for the metal migration. Rate constants for this process have not been determined, but a qualitative comparison of the ^1H NMR spectra of 8 and 12 indicates that

the rate of metal migration in 12 is slightly reduced compared to 8.

The trimethylphosphine substituted derivative of 8 presents a more complex situation. The presence of two isomers, 13a and 13b, is indicated by ^1H NMR and infrared spectroscopy (see Chapter III).



13a



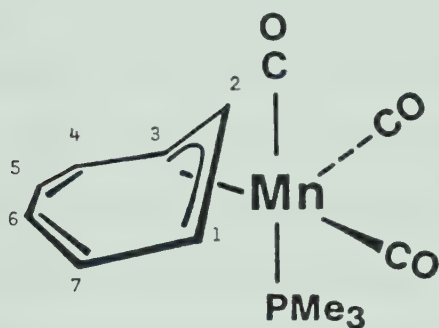
13b

The low temperature limiting ^1H NMR spectrum was obtained in CD_2Cl_2 at -40°C (400 MHz). Spectra in the intermediate exchange region indicate that the pathway of metal migration is a (1,2) shift. At ambient temperature, the cycloheptatrienyl protons of 13a and 13b give a single very broad resonance centered at δ 4.60. The trimethylphosphine protons of 13a and 13b give two distinct doublets at this temperature, indicating that 13a \rightleftharpoons 13b interconversion is not sufficiently rapid at this temperature to cause broadening of the methyl resonances. This is consistent

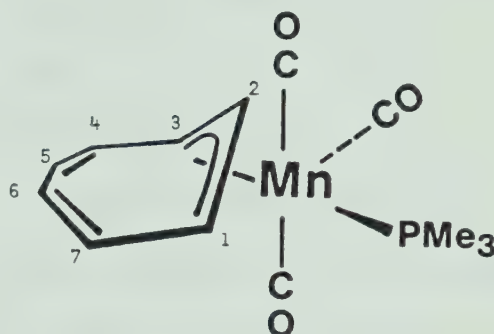
with the lack of carbonyl scrambling accompanying the (1,2) Re migration in 8. In both 8 and 13, the (1,2) Re migration apparently occurs via a mechanism which does not scramble the other ligands attached to the metal.

The manganese analog of 13 has also been investigated.

$(\eta^3\text{-C}_7\text{H}_7)\text{Mn}(\text{CO})_3(\text{PMe}_3)$, (18), also exists as two isomers, 18a and 18b (see Chapter III). The low temperature



18a



18b

limiting spectrum was recorded at -70°C (400 MHz). The $\text{H}_{5,6}$ resonances were least affected by line broadening in the intermediate exchange region, consistent with a (1,2) pathway for Mn migration. A rough estimate of the rate of this process was obtained by fitting of the observed spectrum at 243 K to a spectrum simulated for $k_{12} = 50 \text{ sec}^{-1}$. A value of $\Delta G_{243}^\ddagger = 12.2 \text{ kcal mol}^{-1}$ was obtained from this rate constant.

The appearance of the PMe_3 resonances of 18a and 18b at higher temperatures indicates that isomer interconversion is occurring. The two PMe_3 doublet signals broaden, coalesce and then sharpen to give a well-resolved doublet at ambient temperature. The coalescence temperature for this process was 263 K. The method of Shanan-Atidi and Bar-Eli for estimation of activation parameters from coalescence of two signals of unequal intensity was employed.¹⁸⁵ This procedure gave $\Delta G^\ddagger_{263} = 14.9 \text{ kcal mol}^{-1}$.

The estimated ΔG^\ddagger values for the 18a \rightleftharpoons 18b interconversion and for the (1,2) shift derived above are approximate in the extreme, but some qualitative conclusions regarding the two processes can be made. It is clear that the rate of 18a \rightleftharpoons 18b interconversion is slower than the rate of (1,2) Mn migration. Therefore the (1,2) shift is occurring independently of 18a \rightleftharpoons 18b interconversion.

In the rhenium analog 13, the (1,2) Re migration was observed, but there was no evidence for 13a \rightleftharpoons 13b interconversion at temperatures up to 303 K. If 13a \rightleftharpoons 13b interconversion does occur, it clearly has a lower rate and higher activation energy than the (1,2) Re migration.

Based on observations on the four compounds 3, 8, 13 and 18, the following conclusions can be reached:

1) The rate of (1,2) metal migration in analogous compounds

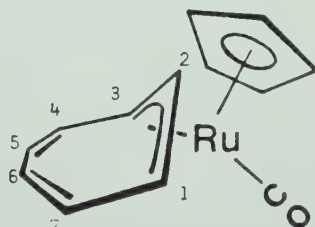
is greater for $M = \text{Mn}$ than for $M = \text{Re}$.

- 2) The rate of metal migration is reduced when a CO group is replaced by PMe_3 .
- 3) The rate of the (1,2) metal migration in 13 and 18 is greater than the respective rates of 13a \rightleftharpoons 13b and 18a \rightleftharpoons 18b interconversion. The two processes are not linked.
- 4) The rate of carbonyl site exchange in 8 (analogous to isomer interconversion in 13 and 18) is less than the rate of (1,2) Re migration.
- 5) 13a \rightleftharpoons 13b interconversion is slower than 18a \rightleftharpoons 18b interconversion, indicating that isomer interconversion rates are greater for $M = \text{Mn}$ than for $M = \text{Re}$.

Section III. Fluxionality of $\text{CpRu}(\text{CO})(\eta^3\text{-C}_7\text{H}_7)$ (25)

The iron analog of 25, $\text{CpFe}(\text{CO})(\eta^3\text{-C}_7\text{H}_7)$ was reported by Rosenblum and Ciappenelli in 1969.¹⁰¹ This iron compound is fluxional, with a (1,2) pathway of metal migration. No activation energy has been reported for this process, but the low temperature limiting ^1H NMR spectrum (100 MHz) was obtained at -50°C .¹⁰⁴

The ^1H NMR spectrum of 25 at ambient temperature shows a sharp singlet cyclopentadienyl resonance and four broad resonances due to the cycloheptatrienyl protons. The low temperature limiting spectrum, indicative of trihapto coordination of the cycloheptatrienyl group, was obtained at -10°C . The resonance due to $\text{H}_{5,6}$ is least affected by line broadening in the intermediate exchange region. As previously noted, this observation indicates that the pathway of metal migration is a (1,2) shift. Since the low



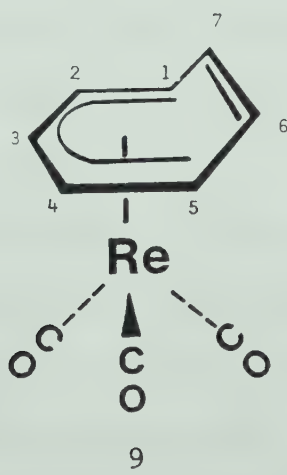
25

temperature limiting spectrum of 25 was obtained at -10°C

with a 400 MHz field, the previous observation of a low temperature limiting spectrum of $\text{CpFe(CO)}(\eta^3\text{-C}_7\text{H}_7)$ at -50°C (100 MHz) indicates that the rate of 1,2 metal migration in these two compounds is similar. Without further data on the iron compound, valid comparisons between the two compounds cannot be made.

Section IV. Fluxional Processes in $(\eta^5\text{-C}_7\text{H}_7)\text{Re}(\text{CO})_3$

As mentioned in the Introduction to this chapter, relatively few examples of pentahapto coordination of cycloheptatriene to a transition metal have been reported. All the reported compounds show fluxional behaviour. With one exception the pathway of metal migration is a (1,2) shift. The ^1H NMR spectrum observed for $(\eta^5\text{-C}_7\text{H}_7)\text{Re}(\text{CO})_3$, (9), (60 MHz, acetone- d_6 , -20°C) is very similar to the spectrum reported for the manganese analog 4. The resonance due to the central proton of the metal bound portion of the ring (H_3) is found at lowest field (δ 7.12). The low temperature limiting spectrum of 9 was obtained at -20°C . The reported low temperature limiting spectrum for 4 was



recorded at -47°C (60 MHz, acetone- d_6).³⁵ The spectrum of 9 observed at 20°C shows substantial broadening of all the

resonances, with the signal due to $H_{6,7}$ least affected. This observation is consistent with a (1,2) metal migration pathway. Similar results were reported for 4. The difference in the temperature required for low-temperature limiting spectra of 4 and 9 leads to the qualitative conclusion that the activation energy for the (1,2) metal migration is lower in 4 ($M = Mn$) than in 9 ($M = Re$).

The rate of (1,2) Re migration in 9 was quantitatively determined at various temperatures by fitting the observed ^{13}C NMR spectra (22.6 MHz, acetone- d_6) to calculated spectra (DNMR3). Rate constants were determined for nine temperatures between 268° K and 313° K. The minimum signal:noise ratio was 15:1. The probe temperature was calibrated and is constant to $\pm 0.5^\circ$ (see Experimental Section). The rate constant data are tablated in Table XIV.

Activation parameters for the (1,2) Re migration calculated from this data are: $\Delta H^\ddagger = 14.8 \pm 0.2 \text{ kcal mol}^{-1}$, $\Delta S^\ddagger = -1.3 \pm 0.7 \text{ eu}$ and $\Delta G_{300}^\ddagger = 15.1 \pm 0.3 \text{ kcal mol}^{-1}$. The reported activation energy for the (1,2) Mn migration in $(\eta^5-C_7H_7)Mn(CO)_3$ is $\Delta G_{300}^\ddagger = 14 \text{ kcal mol}^{-1}$.³⁵ The small difference between these values is of dubious significance, but seems to confirm the observations on the 1H NMR spectra of these compounds. A much lower temperature (ca. 30° lower) was required to observe the low temperature limiting

 Table XIV. Rate Constants for the (1,2) Re migration in 9

T, K	k_{12}^* (sec ⁻¹)
268.0	3
278.0	8
283.0	12
288.0	20
293.0	35
298.0	50
303.0	70
308.0	120
313.0	200

*One-way rate constant.

¹H NMR spectrum of the manganese compound.

In the reported ¹³C NMR study of (n⁵-C₇H₇)Mn(CO)₃ no carbonyl signals were observed, probably due to a combination of long relaxation times and quadrupole coupling effects.³⁵ In contrast to this result for 4, the carbonyl resonances of 9 were readily observed. At low temperatures (193° K), two signals in the ratio 1:2 were observed (22.6 MHz). As the temperature was raised, the signals broaden and coalesce to give a single resonance. Rate constants for

this process were measured by comparing the observed spectra to simulated spectra (DNMR3). The temperature range investigated was 193° K to 283° K. Minimum signal:noise ratio was 10:1. Rate constants for the carbonyl scrambling process are tabulated in Table XV.

Table XV. Rates of CO Scrambling in 9

<u>T, K</u>	<u>k, (sec⁻¹)*</u>
193.0	5
203.0	10
213.0	30
218.0	60
223.0	100
253.0	600
263.0	2000
283.0	5000

*Consistent with previous practice, k is defined as a one-way rate constant.

Activation parameters for the CO scrambling process are $\Delta H^\ddagger = 8.1 \pm 0.1$ kcal mol⁻¹, $\Delta S^\ddagger = -12.8 \pm 0.3$ eu and $\Delta G_{300}^\ddagger = 12.0 \pm 0.1$ kcal mol⁻¹. Comparison of this value

to $\Delta G_{300}^{\ddagger} = 15.1 \pm 0.3 \text{ kcal mol}^{-1}$ calculated for the (1,2) Re migration process shows that carbonyl scrambling occurs much more readily than metal migration. This result is a reversal of the situation in $(\eta^3\text{-C}_7\text{H}_7)\text{Re}(\text{CO})_4$, where metal migration was rapid and carbonyl scrambling was not observable on the NMR time scale.

Site exchange of carbonyl groups in tricarbonyl metal compounds has been observed in a wide variety of compounds. For example, $(\eta^6\text{-C}_7\text{H}_8)\text{M}(\text{CO})_3$ ($\text{M} = \text{Cr}, \text{Mo}$) exhibits CO scrambling with $\Delta H^{\ddagger} = 11\text{-}12 \text{ kcal mol}^{-1}$.¹⁸⁶ The exchange of carbonyl environments in $(\eta^4\text{-C}_6\text{H}_8)\text{Ru}(\text{CO})_3$ has $\Delta G^{\ddagger} = 11.6 \pm 0.2 \text{ kcal mol}^{-1}$.¹⁸⁷ The carbonyl scrambling process observed in 9 has a similar activation energy. A compound very closely related to 9, $(\eta^5\text{-C}_7\text{H}_9)\text{Re}(\text{CO})_3$, has been reported, but no ^{13}C NMR data were obtained for this compound.¹⁸⁷

Section V. Experimental

General

Compounds were prepared as outlined in Chapters II, III and V. Solvents for NMR studies were dried and degassed before use. In the ^{13}C study of $(\eta^3\text{-C}_7\text{H}_7)\text{Re}(\text{CO})_4$, a serum-capped 20 mm NMR tube was employed. The solvent was purged with nitrogen for 15 minutes. In all other cases, 5 mm or 10 mm NMR tubes were used, with vacuum transfer of solvents. Three cycles of freeze-thaw degassing were followed by sealing off under vacuum.

Temperature Calibration

The temperature calibration of the 5 mm ^1H probe of the WH-400 spectrometer was described in Chapter VI. A similar procedure was employed in calibrating the temperature of the 20 mm ^{13}C probe of the WP-200 spectrometer used in the study of the fluxional process in 8. The calibration was carried out using broad-band proton decoupling conditions identical to those employed in recording actual spectra, and the same solvent. This calibration is only strictly valid for this solvent, since the amount of sample heating caused by the proton decoupler is dependent on the solvent dielectric. A linear regression analysis of the data allows

all temperatures in the range of interest to be extrapolated. The measured probe temperatures were constant to $\pm 0.5^{\circ}\text{C}$.

Dial	True	Dial	True
260.000	261.69	291.000	290.33
261.000	262.62	292.000	291.25
262.000	263.54	293.000	292.17
263.000	264.46	294.000	293.10
264.000	265.39	295.000	294.02
265.000	266.31	296.000	294.95
266.000	267.23	297.000	295.87
267.000	268.16	298.000	296.79
268.000	269.08	299.000	297.72
269.000	270.01	300.000	298.64
270.000	270.93	301.000	299.56
271.000	271.85	302.000	300.49
272.000	272.78	303.000	301.41
273.000	273.70	304.000	302.34
274.000	274.62	305.000	303.26
275.000	275.55	306.000	304.18
276.000	276.47	307.000	305.11
277.000	277.40	308.000	306.03
278.000	278.32	309.000	306.95
279.000	279.24	310.000	307.88
280.000	280.17	311.000	308.80
281.000	281.09	312.000	309.73
282.000	282.01	313.000	310.65
283.000	282.94	314.000	311.57
284.000	283.86	315.000	312.50
285.000	284.79	316.000	313.42
286.000	285.71	317.000	314.34
287.000	286.63	318.000	315.27
288.000	287.56	319.000	316.19
289.000	288.48	320.000	317.12
290.000	289.40		

A similar temperature calibration for the Bruker HFX-90 spectrometer has been carried out by T. Brisbane (22.6 MHz ^{13}C spectra were recorded on this instrument). The temperatures quoted in the tabulations of rate constants are the true temperatures, constant to $\pm 0.5^\circ\text{C}$.

REFERENCES

1. F. A. Cotton, J. Am. Chem. Soc., 90 (1968) 6230.
2. "Nomenclature of Inorganic Chemistry" International Union of Pure and Applied Chemistry, 2nd edition, Butterworths, London, 1970, p.51.
3. E. Frankland, Ann., 71 (1849) 171.
4. C. Löwig, J. Prakt. Chem., 60 (1853) 304.
5. G. B. Buckton, Proc. Chem. Soc. (London) 9 (1859) 685.
6. V. Grignard, Ann. Chim. Phys., 24 (1901) 436.
7. G. M. Bennett and E. E. Turner, J. Chem. Soc., (1914) 1057.
8. F. Hein, Chem. Ber., 52 (1919) 195.
9. F. A. Cotton, Chem. Rev. 55 (1955) 551.
10. T. H. Coffield, J. Kosikowski and R. D. Closson, J. Org. Chem., 22 (1957) 598.
11. J. Chatt and B. L. Shaw, J. Chem. Soc., (1959) 705.
12. T. S. Piper and G. Wilkinson, J. Inorg. Nucl. Chem., 3 (1956) 104.
13. G. W. Parshall and J. J. Mrowca, Adv. Organomet. Chem., 7 (1968) 157.
14. A. Shiotani and H. Schmidbaur, J. Am. Chem. Soc., 92 (1970) 7003.
15. G. Yagupsky, W. Mowat, A. Shortland and G. Wilkinson, J. Chem. Soc., Chem. Commun., (1970) 1369.

16. M. R. Collier, M. F. Lappert and M. M. Truelock,
J. Organomet. Chem., 25 (1970) C36.
17. G. Wilkinson, Science, 185 (1974) 109.
18. P. J. Davidson, M. F. Lappert and R. Pearce,
Acc. Chem. Res. 7 (1974) 209.
19. G. Vincow, H. J. Dauben, Jr., F. R. Hunter and
W. V. Volland, J. Am. Chem. Soc., 91 (1969) 2823.
20. R. B. Larrabee, J. Am. Chem. Soc., 93 (1971) 1510.
21. R. Breslow and W. Chu, J. Am. Chem. Soc., 95 (1973)
411.
22. H. J. Dauben and M. R. Rifi, J. Am. Chem. Soc.,
85 (1963) 3041.
23. W. Von E. Doering and P. P. Gaspar, J. Am. Chem.
Soc., 85 (1963) 3043.
24. W. Von E. Doering and L. H. Knox, J. Am. Chem. Soc.,
76 (1956) 3203.
25. E. O. Fischer and H. P. Fritz, Adv. Inorg. Chem.
Radiochem., 1 (1959) 108.
26. E. W. Abel, M. A. Bennett, R. Burton and G. Wilkinson,
J. Chem. Soc., (1958) 4559.
27. R. P. M. Werner and S. A. Manastyrskyj, J. Am.
Chem. Soc., 83 (1961) 2023.
28. J. E. Ellis, Ph.D. Thesis, M.I.T., 1971, p.114.
29. J. E. Ellis, R. A. Faltynek, G. L. Rochfort,
R. E. Stevens and G. A. Zank, Inorg. Chem., 19 (1980)
1082.

30. W. Von E. Doering and W. R. Roth, *Angew. Chem. Int. Ed.*, 2 (1963) 115.
31. F. A. Cotton in "Dynamic Nuclear Magnetic Resonance Spectroscopy", L. M. Jackman and F. A. Cotton, Eds., Academic Press, New York, 1975, Chapter 10.
32. R. B. Woodward and R. Hoffmann, "The Conservation of Orbital Symmetry" Academic Press, New York, 1971.
33. R. B. Woodward and R. Hoffmann, *J. Am. Chem. Soc.*, 87 (1965) 395.
34. R. B. King, *Adv. Organomet. Chem.*, 2 (1964) 157.
35. T. H. Whitesides and R. A. Budnik, *Inorg. Chem.*, 15 (1976) 874; T. H. Whitesides and R. A. Budnik, *J. Chem. Soc., Chem. Commun.*, 1514 (1971).
36. L. E. Orgel, *Inorg. Chem.*, 1 (1962) 25.
37. J. B. Wilford and F. G. A. Stone, *J. Organomet. Chem.*, 2 (1964) 371.
38. F. Calderazzo, K. Noack and V. Schaerer, *J. Organomet. Chem.*, 6 (1966) 265.
39. D. L. S. Brown, J. A. Connor and H. A. Skinner, *J. Organomet. Chem.*, 81 (1974) 403.
40. D. R. Bidinosti and N. S. McIntyre, *J. Chem. Soc., Chem. Commun.*, (1966) 555.
41. G. A. Junk and H. J. Svec, *J. Chem. Soc. A*, (1970) 2102.
42. J. A. Kerr, *Chem. Rev.*, 66 (1966) 465.

43. A. Wojcicki, *Adv. Organomet. Chem.*, 11 (1973) 87.
44. R. B. King and M. Ishaq, *Inorg. Chim. Acta*, 4 (1970) 258.
45. E. W. Abel and S. Moorhouse, *J. Chem. Soc. (Dalton)*, (1973) 1706.
46. B. J. Brisdon, D. E. Edwards and J. W. White, *J. Organomet. Chem.*, 175 (1979) 113.
47. W. Hieber, G. Braun and W. Beck, *Chem. Ber.*, 93 (1960) 901.
48. H. D. Kaesz and M. A. El-Sayed, *J. Molecular Spectroscopy*, 9 (1962) 310.
49. M. J. Webb and W. A. G. Graham, *J. Organomet. Chem.* 93 (1975) 119.
50. F. A. L. Anet, *J. Am. Chem. Soc.*, 86 (1964) 458.
51. F. R. Jensen and L. A. Smith, *J. Am. Chem. Soc.*, 86 (1964) 956.
52. C. H. Bushweller, M. Sharpe and S. J. Weininger, *Tetrahedron Lett.*, (1970) 453.
53. H. Günther, M. Görlitz and H.-H. Hinrichs, *Tetrahedron* 25 (1968) 5665.
54. M. Balci, H. Fischer and H. Günther, *Angew. Chem. Int. Ed.*, 19 (1980) 301.
55. M. Karplus, *J. Chem. Phys.*, 30 (1959) 11.
56. B. E. Mann, B. F. Taylor, N. A. Taylor and R. Wood, *J. Organomet. Chem.*, 162 (1978) 137.

57. J. E. Weidenborner, R. B. Larrabee and A. L. Bednowitz, J. Am. Chem. Soc., 94 (1972) 4140.
58. G. G. Aleksandrov, Yu. T. Struchov and Yu. V. Makarov, Zh. Strukt. Khim., 14 (1973) 98; English translation by Consultants Bureau, New York.
59. N. W. Alcock, J. Chem. Soc. (A), (1967) 2001.
60. D. W. H. Rankins and A. Robertson, J. Organomet. Chem., 105 (1976) 331.
61. V. Koelle, J. Organomet. Chem., 133 (1977) 53.
62. W. D. Bannister, B. L. Booth, M. Green and R. N. Hazeldine, J. Chem. Soc. (A), (1969) 698.
63. T. L. Brown, D. J. Blumer and K. W. Barnett, J. Organomet. Chem., 173 (1976) 71.
64. J. Elzinga and H. Hogeveen, J. Chem. Soc., Chem. Commun., (1977) 705.
65. D. J. Darensbourg and M. Y. Darensbourg, Inorg. Chem., 9 (1970) 1691.
66. M. J. Bennett, J. L. Pratt, K. A. Simpson, L. K. K. Li Shing Man and J. Takats, J. Am. Chem. Soc., 98 (1976) 4810.
67. R. Bau, J. C. Burt, S. A. R. Knox, R. M. Laine, R. P. Phillips and F. G. A. Stone, J. Chem. Soc., Chem. Commun., (1973) 726.
68. E. O. Fischer and S. Breitschaft, Angew. Chem. Int. Ed., 2 (1963) 44.

69. R. B. King and F. G. A. Stone, J. Am. Chem. Soc.,
81 (1959) 5263.
70. G. Engebretson and R. E. Rundle, J. Am. Chem. Soc.,
85 (1963) 481.
71. M. J. S. Dewar and R. Pettit, J. Chem. Soc. (1956)
2021.
72. J. Daub and W. Betz, Chem. Ber., 105 (1972) 1778.
73. B. A. Frenz in "Computing in Crystallography",
H. Schenk, R. Olthof-Hazekamp, H. vanKonigsveld
and G. C. Bassi, Eds., Delft University Press,
Delft, Holland, 1978, pp.64-71.
74. W. Hieber, O. Vohler and G. Braun, Z. Naturforsch.,
13b (1958) 192.
75. W. Hieber and E. Lindner, Chem. Ber., 94 (1961)
1417.
76. cf. P. M. Treichel and D. A. Komar, J. Organomet.
Chem., 206 (1981) 77.
77. C. P. Casey and W. D. Jones, J. Am. Chem. Soc.,
102 (1980) 6154.
78. L. W. Hauk and G. R. Dobson, Inorg. Chem., 5 (1966)
2119.
79. C. A. Tolman, J. Am. Chem. Soc., 92 (1970) 2956.
80. R. J. Angelici, F. Basolo and A. J. Poë, J. Am.
Chem. Soc., 85 (1963) 2215.
81. E. O. Fischer and J. Müller, Z. Naturforsch., 18b
(1963) 413.

82. R. B. King and F. G. A. Stone, *Inorg. Synth.*, 7 (1963) 104.
83. A. Davison, J. A. McCleverty and G. Wilkinson, *J. Chem. Soc.*, (1963) 1133.
84. H. G. Alt, *J. Organomet. Chem.*, 124 (1977) 167.
85. M. Cousins and M. L. H. Green, *J. Chem. Soc.*, (1963) 889.
86. M. L. H. Green and A. N. Stear, *J. Organomet. Chem.*, 1 (1964) 230.
87. K. W. Barnett and D. W. Slocum, *J. Organomet. Chem.*, 44 (1972) 1.
88. G. Wilkinson, *J. Am. Chem. Soc.*, 76 (1954) 209.
89. D. S. Ginley, C. R. Bock and M. S. Wrighton, *Inorg. Chim. Acta*, 23 (1977) 85.
90. J. A. McCleverty and G. Wilkinson, *J. Chem. Soc.*, (1963) 4096.
91. R. B. King and M. B. Bisnette, *J. Organomet. Chem.*, 2 (1964) 15.
92. J. R. Sweet and W. A. G. Graham, *J. Organomet. Chem.*, 217 (1981) C37.
93. R. B. King and A. Fronzaglia, *Inorg. Chem.*, 5 (1966) 1837.
94. C. P. Casey, W. D. Jones and S. G. Harsey, *J. Organomet. Chem.*, 206 (1981) C38.
95. R. P. Stewart, Jr. and G. T. Moore, *Inorg. Chem.*, 14 (1973) 2699.

96. A. Davison and W. C. Rode, *Inorg. Chem.*, 6 (1967) 2124.
97. D. Dong, D. A. Slack and M. C. Baird, *J. Organomet. Chem.*, 153 (1978) 219.
98. R. G. Hayter, *Inorg. Chem.*, 2 (1965) 1031.
99. Robert I. Mink, Ph.D. Thesis, University of Illinois at Urbana-Champaign, 1977, p.36.
100. D. Ciappenelli and M. Rosenblum, *J. Am. Chem. Soc.*, 91 (1969) 3673.
101. D. Ciappenelli and M. Rosenblum, *J. Am. Chem. Soc.*, 91 (1969) 6877.
102. H. Felkin, P. J. Knowles, B. Meunier, A. Mitschler, L. Ricard and R. Weiss, *J. Chem. Soc., Chem. Commun.*, (1974) 44.
103. H. Felkin, P. J. Knowles and B. Meunier, *J. Organomet. Chem.*, 146 (1978) 151.
104. Ph.D. Thesis of D. J. Ciappenelli, Brandeis University, 1971, p.64.
105. ibid, ref. 104, p.70.
106. R. B. King, *J. Am. Chem. Soc.*, 85 (1963) 1918.
107. A. Davison, J. A. McCleverty and G. Wilkinson, *J. Chem. Soc.*, (1963) 1133.
108. F. A. Cotton and T. J. Marks, *J. Am. Chem. Soc.*, 91 (1969) 7523.
109. J. K. Hoyano, Ph.D. Thesis, University of Alberta, 1971, p.192.

110. J. K. Hoyano and W. A. G. Graham, *Inorg. Chem.*,
submitted.
111. P. J. Krusic, P. J. Fagan and J. San Fillipo, Jr.,
J. Am. Chem. Soc., 99 (1977) 250.
112. J. San Fillipo, Jr., J. Silbermann and P. J. Fagan,
J. Am. Chem. Soc., 100 (1978) 4834.
113. P. H. Plesch and A. Stasko, *J. Chem. Soc. (B)*, (1971)
2052 and references therein.
114. K. H. Pannell and D. Jackson, *J. Am. Chem. Soc.*,
98 (1976) 4443.
115. R. W. Fish, W. P. Giering, D. Marten and M. Rosenblum,
J. Organomet. Chem., 105 (1976) 101.
116. A. P. Humphries and S. A. R. Knox, *J. Chem. Soc.*,
(Dalton), (1975) 1710.
117. J. R. Sweet, Ph.D. Thesis, University of Alberta,
1981.
118. B. F. Hallam and P. L. Pauson, *J. Chem. Soc.*, (1956)
3030.
119. R. B. King, L. W. Houk and K. H. Parnell, *Inorg.*
Chem., 8 (1969) 1043.
120. R. B. King, *J. Organomet. Chem.*, 8 (1967) 287.
121. R. K. Pomeroy, private communication to W. A. G.
Graham.
122. A. Mantovani and S. Cenini, *Inorg. Synth.*, 16 (1976)
47.

123. R. B. King, *J. Organomet. Chem.*, 171 (1978) 53.
124. T. Blackmore, M. I. Bruce and F. G. A. Stone,
J. Chem. Soc. (A), (1968) 2158.
125. cf. R. D. Adams and F. A. Cotton in "Dynamic Nuclear
Magnetic Resonance Spectroscopy", L. M. Jackman
and F. A. Cotton, Eds., Academic Press, New York,
1975, Chapter 12.
126. R. D. Adams and F. A. Cotton, *J. Am. Chem. Soc.*, 95
(1973) 6589 and references therein.
127. J. G. Bullitt, F. A. Cotton and T. J. Marks, *J. Am.
Chem. Soc.*, 92 (1970) 2155.
128. R. D. Fischer, A. Vogler and K. Noack, *J. Organomet.
Chem.*, 7 (1967) 135.
129. R. J. Haines and A. L. duPreez, *Inorg. Chem.*, 8
(1969) 1459.
130. R. J. Haines and A. L. duPreez, *J. Organomet. Chem.*,
21 (1970) 181.
131. R. B. King, W. C. Zipperer and M. Ishaq, *Inorg.
Chem.*, 11 (1972) 1361.
132. E. L. Muetterties, "Transition Metal Hydrides",
Marcel Dekker, Inc., New York, 1972, p.77.
133. H. D. Kaesz and R. B. Saillant, *Chem. Rev.*, 72
(1972) 231.
134. D. C. Harris and H. B. Gray, *Inorg. Chem.*, 14 (1975)
1215.

135. D. A. Symon and T. Waddington, *J. Chem. Soc. A*,
(1971) 953.
- 136 S. J. LaCroce, K. P. Menard and A. R. Cutler,
J. Organomet. Chem., 190 (1980) C79.
137. O. S. Mills and J. P. Nice, *J. Organomet. Chem.*,
9 (1967) 339.
138. P. Kalck and R. Poilblanc, *C. R. Acad. Sci. Paris*,
274 (1972) 66.
139. J. K. Hoyano and W. A. G. Graham, *Inorg. Chem.*,
submitted.
140. R. Ball, University of Alberta, Structure Determination
Laboratory Report No. SR:071801-004-80 (October 18,
1981).
141. A. H. Andrist, *J. Org. Chem.*, 38 (1973) 1772.
142. W. Von E. Doering, 18th I.U.P.A.C. Congress, July,
1971. Quoted by Larabee (ref. 143).
143. R. B. Larrabee, *J. Organomet. Chem.*, 74 (1974) 313.
144. A. A. Frost and R. G. Pearson, "Kinetics and
Mechanism", John Wiley and Sons, New York, 1961, p.112.
145. J. Berson, *Acc. Chem. Res.*, 5 (1972) 405.
146. C. W. Spangler, *Chem. Reviews*, 76 (1976) 187.
147. A. G. Anastassiou, *J. Chem. Soc., Chem. Commun.*,
(1968) 15.
148. L. Salem, "The Molecular Orbital Theory of Conjugated
Systems", W. A. Benjamin Inc., New York, 1966,
Chapter 8.

149. M. A. McKinney and D. T. Haworth, *J. Chem. Ed.*,
57 (1980) 110.
150. H. S. Gutowsky, D. W. McCall and C. P. Slichter,
J. Chem. Phys., 21 (1953) 279.
151. L. H. McConnell, *J. Chem. Phys.*, 28 (1958) 430.
152. J. A. Pople, W. G. Schneider and H. J. Bernstein,
"High Resolution NMR", McGraw-Hill, New York, 1959,
Chapter 10.
153. M. J. Bennett, F. A. Cotton, A. Davison, J. W.
Fallor, S. J. Lippard and S. M. Morehouse, *J. Am.*
Chem. Soc., 88 (1966) 4371.
154. F. A. Cotton, *J. Organomet. Chem.*, 100 (1975) 29.
155. F. A. Cotton, *Acc. Chem. Res.*, 1 (1968) 257.
156. H. C. Clark and A. Shaver, *Can. J. Chem.*, 54 (1976)
2068.
157. M. M. Hunt, W. G. Kita, B. E. Mann and J. A. McCleverty,
J. Chem. Soc., (Dalton), (1978) 467.
158. R. D. Holmes-Smith and S. R. Stobart, *J. Am. Chem.*
Soc., 102 (1980) 383.
159. A. P. terBorg, H. Kloosterzeil and N. vanMeurs,
Recl. Trav. Chim. Pays-Bas, 82 (1963) 717.
160. A. P. terBorg and H. Kloosterzeil, *Recl. Trav.*
Chim. Pays-Bas, 82 (1963) 741.
161. K. W. Egger, *J. Am. Chem. Soc.*, 89 (1967) 3688.
162. T. Nozoe and K. Takahashi, *Bull. Chem. Soc. Japan*,
38 (1965) 665.

163. J. A. Berson and M. R. Willicott III, J. Am. Chem. Soc., 88 (1966) 2494.
164. S. Forsén and R. A. Hoffman, Acta Chem. Scand., 17 (1963) 1787; J. Chem. Phys., 39 (1963) 2892; J. Chem. Phys. 40 (1964) 1189.
165. J. W. Faller, in "Determination of Organic Structures by Physical Methods", Vol. 5, F. C. Nachod and J. J. Zuckerman, Eds., Academic Press, New York, 1973, Chapter 2.
166. D. Canet, G. C. Levy and I. R. Peat, J. Mag. Res., 18 (1975) 199.
167. J. H. Noggle and R. E. Shirmer, "The Nuclear Overhauser Effect", Academic Press, New York, 1971.
168. B. M. Fung, J. Am. Chem. Soc., 90 (1968) 219.
169. M. Elian and R. Hoffmann, Inorg. Chem., 14 (1975) 1058.
170. R. Hoffmann, private communication (Tenth ICOMC, Toronto, August, 1981).
171. B. E. Mann, J. Chem. Soc, Chem. Commun., (1977) 626.
172. F. A. Cotton, D. L. Hunter and P. Lahuerta, J. Am. Chem. Soc., 86 (1974) 4723, 7926.
173. B. E. R. Schilling, R. Hoffmann and D. L. Lichtenberger, J. Am. Chem. Soc., 101 (1979) 585.
174. J. C. Green and S. E. Jackson, J. Chem. Soc., (Dalton), (1976) 1698.

175. D. Fabian, T. P. Fehlner, L. S. T. Huang and J. Labinger, *J. Organomet. Chem.*, 191 (1980) 409.
176. G. Binsch, *J. Am. Chem. Soc.*, 91 (1969) 1304.
177. W. Hieber and G. Braun, *Z. Naturforsch.*, 14b (1959) 32.
178. R. Pettit, *J. Am. Chem. Soc.*, 86 (1964) 2589.
179. J. R. Blackborow, K. Hildenbrand, E. A. Koerner von Gustorf, A. Scrivanti, C. Kruger, C. R. Eady and D. Ehntolt, *J. Chem. Soc., Chem. Commun.*, (1976) 16.
180. J. R. Blackborow, R. H. Grubbs, K. Hildenbrand, E. A. Koerner von Gustorf, A. Myashita and A. Scrivanti, *J. Chem. Soc., (Dalton)*, (1977) 2205.
181. J. Müller, C. G. Kreiter, B. Mertschenk and S. Schmidt, *Chem. Ber.*, 108 (1975) 273.
182. J. G. Reuvers, Ph.D. Thesis, University of Alberta, 1979.
183. J. Takats, J. G. Reuvers and S. Gittawong, paper presented at the Tenth ICOMC, Toronto, August, 1981. Abstract #5C08.
184. W. A. G. Graham and I. D. H. Towle, unpublished results.
185. H. Shanan-Atidi and K. H. Bar-Eli, *J. Phys. Chem.*, 74 (1970) 961.
186. C. G. Kreiter and M. Lang, *J. Organomet. Chem.*, 55 (1973) C27.
187. T. H. Whitesides and R. A. Budnik, *Inorg. Chem.*, 14 (1975) 664.

Appendix (Thanks to R. E. D. McClung)

In the magnetization transfer experiment, one measures the z-component of the magnetization in each site i at thermal equilibrium, $M_{z_i}^0$, and under steady state conditions with the k -th resonance saturated, $M_{z_i}^\infty$. It is convenient to describe the saturation transferred in terms of the relative saturation parameters

$$S_i = [M_{z_i}^0 - M_{z_i}^\infty] / M_{z_i}^0, \quad (1)$$

since these parameters are readily obtained by normalizing the integrals in a difference spectrum. It is clear from eq (1) that $S_k = 1$ for the resonance which is saturated, that $S_j = 0$ for sites to which no magnetization transfer occurs and that, in general, $0 \leq S_i \leq 1$. The relationship between the relative saturation parameters, S_i , and the rate constants, k_{ij} , for chemical exchanges between the sites is derived from the Bloch equations modified for chemical exchange.¹ For all sites $i \neq k$, the appropriate Bloch equation for M_{z_i} is

$$\frac{dM_{z_i}}{dt} = \frac{M_{z_i}^0 - M_{z_i}^\infty}{T_{1i}} - \sum_{j \neq i} k_{ij} M_{z_i}^\infty + \sum_{j \neq i} k_{ji} M_{z_j}^\infty = 0, \quad (2)$$

where k_{ij} is the rate of exchange from site i to site j and $M_{z_i}^\infty$ is the steady state magnetization at site i when resonance k is saturated. At thermal equilibrium,

$$k_{ij}M_{z_i}^{\circ} = k_{ji}M_{z_j}^{\circ} . \quad (3)$$

Therefore

$$[M_{z_i}^{\circ} - M_{z_i}^{\infty}]/T_{1i} + \sum_{j \neq i} \{k_{ji}[M_{z_j}^{\infty} - M_{z_j}^{\circ}] - k_{ij}[M_{z_i}^{\infty} - M_{z_i}^{\circ}]\} = 0 \quad (4)$$

Dividing eq (4) by $M_{z_i}^{\circ}$ and introducing S_i from eq (1), we obtain

$$\sum_{j \neq i} k_{ij}[S_j - S_i] = S_i/T_{1i} , \quad (5)$$

which is a set of simultaneous linear equations in the rate constants k_{ij} . For an exchange problem involving n sites, there will be $n-1$ equations which, given measured values of the S_i and T_{1i} , can be solved by standard methods.²

It is appropriate to illustrate the application of eq (5) by considering the ^{13}C saturation transfer in the 7-site monohapto-cycloheptatrienyl fragment. To minimize confusion, we label the sites $a(\text{C}_1 \text{ and } \text{C}_6)$, $b(\text{C}_2 \text{ and } \text{C}_5)$, $c(\text{C}_3 \text{ and } \text{C}_4)$ and $d(\text{C}_7)$. If resonance d is saturated, the relevant linear equations are

$$\begin{aligned} k_{ab}(S_b - S_a) + k_{ac}(S_c - S_a) + k_{ad}(S_d - S_a) &= S_a/T_{1a} \\ k_{ba}(S_a - S_b) + k_{bc}(S_c - S_b) + k_{bd}(S_d - S_b) &= S_b/T_{1b} \\ k_{ca}(S_a - S_c) + k_{cb}(S_b - S_c) + k_{cd}(S_d - S_c) &= S_c/T_{1c} \end{aligned} \quad (6)$$

If the rates of 1-2, 1-3 and 1-4 shifts are represented by the rate constants k_{12} , k_{13} and k_{14} respectively, one can show that

$$\begin{aligned} k_{ab} &= k_{ba} = k_{12} + k_{14} & , & & k_{ad} &= k_{da} = k_{12} & , \\ k_{ac} &= k_{ca} = k_{13} + k_{14} & , & & k_{bd} &= k_{db} = k_{13} & , \\ k_{bc} &= k_{cb} = k_{12} + k_{13} & , & & k_{cd} &= k_{dc} = k_{14} & , \end{aligned} \quad (7)$$

and that eq (6) can be rewritten as

$$\begin{aligned} k_{12}(S_b + S_d - 2S_a) + k_{13}(S_c - S_a) + k_{14}(S_b + S_c - 2S_a) &= S_a/T_{1a} \\ k_{12}(S_a + S_c - 2S_b) + k_{13}(S_c + S_d - 2S_b) + k_{14}(S_a - S_b) &= S_b/T_{1b} \\ k_{12}(S_b - S_c) + k_{13}(S_a + S_b - 2S_c) + k_{14}(S_a + S_d - 2S_c) &= S_c/T_{1c} \end{aligned} \quad (8)$$

In this case the number of relative saturation parameters measured (S_a , S_b and S_c) is equal to the number of rate constants (k_{12} , k_{13} and k_{14}) so that one can solve for the rate constants in a direct fashion. If there are fewer rate constants than equations, methods appropriate to an overdetermined set of equations² would be applied.

References

1. H.M. McConnell, J. Chem. Phys. 28, 430 (1958).
2. F. Scheid, Theory and Problems of Numerical Analysis (McGraw-Hill, New York, N.Y., 1968) Chapters 26 and 28.

B30339